ANDREW RAE DUNCAN

THE PETROLOGY AND PETROCHEMISTRY OF ANDESITE AND DACITE VOLCANOES IN EASTERN BAY OF PLENTY, NEW ZEALAND

Thesis submitted for the degree of
Doctor of Philosophy
in Geology

Victoria University of Wellington
April 1970

CONTENTS

TABLES

* in pocket at back of thesis.

FIGURES

* in pocket at back of thesis.

PLATES

ABSTRACT

The volcanic rocks of Edgecumbe, Whale Island, White Island and Manawahe are andesites and dacites, which are collectively termed the Bay of Plenty volcanics. Edgecumbe is a comparatively young volcano, being active between 1700 and 8000 years B.P.; Whale Island has probably been inactive for at least the last 36,000 years; White Island has probably been active for much of the late Pleistocene, and is still in a stage of solfataric activity with intermittent tephra eruptions; and Manawahe is probably of the order of 750,000 years old (K-Ar date by J.J. Stipp).

The geology of Edgecumbe, Whale Island and White Island is discussed, and the petrography and mineralogy of the Bay of Plenty volcanics is discussed and compared. The rocks of Edgecumbe and Whale Island are extremely similar petrographically, but the rocks of White Island and Manawahe are sufficiently different that they can be distinguished both from one another and from Edgecumbe and Whale Island rocks. Most of the Bay of Plenty volcanics are plagioclase andesites or plagioclase dacites.

New total rock analyses for 28 elements in 44 samples of the Bay of Plenty volcanics are presented, together with analyses for 4 samples from elsewhere in the Taupo Volcanic Zone. Three samples were analysed for an additional 17 elements.

The Bay of Plenty volcanics are calc-alkaline and are predominantly dacites ($\geqslant$ 63% SiO_2) by Taylor et al.'s (1969) definition, but there is chemical continuity from samples with about 61% SiO_2 to samples with about 66% SiO_2. Major and trace element variation trends cannot be

explained entirely by a crystal fractionation hypothesis, and assimilation of upper crustal material of rhyolitic composition best explains the variation trends for Edgecumbe and Whale Island. The variation trends and certain element abundances in White Island rocks suggest the assimilation of marine sediments, and introduction of seawater into the magma.

Taken as a whole, the Bay of Plenty volcanics fit the chemical trends which have been established for the Taupo Zone by earlier workers (e.g. Steiner, 1958; Clark, 1960). The apparent geochemical 'gap' or discontinuity between about 68% and 71.5% SiO_2 noted by Steiner (1958) is further substantiated by the new geochemical data presented here. It is considered likely that basalt, andesite and rhyolite are all primary magmas in the Taupo Volcanic Zone. Their possible origins, and the origins of Taupo Zone dacites are discussed.

ACKNOWLEDGEMENTS

The author particularly wishes to thank Professors R.H. Clark and S.R. Taylor. Professor Clark suggested the thesis topic and has provided guidance and advice on many aspects of the work. Professor S.R. Taylor provided the facilities of his laboratory at Australian National University, Canberra; instructed the author in various techniques of trace and major element analysis; and has spent many hours discussing trace element interpretation in general and the formation of andesites in particular. Professor H.W. Wellman and Drs E.D. Ghent and R.G. Burns have advised the author on various aspects of the research, and have always been willing to discuss problems that have arisen. Professors H.W. Wellman, R.H. Clark and S.R. Taylor have critically read portions of the manuscript, and their constructive criticism has been very helpful.

The author acknowledges financial support from the University Grants Committee in the form of a postgraduate scholarship, which the author held for three years. Additional financial support, both for fieldwork and for air travel to Australia and back has been provided by the Internal Research Committee of Victoria University of Wellington.

During fieldwork the author had accommodation provided for him by courtesy of the Tasman Pulp and Paper Co. Ltd at Kawerau. Mr J.A. Okeby and Mr J. Mitchell, both of Tasman, were particularly helpful to the author and their assistance is gratefully acknowledged. Staff of the N.Z. Geological Survey at the Rotorua District Office, particularly Messrs J. Healy, D. Rishworth and E. Lloyd, have always been willing to discuss field problems with the author, and have given valuable

suggestions and advice on many occasions. During field interpretation of tephra sections the author was guided by Messrs C.G. Vucetich and A.Pullar, and was assisted by Mr P. Wellman. Sample collection on Edgecumbe was aided by members of the 1967 B.Sc. (Hons.) course in Geology from Victoria University, who assisted the author for a day.

Thanks are due to Professor J.C. Jaeger, Chairman of the Department of Geophysics and Geochemistry at A.N.U. for accepting the author as a temporary research student in his department during the six months that the author spent at A.N.U. The co-operation of Professor D.A. Brown, Chairman of the Department of Geology at A.N.U., who allowed the author use of analytical equipment in his department is gratefully acknowledged. Advice on analytical techniques and many hours of cheerful assistance were given the author by Mrs M.J. Kaye, and her help was much appreciated. In addition, Mrs Kaye made major element analyses of four samples, and spark-source mass spectrographic analyses of three samples. Dr B.W. Chappell instructed the author in x-ray fluorescence analytical techniques, and permitted the author to make major element analyses using equipment in his charge. Advice on the techniques of gamma-ray spectrography was given by Dr K. Heier.

The author thanks the Director, N.Z. Geological Survey, for allowing the use of x-ray fluorescence and electron microprobe equipment. Analytical advice from members of Geological Survey, in particular Drs A. Ewart, G.A. Challis, P. Wood, P. Blattner and Mr J. Hunt is acknowledged.

Manuscript copies of papers were made available to the author prior to their publication by courtesy of the following authors:

Drs S.R. Taylor, A. Ewart, T. Hatherton, J.J. Stipp, Philippa M. Black, J. Hulston, J.B. Gill, and Mr M. Stewart.

Apart from computer programmes written by the author, programmes written by the following people were used in data reduction and statistical analysis: Dr P. Arriens, Mrs M.J. Kaye, Mrs J. Widdowson, Messrs M. Cook, D. Kinneburgh, R. Cochrane and K. Rodgers.

Discussions with a large number of people were responsible for clarification and development of some of the ideas expressed in this thesis, the author would like to thank the following people in particular: Professors R.H. Clark, S.R. Taylor, H.W. Wellman, J. Bradley; Drs A. Ewart, E.D. Ghent, R.G. Burns, A.J.R. White, J.W. Cole, J.J. Stipp, T. Hatherton, J. Hulston, P. Wood; Messrs C.G. Vucetich, A. Pullar, J. Healy, J.D. Milne, P. Wellman, B.P. Kohn, and P. Browne.

Transport to White Island has been provided by courtesy of the R.N.Z.N. and the R.N.Z.A.F.

The thesis has been typed by my wife, and her assistance in this respect, together with the considerable help she has given in the preparation of manuscript has been invaluable.

Credits

Reproduction of line drawings: Mrs A. Adams

Reproduction of tables: V.U.W. Multilith department

Ammonia prints and photostats: Gordon H. Burt Ltd.

Binding: Bookbinding Specialists Ltd.

PART 1

GEOLOGY, PETROGRAPHY AND MINERALOGY OF EDGECUMBE, WHALE ISLAND, WHITE ISLAND AND MANAWAHE

INTRODUCTION

Quaternary calc-alkaline volcanism in general, and andesitic volcanism in particular, is closely associated with active continental margins and island arcs. Active continental margins and andesitic volcanism border most of the Pacific, forming an almost continuous chain of volcanoes from the Andes of South America through Central America to the Cascades of North America, from there through the Alaskan peninsula and Aleutian and Kurile arcs to Japan, and thence through the Bonin-Marianas arc, the Solomon Islands, and the Fiji, Tonga and Kermadec Islands to New Zealand. This remarkable volcanic chain which is semi-continuous for more than 20,000 miles has been termed the "girdle of fire" round the Pacific. The boundary between circum-pacific andesitic volcanism and the tholeiitic and alkalic volcanism within the Pacific basin has been termed the "andesite line", and has played an important part in many petrogenetic theories for the origin of the calc-alkalic volcanic association.

In the centre of North Island, New Zealand, Holocene volcanism has occurred principally in the Taupo Volcanic Zone (Fig. 1.), which extends from Ohakune to White Island. The structure of the Taupo Volcanic Zone, the distribution of eruptive rocks within it and the volcanic mechanisms controlling eruption have been discussed by Healy (1962, 1964), Thompson (1964) and Modriniak & Studt (1959). Clark (1960 a, b.) noted that surface outcrops of the rock types present show an apparent symmetry, with andesitic eruptives being located at the southwestern and northeastern ends of the zone, separated by rhyolitic eruptives and minor amounts of dacitic eruptives.

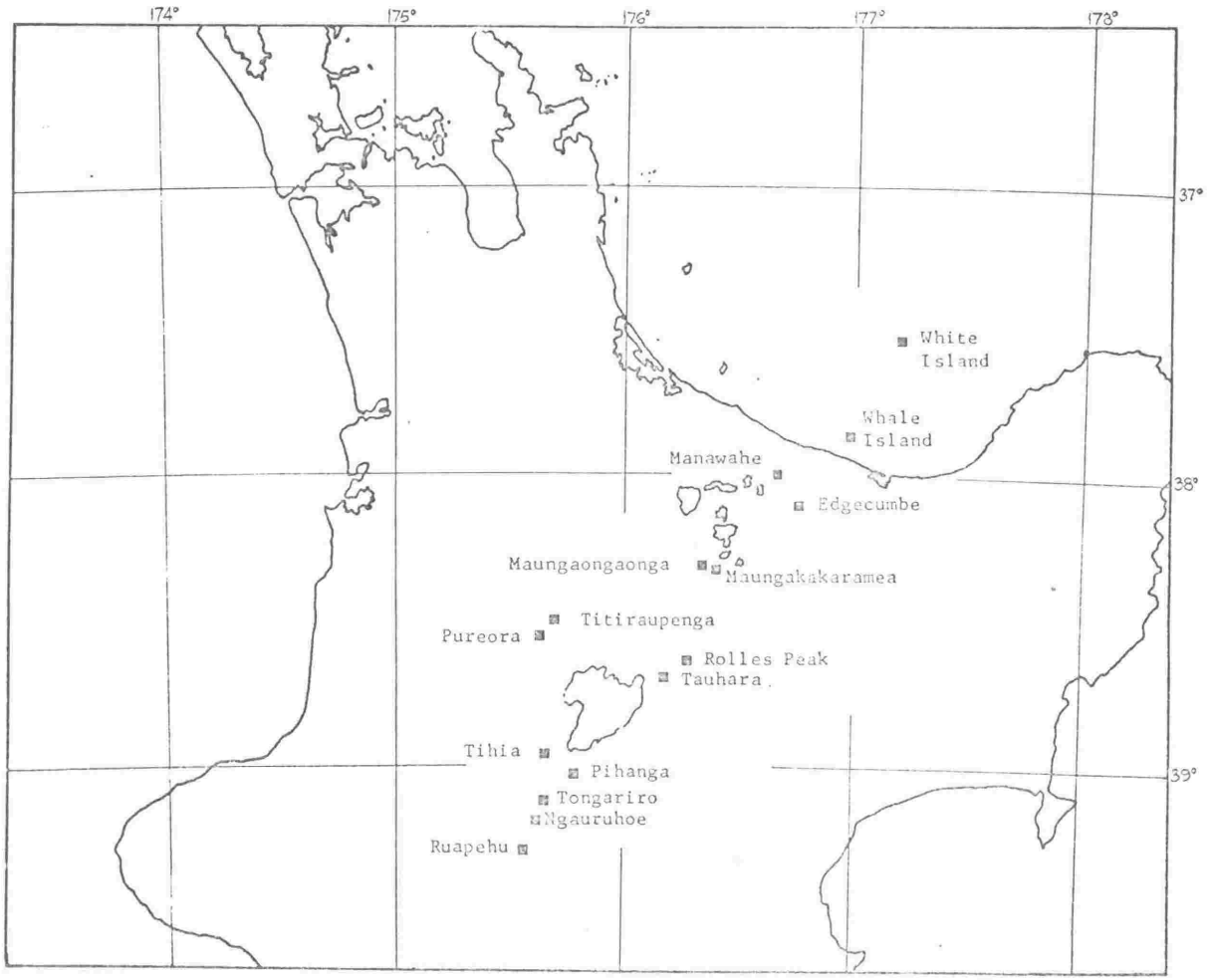

Fig. 1. - Map of the central part of North Island showing the locations of andesite and dacite volcanoes in the Taupo Volcanic Zone.

For the intermediate calc-alkaline volcanics, some of which are the subject of this thesis, the distribution is as follows. Volcanoes termed "young" are thought to have been active within the last 50,000 years.

By far the greatest volume of andesite erupted in the Taupo Zone has been from the volcanoes of Tongariro National Park; Ruapehu, Ngauruhoe and Tongariro; and from Pihanga and Tihia just to the north of the park. The central part of the zone contains three small dacite volcanoes; Tauhara, Maungaongaonga and Maungakakaramea; and three old andesite volcanoes; Pureora, Titiraupenga and Rolles Peak. The northeastern portion of the zone contains the young volcanoes Edgecumbe, Whale Island and White Island together with the old volcano Manawahe; all four of these volcanoes have been described as andesitic by Healy, Schofield & Thompson (1964). However the lavas of the four volcanoes are shown here to be more acidic than the andesites of the Tongariro National Park volcanoes, and would be better described as transitional in composition from andesite to dacite.

The young volcanoes Edgecumbe, Whale Island and White Island lie approximately 40 km apart on the flanks of the Whakatane Graben, described by Macpherson (1944), and its proposed offshore extension the White Island Trench (Fleming, 1952). The dissected remnants of the old volcano Manawahe also lie on the flank of the Whakatane Graben, some 15 km north of Edgecumbe. Thus the positions of the andesitic and dacitic volcanoes at the northeast end of the Taupo Volcanic Zone appear to be related to the position of the Whakatane Graben.

The Whakatane Graben is a complex depression, bounded on the northwest by normal faults and bounded on the southeast by intersecting north-south trending transcurrent faults and northeast trending normal faults (Healy, Schofield & Thompson; 1964). Where the graben crosses the coast the basement (Mesozoic greywacke) lies at least 2100 m below the surface, shallowing to about 1500-1800 m at Kawerau. From samples recovered from drillholes for steam production at Kawerau, the graben appears to be filled with rhyolitic lavas, tuffs and flow breccias; ignimbrite; andesite; and volcanigenic siltstones.

For convenience of description the rocks of Edgecumbe, Whale Island, White Island, and Manawahe volcanoes are collectively termed the "Bay of Plenty volcanics"; and although other andesites and dacites crop out in the Bay of Plenty region (e.g. Motiti Island) these are not included in the present usage of this collective term.

PETROGRAPHIC NOMENCLATURE

Rocks can be named according to petrographic or chemical criteria, but in general few rocks from any particular suite are analysed, thus necessitating a dual classification using either criterion. Such classifications, one chemical and one petrographic, will often result in different names for the same rock. Since the intermediate calc-alkaline volcanics are petrographically classified according to their phenocryst assemblage, which often represents only 20-30% by volume of the rock, differences between chemical and petrographic classification are quite frequent. Throughout the sections on the geology, petrography and mineralogy of the Bay of Plenty volcanics a petrographic classification, discussed below, is used.

A mineralogical criterion which closely corresponds to the chemical dividing line between andesite and dacite, chosen at 63% SiO_2 in accordance with Taylor et al.'s (1969) recommendation, is the presence (dacite) or absence (andesite) of modal quartz. All samples from Edgecumbe, Whale Island, White Island and Manawahe are chemically either andesitic or dacitic. All chemically analysed rocks petrographically classified as dacites are also dacitic in chemistry ($\geqslant$ 63% SiO_2). However, a number of "chemical dacites" do not contain modal quartz; thus the petrographic classification adopted provides an underestimate of the proportion of rocks with dacitic chemistry in the volcanics sampled. A more extensive account of the relationships between mineralogy and chemistry in the rocks analysed is given in the section on Geochemistry.

Petrography is also used for sub-division of the andesites and dacites. With one modification, the mineralogical sub-divisions adopted are essentially the same as those of Clark (1960 b.). As the plagioclase from the Bay of Plenty andesites and dacites is more sodic than that in the rocks of Tongariro National Park, Clark's labradorite and labradorite-pyroxene prefixes have been altered to plagioclase and plagioclase-pyroxene. With this alteration Clark's petrographic classification of the andesites is applicable to both andesites and dacites, allowing simple comparison of their mineralogy.

The petrographic subdivisions used in this thesis are detailed below:-

(1) Plagioclase andesite/dacite - porphyritic plagioclase dominant over pyroxene phenocrysts.

(2) Plagioclase-pyroxene andesite/dacite - proportion of pyroxene to plagioclase phenocrysts substantial. Quantitative distinction from (1) made according to the value of the ratio (porphyritic pyroxene x 100)/(porphyritic plagioclase + pyroxene), samples with a ratio less than 33.3 are classified as plagioclase andesites/dacites.

Since none of the Bay of Plenty volcanics sampled have substantial concentrations of olivine or hornblende, Clark's subdivisions requiring significant amounts of these minerals are not used in this thesis. Similarly, pyroxene is never the dominant phenocryst in the Bay of Plenty volcanics sampled, and a pyroxene andesite/dacite definition is not required.

EDGECUMBE

Edgecumbe is a young volcano 3 km southeast of the town of Kawerau in the Bay of Plenty region. Its summit is 821 m above sea-level, and its base about 70 m above sea-level. The rocks of which it is composed have been erupted onto the tephra-covered surface of the eroded Matahina Ignimbrite.

Edgecumbe was described as a young-looking hypersthene-andesite volcano by MacPherson (1944), and was similarly described by Healy, Schofield & Thompson (1964) who, in addition, inferred on the basis of tephrachronology an age for Edgecumbe of little more than 1,000 years. A more extensive geological description has been given recently by Healy (1967); but no systematic geological, petrological or petrochemical study of the volcano has been made previously. Studt (1958) made a geophysical investigation of the Kawerau area which showed that Edgecumbe has very little effect on the geomagnetic contours and because of the marked susceptibility difference between the andesite and the underlying ignimbrite he therefore inferred that the andesite does not extend far below the surface.

GEOLOGY

Edgecumbe rises abruptly from the tephra-covered surface of the Matahina Ignimbrite and is virtually undissected. The lack of dissection is due both to its youthfulness and to a large proportion of the drainage being sub-surface, emerging as springs at the base of the lowest lava flows. The outer boundary of lava flows at the base of the volcano is well defined and on the mountain itself features such as

Plate 1. - View of Edgecumbe from the northwest, the ignimbrite Roof Dome can be seen at the foot of the Main Cone (left centre).

flows and groups of flows can be determined from air photographs and detailed contour maps.

The geology is depicted on two single-factor maps. Fig. 2 is a detailed contour map of Edgecumbe and the surrounding area. Fig. 3 is an interpretative map showing all recognisable individual flows and the vents from which they are thought to have come. Relative age of the flows from any one vent is also indicated wherever it can be deduced from topography, air photographs or ground inspection. In many cases it is harder to observe flow boundaries and contact relationships on the ground than in air photographs, mainly because of the chaotic and broken surface of the flows and the heavy bush cover. Table 1 lists the grid co-ordinates of the vents and groups the vents, and flows from them according to locality.

Where flows can be ascribed to a particular vent they are given the vent number, and a number of flows apparently from the same vent are termed a flow series. The relative age of the flows in each flow series is indicated in Fig. 3, the letters 'a', 'b' and 'c' after the vent number indicating increasing age with 'a' being the youngest recognised flow from that vent. In cases where a flow series can be recognised but the vent from which it was erupted is not recognisable, then all the flows in any one series are identified by capital letters. Thus flow series A contains three flows Aa, Ab and Ac, in order of increasing age.

It has not been possible to determine the location of the vents from which the lowest flows around the base of the volcano were erupted, nor do the flows form clearly defined flow series. They have therefore been grouped according to their location into the Northern, Southern and Western Base Flows.

TABLE 1

LOCATIONS AND NAMES OF EDGECUMBE VENTS AND VOLCANIC UNITS

Vent No.	Grid Co-ordinates	Grouping
1.	N77/163070	
2.	N77/164072	Western Vents, Flows.
3.	N77/165071	
4.	N77/168071	
5.	N77/172071	Main Dome.
6.	N77/179075	Main Cone Vents, Flows.
7.	N77/181087	North Dome.
8.	N77/184076	
9.	N77/185075	Main Cone Vents, Flows.
10.	N77/186075	
11.	N77/187074	

A striking feature of the volcanism at Edgecumbe is the marked linear distribution of nearly all the vents. Ten out of the eleven recognised vents fall inside a band 300 m wide and 3 km long trending 85°. This trend is not parallel to the 50° trend of the Tarawera rift or its postulated extension as a concealed fault down the Tarawera River valley to the west of Edgecumbe, nor is it parallel to the main north-south or northeast-southwest fault trends in the area. There is no topographic indication of recent faulting displacing the surface of the Matahina Ignimbrite in the area immediately surrounding Edgecumbe. The vent trend is inferred to be controlled by a major fracture zone, but vertical or horizontal displacements on this zone have not been observed.

Western Flows

The western Base Flows are very similar in topographic expression to the northern and southern Base Flows, and all three are probably about the same age. The relative ages of vents 1, 2, 3, and 4 are not certain as flows from these vents are separated by areas of western Base Flows. Flows 1a, 1b, 2b and 3c do not have any well-preserved flow features and are thought to be rather older than flows 2a, 3a, and 3b. The latter flows have well-preserved ridges parallel to the flow front, together with clearly defined levées. The small flow from vent 4 is certainly younger than Main Dome (extruded from vent 5) since it has been constrained to the valley between Main Dome and Western Flows; it is also probably younger than the flows from vents 2 and 3.

It seems probable that early eruptions from vents 1, 2, and 3 were approximately contemporaneous, but that eruptions continued from vents 2 and 3 after vent 1 had become inactive. The lava flow from vent 4

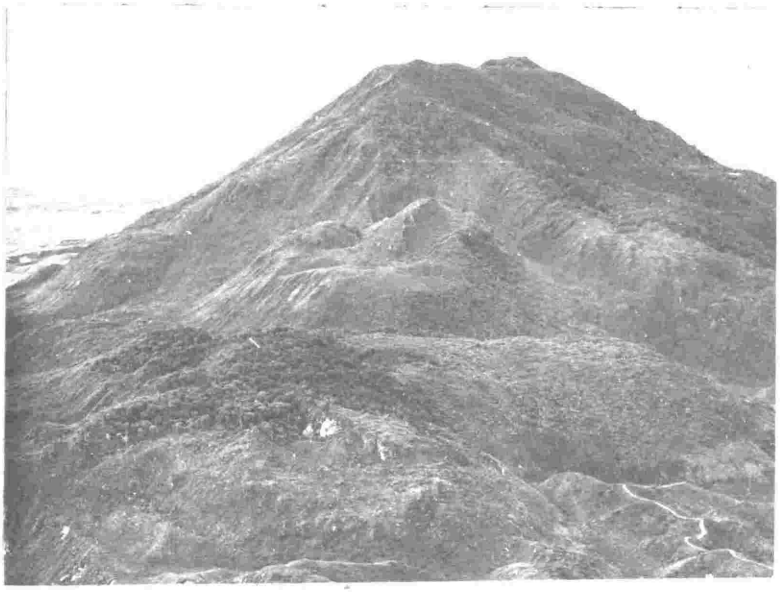

Plate 2. - Alignment of vents comprising the Edgecumbe volcano; western vents in the foreground with the Main Dome, and Main Cone vents behind them.

Plate 3. - Main Dome, Edgecumbe.

probably postdates flows from vents 2 and 3, thus indicating a pattern of a slowly eastward-migrating focus of eruption.

Steep sides and fronts (up to 40°) on most of the flows, and remnants of extrusive spines at vents 2 and 3 are indications of relatively high magma viscosity.

Main Dome

Main Dome lying between Main Cone and the Western Flows is one of the most conspicuous features on Edgecumbe. It is extremely steep-sided (up to 48°) and was extruded as a single unit, but lava protrusions broke through the cooling-surface at two points to form small spines. A number of blocks of non-vesicular lava on top of the Dome are capped by a welded breccia of rather vesicular lava. As the contact between the welded breccia and the underlying lava is gradational, the breccia is probably the auto-brecciated top of the lava dome rather than air-fall agglomerate.

Main Dome is apparently younger than flow 6a, one of the youngest flows on Main Cone, since the foot of flow 6a is covered by the eastern margin of the Dome. The Dome is probably younger than all the flows on Main Cone with the possible exception of flow 8a. It is older than the flow from vent 4, but may be the same age as one or more of the other Western Flows.

Domes of this type and size are common in volcanoes of intermediate calc-alkaline composition (Williams, 1932) and their formation is often accompanied by eruptions of the nuée ardente type. Dome growth accompanied by nuée ardente eruptions is well illustrated by the eruptions of Mt Lamington in 1951 (Taylor, 1958). Main Dome, however, seems to have grown quietly with no accompanying explosive activity.

Nowhere around the base of the Dome are there any extensive talus fans, and no breccia deposits of nuée ardente type are found either on the volcano or on the surrounding tephra-covered ignimbrite.

The approximate volume of the Main Dome together with the approximate volumes of the other volcanic units making up the Edgecumbe volcano are given in Table 2.

Main Cone

Main Cone includes by far the largest volume of volcanic material in the Edgecumbe volcano (Table 2.). Flows forming the base of Main Cone were erupted from vents which are no longer visible, and are probably coulées from vents which are now covered both by the basal flows themselves and by subsequent flows.

The mode of growth in Main Cone appears to have been by successive eruption of massive coulées of highly viscous lava from vents near the centre of the Cone. Thinner flows of "aa" type were erupted mainly in the late stages of activity.

On the north side of Main Cone there are three well defined ridges, each formed by successive coulées and flows following nearly the same path but for progressively shorter distances from their common vent. Flows 6a, 6b and 6c followed the same path, which after flow 6c must have been a ridge. Similarly flows Aa and Ab followed the ridge formed by flow Ac; and flow Ba followed the ridge formed by flow Bb, a ridge to the east of the one formed by flow series A. In flow series A, B and C the volumeof individual flows decreases with decreasing age, the same trend shown by flows from vent 6. The vents from which flow series A, B, and C were erupted cannot be identified, but from the distribution of the flows the lavas must have been erupted from vents 9 and 10, or from vents close to these localities.

TABLE 2

APPROXIMATE VOLUME OF VOLCANIC UNITS

COMPRISING EDGECUMBE VOLCANO

Western Flows = 6.58×10^7 m^3.

Main Dome = 2.98×10^7 m^3.

North Dome = 1.18×10^6 m^3.

Main Cone = 1.51×10^9 m^3.

total volume = 1.61 km^3 = 0.39 $mile^3$

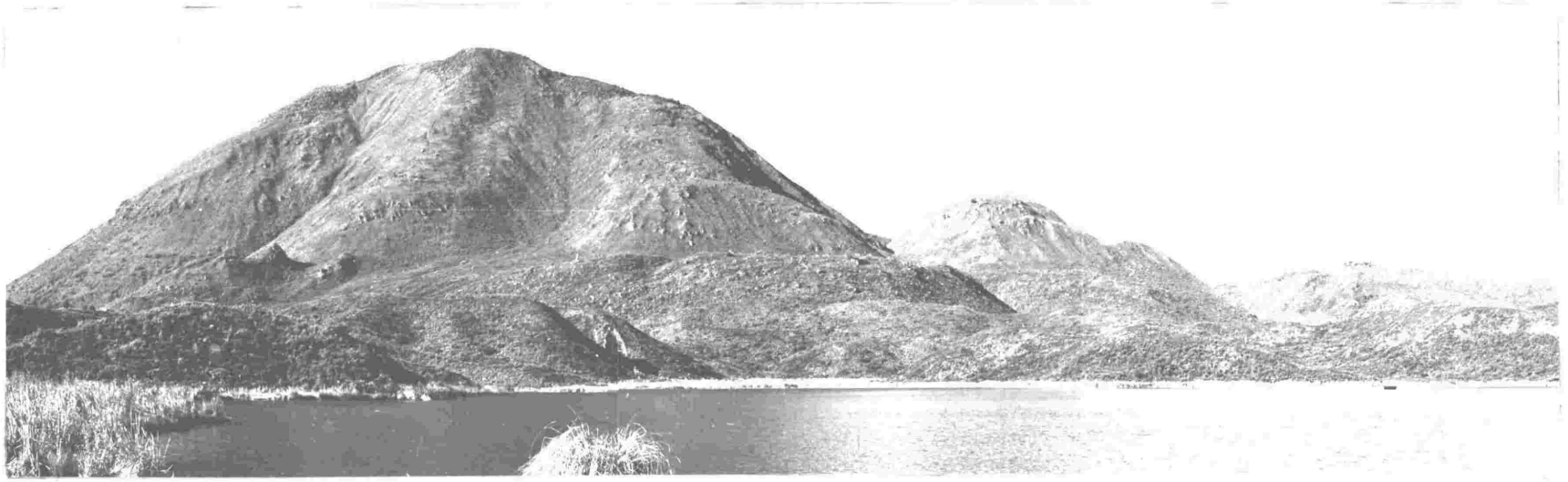

Plate 4. - Panorama of Edgecumbe from the west, Lake Pupuwharau in foreground.

The western flank of Main Cone, between the northeastern flows from vent 6 (6a, 6b and 6c) and the flows from vent 8 (8a and 8b), is sub-arcuate with the arc centered approximately on Main Dome. This suggests that the western side of Main Cone was sculptured either by explosion or collapse related to activity from vent 5. A major explosion in this area appears to be ruled out by the lack of fragmentary andesitic material or andesitic ash on or within the tephra deposits covering the Matahina Ignimbrite at the foot of the mountain. However, as shown in Fig. 3, extensive scree slopes on the western flank of Main Cone might have been formed by collapse along an arcuate fracture associated with vent 5. A flow from vent 6 apparently postdates this scree formation but predates the extrusion of Main Dome from vent 5.

On the south side of Main Cone there are four major coulées, which have been assigned to flow series D as it is likely that the vents from which they were erupted (possibly 9 and/or 10) were close together or coincident. Flow 8a postdates flows Da and Dd and from its surface appearance is probably the youngest of the flows on Main Cone. Flow 8b, which is largely covered by flow 8a, may be contemporaneous with some of flow series D.

A smooth surfaced fan-shaped lahar deposit, with its apex at the present summit of Edgecumbe, covers the eastern side of Main Cone. Its upper margins lie at the rim of an old breached crater, within which a small tholoid or vent plug was extruded from vent 11. It contains all sizes of volcanic material from 15 m blocks down to sand size particles, and extends for about 1 km northeast of the volcano, following the floor of a valley in the ignimbrite. Part of the lahar

debris consists of blocks which are chemically indistinguishable (see p.302) from samples taken from the small plug tholoid in vent 11, and thus the plug may be the remnant of a larger extrusive spine, whose collapse provided much of the material incorporated in the lahar.

The two small craters at the top of Main Cone are explosion pits (vents 9 and 10), and with the possible exception of flow 8a are probably the youngest features on the cone. The amount of ejecta produced by the explosions must have been small as andesitic ash and lapilli were only found at two sites on the south side of the Main Cone. No andesitic ash or lapilli were found in the tephra sheet covering the Matahina Ignimbrite at the base of the volcano.

North Dome

North Dome is notable since it was extruded from the only vent on Edgecumbe which does not lie within the 300 m wide band enclosing the other vents. It is even smaller than the plug tholoid in vent 11 and is topped by a small 25 m high extrusive spine which has strongly ribbed sides, probably due to scoring by the sides of the vent during extrusion. The relative age of North Dome is unknown as it is separated from other flows by scree debris from flows higher on the mountain.

Ignimbrite Roof Dome

On the northeast side of Edgecumbe volcano, 300 m beyond the foot of the lowest flow from Main Cone, there is a topographic dome composed of Matahina Ignimbrite which was described by Healy (1967) as a "roof mountain". Healy considered that it had "been thrust and lifted upwards, presumably by an intrusion of lava beneath it, until it stands 400 ft above its surroundings."

It can be seen from Fig. 4 that the ignimbrite was not merely pushed up vertically from below, but was also tilted downwards to the northeast in the process. Thus a sheath of the unwelded top of the ignimbrite bounds the Roof Dome on the north and east flanks. An arcuate valley on the top of the Roof Dome, together with collapse pits along the floor of this valley, suggest that part of the Dome collapsed back into the underlying vent along a ring-fracture. Strong hydrothermal alteration of welded ignimbrite is exposed on the northern, northeastern and northwestern flanks of the highest portion of the Roof Dome, inside the inferred arcuate fracture.

No andesite is exposed either on or around the base of the Roof Dome. As Healy (1967) said: "it represents an incipient volcano, the lava of which did not reach the surface". The age of the Roof Dome relative to the volcanic activity on Edgecumbe cannot be determined directly as the two are not in contact; it is however discussed further in the section on tephra stratigraphy and chronology.

TEPHRA STRATIGRAPHY AND CHRONOLOGY

The assistance of Mr C.G. Vucetich and Mr W.A. Pullar was invaluable in identifying and measuring the three distinctive ash layers recorded on Edgecumbe volcano. In order to determine the tephra stratigraphy flattish sites were carefully selected on the very rough surface of the block flows, and each site was dug out in the form of a narrow trench in order to measure the average thickness of each layer, and in order to avoid erosion breaks associated with the rough topography. Three ash layers, which are briefly described below,

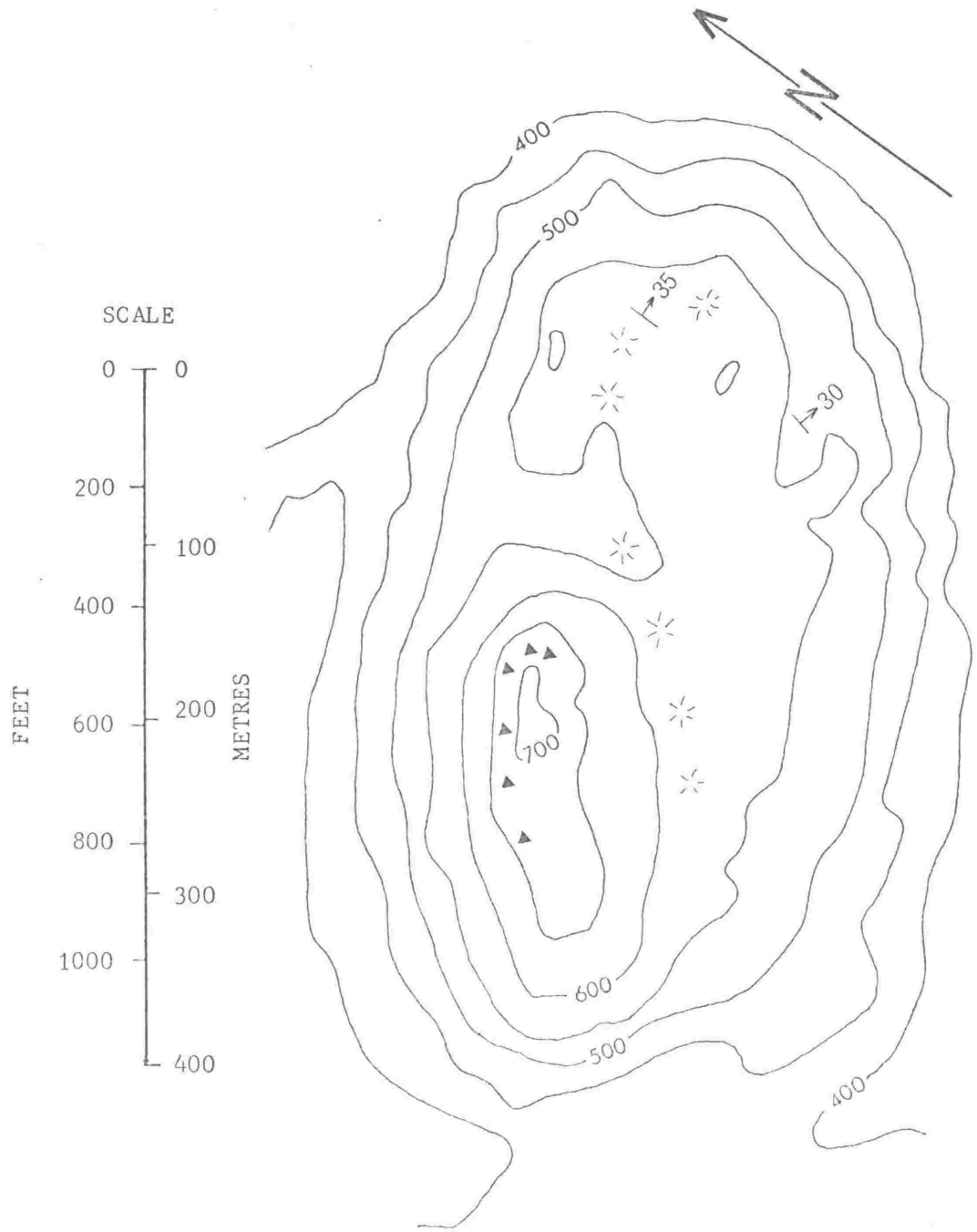

Fig. 4. - Map of ignimbrite Roof Dome. Contour interval is 100 ft. Symbols: ▲ denotes hydrothermal alteration area; collapse structure with pit at ground surface; ⊢→ 30, indicates dip of lenticular zones in ignimbrite.

were found at all the selected sites on the Western Flows, Main Dome and Main Cone; the thicknesses found at each site are given in Table 3.

(1) Tarawera Ash: dark-brown to black, glassy, fine lapilli, and near-white accessory rhyolite scavenged from the vent walls.

(2) Kaharoa Ash: capped by a very black paleosol contrasting with the underlying pale-brown to white, shower-bedded, dense fine ash.

(3) Taupo Lapilli: shower-bedded coarse ash at the base, overlain by a brown paleosol containing soft, highly vesicular pumice fragments.

Towards the top of Main Cone the colours and the weathering expression of the ash layers change due to higher rainfall. In particular the Taupo Lapilli is stained dark-brown and allophanic colloid extends throughout. However the coarse-ash basal layers of the Taupo Lapilli are still recognisable.

At site 6, on the summit of Main Cone, a well-weathered fine ash, about 5 cm thick, underlies the basal layer of the Taupo Lapilli. It is ill-defined and the form of the pumice and the accessory minerals are hard to determine. The ash is most unlikely to be the Whakatane Ash which is usually 100 cm thick in this area, and is tentatively correlated with the Waimihia Ash. At site 8 on the southern side of the Main Cone the basal fine ash layer is also present, and again about 5 cm thick. It overlies about 8-10 cm of andesitic lapilli and ash which is thought to represent ejecta from the explosion pits at vents 9 and 10. It is likely that nearer the explosion pits the ejected debris is coarser and harder to distinguish from the surface of the underlying flows.

TABLE 3

EDGECUMBE TEPHRA STRATIGRAPHY

Site	THICKNESS OF TEPHRA LAYERS IN CM. Tarawera Ash	Kaharoa Ash	Taupo Lapilli	Other
1. N77/160070	*	*	*	
2. N77/172073	*	*	*	
3. N77/171085	*	*	*	
4. N77/183078	25	43	3	
5. N77/184076	30	36	30	
6. N77/189073	33	43	33	5
7. N77/189068	33	71	38	?
8. N77/189064	33	56	25	15
9. Lahar Flow (mean of 7 sites)	36	37	16	

* indicates presence of particular tephra, but thickness uncertain.

Site Identification

1. Flow 1a.
2. Main Tholoid.
3. Northern Base Flows.
4. Flow Aa.
5. Main Cone, West Peak.
6. Flow 11a.
7. Flow Db.
8. Flow Dc.
9. Lahar Flow, grid references for sites as below: N77/: 203082, 202083, 201083, 205086, 206087, 207089, 207091.

The site chosen on the Roof Dome (grid ref: N77/197091) is over a part of the ignimbrite which is moderately welded, not on the unwelded upper part of the ignimbrite. Thus the tephra section measured postdates the formation of the dome, during which the updomed part of the ignimbrite was tilted to expose lower stratigraphic horizons within it. The following ash section was found:

Tarawera Ash	25 cm
Kaharoa Ash	36 cm
Taupo Lapilli	nil
Whakatane Ash	86 cm

A critical section in a road cutting 500 m southeast of the Roof Dome (grid ref: N77/200086) shows a boulder of Edgecumbe andesite resting on the paleosol capping the Rotoma Ash, and surrounded and covered by the Whakatane Ash.

The tephra cover on the lahar flow on the eastern side of Main Cone was studied at seven sites and the mean thickness of each ash layer given in Table 3. Tarawera Ash, Kaharoa Ash and the Taupo Lapilli are present at six out of the seven sites, but at the seventh the Kaharoa Ash is missing.

Chronological Conclusions

The minimum age of the lava flows on Edgecumbe and of the lahar flow from the Main Cone, at the sites examined, is 1700 years B.P., the age of the Taupo Lapilli. If the basal fine ash layer at sites 6 and 8 is the Waimihia Ash (as seems probable), then the minimum age for the flows underlying these two sites is 3200 years B.P., the age of the Waimihia Ash. The age of the uplift which formed the ignimbrite Roof

Dome is between 5000 years and 8000 years B.P. (Whakatane Ash: 5000 B.P.; Rotoma Ash: 8000 B.P.) The block of Edgecumbe andesite resting on the paleosol capping the Rotoma Ash has probably rolled downhill from the front of flow Cb, a distance of 60 m; indicating that there was effusive volcanism on the northeast flank of Main Cone between 5000 years and 8000 years B.P.

This conclusion differs from that reached by Healy, Schofield, & Thompson (1964) who found only the Tarawera and Kaharoa ashes on Edgecumbe, and thus inferred an age for the volcano of little more than 1000 years.

PETROGRAPHY

75 thin sections of samples from Edgecumbe volcano were studied and 50 representative samples were chosen for modal analyses. All the samples, apart from xenoliths, are porphyritic plagioclase andesites or plagioclase dacites. They all contain phenocrysts of zoned plagioclase (An_{70}-An_{30}), clinopyroxene (augite), orthopyroxene (hypersthene-bronzite), and opaque oxides (magnetite, titanomagnetite). The groundmass invariably contains small laths of plagioclase, and crystals of orthopyroxene, opaque oxides, apatite and rutile; in addition about half the samples have recognisable cristobalite in the groundmass. Biotite, quartz and hornblende are present as phenocrysts in 50%, 40% and 25% respectively of the samples.

Glomeroporphyritic aggregates of varying proportions of plagioclase, pyroxenes and opaque oxides occur in most samples. Most groundmass textures are pilotaxitic, but some are hyalopilitic, usually with the

glass partially devitrified. Two of the thin sections examined have amygdaloidal texture with cristobalite amygdales.

Sample locations for the 50 selected samples and their modal analyses and phenocryst proportions are given in Table 4. At least 1500 points were counted on each thin section. In order to evaluate the precision of a modal analysis and the degree to which it is representative, six modal analyses of the same thin section were made, followed by six modal analyses of different thin sections from the same sample and a further six modal analyses of one thin section from each of six samples from Main Dome. The results of this test are given in Table 5 in the form of the relative deviation for each mineral within one thin section, between thin sections and between samples. Table 5 shows that the relative deviation is much less for major constituents than for minor constituents, as would be expected. There is also a general tendency towards higher relative deviation for any mineral between thin sections than within a thin section, and a tendency towards higher relative deviation between samples than between thin sections. Thus a single sample can be considered mineralogically representative of the volcanic unit from which it was taken only as an approximation, and analysis of a number of samples from the same flow will greatly increase the precision of the mode, and the degree to which it is representative.

Comparative Petrography of Edgecumbe Volcanic Units

The following discussion of comparative petrography is based on the average analyses of samples from each unit, presented in Table 6. Where there was only one sample from a unit, and averages could not be taken, it is marked with an asterisk in Table 6 to indicate the lower reliability.

TABLE 4

LOCATIONS, MODAL ANALYSES AND PHENOCRYST PR(

LOCALITY	SAMPLE NO.	PETROGRAPHIC CLASSIFICATION	MODAL ANALYSIS					
			Groundmass	Plagioclase	Ortho-Pyroxene	Clino-Pyroxene	Quartz	Hornblende
Base Flows N	11205	Plagioclase Andesite (D)*	77.2	16.6	2.2	1.6	-	0.5
	11253	Plagioclase Andesite	69.9	22.9	3.2	2.3	-	-
	11365	Plagioclase Dacite	67.2	28.1	2.3	1.6	-	-
W	11366	Plagioclase Andesite	74.6	18.6	2.6	2.9	-	-
	11206	Plagioclase Andesite (A)*	69.3	25.9	2.9	0.8	-	-
S	11367	Plagioclase Dacite	55.9	30.7	6.8	3.1	1.3	1.0
	11368	Plagioclase Andesite	56.3	31.2	6.0	4.9	-	-
	11213	Plagioclase Andesite (D)	74.9	17.4	3.9	2.5	-	-
Western Flows 1.	11319	Plagioclase Andesite	72.4	23.8	1.9	1.2	-	-
	11320	Plagioclase Andesite	72.9	18.0	2.9	5.0	-	-
3.	11321	Plagioclase Andesite	77.2	16.0	2.4	1.4	-	-
	11322	Plagioclase Andesite	71.9	20.5	3.3	2.7	-	-
	11323	Plagioclase Andesite	76.5	16.9	3.6	1.7	-	-
	11324	Plagioclase Dacite	74.1	19.6	3.0	1.0	1.3	-
4.	11325	Plagioclase Andesite	73.0	20.7	2.0	2.9	-	-
Main Dome 5.	11210	Plagioclase Dacite (D)	56.7	25.0	0.5	1.8	8.5	1.0
	11211	Plagioclase Dacite (D)	61.5	26.7	6.6	1.6	1.1	0.1
	11326	Plagioclase Dacite	61.7	27.4	3.8	2.6	1.4	0.7
	11327	Plagioclase Dacite	65.0	24.6	4.8	0.7	3.0	0.8
	11328	Plagioclase Dacite	65.0	21.8	2.9	1.1	5.4	0.4
	11329	Plagioclase Dacite	61.3	19.1	3.0	6.3	6.9	1.3
	11212	Plagioclase Dacite (D)	61.5	27.6	4.2	2.6	2.5	0.1
Main Cone 6.	11252	Plagioclase Dacite	61.6	27.1	5.1	2.6	0.5	0.9
	11330	Plagioclase Andesite	60.0	27.1	7.2	4.0	-	-
	11331	Plagioclase Andesite	58.5	29.7	4.5	3.1	-	-
	11332	Plagioclase Dacite	51.8	41.0	3.6	2.4	0.3	-
8.	11333	Plagioclase Andesite	57.4	32.6	5.3	3.0	-	-
	11334	Plagioclase Dacite	66.2	20.8	5.2	1.8	2.0	0.1
11.	11214	Plagioclase Andesite (D)	65.6	25.0	3.8	4.5	-	-
	11335	Plagioclase Andesite	67.9	23.4	2.7	1.5	-	2.7
A.	11207	Plagioclase Andesite (D)	57.9	27.6	8.4	4.4	-	-
	11336	Plagioclase Andesite	61.9	28.1	4.3	4.0	-	-
	11337	Plagioclase Dacite	58.0	33.6	1.7	1.8	0.7	-
B.	11338	Plagioclase Dacite	63.8	27.8	1.4	4.4	1.0	-
	11339	Plagioclase Andesite	58.7	31.2	4.8	3.2	-	-
	11340	Plagioclase Dacite	55.9	29.2	7.4	3.4	1.8	-
	11216	Plagioclase Andesite (A)	54.1	31.6	5.9	6.9	-	-
C.	11341	Plagioclase Andesite	76.7	19.5	2.0	0.7	-	-
	11342	Plagioclase Andesite	77.3	16.1	3.2	2.2	-	-
D.	11343	Plagioclase Dacite	72.1	21.9	3.2	1.0	0.6	-
	11344	Plagioclase Dacite	63.7	25.7	3.2	2.3	2.3	-
	11345	Plagioclase Andesite	68.1	23.0	3.3	4.2	-	-
North Dome 7.	11346	Plagioclase Dacite	58.8	24.8	3.9	5.5	5.8	-
	11347	Plagioclase Andesite	65.4	28.6	4.0	0.6	-	-
	11348	Plagioclase Andesite	64.9	23.4	5.5	4.2	-	-
Lahar Flow	11349	Plagioclase Dacite	55.3	32.0	2.4	2.6	1.5	3.8
	11215	Plagioclase Dacite (D)	64.0	29.0	3.7	1.6	0.1	0.6
	11350	Plagioclase Andesite	63.6	28.8	3.5	2.1	-	0.3
	11217	Plagioclase Dacite (D)	60.8	31.2	2.4	1.4	1.6	0.7

Note: Most sections contain aggregates of pyroxene, opaques and plagioclase which are very probably pseudomorphs after biotite and hornblende. Where some of the biotite or hornblende remain the pseudomorph is counted as the primary mineral, where alteration is complete the pseudomorph is counted as the secondary minerals.

TABLE 5

PRECISION AND SAMPLE REPRODUCIBILITY OF POINT-COUNT ANALYSES

Mineral Constituents	Variation* in Section	Variation * between Sections	Variation * between Samples	Mean % of Mineral
Groundmass	3.4	5.0	5.0	62.3
Plagioclase	6.8	9.5	13.2	25.1
Orthopyroxene	30.0	20.3	55.7	4.2
Clinopyroxene	32.9	40.4	85.0	2.5
Quartz	20.0	47.1	61.7	2.3
Hornblende	130.0	87.1	83.3	0.5
Biotite	57.5	74.6	81.1	1.3
Opaques	72.0	38.2	65.3	1.8

* expressed as relative deviation: $\frac{\text{Standard Deviation} \times 100}{\text{Mean}}$

Note: 6 point-count analyses were made in order to determine the variation in each column, 1500 counts were made for each point-count analysis.

TABLE 6

AVERAGE MODAL ANALYSES OF EDGECUMBE VOLCANIC UNITS

LOCALITY		MODAL ANALYSIS								RATIOS	
		Groundmass	Plagioclase	Ortho-Pyroxene	Clino-Pyroxene	Quartz	Hornblende	Biotite	Opaques	$\frac{\text{Pyroxene}}{\text{Plagioclase}}$	$\frac{\text{Orthopyroxene}}{\text{Clinopyroxene}}$
Base Flows	N	71.4	22.5	2.6	1.8	-	0.2	0.1	1.4	0.20	1.40
	W	71.9	22.2	2.3	1.9	-	-	-	1.2	0.21	1.40
	S	62.5	26.4	5.6	3.5	0.4	0.3	-	1.3	0.35	1.58
Western Flows	1.	72.6	20.9	2.4	3.1	-	-	-	1.0	0.26	0.77
	3.	74.9	18.3	3.1	1.7	0.3	-	-	1.7	0.26	1.83
	4.*	73.0	20.7	2.0	2.9	-	-	0.2	1.2	0.24	0.69
Main Dome	5.	61.8	24.6	3.7	2.4	4.1	0.6	1.0	1.8	0.25	1.54
Main Cone	6.	58.0	31.2	5.1	3.0	0.2	0.2	0.7	1.6	0.27	1.69
	8.	61.7	26.6	5.3	2.4	1.0	0.1	1.2	1.7	0.29	2.22
	11.	66.7	24.1	3.3	3.0	-	1.4	0.1	1.4	0.26	1.08
	A.	59.2	23.8	4.8	3.4	0.2	-	0.1	2.5	0.28	1.39
	B.	58.0	30.0	4.9	4.5	0.7	-	-	1.9	0.31	1.05
	C.	77.0	17.8	2.6	1.5	-	-	-	1.1	0.23	1.76
	D.	68.1	23.5	3.2	2.5	1.0	-	0.6	1.1	0.24	1.32
North Dome	7.	63.1	25.6	4.5	3.4	1.9	-	0.1	1.4	0.31	1.36
Lahar Flow		60.8	30.3	3.0	1.9	0.8	1.4	0.5	1.3	0.17	1.61

* One sample only, not an average.

The northern and western Base Flows have almost identical proportions of groundmass, plagioclase and total pyroxene. Their orthopyroxene/clinopyroxene ratios are identical and the only difference between them is that a trace of hornblende and biotite is present in the northern Base Flows but not in the western Base Flows. The southern Base Flows differ from the northern and western Base Flows in having a considerably lower proportion of groundmass, more total pyroxene and a much higher pyroxene/plagioclase ratio; they also have a trace of quartz, which is not present in the other Base Flows.

The Western Flows are petrographically very similar to one another and are also very similar to the northern and western Base Flows. The main difference between different flow series in the Western Flows is the much higher orthopyroxene/clinopyroxene ratio in flow series 3 compared to that in flow series 1 and 4. Other differences between them are the presence of a trace of quartz in flow series 3 and a trace of biotite in flow series 4.

Main Dome is the most distinctive petrographic unit on Edgecumbe, having a low groundmass content, high quartz content and significant amounts of hornblende and biotite (particularly the latter). It is the only volcanic unit on Edgecumbe whose petrography is distinctive enough for it to be recognised solely on the basis of its modal analysis. A comparison with the flow from vent 4 is of interest since this vent is very close to vent 5, and flow 4a was probably erupted shortly after the extrusion of Main Dome from vent 5. Flow 4a has a very much higher groundmass content than Main Dome, lacks quartz and hornblende and has only a trace of biotite. Even considering the comparatively small range

of variation in the samples (Table 6), the differences between flow 4a and Main Dome obviously represent a significant difference in the petrography of lava erupted from the two nearly coincident vents in this area.

Table 6 shows that the petrography of flow series on Main Cone is extremely variable, with the minerals showing the most variation being quartz, hornblende and biotite. The orthopyroxene/clinopyroxene ratio for all flow series on Main Cone is greater than 1. Since the relative age of the flow series on Main Cone is not sufficiently well known, it is impossible to determine if there is systematic petrographic variation with age. Within flow series 6, however, there is a systematic decrease in the proportion of groundmass with decreasing age; from 61.6% groundmass in flow 6c, through 58.5% in flow 6b to 51.8% in flow 6a. Being based on modal analyses of single samples from each flow the validity of this trend is uncertain; but such a trend of increasing crystallinity with time would be expected in successive flows from one body of cooling magma. Flow series 6 also shows a similar systematic decrease in the orthopyroxene/clinopyroxene ratio.

North Dome is similar in modal composition to Main Dome but the quartz content is slightly lower and it lacks hornblende. The steep sides and general topographic forms of Main Dome and North Dome suggests that their magma was particularly viscous at the time of its extrusion. High quartz and low groundmass percentages suggest that they were more crystalline prior to extrusion than any of the other volcanic units.

The modal composition of the lahar flow, having significant proportions of quartz, hornblende and biotite, suggest that it is

largely composed of material from a tholoid or spine similar in composition to Main and North Domes. In the section on Edgecumbe geology it was concluded that a spine is likely to have formed part of the plug tholoid extruded from vent 11.

As a whole, there does not appear to be any systematic variation in modal composition with age for the Edgecumbe volcano, but there are suggestions of a cyclic variation of increasing crystallinity and quartz content, and decreasing orthopyroxene/clinopyroxene ratio with decreasing age in a flow sequence. The overall similarity of modal mineralogy on Edgecumbe, and the close similarity between some flows of different ages and from different vents (e.g. northern Base Flows and flow series 1) suggest a parental magma at depth whose composition has varied little during Edgecumbe's period of activity. The modal variations observed are considered to be due to processes within magma held at shallow depths beneath the volcano immediately prior to eruptions. The modal mineralogy of lava erupted from such a "magma chamber" would depend on the amount of magma in the "chamber" prior to a particular eruption, the rate of cooling and the load and vapour pressures on the magma.

WHALE ISLAND

Whale Island is the upper portion of the eroded remnants of a volcano lying 12 km north of the town of Whakatane, and 8 km off the coast in the Bay of Plenty. It has a central peak 347 m high, which is the southern portion of an eroded volcanic cone, and lower peaks to the east and west which are separated from the Central Cone by short valleys. The north coast of the island is precipitous with continuous cliffs between 20 and 300 m high. The geology of Whale Island was described by MacPherson (1944), who stated that "practically the whole island is occupied by andesitic rock, excepting minor areas of sinter, bedded rhyolite tuff, greywacke conglomerate, and dune sand." Healy (1967) described the northern cliffs as a comparatively recent fault scarp. Hutton in an appendix to MacPherson's (1944) paper described a thin section of a sample collected from the south coast of the island as an augite-hypersthene andesite very similar to Edgecumbe samples.

GEOLOGY

The geology of Whale Island is depicted on two single-factor maps with Fig. 5 an approximate contour map drawn by radial line plotting from air photographs with heights by parallax measurements; and Fig. 6 a map showing surface geology and inferred vent locations.

Central Cone rocks are well exposed on the island's precipitous northern face and are also exposed in low coastal cliffs on the south side of the island. MacPherson (1944) described layers of andesite lava, agglomerate, and breccia, with minor layers of rhyolitic tuff exposed in the north cliff section.

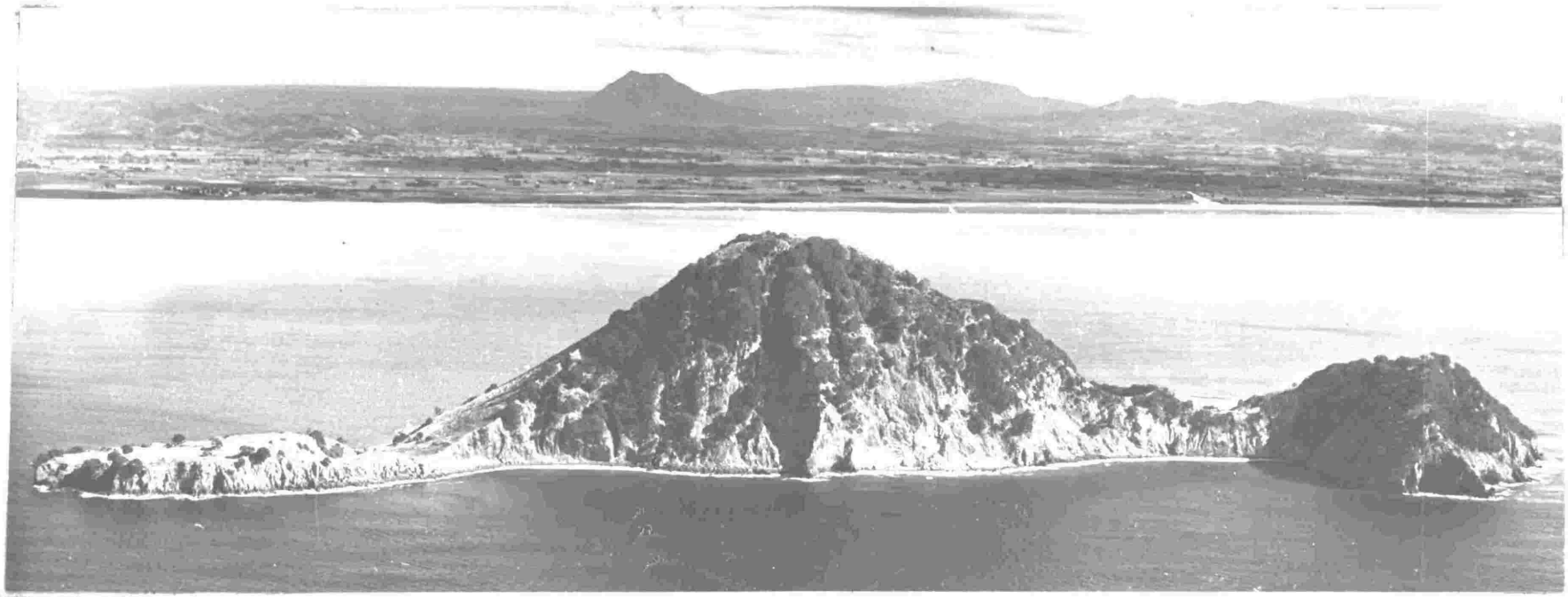

Plate 5. - Whale Island from the north, East Dome (left), Central Cone (centre), West Dome (right). Edgecumbe and Tarawera can be seen on the horizon behind.

Massive homogeneous andesite crops out at the base of Central Cone in the north cliff section and is thought to be part of a single tholoid or coulée, which has been named for convenience as the "Cone Tholoid". The Cone Tholoid is covered by an even layer, 1 m thick, of volcanic material thought to be of nuée ardente origin. The bulk of the material above the nuée ardente deposit is volcanic breccia, consisting of a poorly sorted mass of angular and sub-angular blocks of lava in a matrix of smaller boulders of lava and finer, mainly ash grade, volcanic material. The volcanic breccia has rudimentary bedding with the stratification nearly parallel to the present cone surface, it is not possible, however, to place boundaries on a particular bed. A second nuée ardente deposit, very similar in appearance and thickness to the lower one, occurs within the volcanic breccia about 70 m stratigraphically above the Cone Tholoid. It is conformable with the stratification in the volcanic breccia and has smooth upper and lower contacts. A massive and homogeneous dacite with near-vertical sides about 80 m high, crops out in the upper central portion of the north cliff section, and is surrounded on all visible sides by volcanic breccia. Where they are exposed the contacts between this dacite and the volcanic breccia are abrupt, and there is no evidence that the dacite intrudesthe breccia.

The nuée ardente deposits are poorly sorted material consisting of lapilli-size fragments of andesite and dacite in a pale-coloured matrix of dacitic composition. Thickness is constant along the outcrop (about 300 m) and the deposit lacks shower-bedding. The poor sorting and lack of bedding suggest that the source is local, but the

Plate 6. - North coast of Whale Island, view from East Dome across the eroded face of Central Cone to West Dome. The prominent rock buttress at sea-level on the Central Cone is part of the Cone Tholoid.

constant thickness indicates that the deposit is unlikely to be tephra from a local source (see p.138 for thickness measurements on recent White Island tephra eruptions). It is therefore considered that the deposits were formed by two small nuée ardente eruptions from a vent on the Central Cone.

The origin of the volcanic breccia referred to above (p.35) is problematical. If it is air-fall agglomerate, then it is reasonable to assume that eruptions which produced agglomerate on such a large scale, must also have produced large amounts of finer-grade tephra. However there are no deposits of andesitic or dacitic tephra interbedded with the volcanic breccia on Whale Island, nor are any such deposits found in a Lower Pleistocene-Recent section (Whale Island is probably late Pleistocene), described by Healy & Ewart (1965), in the mainland cliffs west of Matata, some 20 km from Whale Island. Hence the volcanic breccia is unlikely to be airfall agglomerate, although it was originally described as such by MacPherson (1944).

A second possiblity is that the volcanic breccia is composed of completely auto brecciated lava flows. The precise geometrical shape of the Central Cone implies that if it is composed almost entirely of auto-brecciated lava flows, then these flows must have been thin and evenly distributed. Search of the literature has failed to provide examples of a comparable succession of totally auto-brecciated thin dacitic lavas. If the volcanic breccia represents a flow succession then the massive dacite cropping out in the north cliff section (p.35) would be interpreted as a vent plug, and would be expected to show an intrusive contact with some of the basal flows,

however the contact zone observed in the outcrop is not of this type. The volcanic breccia is thus unlikely to have been formed by a succession of auto-brecciated lava flows.

The author's preferred hypothesis is that the massive dacite is the remnant of a large spine of lava, whose upper portions have collapsed during extrusion to form a conical fan of debris surrounding the spine. The spine continued to collapse or be broken down by erosion until it was no higher than the fan of debris surrounding it. The Central Cone half angle is 32°-38°, about the usual angle of rest for poorly sorted debris. The break in slope on the western flank of Central Cone is not interpreted as a parasitic vent, but as a secondary lava spine protruding slightly above the level of collapse debris. Stages in the growth of Central Cone, according to this interpretation, are shown diagramatically in Fig. 7.

The low lying part of the island east of Central Cone is one large flat-topped lava dome, here named "East Dome". The Dome is well exposed in 30 m high sea-cliffs on its northern side and is composed of massive, columnar-jointed lava. The western margin of East Dome is exposed in the north cliffs and along the eastern side of McEwans Valley, which runs down between the Dome and Central Cone to McEwans Bay on the south coast. In the north cliff exposures the western margin has a conspicuous pale grey coloured fine-grained border zone containing many near-spherical, dark grey xenoliths about 2-5 cm in diameter. This conspicuous border zone is not present on the side of McEwans Valley, about 250 m from the north coast, but in McEwans Valley the western margin has been extensively altered by hydrothermal activity.

Fig. 7. - (See next page). Interpretation of stages of growth of Central Cone, Whale Island, details of each stage are given below.

(1) Extrusion of Cone Tholoid.

(2) Start of extrusion of central spine, accompanied by a small nuée ardente eruption.

(3) Extrusion of central spine continues, accompanied by semi-continuous collapse of portions of the spine which results in a cone of volcanic breccia being built up around the base of the spine. Start of extrusion of western spine (probably more dome-shaped than central spine).

(4) Small nuée ardente eruption from eastern flank of the central spine, continued spine growth and collapse.

(5) Both central and western spines grow to their maximum height, probably accompanied by continuous spine collapse. After spines cease growing their height is reduced by erosion until their tops are level with the cones of collapse debris surrounding them.

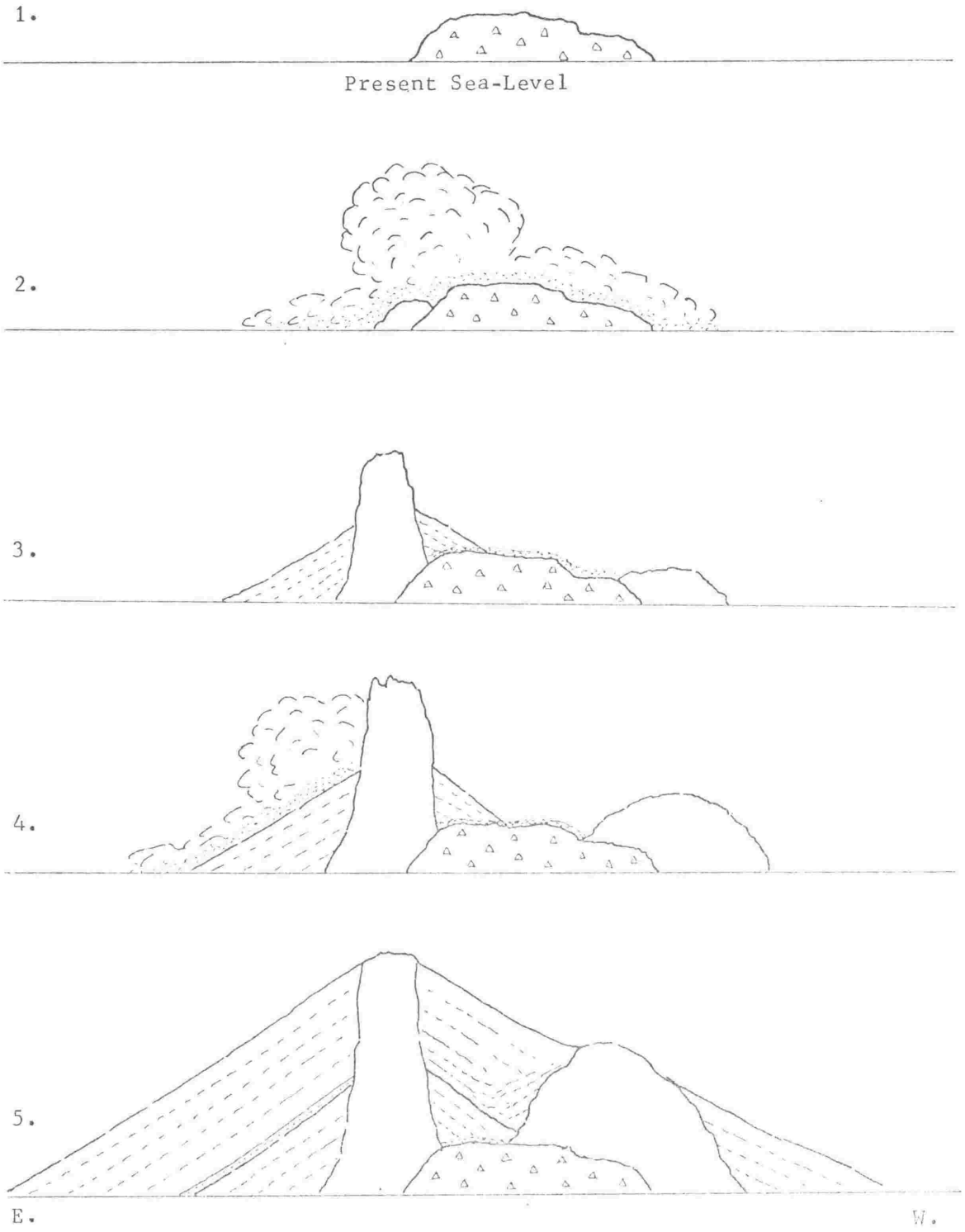

Fig. 7. - See previous page for captions.

At the north end of McEwans Valley are valley-floor deposits consisting of lenses of loess and dacitic tuff (some of it sub-aqueous), which overlie Central Cone volcanic breccia, and which have been tilted so that they now dip 40° towards the Cone. Tilting of these beds decreases rapidly away from the margin of East Dome and is therefore thought to be due to its extrusion. Hence East Dome is considered to be younger than Central Cone. Extrusion of the Dome caused eastward migration of the axis of maximum deposition in McEwans Valley and a lense of loess and rhyolitic tephra was deposited 30 m west of the tilted deposits, after the extrusion of the Dome.

The peak at the west end of the island is formed by a massive outcrop of lava with both columnar and onion-skin jointing shown in exposures around the coast. The northern half of this western portion of the island appears from ground, sea and aerial observations to consist of a single dome, here named "West Dome". The southern half of this western portion of the island is composed of pumiceous marine sandstones and siltstones, some of which are current bedded, and which at the southern end of the cliff exposure dip 10° south but which are overturned and dip 80° north at their contact with West Dome. A zone of reddish, baked, hydrothermally-altered siltstones forms a band about 5 m wide along the contact. Two stages in the up-doming have been recognised. After the first part of the up-doming a 5 m cliff was cut by the sea at the south end of the section, a lahar from West Dome then flowed over this cliff, forming a wedge of lahar debris on the seaward side. In the final stages of up-doming some of the uplifted sediments slumped southwards over the lahar debris, and were

then eroded to form another sea-cliff to the south of the previous one. A second lahar from West Dome then filled in another wedge of debris on the seaward side of the new cliff. Photographs of the western end of the island showing these features are given as Plates 7, 8, and 9, and a north-south cross-section is given as Fig. 8.

The pumiceous marine sandstones and siltstones are lithologically very similar to the fossiliferous Castlecliffian sediments described by Healy & Ewart (1965) in the section on the mainland coast between Matata and Otamarakau, 20 km from Whale Island. Castlecliffian sediments also occur on the Rurima Rocks, 8 km west of Whale Island.

The andesite and dacite forming the sides and floor of Sulphur Valley, the valley immediately to the west of Central Cone, has suffered extensive hydrothermal alteration and fairly thick deposits of siliceous sinter carpet the valley floor. Six small fumaroles are still discharging steam, and steam is emitted from the beach sands in Brimstone Bay at low tide, however only one small boiling pool remains. The total area of the sinter deposits is about 0.016 km^2; they form a dumb-bell shape with the two largest parts being approximately circular and 80-100 m in diameter. Between the two main areas of sinter deposition in the valley there are remnants of water-laid rhyolitic ash beds, which are probably tephra which has been washed off the Central Cone and deposited in a pool in the thermal area. From its appearance the re-deposited tephra is probably the Rotoma Ash dated at about 8,000 years B.P., and since the water-laid beds overlie thick deposits of sinter it would seem that the major part of the hydrothermal activity in Sulphur Valley took place prior to 8,000 years B.P.

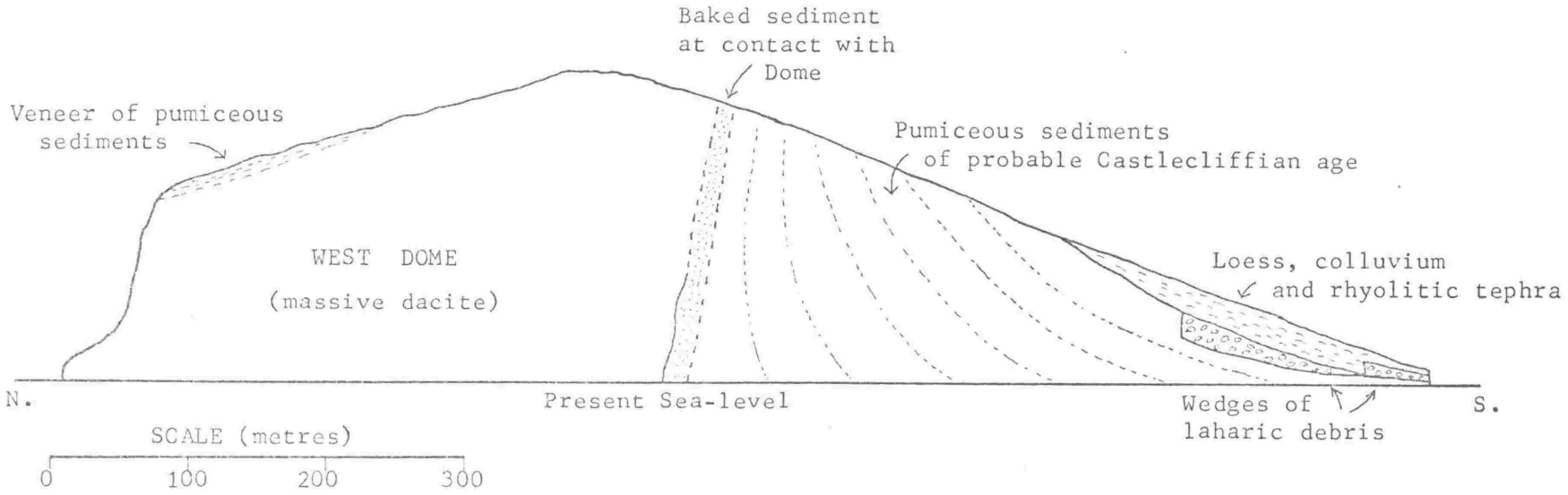

Fig. 8. - Diagramatic cross-section of the western portion of Whale Island. Pumiceous sediments of probable Castlecliffian age were updomed and locally overturned during the extrusion of the West Dome. Approximate dips in the pumiceous sediments are indicated by the dotted lines, structure has been simplified in this representation, as slumping and local contortion of beds is common.

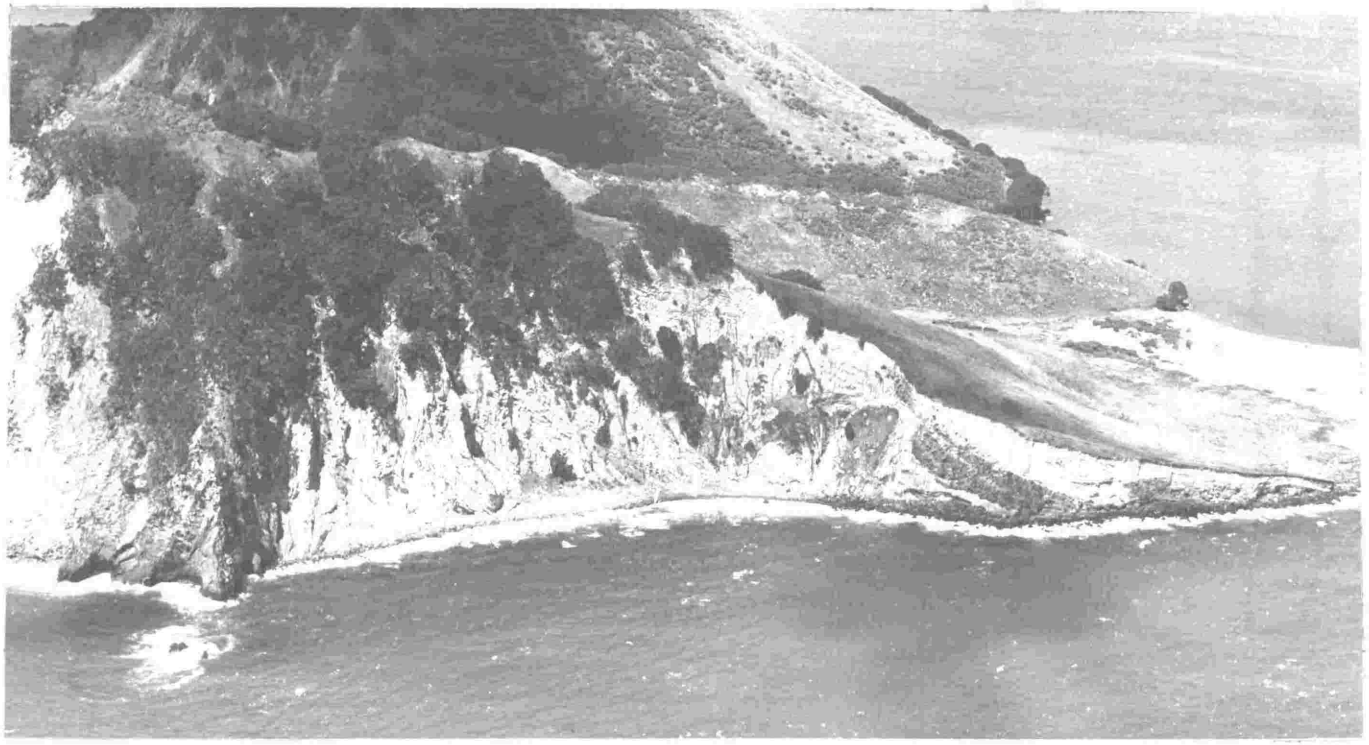

Plate 7. - Cliff section on west coast of West Dome. Pale coloured beds in centre are pumiceous sediments of probable Castlecliffian age. Contact with lava of West Dome just to the right of the Spur running down to the sea at the left of the photograph. cf. Fig. 8.

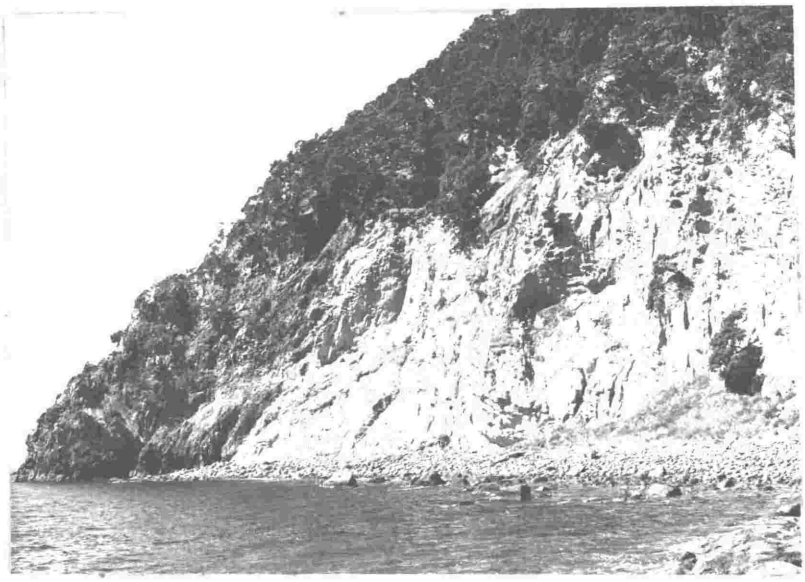

Plate 8. - Cliff section on west coast of West Dome. Pumiceous sediments in foreground, dacitic lava in background, with contact dipping about 80° away from viewpoint (sediments are locally overturned). Direction of view is approximately normal to strike of contact.

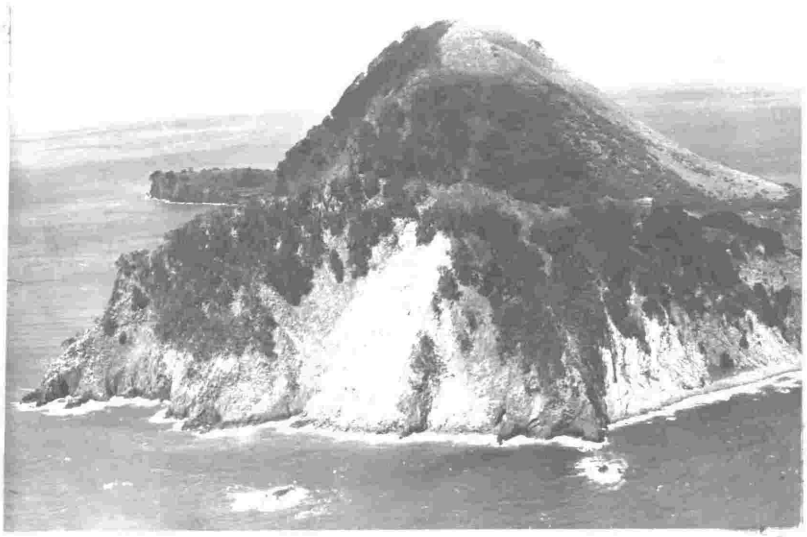

Plate 9. - West Dome with Central Cone and East Dome in background.

The western wall of Sulphur Valley is formed by a lava flow, Flow A, which flowed to the south from a vent on the western side of the Central Cone, which has now been eroded away. At the north cliffs Flow A is composed of about 10 m of massive lava, capped by about 3 m of blocky lava.

The degree of slumping has made it difficult to interpret cliff exposures on the north coast between Central Cone and West Dome. The lower part of the cliff section adjacent to West Dome apparently contains pumiceous sandstones and siltstones similar to those exposed in the west cliffs south of West Dome. The upper part of the section is composed of lahar debris from West Dome, covered by a few metres of loess and rhyolitic tephra. On the axis of Sulphur Valley, scree debris from Central Cone is inferred to be faulted against the pumiceous sediments, but the fault plane is obscured by slumps. A high-angle fault in this position was also postulated by MacPherson (1944), who related the hydrothermal activity in Sulphur Valley to the southward extension of such a fault zone.

Healy (1967) states that "the whole island has been faulted along the northern coast with the formation of steep cliffs which cut across the three elevated parts as well as the heads of the two valleys". A simpler explanation is that unconsolidated volcanic breccia on the north side of Central Cone has been eroded by the sea, exposing the more resistant Cone Tholoid and central spine and steepening the cone angle on the north face from 30° to 70°. West Dome being composed of massive lava and hence being more resistant to marine erosion extends further seaward than the remnants of Central Cone. Sea cliffs 80 m high on the south side of Central Cone show the

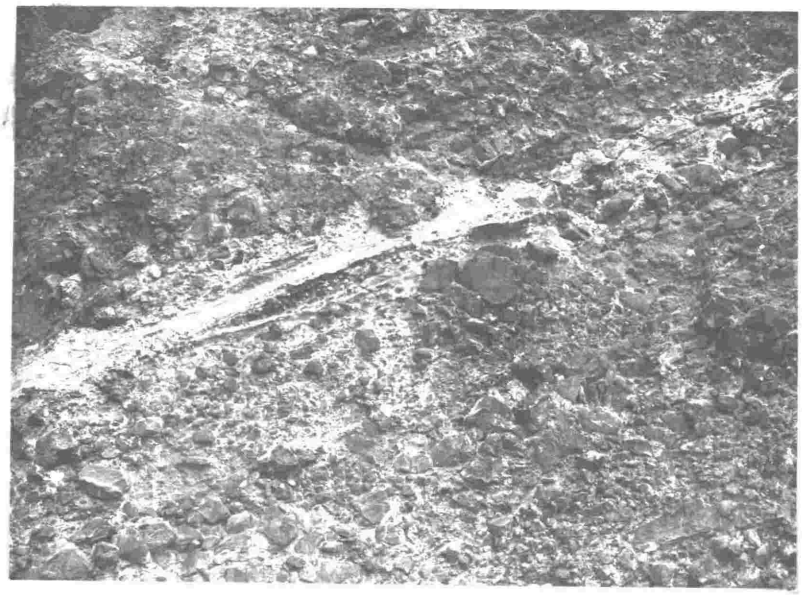

Plate 10. - Bedded volcanic breccia on North cliff section through Central Cone. Pale coloured band (about 1 m thick) is a probable nuée ardente deposit.

Plate 11. - Whale Island from the east with East Dome in foreground and Central Cone in background. Note cliffing and erosion on northern side.

amount of erosion relative to present sea level achieved in an area where the sea waves had a fetch of only 8 km. The amount of erosion that has occurred on the north side of Central Cone in the same time is therefore quite reasonable in view of its much greater exposure to seas and swell, as it faces the open ocean. Healy also comments on what he considers the lack of an appreciable wave-cut platform on the north side of the island. However, the present author considers that there is insufficient bathymetric data to decide whether or not the size of the wave-cut platform is comparable with the base area of the eroded portion of the island.

East Dome consists of massive lava and is thought to have been only slightly eroded to form the cliffs on its north and east sides. West Dome is also thought to be close to its original size; but it is very likely that the Dome would have been mantled on its western and northern sides by up-domed sediments, similar to those preserved on its eastern and southern sides. Any such mantling sediments have been almost completely eroded away from the northern and western sides of the Dome, with just a few remnants preserved about 180 m above sea level on its northern flank.

TEPHRA STRATIGRAPHY AND CHRONOLOGY

In order to determine the tephra stratigraphy, sections through air-fall cover beds on the north and west cliffs of the island were carefully examined, and a number of pits were dug to provide inland sections on East and West Domes and Central Cone. Tephra layers were identified by Mr C.G. Vucetich.

Air-fall cover beds in all sections include a significant proportion of loess and dune sand. The loess beds have strong cohesion and a

"massive" appearance when weathered. Buried dune sands, on the other hand, tend to be incohesive and are friable when weathered. An initial proportion of fine-grained material in the loess has been converted to colloids by soil processes, and apart from this colloid there is no clear difference in the grain-size of the material comprising loess and dune sands.

The most complete section of air-fall cover beds on Whale Island is a lensoid deposit in the cliff face at the truncated north end of McEwans Valley. The base of the section is stratified volcanic breccia from Central Cone, overlain by a bed of yellow-brown clay containing abundant chips of andesite and dacite. The overlying part of the section consists of six rhyolitic tephra layers, interbedded with loess and buried dune sands. The tephra layers are correlated, in order of decreasing age, with the Rotoehu Ash, Waiohau Ash, Rotoma Ash, Taupo Lapilli, Kaharoa Ash and Tarawera Ash (Fig. 9 is a stratigraphic column for this section). Since the cover beds were deposited after the westward displacement of the valley axis during the extrusion of East Dome, they are clearly younger than both Central Cone and East Dome; which thus have a minimum age of 36,000 years B.P., the age of the Rotoehu Ash.

Sections in pits dug on East Dome and the southern side of Central Cone are incomplete. In most of the pit sections no volcanic ashes could be recognised, only variable thicknesses of loess being present. The oldest ash found in any of the pit sections is the Rotoma Ash, dated at 8,000 years B.P.

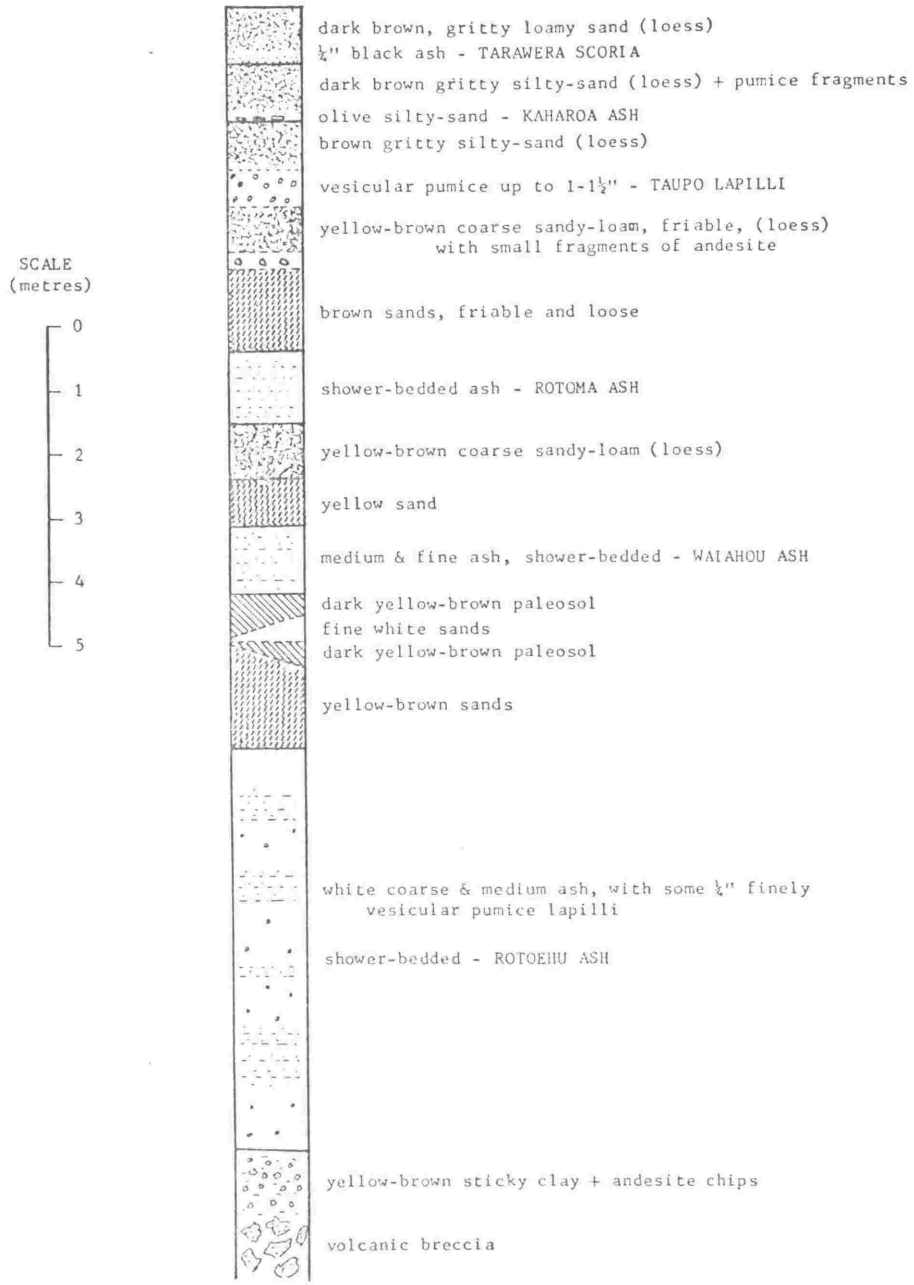

Fig. 9. - Section through airfall cover-beds at the north end of McEwans Valley, Whale Island.

The Rotoma Ash is also the oldest ash recognised in cover beds overlying lahars from West Dome in a cliff section at the southwest corner of the island. Thus the minimum age of the West Dome is 8,000 years B.P., but as the section is very possibly incomplete the Dome may be much older.

PETROGRAPHY

Fifty thin sections of samples from Whale Island lavas were studied and 25 representative sections were chosen for modal analysis (Table 7). All non-xenolithic samples except one are porphyritic plagioclase dacites or plagioclase andesites; the exception being a single plagioclase-pyroxene dacite from the Central Cone. All non-xenolithic samples contain phenocrysts of intermediate-calcic plagioclase, augite, hypersthene-bronzite and titanomagnetite. Quartz, hornblende and biotite are present as phenocrysts in 70%, 50% and 40% respectively of the samples. Groundmass constituents are plagioclase, orthopyroxene, titanomagnetite, apatite, rutile and cristobalite. Groundmass textures are pilotaxitic or hyalopilitic and in some cases there is marked flow alignment of plagioclase laths in the groundmass.

The lavas of Whale Island contain a large number of xenoliths, which are particularly well exposed in the abraded and rounded lava beach boulders found around the coast of the island. In the beach boulders xenoliths crop out at an average of one xenolith for every square metre of lava surface exposed. On weathered surfaces of lava still in place, such as in the cliffs on the sides of West Dome, xenoliths are not easily recognised since the surface weathering

TABLE 7

LOCATIONS, MODAL ANALYSES AND PHENOCRYST PROPORTIO

LOCALITY	SAMPLE NO.	PETROGRAPHIC CLASSIFICATION	MODAL ANALYSIS						
			Groundmass	Plagioclase	Ortho-Pyroxene	Clino-Pyroxene	Quartz	Hornblende	Biot
Central Cone	11225	Plagioclase Dacite (D)*	68.3	20.7	6.6	1.6	1.9	-	-
	11227	Plagioclase Dacite (D)	65.0	24.8	4.8	2.1	1.6	0.1	-
	11351	Plagioclase Dacite	58.6	32.6	4.4	1.3	0.1	0.1	-
	11233	Plagioclase Dacite	71.6	19.5	4.4	3.3	0.7	-	-
	11234	Plagioclase Andesite(D)	67.1	23.0	5.0	2.9	-	-	-
	11235	Plagioclase Dacite (D)	61.2	26.8	4.6	2.0	2.4	1.4	0.
	11236	Plagioclase Dacite (D)	64.6	22.7	5.7	2.3	3.4	0.3	0.
	11237	Plagioclase Dacite (D)	64.9	21.0	6.4	1.7	4.4	0.5	-
	11238	Plagioclase Dacite (D)	63.3	25.3	4.7	1.8	3.7	0.6	0.
	11239	Plagioclase Dacite (D)	64.9	24.6	4.7	3.0	1.2	0.5	-
	11352	Plagioclase Dacite	70.0	19.9	4.3	2.9	1.9	0.1	-
	11353	Plagioclase Dacite	67.8	24.1	3.4	2.6	1.1	-	0.
	11354	Plagioclase-Pyroxene Dacite	67.0	16.2	5.4	4.1	1.8	-	-
East Dome	11224	Plagioclase Andesite(D)	67.5	25.8	2.0	3.9	-	-	0.
	11355	Plagioclase Andesite	70.5	20.0	5.3	2.7	-	-	0.
	11356	Plagioclase Andesite	77.4	16.5	4.1	0.8	-	-	-
	11357	Plagioclase Andesite	79.6	12.6	3.9	2.0	-	-	0.
	11231	Plagioclase Andesite(D)	76.9	19.0	2.5	0.7	-	-	0.
West Dome	11218	Plagioclase Dacite (D)	51.5	34.2	3.3	2.3	7.8	0.2	-
	11220	Plagioclase Dacite (D)	64.0	24.6	3.7	3.3	3.1	0.5	0.
	11221	Plagioclase Dacite (D)	58.2	26.7	4.8	4.0	4.6	1.1	-
	11358	Plagioclase Dacite	72.3	17.3	3.2	4.8	1.3	-	-
	11359	Plagioclase Dacite	68.5	19.3	4.0	1.3	1.9	4.0	-
Flow A	11360	Plagioclase Dacite	68.6	24.6	2.2	3.2	0.6	0.1	0.
	11361	Plagioclase Andesite	68.5	21.5	3.1	3.8	-	-	-

Note: Most sections contain aggregates of pyroxene, opaques and plagioclase which are very probably pseudomorphs after biotite and hornblende. Where some of the biotite or hornblende remain the pseudomorph is counted as the primary mineral, where alteration is complete the pseudomorph is counted as the secondary minerals.

obscures the differences in colour and texture between the xenoliths and the host lava. It is unlikely that the lavas of Whale Island are any more xenolithic than those of Edgecumbe, as the proportion of random samples containg xenoliths is about the same for each volcano. The majority of the xenoliths are andesites, and pyroxene and pyroxene-hornblende microdiorites, whose petrography and petrogenesis are discussed in a later section.

Comparative Petrography of Whale Island Volcanic Units

All except one of the 13 modally analysed samples from Central Cone contain quartz, but the presence of hornblende and biotite is more variable, with a general tendency for samples with high quartz contents to contain more hornblende and biotite. The Cone Tholoid at the base of Central Cone has the lowest phenocryst content of any Central Cone sample, but is not notably different in any other respect. The major variation between samples from different localities on Central Cone is in their plagioclase and pyroxene contents. A set of samples from the stratified volcanic breccia exposed on the north face of Central Cone shows an inverse relationship between the plagioclase and total pyroxene contents. There is no systematic presence or absence of quartz, hornblende and biotite within any particular area of the Central Cone; this is considered to be due to the inherent inaccuracies of the sampling technique and point-counting when applied to minor constituents, as discussed on p.26, and as shown in Table 5. The modal mineralogy of the central spine (sample 11353) and the volcanic breccia (samples 11234-11239) are very similar and quite consistent with the volcanic breccia having formed by

collapse of the upper part of the spine. The relatively high pyroxene content of the plagioclase-pyroxene dacite sampled on the southwest flanks of the Central Cone may be due to derivation from the western spine rather than the central spine. However, surface samples from the western spine are too altered by weathering for modal analysis. Flow A is very similar to the Central Cone but has less quartz and a distinctly lower orthopyroxene/clinopyroxene ratio.

The mineralogy of the altered lavas and scree deposits on the flanks of Sulphur Valley was determined optically and by x-ray diffraction. The end-product of this hydrothermal alteration consists almost entirely of silica minerals; being mainly opaline silica and cristobalite with lesser amounts of quartz. In some samples a trace of plagioclase still remains but ferromagnesian minerals are apparently altered and leached at an early stage in this alteration of the rock. Secondary minerals not found in any of the samples include clays, mica, felspar and zeolites.

None of the East Dome samples contain quartz or hornblende, and this clearly separates rocks of this unit from rocks of the other volcanic units on the island. Comparison of the average modal analyses of the units given in Table 8 also shows that the East Dome is distinctly lower in phenocryst content than any other unit. There is thus evidence from the modal analyses for considering the East Dome to be the product of a different magmatic event from that which produced the rest of the island. Additional chemical, mineralogical and xenolithic evidence is discussed in later sections.

TABLE 8

AVERAGE MODAL ANALYSES OF WHALE ISLAND VOLCANIC UNITS

	MODAL ANALYSIS								RATIOS	
LOCALITY	Groundmass	Plagioclase	Ortho-Pyroxene	Clino-Pyroxene	Quartz	Hornblende	Biotite	Opaques	$\frac{\text{Pyroxene}}{\text{Plagioclase}}$	$\frac{\text{Orthopyroxene}}{\text{Clinopyroxene}}$
Central Cone	65.6	23.2	5.0	2.5	1.9	0.3	0.1	1.4	0.32	2.00
East Dome	74.4	18.8	3.6	2.0	-	-	0.4	0.8	0.29	1.81
West Dome	62.9	24.4	3.8	3.1	3.7	1.2	0.1	0.8	0.28	1.21
Flow A	68.4	23.0	2.7	3.5	0.3	0.1	0.2	1.8	0.27	0.77

West Dome samples have the highest average quartz and hornblende content of any unit, but are otherwise very similar to Central Cone rocks. Modal analyses of samples from West Dome show much more variation in their groundmass and plagioclase contents than samples from any other units. This variation, since it applies to major constituents, is considered to be real and not merely a result of sampling and point-counting technique. Such a variation could be due either to the extrusion of magma whose phenocryst distribution was inhomogeneous or to successive extrusion of magma pulses from a body of magma whose phenocryst content was changing with time. As the efficiency of magma movement and extrusion as a homogenising process is not known, it is not possible to decide between these two alternatives. Jointing patterns vary in different parts of the West Dome but there are no clearly identifiable individual cooling units.

In general, the variation in modal analyses between samples from the same volcanic units is comparable to that in volcanic units on Edgecumbe. The variations between West Dome rocks are comparable to variations between the units comprising the Main Cone of Edgecumbe.

The only volcanic unit on Whale Island within which stratigraphic sequence can be established is the Central Cone. However, although the volcanic breccia which forms the bulk of the exposed part of the cone is bedded, it is not possible to tell if the order in which the beds were deposited corresponds to the order in which the lava was extruded from the vent to form the central spine. It is thus impossible to determine the successive variations in modal mineralogy during a single extrusive phase on Whale Island. If one considers the Central Cone

and the West Dome to have been formed from the same high-level magma body, as seems very possible from their petrographic similarity, then a discontinuous sequence is established which can be placed in order of age from the field evidence. Considering the sequence from the tholoid at the base of the Central Cone, to the Central Cone breccias and then to the West Dome there is a trend of increasing quartz and hornblende content and decreasing groundmass and total pyroxene content with decreasing age. This compositional trend is the same as that inferred from modal analyses of Edgecumbe samples. At Edgecumbe this trend was apparently cyclic; and this may also be the case at Whale Island. Extrusion of the East Dome may represent the start of a second cycle.

WHITE ISLAND VOLCANIC COMPLEX

White Island is an active volcano in the Bay of Plenty, about 48 km northeast of Whakatane. It lies immediately to the west of the White Island Trench (Fleming, 1952) and is part of a large volcanic edifice, here named the White Island Massif, whose other parts above sea-level are the Volckner and Club Rocks. A number of dacitic and andesitic seamounts described by Pantin (in prep.) and Duncan (in press) lie between 6 and 44 km from White Island, and are mainly to the west and northwest of the island. The seamounts together with the White Island Massif comprise the "White Island Volcanic Complex", the geology and petrography of which is described below.

WHITE ISLAND

White Island (Fig. 10) is approximately 2.4 km from east to west and 2.0 km from north to south, its highest point, Mt Gisborne, being 321 m above sea-level. The White Island Massif extends down to between the 300 and 400 m isobaths, but only half of its height and a very small portion of its volume are above sea-level. Two groups of seamounts to the northwest of the island have comparable volume to the White Island Massif and one of these, the Mahina seamount (Pantin, in prep.), has a form similar to that of White Island, being a breached cone with crater walls 200-300 m high. The approximate volume of volcanic rocks in the White Island Volcanic Complex is estimated to be 78 km^3, compared with a volume of 800 km^3 (Clark, per. comm.) for the andesitic volcanoes of Tongariro National Park.

White Island has been in a state of continuous solfataric eruption, with intermittent ash eruptions, ever since 1826, when it was first

examined by Europeans. A comprehensive review of the literature concerning the volcanic and economic history of the White Island crater from 1826-1940 was given by Luke (1959). Since the 1920's the island has been studied at intervals by scientists from the N.Z. D.S.I.R., in particular those from the Geological Survey and Chemistry Division. D.S.I.R. Bulletin 127 (1959) summarised much of this work with papers on the general physiography and geology (Hamilton & Baumgart); physical and chemical investigations 1939-1955 (Wilson); soils (Baumgart, Stout, Johnston & Vernon); vegetation (Hamilton); and birds (Wodzicki & Robertson). More recent papers on the geology and volcanology of the island are those by Thompson (1965), Healy (1967) and Black (1970). Tephra eruptions between 1966 and 1969, together with related inflation and deflation of the ground surface in the crater, have been described by Clark (in press) and Duncan & Vucetich (in press).

Geological mapping and investigations of White Island have been made by Mr J. Healy (N.Z.G.S.) and the results are in preparation for publication. Consequently the present author has largely confined his investigations to the crater, and to a reconnaissance petrographic and geochemical investigation of that portion of the island east of Mt Gisborne. The details of White Island petrography and geochemistry described by Black (1970) are largely complementary to the present investigation, since Black's work was mainly concerned with the area north and west of Mt Gisborne.

Geology of White Island

White Island was described by Hamilton and Baumgart (1959) and Thompson (1965) as consisting of three overlapping, and partly eroded, cones of different ages. The first cone, the oldest, forms the western

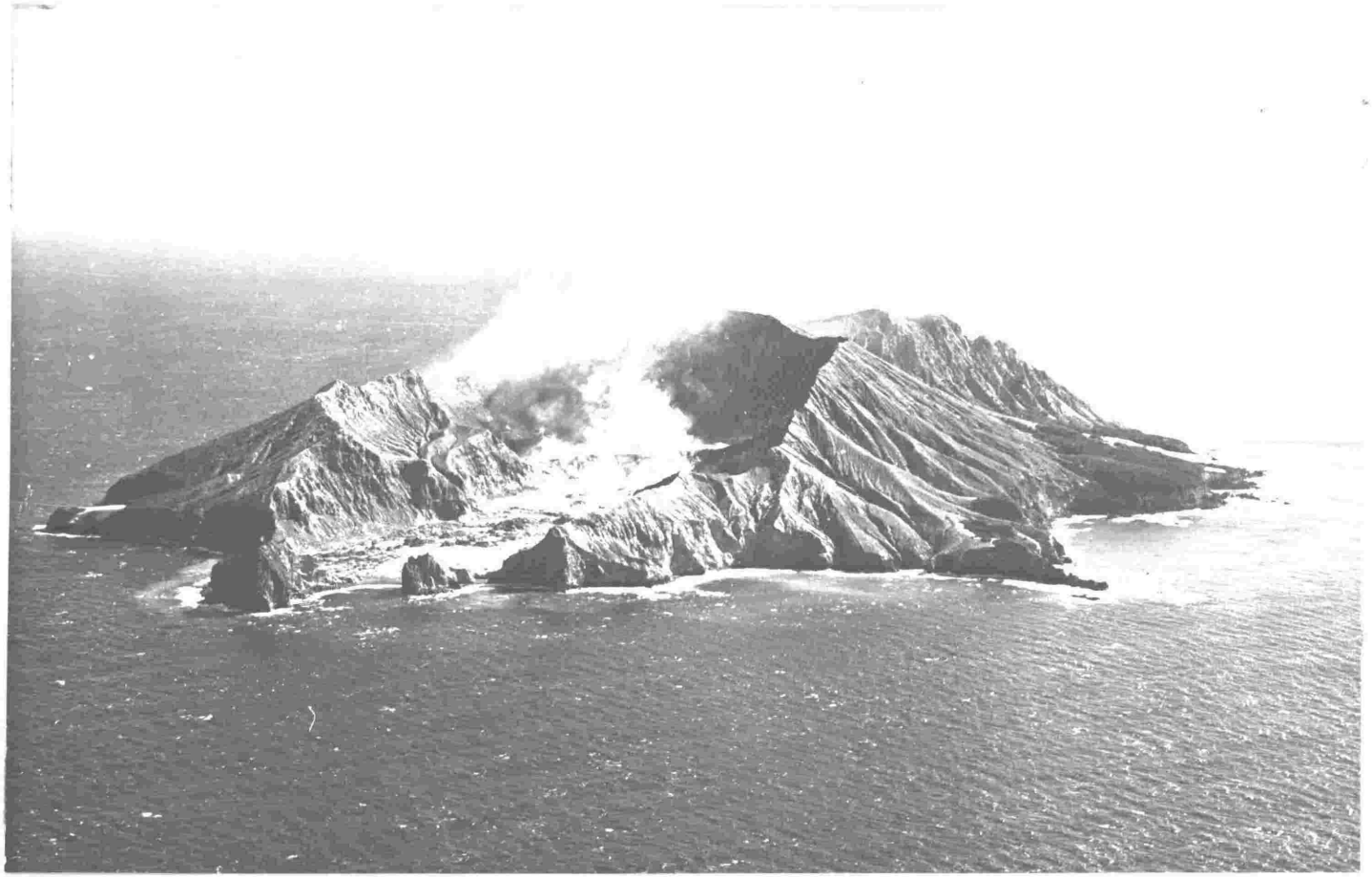

Plate 12. - White Island (viewed from the east).

portion of the island in the Mt Ngatoro-Te Matawiwi area (Fig. 10), and was thought by Hamilton and Baumgart (1959) and Thompson (1965) to include Volckner Rocks and Club Rocks. The second cone was considered by these authors to include Troup Head and Pinnacle Head. The third cone consists of the central portion of the present island and it has surmounted both the older cones.

The attitude of lavas and agglomerates forming the western portion of White Island indicate a sea-level diameter of less than 4 km for the cone of which Mt Ngatoro is part. The present author therefore considers it unlikely that the Volckner Rocks (lying 5.5 km northwest of the western end of White Island) were part of the first cone. The bathymetry (Duncan, in press; Fig. 1) indicates that Volckner Rocks are the remnants of a separate volcano whose summit was probably 100-200 m above present sea-level. A submarine ridge that links Volckner Rocks with White Island was probably formed by eruptions from a number of vents.

Healy (1967) considers that the centre of the top of the oldest cone would have been situated on the northeast part of the present island, possibly near North Bench. However, because the lava flows in the cliffs on the northwest side of the island dip 30° at 20°, it is more likely that the centre of the oldest cone was to the northwest, and probably no more than 500 m from Mt Ngatoro.

Club Rocks, considered by Hamilton and Baumgart (1959) to be part of the first cone, are more likely to mark the site of a parasitic vent south of the cones comprising White Island, and their age relative to any part of White Island cannot be easily inferred.

The youngest cone forms the eastern and central portions of the island. Its crater is divided into two sections by a spur at the eastern end of South Crater Bench and by a spur on the north crater wall. The crater therefore appears to be two coalescent craters which are named for convenience as the east and west sub-craters. The once-continuous eastern crater wall is now breached at three points on the coast, at Crater, Wilson, and Shark Bays.

Lavas at the base of Troup Head on the eastern side of Crater Bay closely resemble lavas at the base of the crater wall on the western side of Crater Bay and pale-coloured, poorly-sorted pyroclastics on Troup Head are identical with those in the crater wall below South Crater Bench. In view of these correlations between Troup Head and Central Cone sequences, suggestions by previous authors' (Baumgart & Hamilton, 1959; Thompson, 1965; and Healy, 1967) that Troup Head and Pinnacle Head are remnants of an earlier cone seem unlikely. However, a massive andesite (probably a tholoid or coulée) at the base of Troup Head was probably extruded from a parasitic vent on the east flank of the Central Cone.

The present author therefore concludes that White Island consists of two, and not three cones as has previously been suggested. The eroded older cone, forming the western portion of the island, is surmounted by the younger Central Cone which forms the bulk of the present island. Club Rocks mark the site of a parasitic vent, but their age relative to the two cones is unknown. A second parasitic vent, on the east flank of the Central Cone, is indicated by the

massive andesite at the base of Troup Head. Volckner Rocks are considered to be the remnants of a separate volcano lying to the northwest of White Island.

Both cones are composed of lava flows, agglomerates, volcanic breccias (including lahars), pyroclastics, and dykes. Black (1970) has also reported an ignimbritic flow on the northeast flank of the Central Cone. There are numerous examples of eroded gullies which have been filled with volcanic material and subsequently re-eroded, indicating that the volcano has had a complex geological history with alternating periods of activity and quiescence.

Development of the White Island Crater

Hamilton and Baumgart (1959) suggested that the present White Island crater was produced by collapse of parts of their second and third cones. However, there appears to be little evidence to support this view and it is considered more likely that the crater was explosively excavated.

The stages of formation of the crater can be inferred from the pyroclastics exposed in the upper parts of the crater wall sections. The section near the present crater rim above South Crater Bench consists of three pyroclastic units. The lowest unit, A, consists of 30-40 m of ill-defined beds, approximately 1-2 m thick, composed predominantly of andesitic blocks in a reddish brown matrix.
The middle unit, B, consists of 20 m of andesitic blocks (considerably smaller than those in unit A) and lapilli set in a bedded matrix of cream-coloured andesitic ash which contains appreciable gypsum and sulphur. Unit B differs from unit A in its colour, overall finer grain size, comparative scarcity of blocks, and generally thinner

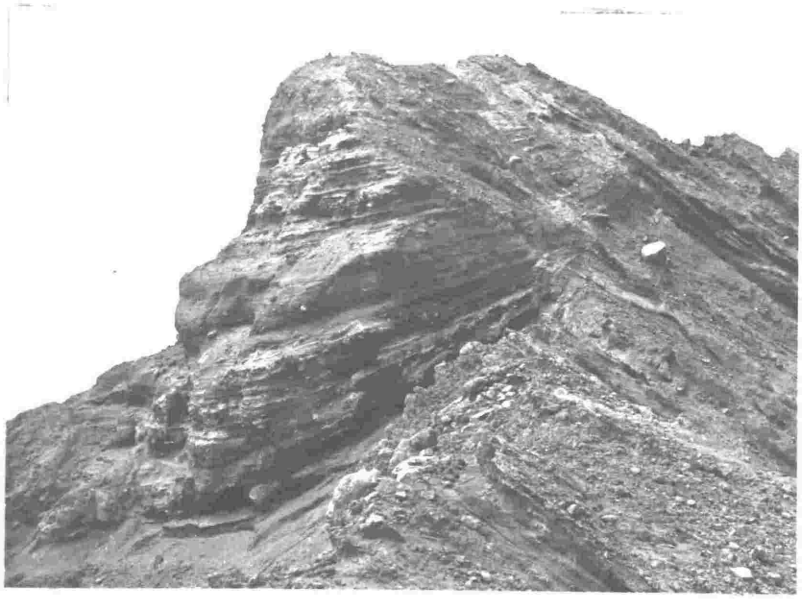

Plate 13. - Pyroclastic unit B on Troup Head, White Island.

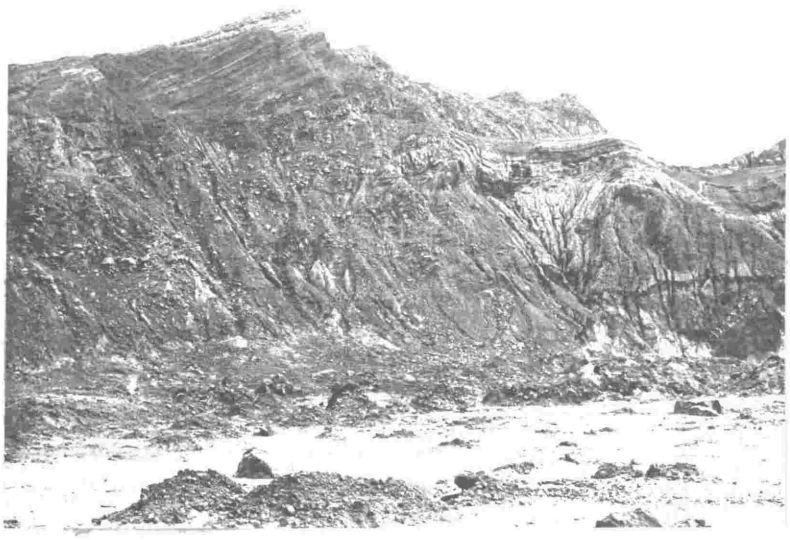

Plate 14. - Pyroclastic Units A and B exposed in the walls of the crater, and on the flanks of South Crater Bench.

beds (1cm - 1 m) with more clearly defined bedding planes. Units A and B are overlain by 1-3 m of pyroclastics, unit C, consisting of bedded sandy ash and lapilli capped by the finer ashes produced by historic eruptions.

Unit A occurs in many places on the outer slopes of the island and is exposed in cliffs on the northern and southern shores, with its greatest thickness on the southern side of the island. Unit B has been largely eroded off the outer slopes of the cone but is preserved in coastal sections, particularly near Ohauora Point and on North Bench. Unit A and unit B are not found on the present crater floor, nor were they observed in pits dug into the Crater floor.

Pyroclastic units A and B represent the most recent major eruptions on White Island, and are therefore thought to be the pyroclastic deposits that record the formation of the present crater. It has been suggested above that the crater actually consists of two coalescing "sub-craters"; unit A is considered to have been erupted during the formation of one sub crater, and unit B during the formation of the other. It remains to determine which unit came from which sub-crater.

Critical sections are exposed on the north and west sides of Troup Head (Plates 15 and 16), and they are interpreted in a cross-section (Fig. 11). The base of the north face section is a massive andesite tholoid or coulée, capped by 1 m of pale-coloured, bedded, andesitic ash. Above the ash layer there are a few lava flows, some of which are massive and others are brecciated. There is a near vertical andesitic dyke at the western end of the section, the western side of which is considered to be the original margin of the east sub-crater. The deposits in the west face section are thus interpreted

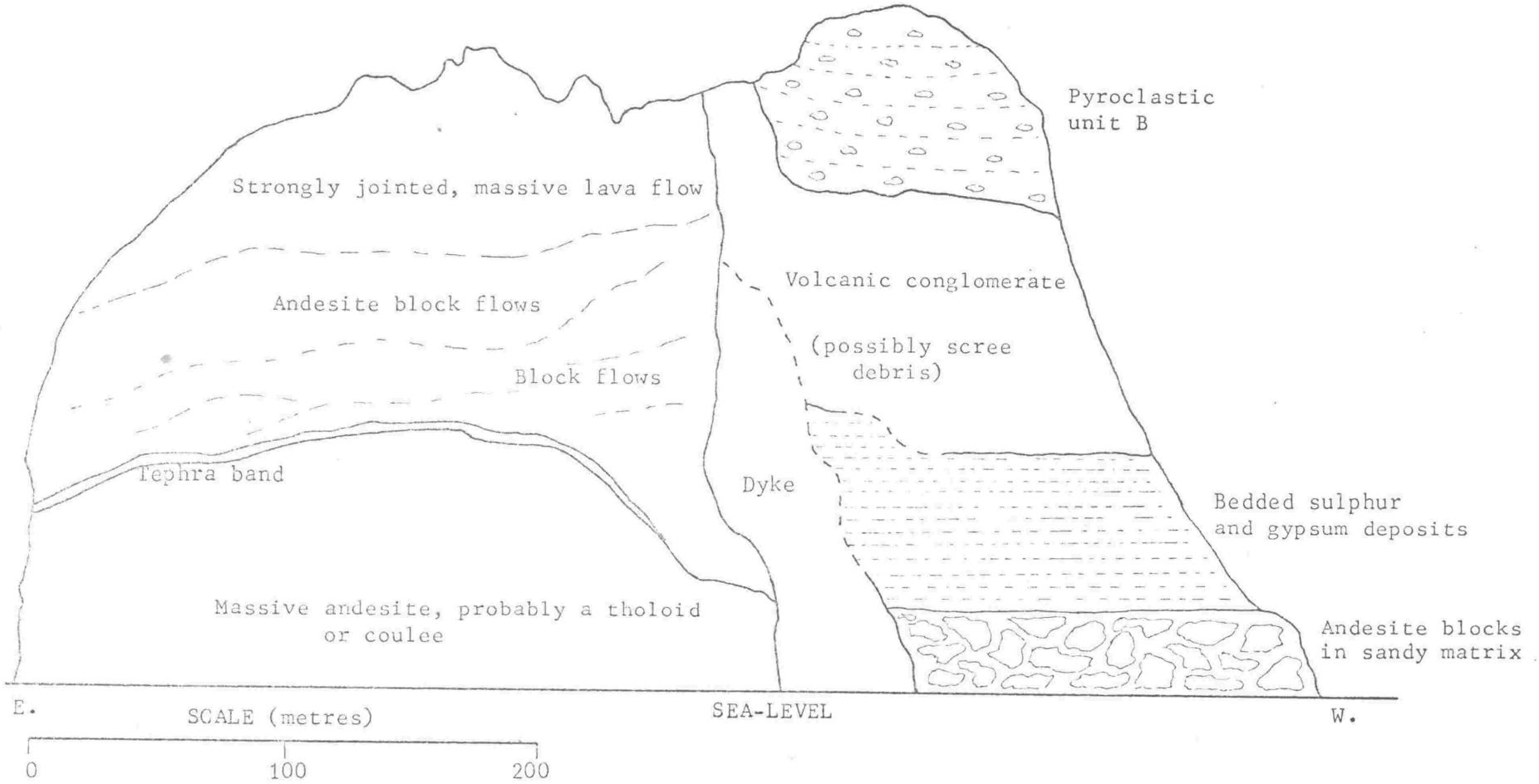

Fig. 11. - Diagramatic cross-section on an east-west line through the northern portion of Troup Head (White Island). Vertical exaggeration approximately 3 x.

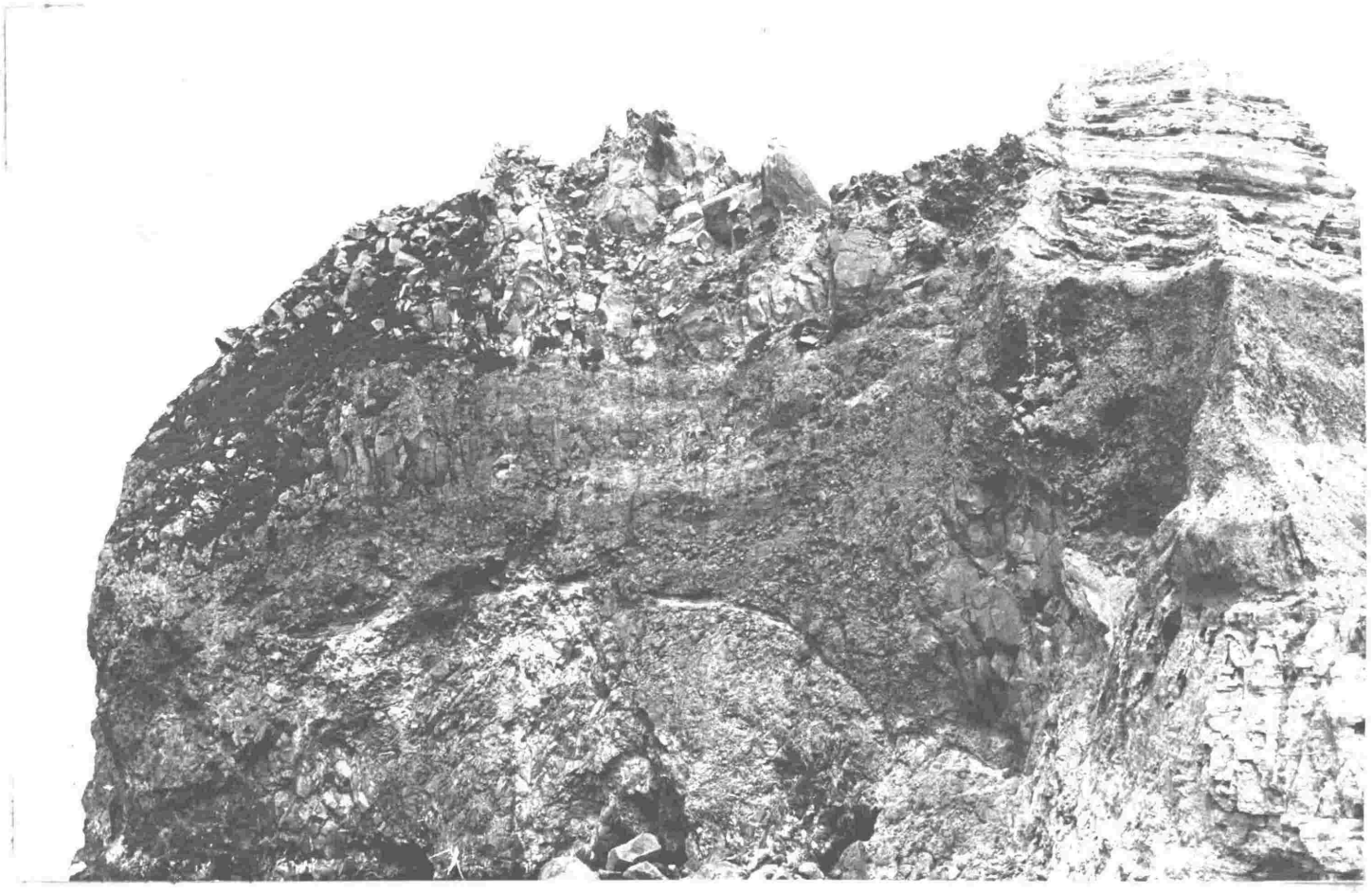

Plate 15. - Section on northern face of Troup Head, cf. Fig. 11.

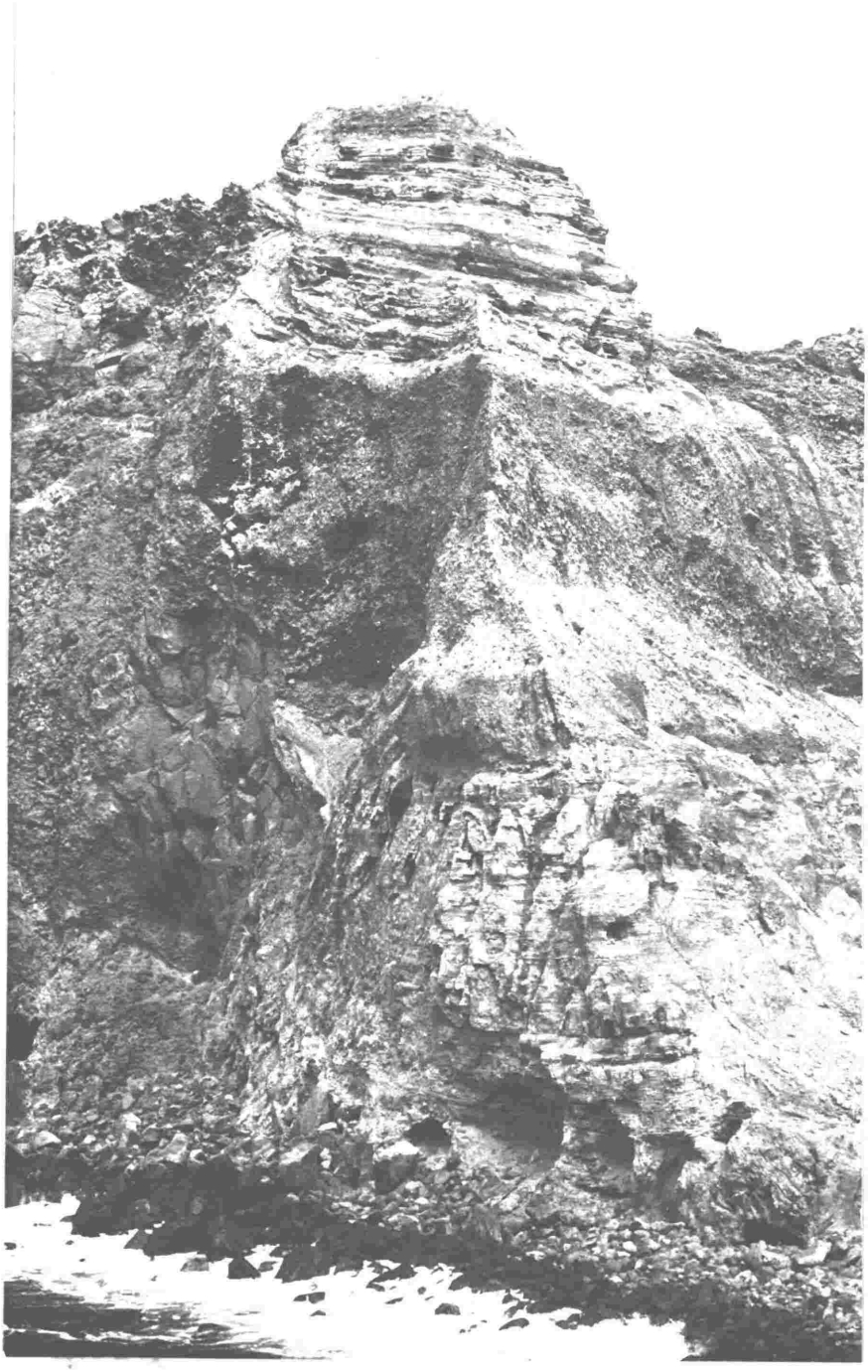

Plate 16. - Section on northwestern corner of Troup Head, cf. Plate 15 and Fig. 11.

as crater floor deposits formed after the east sub-crater had been explosively excavated. The west face section consists of blocks of andesite set in a sandy andesitic matrix, overlain by about 30 m of thinly-bedded, horizontal, gypsum and sulphur deposits; which are in turn overlain by 30 m of andesitic blocks (probably scree or lahar debris). The uppermost part of the section consists of about 20 m of pyroclastic unit B.

The presence of unit B at the top of a section on what was the floor of the east sub-crater indicates that the east sub-crater was formed prior to the west sub-crater, unit A being erupted during the formation of the east sub-crater and unit B during the formation of the west sub-crater.

After its formation the east sub-crater was largely filled with horizontally bedded gypsum and sulphur deposits; remnants of which are preserved on the south wall of the crater, in the west face section on Troup Head, and to a heights of 70-80 m above the present crater floor on the north crater wall. The deposits are extremely similar to those that formed in a lake which occupied much of the crater floor at the end of the last century, and it is likely that they were also formed in a lake.

The level of the lake is unlikely to have been more than 20 m above or below sea-level because the crater walls are not sufficiently impermeable. It would thus seem that shore-level was some 70-80 m higher at the time when the bedded sulphur and gypsum deposits on the north crater wall were formed. Since it is generally accepted that Pleistocene sea-levels have not been markedly higher than they

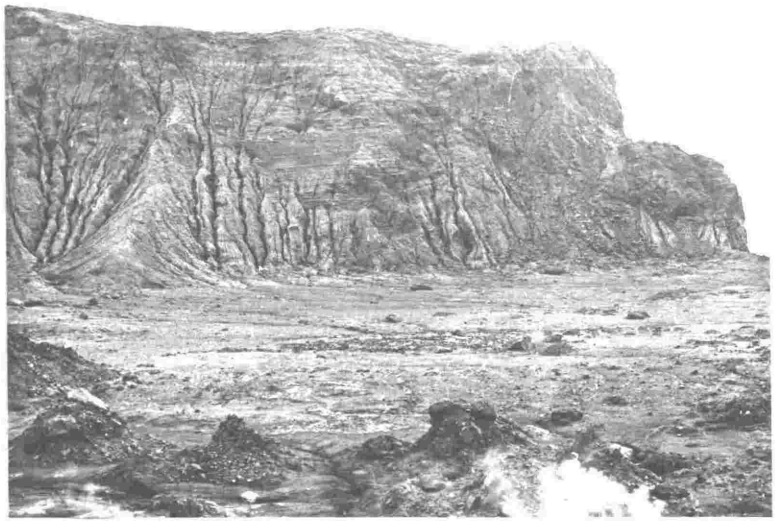

Plate 17. - Gypsum and sulphur beds preserved in a section on the north wall of White Island crater.

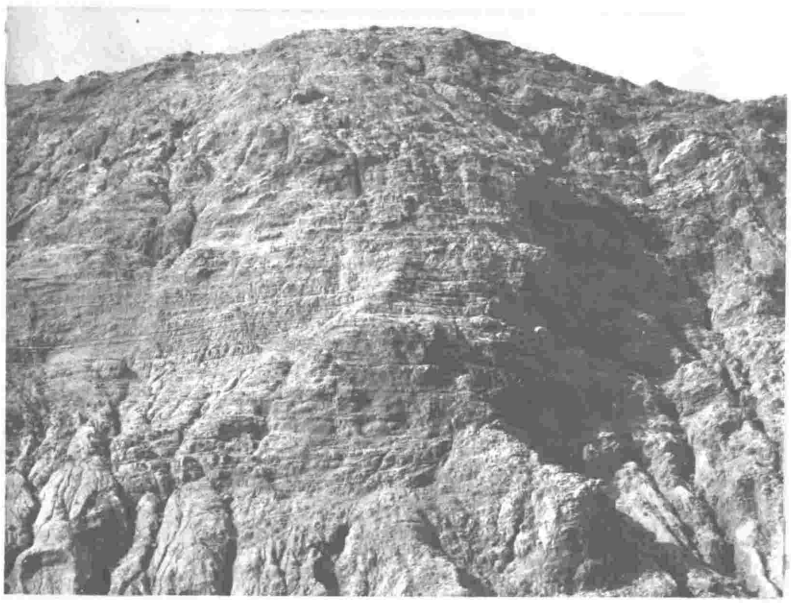

Plate 18. - Detail of gypsum and sulphur beds on north crater wall.

are at present, White Island is inferred to have been uplifted about 70-80 m since the formation of these deposits.

At the coast in Crater Bay and Wilson Bay there is a clearly defined Holocene planar surface cut into old lahar debris. This surface probably formed close to sea-level, but it now stands about 3 m above present sea-level. Eustatic sea-level curves for the last 10,000 years are not sufficiently accurate for a reliable uplift rate to be inferred for a surface so close to present sea-level. However, it is very likely that the uplift rate is less than 1 mm per year. An alternative method of deriving the uplift rate is to make use of the known maximum height for the north wall sulphur and gypsum deposits. In view of the probable uplift rate of less than 1 mm per year, these deposits almost certainly formed during an interglacial, hence a maximum uplift rate for White Island is determined by assuming this interglacial to be the last interglacial. The maximum uplift rate so derived is 0.7 mm per year.

The sulphur and gypsum beds on the east sub-crater have been largely removed by erosion, probably marine erosion following the breaching of the crater. The breaching itself was very likely a result of marine erosion since there is no evidence of explosive activity in the east sub-crater after its formation. As shown on the west face section on Troup Head, pyroclastic unit B was deposited at an intermediate stage in the erosion of the material filling the east sub-crater, and the west sub-crater is therefore appreciably younger than the east sub-crater.

The well-bedded character of pyroclastic unit B indicates that the west sub-crater was not formed by a single paroxysmal eruption,

but rather by a series of smaller eruptions spread over some time; the absence of any significant weathering breaks within the sequence indicates that the interval between eruptions is unlikely to be greater than a few hundred years.

After the erosion and removal of gypsum and sulphur beds in the east sub-crater, and explosion debris deposited on both, lahars and pyroclastics of unit C were deposited over the whole crater to form its present floor. Some bedded gypsum and sulphur deposits were also formed as sediments in a lake about 12 m above present sea-level.

No lava flows which apparently post-date the formation of the west sub-crater have been observed on the crater floor. However, Black (1970) considers the youngest lava flow on the island to be at the summit of Mt Gisborne, overlain by only a thin layer of bedded tephra. The age of this flow is unknown but from its situation it seems most unlikely to post-date crater formation.

PETROGRAPHY

Forty thin sections of samples from White Island were studied and thirteen representative sections were chosen for modal analysis. A large proportion of the samples collected showed signs of alteration, both by weathering and by hydrothermal processes. Weathering processes appear to be particularly rapid on White Island (they were described as "intense" by Baumgart, 1959), probably due to the acid fumes and to the low pH (1-4.5) of the ground water. Samples collected included lavas, agglomerates, dykes, volcanic breccias, pyroclastics and volcanigenic sediments. Tephra erupted during the period 1966-1969

was also sampled and its petrography, grain size distribution and mineralogy was described by Duncan & Vucetich (in press).

The lavas, dykes and agglomerates collected comprise plagioclase andesites, plagioclase-pyroxene andesites, plagioclase dacites and plagioclase-pyroxene dacites. Their mineralogy is similar to that of Edgecumbe and Whale Island samples in that they contain intermediate -calcic plagioclase, augite, hypersthene-bronzite and titanomagnetite as the major constituents. However hornblende and biotite which often occur in the Edgecumbe and Whale Island lavas are absent from the White Island lavas sampled (Black, 1970, reported biotite as a constituent in some samples). The only occurrence of olivine observed by the author in the Bay of Plenty volcanics is in sample 11362, which was collected west of Poroporo on the south coast of White Island. Generally speaking the White Island samples contain more pyroxene and less quartz than the other Bay of Plenty volcanics.

Volcanigenic sediments sampled from the crater consist of a mixture of weathered andesitic debris, sulphur, and gypsum, together with minor anhydrite. Horizontal beds of almost pure gypsum crop out in a low cliff near the coast in Crater Bay and pure sulphur is deposited at the mouths of many fumaroles.

The groundmass texture of White Island volcanic rocks is generally hyalopilitic or pilotaxitic. The volcanic glass which comprises most of the hyalopilitic groundmasses is pale-brown to dark brown in colour and generally contains few crystallites (mainly felspar). The proportion of rocks with hyalopilitic groundmass is higher in White Island volcanics than in any of the other Bay of

Plenty volcanics except Manawahe. Pilotaxitic groundmasses of White Island rocks often contain pale coloured patches, composed largely of cristobalite, some of which have "cores" of quartz. Brownish patches in a number of pilotaxitic groundmasses are considered to be due to formation of hydrated iron oxides and hydroxides.

Accessory minerals comprise apatite, rutile and a little zircon.

Comparative Petrography of White Island Volcanic Units

Modal analyses of White Island samples and sample locations are given in Table 9.

Twenty samples were collected from the south coast, and nine of these were sufficiently unaltered to warrant modal analysis. There was no systematic petrographic variation observed either between flows from a particular cliff section, or between flows from different cliff sections. Relative ages of flows in different cliff sections could not be established and it is thus impossible to say whether there were any petrographic trendswith time during the formation of the Central Cone.

A massive lava (sample 11246) at the base of Troup Head has the lowest groundmass content of any White Island sample studied, and it has the highest plagioclase/pyroxene ratio. This sample has distinctly different petrography from any Central Cone sample. A sample (11370) from a dyke in Troup Head is very similar petrographically to Central Cone examples, except that it contains 1.4% chalcedony.

TABLE 9

LOCATIONS, MODAL ANALYSES AND PHENOCRYST PROPO

LOCALITY	SAMPLE NO.	PETROGRAPHIC CLASSIFICATION	MODAL ANALYSIS					
			Groundmass	Plagioclase	Ortho-Pyroxene	Clino-Pyroxene	Quartz	Chalced
South Coast	11362	Plagioclase-Pyroxene Andesite	60.9	23.2	7.0	8.2	-	-
	11363	Plagioclase-Pyroxene Andesite	73.1	16.7	5.3	4.6	-	-
	11364	Plagioclase Dacite	71.5	17.3	4.3	4.1	1.2	-
	11369	Plagioclase Andesite	68.2	23.4	3.6	4.3	-	-
	11241	Plagioclase-Pyroxene Andesite (D)*	67.2	17.3	6.1	8.9	-	-
Crater Bay	11244	Plagioclase Andesite (D)	69.1	21.1	5.1	4.4	-	-
	11245	Plagioclase-Pyroxene Andesite (D)	60.0	21.1	12.0	6.3	-	-
	11371	Plagioclase Dacite	69.0	22.4	4.5	2.6	0.8	-
	11372	Plagioclase Andesite	69.7	21.4	5.1	3.1	-	-
Troup Head	11246	Plagioclase Andesite (A)*	53.1	37.1	4.9	4.6	-	-
	11370	Plagioclase-Pyroxene Dacite	69.4	18.5	3.9	5.8	-	1.4
S.E. Crater Wall	11243	Plagioclase-Pyroxene Andesite (D)	67.3	19.8	8.1	3.8	-	-
N.E. Crater Wall	11373	Plagioclase-Pyroxene Andesite	55.9	27.9	11.0	4.4	-	-

*(A) Chemical andesite.

*(D) Chemical dacite.

MANAWAHE

The eroded remnants of the Manawahe volcano lie about 8 km northeast of the town of Manawahe, on the west flank of the Whakatane Graben. It was correlated with Beeson's Island volcanics of possible Miocene age by Healy, Schofield and Thompson (1964), but has been recently dated by the K-Ar method (J.J. Stipp, pers. comm.) at approximately 750,000 years B.P. No detailed geological study of the volcano has been made.

Petrography of Manawahe

Eighteen samples, collected both on the surface and from drillholes (drillhole samples supplied by D. Rishworth, N.Z.G.S.) were selected for thin-sectioning, and 15 of these were modally analysed (Table 10). Phenocryst constituents found in all samples are intermediate plagioclase, augite, bronzite-hypersthene and titanomagnetite. One sample contains phenocrystic cristobalite and biotite, and another sample contains phenocrystic quartz.

All samples listed in Table 10 except for 11383 have hyalopilitic textures with the groundmass glass in varying degrees of devitrification. Sample 11383 has the lowest groundmass content of any sample and has a pilotaxitic groundmass texture. Groundmass minerals are microlites of felspar and orthopyroxene, and grains of opaques. Cristobalite is a common groundmass mineral in many samples, it usually occurs as patches in the groundmass which are often surrounded by a rim of groundmass glass which is darker than the rest of the groundmass glass.

Plagioclase phenocrysts often show patchy zonation with extensive formation of glass in their cores, and in some cases the cores are

TABLE 10

LOCATIONS, MODAL ANALYSES AND PHENOCRYST P

SAMPLE NO.	LOCALITY	DEPTH (m below Surface)	PETROGRAPHIC CLASSIFICATION	MODAL ANALYSIS					
				Groundmass	Plagioclase	Ortho-Pyroxene	Clino-Pyroxene	Quartz	Cristo
11247	N68/120253	0	Plagioclase Dacite (D)*	75.2	19.2	3.5	1.0	-	0.
11248	N68/123253	0	Plagioclase Andesite (D)	79.8	16.7	1.8	1.0	-	-
11249	N68/132230	0	Plagioclase Dacite (D)	77.0	18.6	1.9	0.6	1.0	-
11374	N68/113250	0	Plagioclase Andesite	79.3	15.7	2.5	1.6	-	-
11375	N68/114250	0	Plagioclase Andesite	80.0	16.4	1.1	1.9	-	-
11376	N68/120255	31.5	Plagioclase Andesite	75.2	18.8	2.4	2.4	-	-
11377	N68/120255	40.4	Plagioclase Andesite	74.5	18.3	4.7	2.0	-	-
11378	N68/116254	35.3	Plagioclase Andesite	74.7	21.4	2.1	1.0	-	-
11379	N68/120252	29.3	Plagioclase Andesite	79.1	17.0	2.2	1.1	-	-
11380	N68/120252	38.7	Plagioclase Andesite	74.8	21.1	2.4	1.2	-	-
11381	N68/120252	54.9	Plagioclase Andesite	77.9	18.6	2.1	0.9	-	-
11382	N68/120252	58.3	Plagioclase Andesite	74.6	20.8	2.3	1.5	-	-
11383	N68/118251	59.7	Plagioclase Andesite	65.4	29.3	3.1	0.9	-	-
11384	N68/118251	74.1	Plagioclase Andesite	75.3	19.8	2.5	1.5	-	-
11385	N68/118251	80.3	Plagioclase Andesite	72.2	23.2	2.0	2.1	-	-

* (D) Chemical dacite.

altered to clay minerals. Clay minerals were not observed as major alteration products of plagioclase in the rest of the Bay of Plenty volcanics, but minor amounts of clay are probably present in the other volcanics. The clay alteration product was identified by X-ray diffraction as hydrated halloysite (endellite) on the basis of its 9.9 Å peak, which increases to 10.8 Å on glycollation, and decreases irreversibly to 7.0 Å on drying at 110° C for 24 hours. Endellite, chlorite and hematite-limonite veins are common in altered drillhole samples.

Petrographically, all of the samples examined are very similar, with 13 out of 15 being plagioclase andesites, and the remaining two samples being plagioclase dacites. Three samples were chemically analysed and all were found to be chemical dacites, but one of the three is a petrographic andesite (sample 11248). Samples taken from boreholes do not show any systematic petrographic variation with depth, and together with surface samples do not show groupings of petrographic types according to areal distribution within the Manawahe volcano.

PETROGRAPHIC COMPARISONS BETWEEN EDGECUMBE, WHALE ISLAND, WHITE ISLAND AND MANAWAHE

The means and standard deviation for the modal compositions of samples from each of Edgecumbe, Whale Island, White Island and Manawahe are given in Table 11.

The most obvious differences between the modal analyses of the four volcanoes are for those minerals which are present in the rocks from some volcanoes but not in the rocks from others. Thus modal olivine is found only in White Island samples and modal cristobalite (phenocrystic) only in Manawahe samples. Hornblende is found in rocks from Edgecumbe and Whale Island but not in rocks from White Island and Manawahe. Biotite is not found in White Island rocks (c.f. Black, 1970) but is found in rocks from the other three volcanoes.

Comparisons of the variance and the mean of the six ubiquitous modal constituents (groundmass, plagioclase, orthopyroxene, clinpyroxene, quartz, and titanomagnetite) in each of the four volcanoes are made using the statistical parameters "F" and "Student's 't' ". The parameter "F" is the ratio of the squares of the standard deviations for two distributions, and is used to test whether there is any significant difference between the variances of the two distributions. Student's 't' is a parameter used to test for significant difference between the means of two distributions. In order to compare all possible pairs of distributions for the four volcanoes a 4 x 4 matrix of F and t values for each of the six ubiquitous modal constituents was computed and is given as Table 12.

TABLE 11

COMPARISON OF MODAL ANALYSES

	EDGECUMBE		WHALE ISLAND		WHITE ISLAND		MANAWAHE	
	Mean %	S.D.	Mean %	S.D.	Mean %	S.D.	Mean %	S.D.
Groundmass	65.0	7.3	67.1	6.2	65.7	6.2	75.7	3.7
Plagioclase	25.2	5.5	22.5	4.9	22.1	5.5	19.7	3.4
Orthopyroxene	3.8	1.7	4.3	1.2	6.2	2.7	2.4	0.8
Clinopyroxene	2.7	1.5	2.6	1.1	5.0	1.9	1.4	0.5
Quartz	1.1	2.0	1.7	1.9	0.3	0.5	0.07	0.3
Cristobalite	-	-	-	-	-	-	0.04	0.2
Biotite	0.3	0.6	0.1	0.2	-	-	0.01	0.03
Hornblende	0.3	0.7	0.4	0.8	-	-	-	-
Olivine	-	-	-	-	0.02	0.06	-	-
Opaques	1.6	0.8	1.3	1.1	0.7	0.4	0.7	0.3

TABLE 12

F AND t MATRICES FOR MODAL ANALYSES

ANALYTICAL GROUPS ARE IDENTIFIED IN THE TEST MATRICES BY THE FOLLOWING NUMBERS

1 - Edgecumbe Volcano
2 - Whale Island Volcano
3 - White Island Volcano
4 - Manawahe Volcano

F Test Matrix - Groundmass

	1	2	3	4
1	0.00 (0, 0)	1.39 (49,24)	1.39 (49,12)	3.89 (49,14)*
2	1.39 (49,24)	0.00 (0, 0)	1.00 (24,12)	2.81 (24,14)
3	1.39 (49,12)	1.00 (12,24)	0.00 (0, 0)	2.81 (12,14)
4	3.89 (49,14)*	2.81 (24,14)	2.81 (12,14)	0.00 (0, 0)

F Test Matrix - Clinopyroxene

	1	2	3	4
1	0.00 (0, 0)	1.86 (49,24)	1.60 (12,49)	9.00 (49,14)*
2	1.86 (49,24)	0.00 (0, 0)	2.98 (12,24)	4.84 (24,14)*
3	1.60 (12,49)	2.98 (12,24)	0.00 (0, 0)	14.44 (12,14)*
4	9.00 (49,14)*	4.84 (24,14)*	14.44 (12,14)*	0.00 (0, 0)

F Test Matrix - Plagioclase

	1	2	3	4
1	0.00 (0, 0)	1.26 (49,24)	1.00 (49,12)	2.62 (49,14)
2	1.26 (49,24)	0.00 (0, 0)	1.26 (12,24)	2.08 (24,14)
3	1.00 (12,49)	1.26 (12,24)	0.00 (0, 0)	2.62 (12,14)
4	2.62 (49,14)	2.08 (24,14)	2.62 (12,14)	0.00 (0, 0)

F Test Matrix - Quartz

	1	2	3	4
1	0.00 (0, 0)	1.11 (49,24)	15.38 (49,12)*	59.17 (49,14)*
2	1.11 (49,24)	0.00 (0, 0)	13.88 (24,12)*	53.40 (24,14)*
3	15.38 (49,12)*	13.88 (24,12)*	0.00 (0, 0)	3.85 (12,14)*
4	59.17 (49,14)*	53.40 (24,14)*	3.85 (12,14)*	0.00 (0, 0)

F Test Matrix - Orthopyroxene

	1	2	3	4
1	0.00 (0, 0)	2.01 (49,24)	2.52 (12,49)	4.52 (49,14)*
2	2.01 (49,24)	0.00 (0, 0)	5.06 (12,24)*	2.25 (24,14)
3	2.52 (12,49)	5.06 (12,24)*	0.00 (0, 0)	11.39 (12,14)*
4	4.52 (49,14)*	2.25 (24,14)	11.39 (12,14)*	0.00 (0, 0)

F Test Matrix - Opaques

	1	2	3	4
1	0.00 (0, 0)	1.89 (24,49)	4.67 (49,12)*	8.78 (49,14)*
2	1.89 (24,49)	0.00 (0, 0)	8.84 (24,12)*	16.60 (24,14)*
3	4.67 (49,12)*	8.84 (24,12)*	0.00 (0, 0)	1.88 (12,14)
4	8.78 (49,14)*	16.60 (24,14)*	1.88 (12,14)	0.00 (0, 0)

t Test Matrix - Groundmass

	1	2	3	4
1	0.00 (0)	1.24 (73)	0.32 (61)	5.59 (63)*
2	1.24 (73)	0.00 (0)	0.66 (36)	4.99 (38)*
3	0.32 (61)	0.66 (36)	0.00 (0)	5.44 (26)*
4	5.59 (63)*	4.99 (38)*	5.44 (26)*	0.00 (0)

t Test Matrix - Clinopyroxene

	1	2	3	4
1	0.00 (0)	0.30 (73)	4.68 (61)*	3.46 (63)*
2	0.30 (73)	0.00 (0)	5.14 (36)*	4.18 (38)*
3	4.68 (61)*	5.14 (36)*	0.00 (0)	8.29 (26)*
4	3.46 (63)*	4.18 (38)*	8.29 (26)*	0.00 (0)

t Test Matrix - Plagioclase

	1	2	3	4
1	0.00 (0)	2.08 (73)	1.81 (61)	3.71 (63)*
2	2.08 (73)	0.00 (0)	0.23 (36)	1.97 (38)
3	1.81 (61)	0.23 (36)	0.00 (0)	1.45 (26)
4	3.71 (63)*	1.97 (38)	1.45 (26)	0.00 (0)

t Test Matrix - Quartz

	1	2	3	4
1	0.00 (0)	1.25 (73)	1.58 (61)	2.17 (63)
2	1.25 (73)	0.00 (0)	2.93 (36)*	3.85 (38)*
3	1.58 (61)	2.93 (36)*	0.00 (0)	1.34 (26)
4	2.17 (63)	3.85 (38)*	1.34 (26)	0.00 (0)

t Test Matrix - Orthopyroxene

	1	2	3	4
1	0.00 (0)	1.33 (73)	4.06 (61)*	2.94 (63)*
2	1.33 (73)	0.00 (0)	3.27 (36)*	5.24 (38)*
3	4.06 (61)*	3.27 (36)*	0.00 (0)	5.82 (26)*
4	2.94 (63)*	5.24 (38)*	5.82 (26)*	0.00 (0)

t Test Matrix - Opaques

	1	2	3	4
1	0.00 (0)	1.36 (73)	4.13 (61)*	4.48 (63)*
2	1.36 (73)	0.00 (0)	2.12 (36)	2.31 (38)
3	4.13 (61)*	2.12 (36)	0.00 (0)	0.17 (26)
4	4.48 (63)*	2.31 (38)	0.17 (26)	0.00 (0)

Note (1) Figures in brackets denote the number of degrees of freedom for a particular value of F or t.

(2) Values of F and t marked with an asterisk are statistically significant at the 1% level, i.e. the two variances or the two means being tested have less than one chance in a hundred of being drawn from the same distribution, and are therefore considered to represent two statistically different distributions.

Detailed inferences as to significant differences in a particular modal constituent between pairs of volcanoes can be made from Table 12 and will not be listed here. The principal conclusions are: (1) for all modal constituents Edgecumbe and Whale Island rocks are indistinguishable; (2) White Island rocks and Manawahe rocks can be statistically distinguished from each other and from Edgecumbe and Whale Island rocks by their orthopyroxene and clinopyroxene content; (3) Manawahe rocks have significantly higher groundmass contents than any of the other Bay of Plenty volcanics; (4) the variance of quartz is significantly different in the distributions for White Island and for Manawahe when compared to each other, or to Edgecumbe and Whale Island distributions.

MINERALOGY

PLAGIOCLASE

Plagioclase is present in all the Bay of Plenty volcanics, and is the most abundant phenocryst in all samples. The modal percentage of plagioclase lies in the range 15.7% - 41.0% and plagioclase expressed as a proportion of the total phenocryst content lies in the range 49.1% - 86.3%. Differences in the plagioclase abundance distributions between rocks from Edgecumbe, Whale Island, White Island and Manawahe are shown in Tables 11 and 12.

Within any one rock there is a large range in the size of plagioclase phenocrysts, from about 6 mm to less than 0.1 mm for the maximum dimension. There is an apparent correlation in rocks from the same volcano, between the modal size of plagioclase phenocrysts and the total crystallinity of the sample, but this cannot usually be observed unless the difference in crystallinity is marked (i.e. exceeds 10%). The distribution of the maximum dimension of plagioclase phenocrysts in Edgecumbe lavas was determined by measurements on 250 randomly selected crystals, ten crystals being selected from each of 25 rock samples of comparable crystallinity. The distribution obtained (Fig. 12) is bimodal with modal sizes at 0.6 mm and 1.0 mm; it is strongly skewed, with a larger number of small phenocrysts than large ones. The continuity of the distribution suggests that plagioclase nucleation has continued throughout its crystallisation history and the bimodal nature of the distribution infers two periods of increased nucleation (dependant on the assumption that maximum dimension of plagioclase crystals in the same rock sample is an indication of

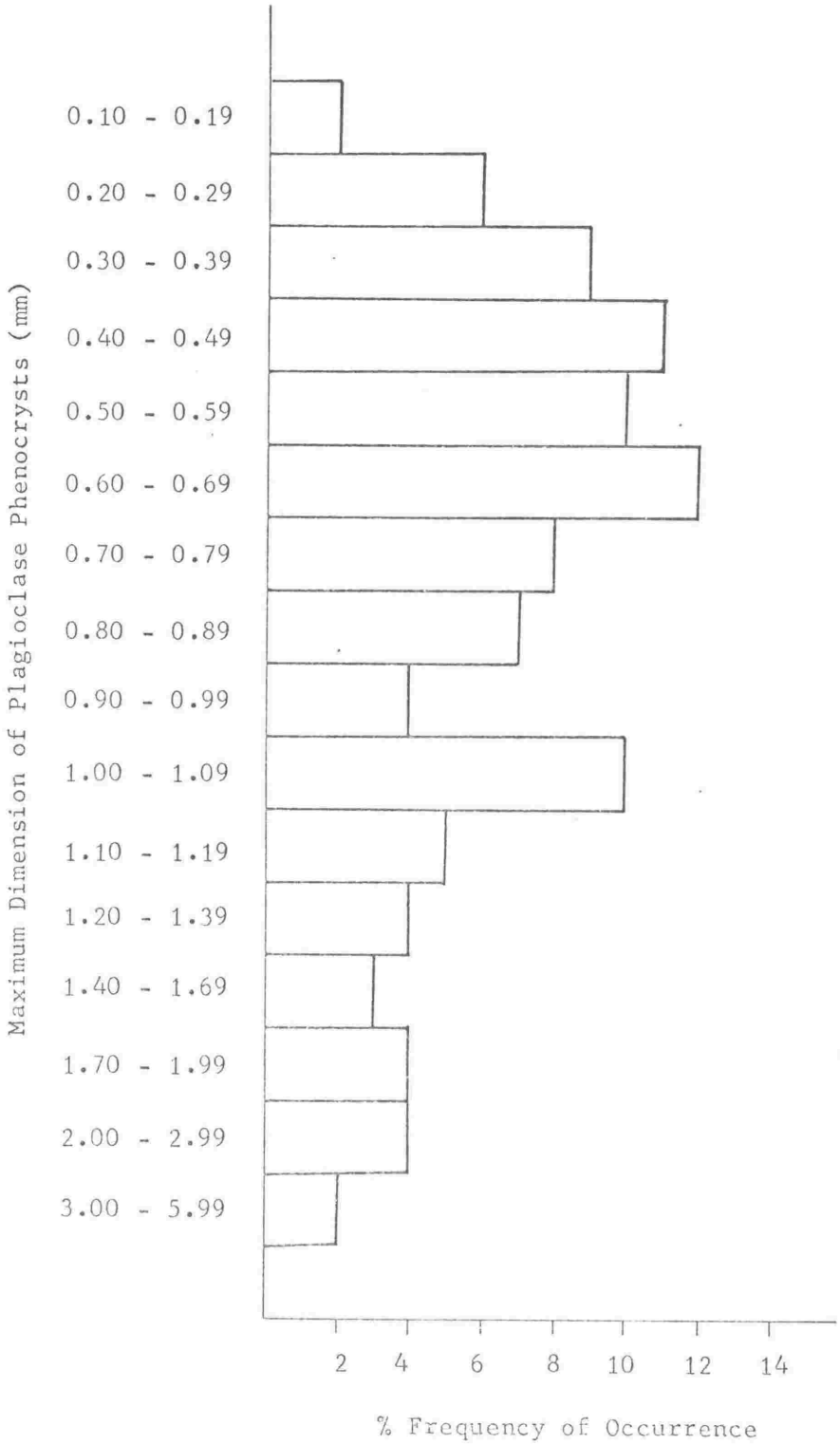

Fig. 12. - Histogram showing size distribution of plagioclase phenocrysts in 25 Edgecumbe rock samples.

relative age, this assumption is discussed below). Since the distribution is obtained by combining data from 25 discrete rock samples of different ages (age of extrusion) the two periods of nucleation could be due to change in physical and chemical changes within a single magma body, or could be due to the samples being taken from two magma bodies of different ages and crystallisation history. Alternatively, the bimodality of the distribution is a result of sampling error.

Plagioclase is also a ubiquitous groundmass constituent and occurs as small (2-10 micron) lath-like crystals in both pilotaxitic and hyalopilitic groundmasses.

Composition

Plagioclase compositions were determined by measuring the extinction angle $X' \wedge (010)$ in sections oriented $\perp$ a, using the chart given by Tobi (1963, Fig. 6B). In order that a reasonable number of determinations for plagioclase in each selected thin-section could be made, a universal stage was used to rotate selected plagioclase crystals into an orientation $\perp$ a. Using this technique the core compositions of at least 10 plagioclase phenocrysts in each of 50 selected thin sections from Edgecumbe, Whale Island, White Island and Manawahe were determined. The core compositions were chosen because the complex zonation patterns shown by virtually all the plagioclase phenocrysts necessitated measurement of a particular zone within all crystals if meaningful interpretations were to be made. The range of plagioclase core compositions determined for phenocrysts in a single sample are frequently comparable with the range of compositions shown by all the

plagioclase phenocrysts determined. It is therefore impossible to distinguish a particular range of plagioclase core compositions in samples from a particular volcanic unit from the range of compositions in samples from another volcanic unit, nor is the range of plagioclase core compositions distinctive for samples from any particular volcano comprising the Bay of Plenty volcanics. In general, plagioclase core compositions for the Bay of Plenty volcanics range from An_{35} to An_{83} with the most frequently observed values in the range An_{55}-An_{65}. The most sodic rim composition determined was An_{21}.

There is a reasonable correlation between the core composition of a plagioclase phenocryst and its size (expressed as $\sqrt{xy}$ where x and y are the maximum and minimum dimensions of a section $\perp$ a.), with smaller phenocrysts having more albite-rich cores than larger phenocrysts (Fig. 13). It is considered that volcanic plagioclase is in disequilibrium with the magma after its crystallisation (as indicated by extreme zonation patterns), and that the core compositions of plagioclase crystals are therefore dependant on the composition of the residual liquid in the magma at the time of their crystallisation. Thus it can be inferred that the size of a plagioclase phenocryst within a particular rock sample of the Bay of Plenty volcanics is largely dependent on its relative age.

Determinations of the x-ray diffraction parameters Υ ($2V_{131}+2V_{220} - 4V_{\bar{1}31}$ for Cu radiation) and B ($2V_{\bar{1}11} - 2V_{\bar{2}01}$ for Cu radiation) were made (Table 13) for plagioclases separated from 12 rock samples of the Bay of Plenty volcanics. The values of the parameters are dependent on the plagioclase composition and on

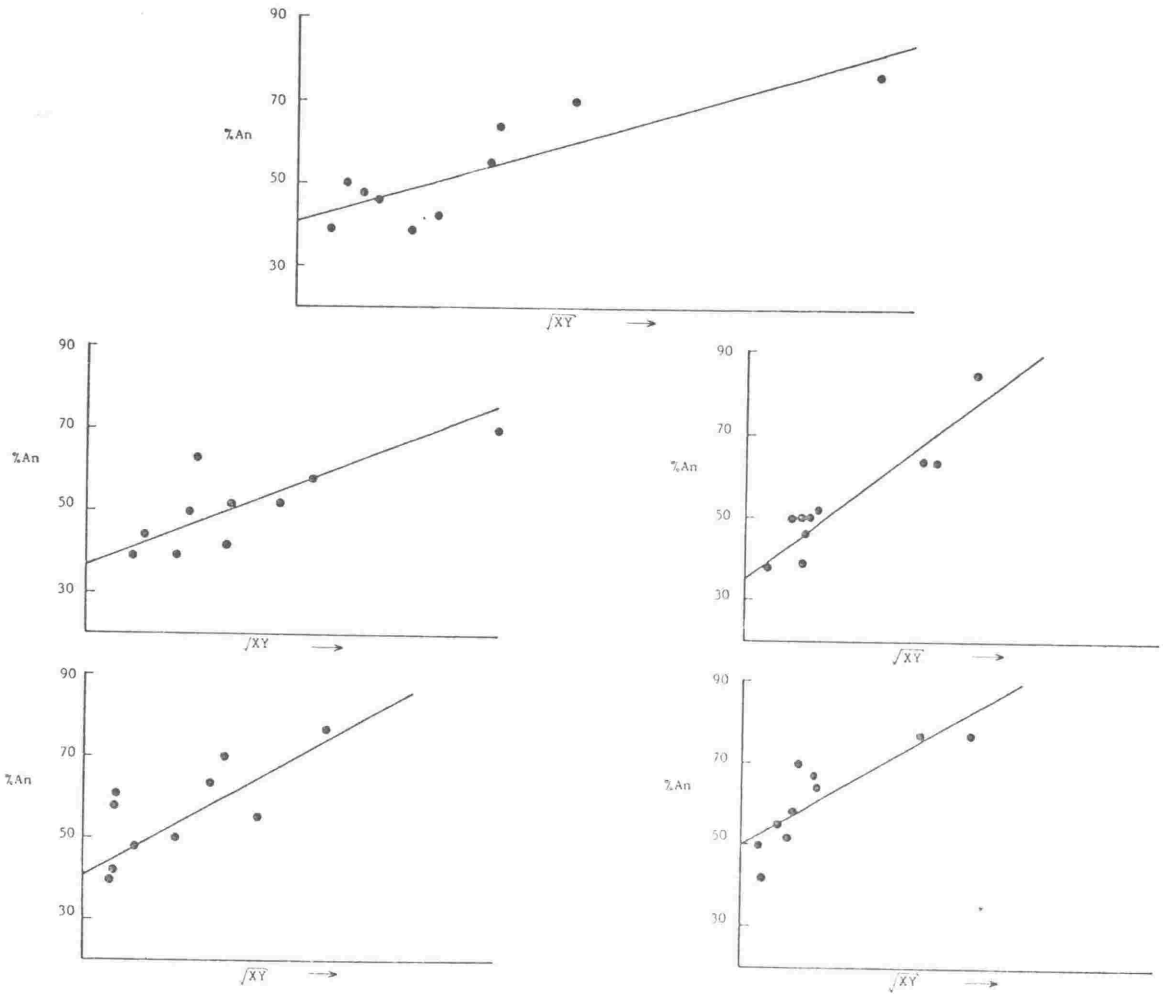

Fig. 13. - Graphs of plagioclase phenocryst size against core composition for five rock samples from Central Cone, Whale Island. In the graph for each sample, phenocryst size is expressed as $\sqrt{XY}$ (increasing to the right), where X and Y are the maximum and minimum dimensions of phenocryst sections $\perp$ a (X and Y were measured in arbitrary units). Lines are RMA regression lines fitted to the data plotted.

TABLE 13

X-RAY DIFFRACTION PARAMETERS FOR PLAGIOCLASE

SAMPLE NO.	γ	B
11251	1.02	0.81
11219	0.90	0.85
11206	1.30	0.75
11228	1.30	0.76
11386	0.99	0.82
11327	1.27	0.80
11387	1.30	0.78
11352	1.07	0.78
11349	1.20	0.77
11215	1.18	0.76
11388	1.18	0.78
11389	1.05	0.75

$$\gamma = 2V_{131} + 2V_{220} - 4V_{\bar{1}31}$$

$$B = 2V_{\bar{1}11} - 2V_{\bar{2}01}$$

its structural state (Smith & Gay, 1958). A plot of Υ against B for the plagioclase analysed (Fig. 14) shows no significant differences between samples from each of the four volcanoes.

Most plagioclase phenocrysts are twinned, and twinning of carlsbad, albite, combined carlsbad-albite, and pericline types was recognised.

Zoning

Nearly all plagioclase phenocrysts are zoned, the most common zonation patterns being normal oscillatory, or oscillatory with different compositional groups but no overall compositional trend. In all cases where it was examined in detail the pattern of oscillatory zoning is of groups of zones with successive zones in each group having the same average composition, but with abrupt compositional changes between groups of zones. In plagioclase phenocrysts in samples of the Bay of Plenty volcanics the overall change in the mean composition of groups of oscillatory zones between core and rim of the phenocryst may show a normal trend (decreasing %An outwards), a reverse trend, or no trend at all. Detailed compositional cross-sections (obtained by measurement of extinction angles $X' \wedge (010)$ in sections oriented $\perp$ a.) of two plagioclase phenocrysts with complex zoning patterns are shown in Figs. 15 and 16. Ewart (1963) in his description of plagioclase phenocrysts from tephra in the Taupo Sub-Group noted that plagioclase phenocrysts from particular ash members often showed a characteristic number of sharp and discordant breaks in their zoning patterns. He correlated these zoning breaks with previous eruptions in the Taupo sequence. Similar discordant breaks are observed in the zoning patterns of plagioclase phenocrysts from the Bay of Plenty

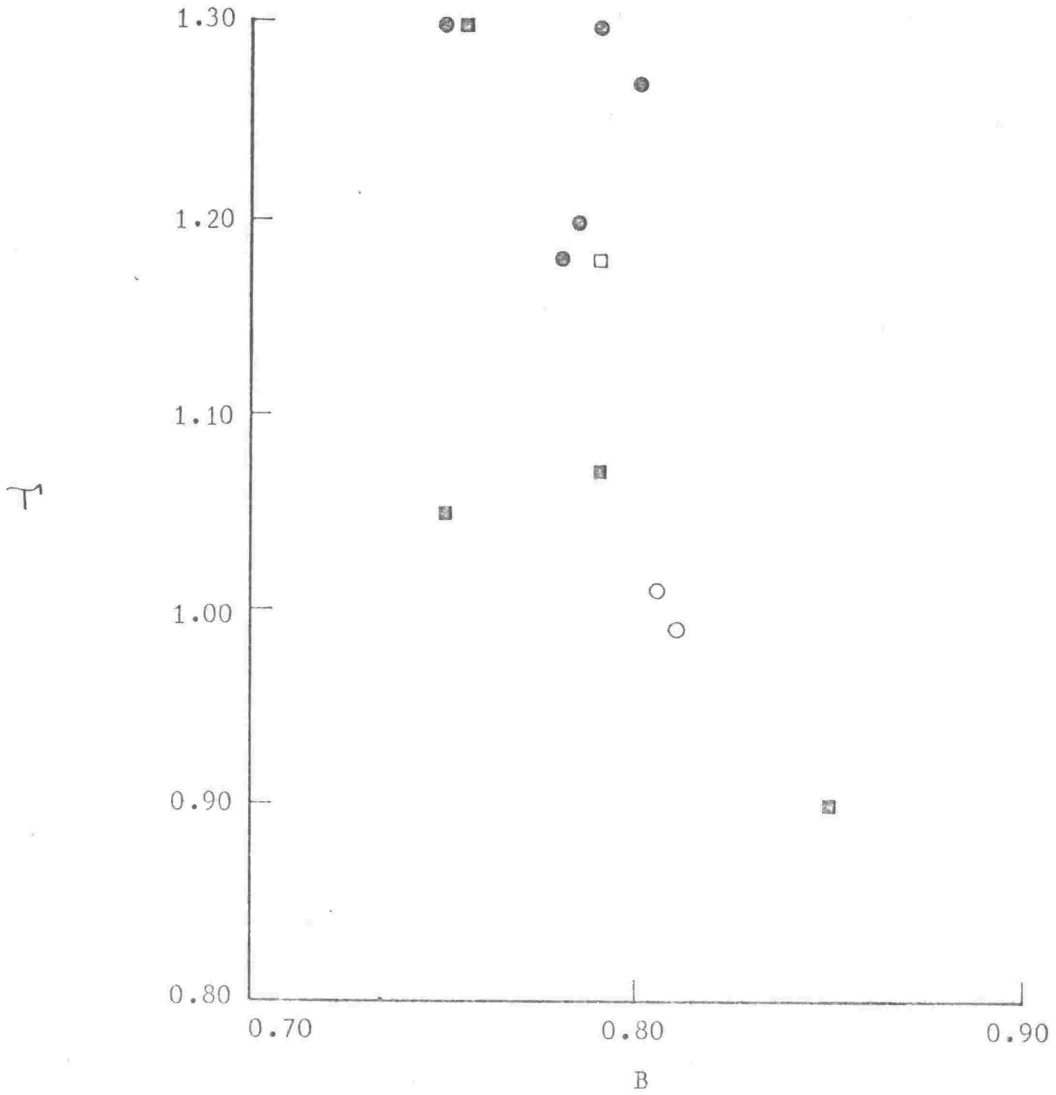

Fig. 14. - Values of the x-ray diffraction parameters T and B for plagioclase from samples of the Bay of Plenty volcanics. Symbols: ● Edgecumbe, ■ Whale Island, ○ White Island, □ Manawahe.

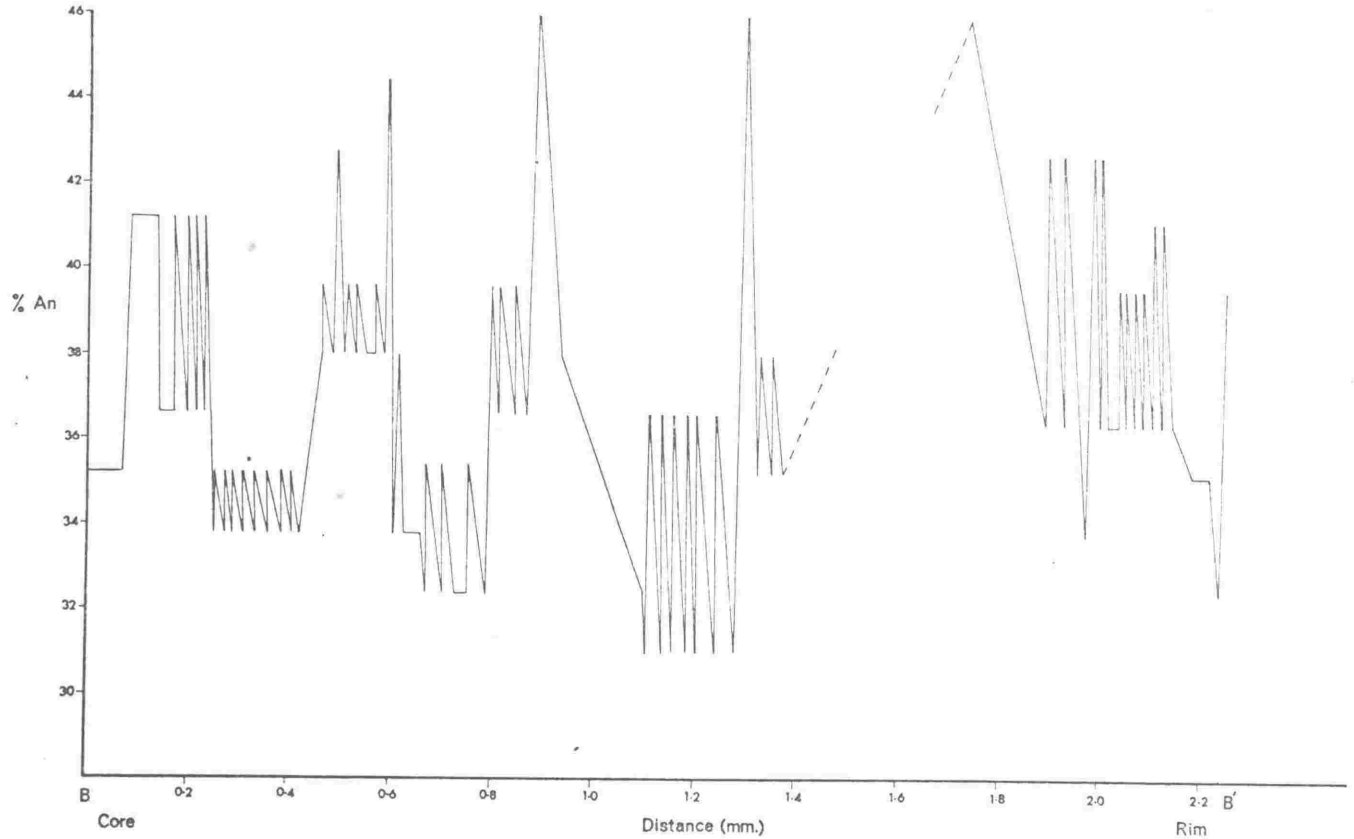

Fig. 15. - Compositional cross-section of plagioclase phenocryst from sample 11328. Composition determinations made by measuring extinction angle $X' \wedge C$ in section $\perp a$.

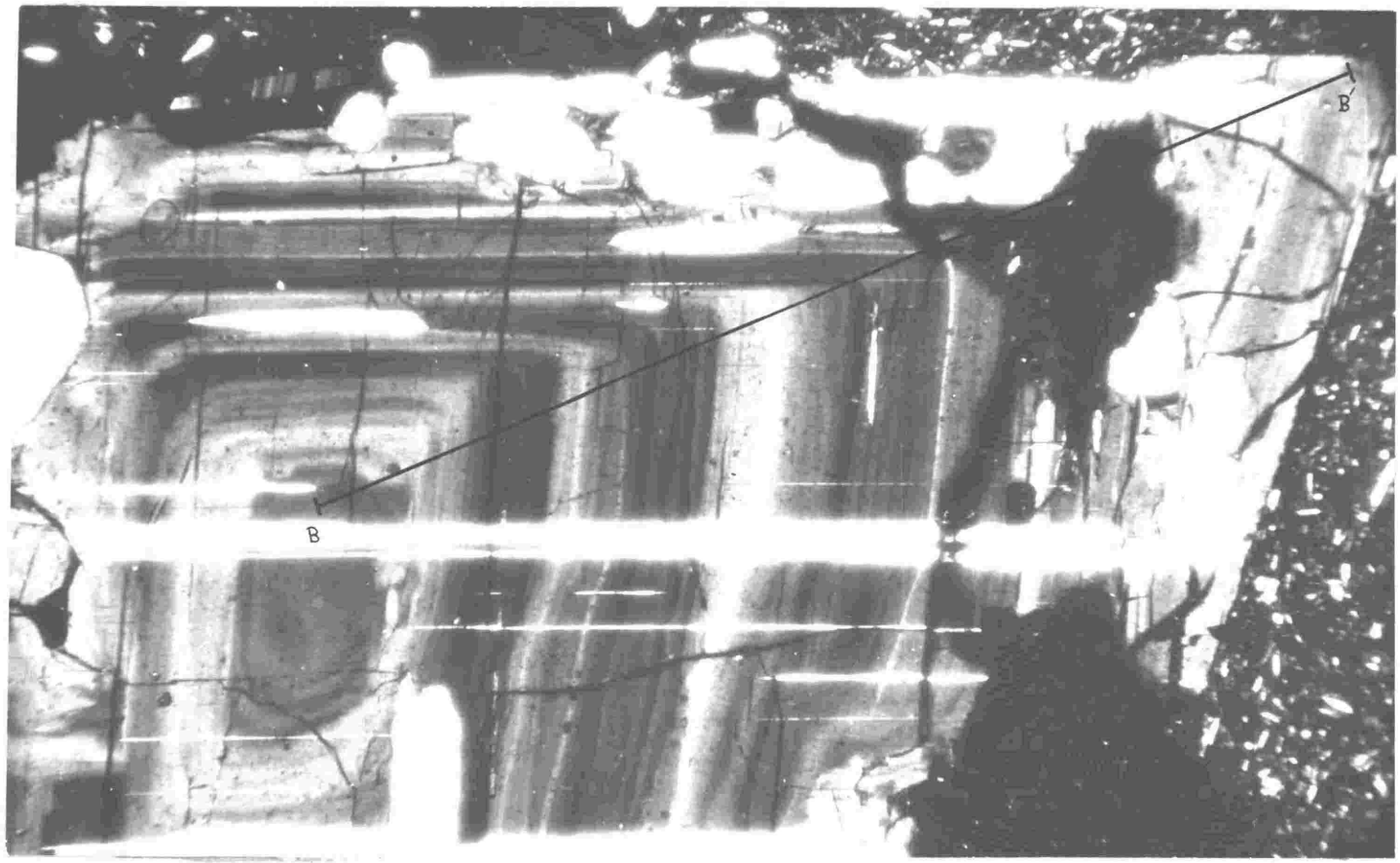

Plate 19. - Photomicrograph of plagioclase phenocryst from sample 11328. A compositional cross-section (B-B') for this crystal is given in Fig. 15. x 65.

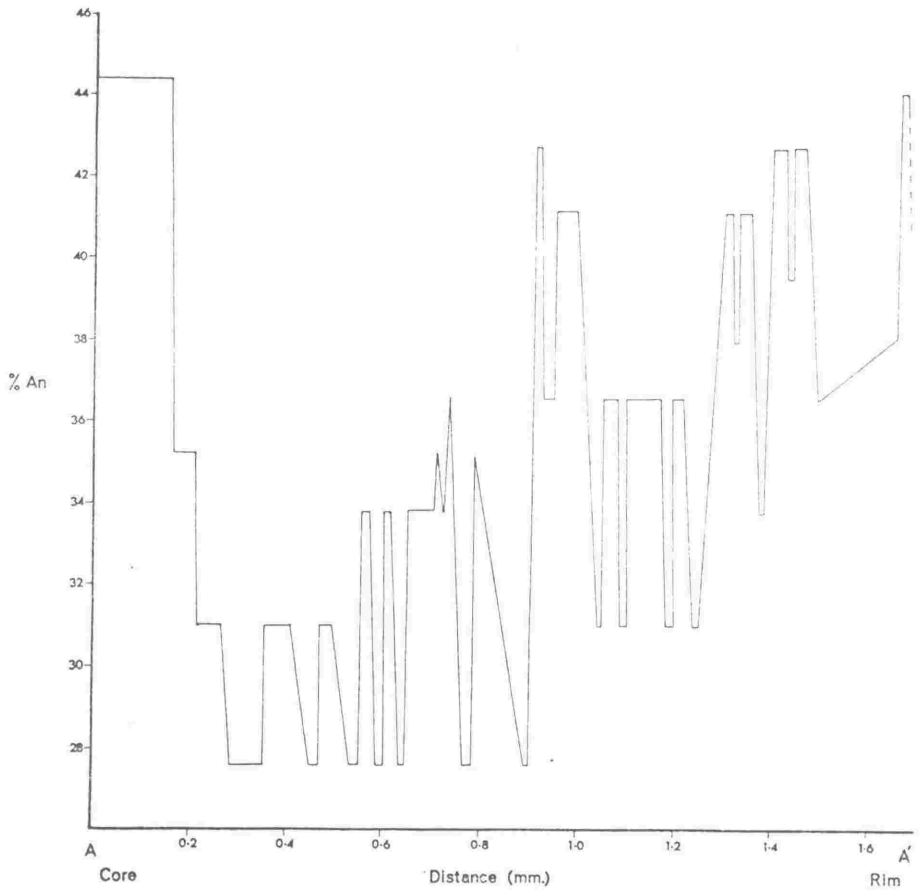

Fig. 16. - Compositional cross-section of plagioclase phenocryst from sample 11373. Composition determinations made by measuring extinction angle $X' \wedge C$ in section $\perp$ a.

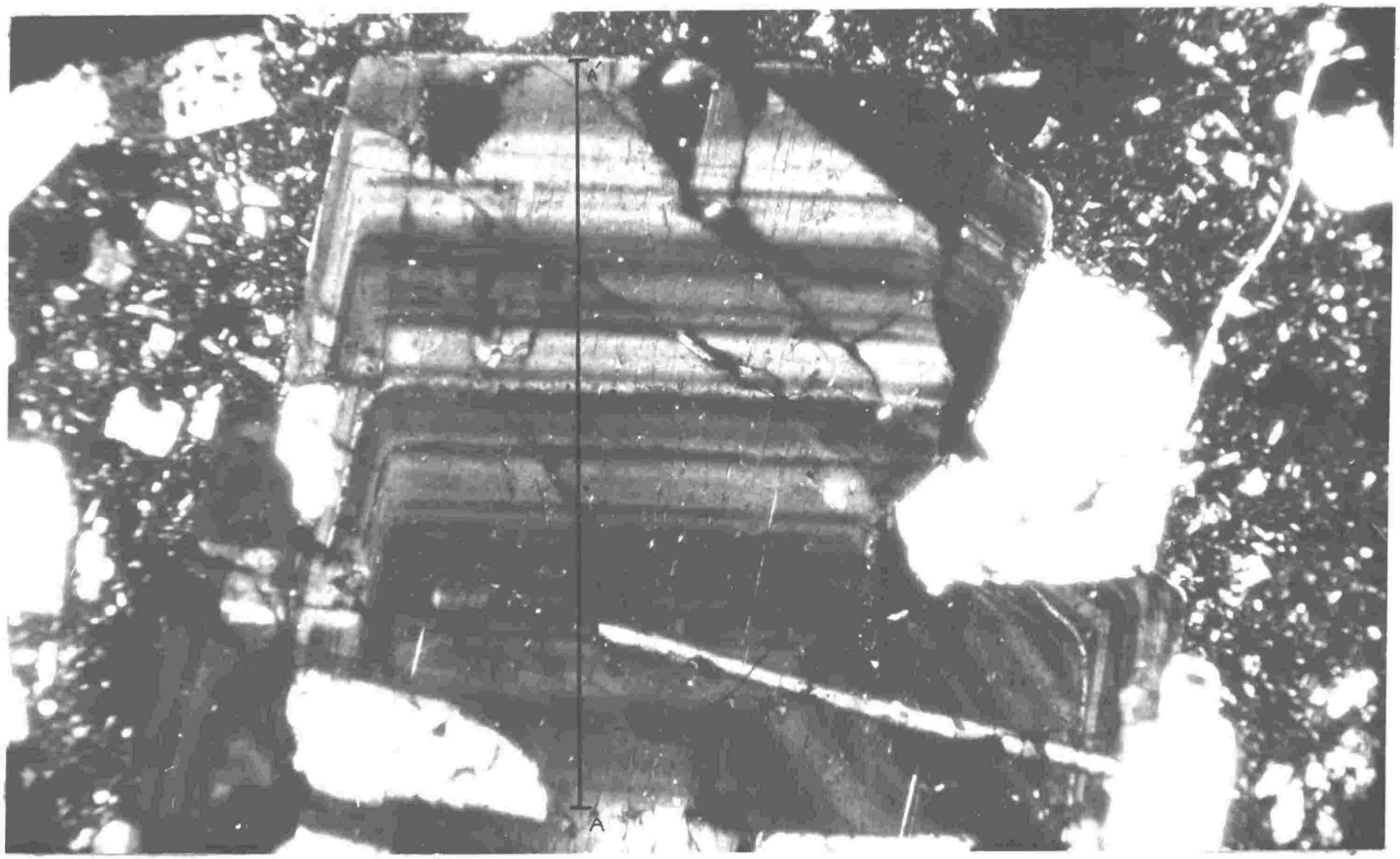

Plate 20. - Photomicrograph of plagioclase phenocryst from sample 11373. A compositional cross-section (A-A') for this crystal is given in Fig. 16. x 65.

volcanics. But here there is no association of a particular number of discordant breaks with a particular volcanic unit, and correlation of zoning breaks with previous eruptions is not clear-cut.

Theories on the origin of oscillatory zoning were discussed by Vance (1962), who concluded that oscillatory zoning forms in response to "recurrent supersaturation of the melt in anorthite, adjacent to the individual crystals" (a hypothesis originally advanced by Harloff in 1927). Bottinga, Kudo & Weill (1966) demonstrated the existence of large concentration gradients for a number of elements in the boundary zones (in a glass matrix) immediately surrounding plagioclase crystals. They were thus able to infer that plagioclase growth rates are diffusion controlled, which is a requirement of Harloff's theory for the origin of oscillatory zoning. They inferred from electron microprobe determinations of boundary-zone glass that the controlling diffusion rate in oscillatory zone formation is that of Al, not that of Ca and/or Na as had previously been postulated (Harloff, 1927; Vance, 1962). The cycle of oscillatory plagioclase crystallisation was considered by Bottinga, Kudo & Weill to be due to the systematic change in character of the crystal-liquid interface during diffusion-controlled crystallisation (Bottinga, Kudo & Weill, 1966, p. 801).

Resorption of plagioclase phenocrysts, particularly the cores of phenocrysts, resulting in inclusions of colourless or pale-brown glass (or occasionally sodic plagioclase) is a common feature in samples of the Bay of Plenty volcanics. Measurements on 250 plagioclase phenocrysts in 25 samples shows a strong correlation between the occurrence of plagioclase resorption and phenocryst size, more large phenocrysts

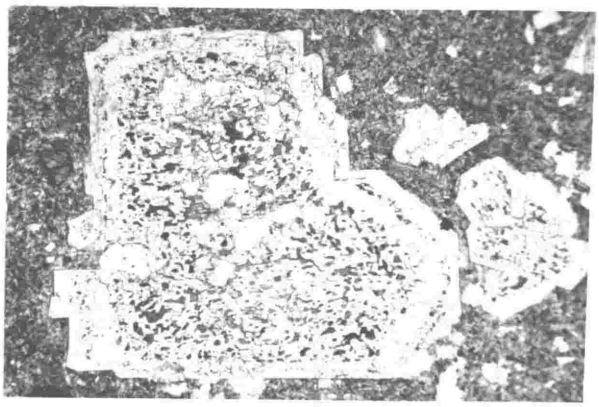

Plate 21. - Glass resorption zones in plagioclase phenocrysts. Photomicrograph, x 32.

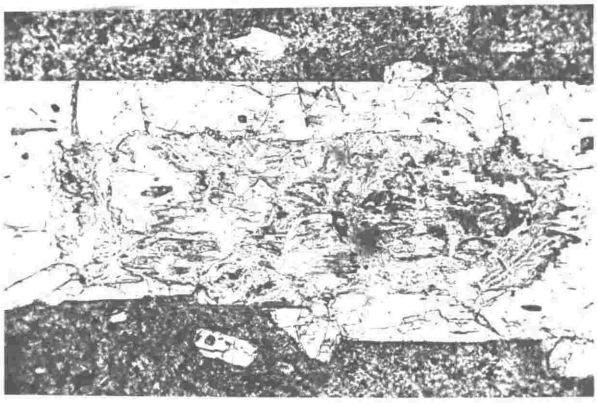

Plate 22. - Glass resorption zone in core of plagioclase phenocryst. Photomicrograph, x 70.

Plate 23. - Euhedral patches of glass formed by plagioclase resorption. Photomicrograph, x 460.

show resorption than do small phenocrysts (Fig. 17). Plagioclase resorption of this type is closely analogous to patchy zoning in plagioclase as described by Vance (1965). However, in Vance's examples the areas which were resorped were subsequently filled with a plagioclase more sodic than their original composition. The formation of a sodic plagioclase in patchy zones is seldom found in plagioclases of samples from the Bay of Plenty volcanics.

Although resorption zones are particularly common in the cores of phenocrysts from the Bay of Plenty volcanics, they are also found as discrete bands in the outer zones of plagioclase phenocrysts. Some phenocrysts have been observed with three or four discrete bands of resorption zones, but it has not been possible to determine whether these bands formed simultaneously or sequentially. Resorption patches tend to be subhedral, with strong crystallographic control over their form, the more euhedral patches being bounded by (001), (010) and (100) and showing quasi-rectangular outlines in section. Poikilitic inclusions in plagioclase cores are found more frequently in the phenocryst cores which are resorped, than in the cores which are not; supporting Vance's (1965) contention that the resorped patches are at least partially filled with magmatic material. Poikilitic inclusions in plagioclase from the Bay of Plenty volcanics consist predominantly of opaques, clinopyroxene, and orthopyroxene, with minor apatite. Vance (1965) considers that resorption of plagioclase in the formation of patchy zoning is probably due to fall in hydrostatic pressure related to upward displacement of the magma and this hypothesis is consistent with the available data from the Bay of Plenty volcanics.

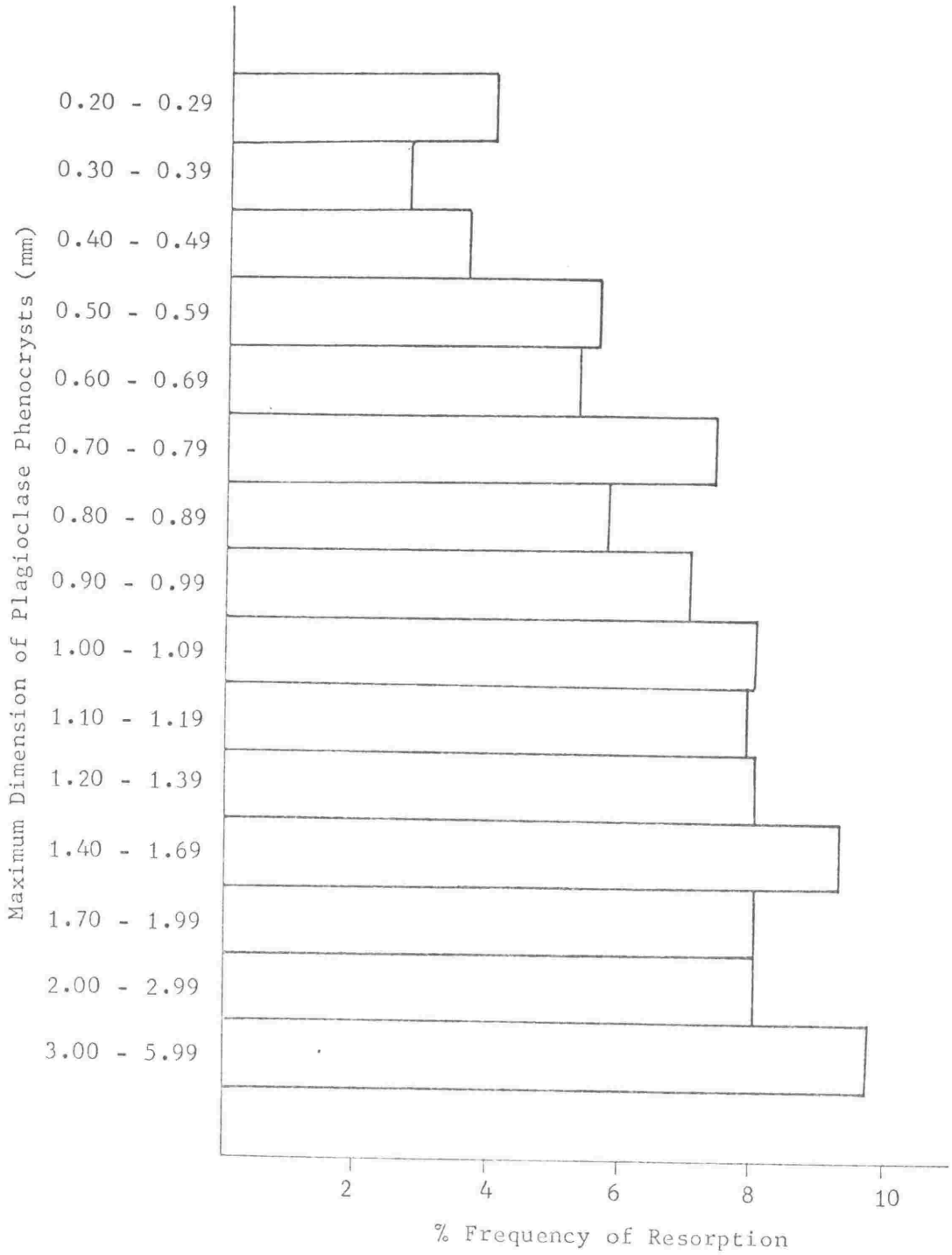

Fig. 17. - Histogram of frequency of resorption in plagioclase phenocrysts compared to their size, data from 25 Edgecumbe rock samples.

PYROXENE

Pyroxene is the second most abundant phenocryst mineral in the Bay of Plenty volcanics and both orthopyroxene and clinopyroxene occur in all samples examined. Modal pyroxene is in the range 2.3% - 18%, with total pyroxene as a proportion of the phenocrysts in the range 5% - 28%. Five pyroxene types have been recognised in samples of the Bay of Plenty volcanics; bronzite, hypersthene, ferro-hypersthene, augite and sub-calcic augite. Pigeonite, reported by Clark (1960 b) in the Tongariro National Park andesites, was not found in the Bay of Plenty andesites and dacites. The orthopyroxene : clinopyroxene ratio is extremely variable, but modal orthopyroxene generally exceeds modal clinopyroxene and the average value of the ratio would be about 2 : 1.

Pyroxene in the Bay of Plenty volcanics occur both as discrete phenocrysts and as components in glomeroporphyritic aggregates. Clinopyroxenes are more frequently found as components of glomerophenocrysts than are orthopyroxenes.

A large proportion of pyroxene phenocrysts are zoned, most showing normal zoning (i.e. decreasing Mg/Fe ratio from the core outwards) but some showing reverse zoning. Electron microprobe analyses of 40 phenocrysts from 5 samples show that about 20% of zoned pyroxene phenocrysts are reverse zoned, and that a higher proportion of clinopyroxenes than orthopyroxenes are reverse zoned.

Optical data for orthopyroxenes and clinopyroxenes in rock samples from Edgecumbe, Whale Island and White Island is given in Table 14.

TABLE 14

OPTICAL DATA FOR PYROXENES IN THE BAY OF PLENTY VOLCANICS

VOLCANO	SAMPLE NO.	ORTHOPYROXENE				CLINOPYROXENE				
		γ	2V	Composition (atomic %)		β	2V	Composition (atomic %)		
				Mg	Fe			Mg	Fe	Ca
EDGECUMBE	11206	1.695	70°	75	25	1.701	47°	35	27	38
	11327	1.705	63°	70	30	1.710	49°	33	29	38
	11387	1.698	69°	73	27	1.700	48°	36	26	38
	11349	1.700	67°	72	28	1.698	54°	36	23	41
	11215	1.701	66°	71	29	1.704	48°	33	29	38
WHALE ISLAND	11219	1.700	68°	73	27	1.697	49°	37	23	40
	11220	1.699	74°	75	25	1.698	48°	36	24	40
	11352	1.700	59°	68	32	1.701	46°	35	28	37
	11389	1.700	58°	68	32	1.702	50°	34	26	40
	11228	1.700	68°	72	28	1.701	51°	33	25	42
WHITE ISLAND	11386	1.700	70°	73	27	1.699	48°	35	26	39
	11363	1.698	60°	70	30	1.698	47°	37	25	38

NOTES (1) Values of γ, β and 2V are means of 5-10 determinations on different crystals from each sample. R.I. determinations are $\pm$ 0.002, and 2V determinations are $\pm$ 2°.

(2) Orthopyroxene compositions determined from optical data using Fig. 10 in Deer, Howie and Zussman (1963), Vol. 2, p.28.

(3) Clinopyroxene compositions determined from optical data using Fig. 41 in Deer, Howie and Zussman (1963), Vol. 2, p.132.

The mean orthopyroxene composition in most rocks appears from the optical data to be a bronzite, although the majority of orthopyroxenes analysed by electron microprobe proved to be hypersthenes. The optical properties of the ortho- and clinopyroxene show no significant differences between the three volcanoes. Hypersthenes and bronzites from the Bay of Plenty volcanics are weakly pleochroic with X = pale pinkish-brown, Y = neutral yellowish-brown colour, and Z = pale green.

A total of forty pyroxene phenocrysts from 5 rock samples were analysed by electron microprobe (A.E.I. model S.E.M.2) for the elements Mg, Fe and Ca. Analyses were made with an accelerating voltage of 30 kV and a beam current of 0.2mA. Two previously analysed augites were used as standards. Since only two standards were used, and since no orthopyroxene standards were available to the author, the analyses are not considered to be accurate (errors could be as high as $\pm$ 10-20% relative). However, precision is estimated to be $\pm$ 5% (relative deviation), which allows reasonable comparison of values to be made. For all phenocrysts showing zoning at least two analyses were made, one of the core of the phenocryst, and one of its rim. The full set of analyses are given in Appendix 1, and a set of average analyses for the core and rim of both orthopyroxene and clinopyroxene crystals in all analysed samples is given in Table 15. Ternary diagrams showing the total range of pyroxene analyses, and tie-lines joining coexisting ortho- and clinopyroxenes are given in Fig. 18. All analyses for pyroxenes in each of the five analysed samples are given as ternary diagrams in Fig. 19.

The range of Mg/Fe ratios in zoned phenocrysts varies considerably but tends to be similar in phenocrysts from the same rock sample.

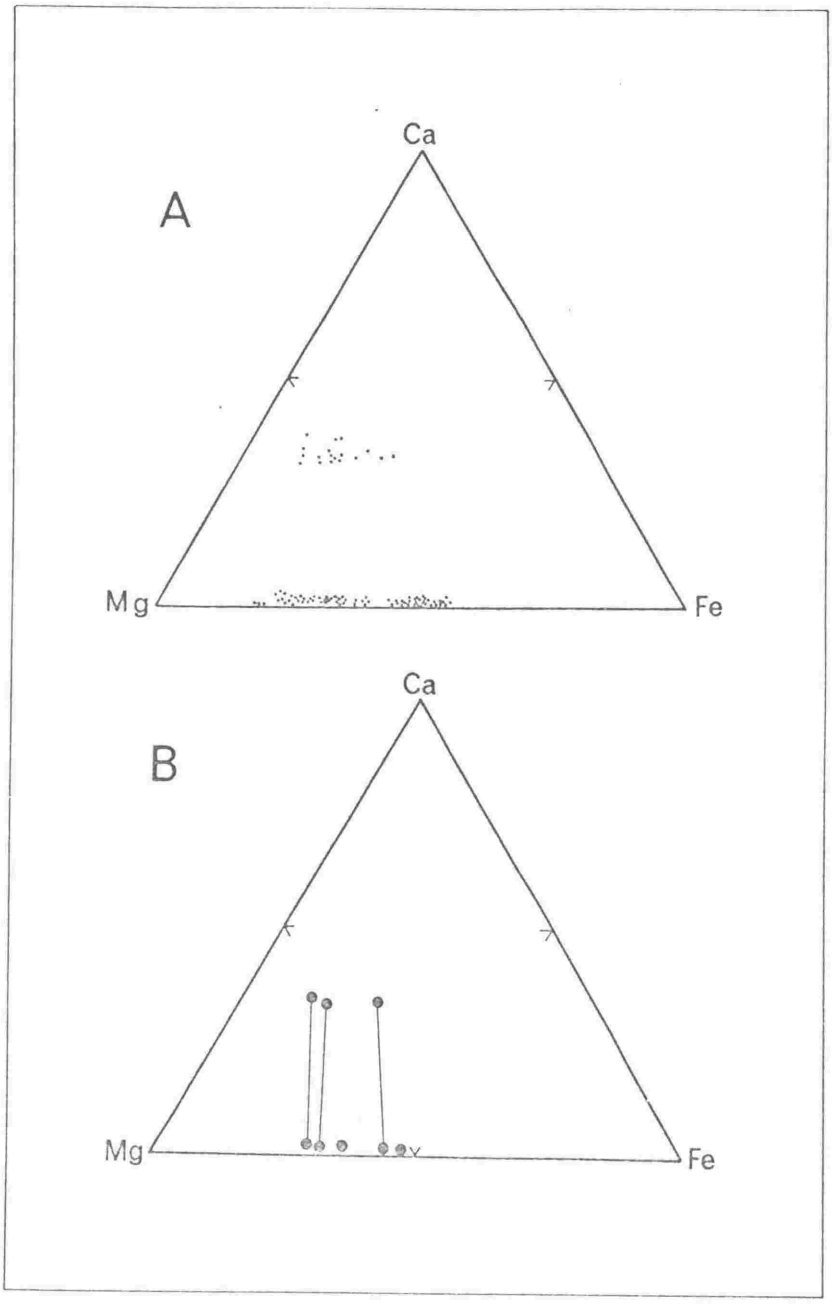

Fig. 18. - Electron microprobe analyses of pyroxene phenocrysts in the Bay of Plenty volcanics, shown as atomic percent Ca, Mg, Fe. (A) all analyses of pyroxene phenocrysts from the Bay of Plenty volcanics, analyses of pyroxenes in each of five rock samples are given separately in Fig. 19. (B) average pyroxene analyses in five rock samples of the Bay of Plenty volcanics, tie-lines join co-existing pyroxene pairs from three of the samples.

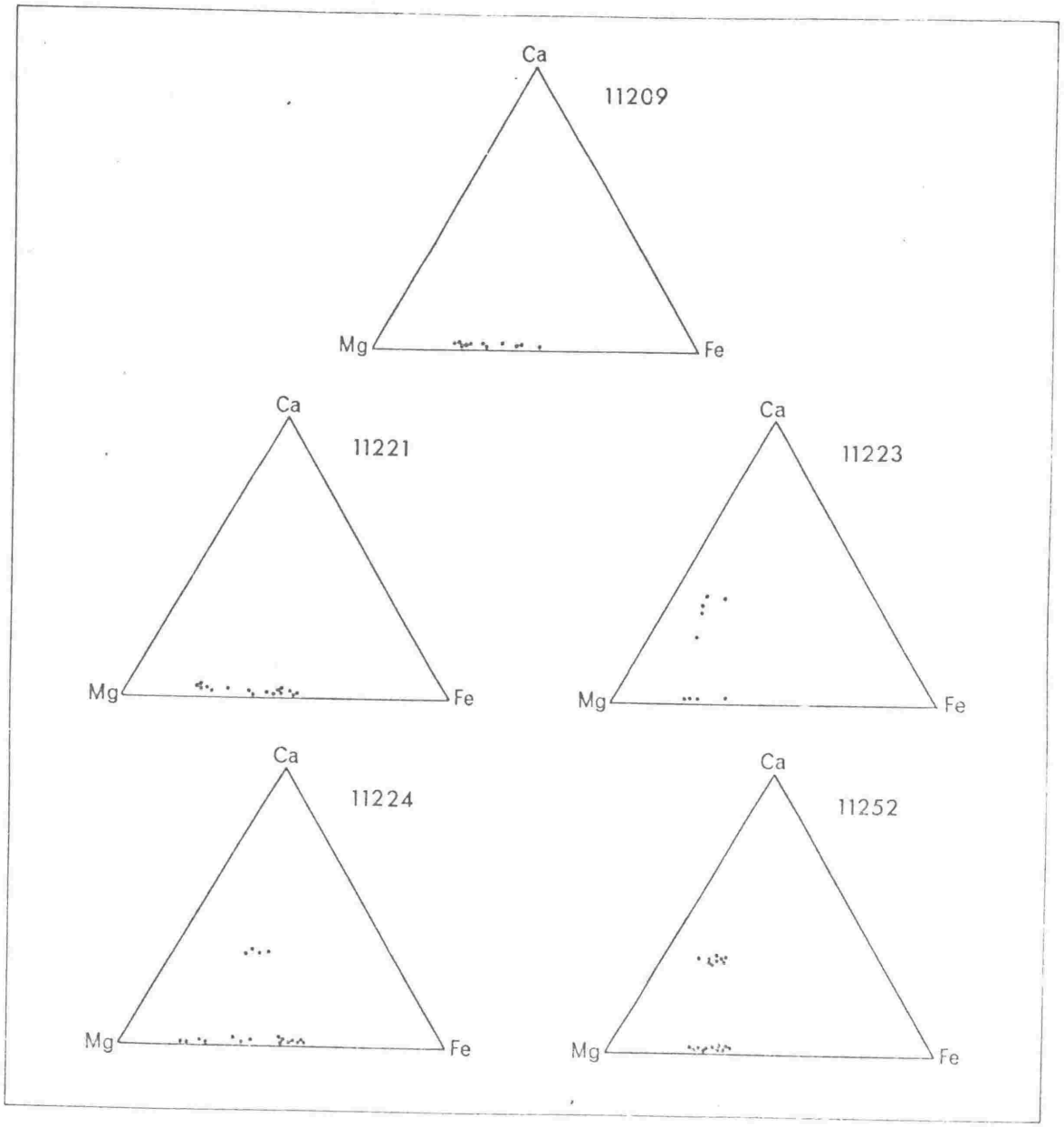

Fig. 19. - Electron microprobe analyses of pyroxene phenocrysts in each of five rock samples of the Bay of Plenty volcanics, plotted as atomic percent Ca, Mg, Fe. Analyses plotted here are listed in Table 37 (Appendix 1).

TABLE 15

ELECTRON PROBE ANALYSES OF PYROXENES - AVERAGES

SAMPLE NO.	PYROXENE TYPE	NO. OF CRYSTALS ANALYSED	ANALYSIS POSITION	ATOMIC PERCENT Fe	Mg	Ca	Mg/Fe RATIO
11252	Orthopyroxene	9	Core	30.84	66.92	2.24	0.94
			Rim	32.39	65.36	2.25	0.88
	Clinopyroxene	5	Core	17.53	49.36	33.11	1.23
			Rim	15.73	50.57	33.70	1.40
11209	Orthopyroxene	7	Core	28.92	68.86	2.22	1.04
			Rim	43.14	55.25	1.61	0.56
11221	Orthopyroxene	7	Core	46.41	52.12	1.47	0.49
			Rim	47.56	51.07	1.37	0.47
11223	Orthopyroxene	2	Core	23.75	74.06	2.19	1.36
			Rim	34.59	63.44	1.97	0.80
	Clinopyroxene	3	Core	11.13	53.76	35.11	2.10
			Rim	15.93	51.20	32.87	1.40
11224	Orthopyroxene	8	Core	37.31	61.09	1.60	0.71
			Rim	50.36	47.93	1.71	0.41
	Clinopyroxene	2	Core	25.86	40.52	33.62	0.68
			Rim	25.36	40.70	33.94	0.70

The maximum range in Mg/Fe ratio measured for a single phenocryst is 1.14-0.39, in an orthopyroxene whose core composition was $Mg_{70.7}$ $Fe_{27.1}$ $Ca_{2.2}$ and whose rim composition was $Mg_{46.9}$ $Fe_{52.0}$ $Ca_{1.1}$.

From the electron probe analyses it would seem that pyroxenes in the Bay of Plenty volcanics are predominantly augite and hypersthene, with ferro-hypersthene developed as a narrow zonal rim around many hypersthene phenocrysts. The rim of one augite crystal was the only sub-calcic augite analysed.

Electron probe analyses were made of crystals from too few samples to allow meaningful comparison of the pyroxene compositions in rocks from Edgecumbe and Whale Island. However, it can be seen that the core compositions of orthopyroxene phenocrysts in microdiorite xenoliths from both volcanoes are of higher Mg/Fe ratio than core compositions of pyroxenes in non-xenolithic samples.

SILICA MINERALS

Quartz

Quartz is the most abundant phyric silica mineral in the Bay of Plenty volcanics, occurring as a modal constituent in about 50% of Edgecumbe and Whale Island samples, but only in 10% of White Island and Manawahe samples. Its maximum modal concentration is 8.5% in a sample from Main Dome on Edgecumbe.

Quartz phenocrysts vary in size from 0.1 mm to 2.0 mm and virtually all of them are strongly resorped and show deeply embayed outlines. Some are surrounded by narrow reaction rims of pyroxene. Most quartz phenocrysts are cracked, and the position of embayments is controlled by the distribution and form of the cracks.

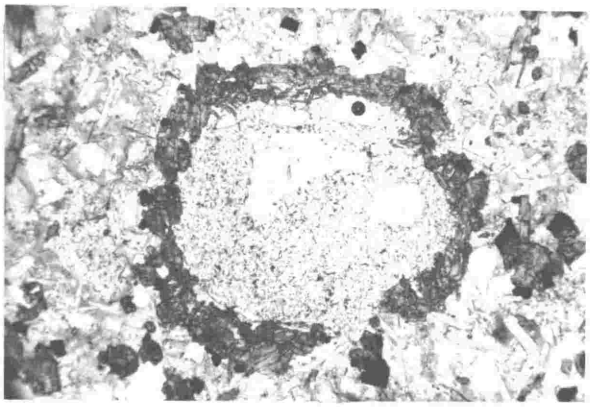

Plate 24. - Resorped quartz phenocryst rimmed by augite crystals. Photomicrograph, x 25.

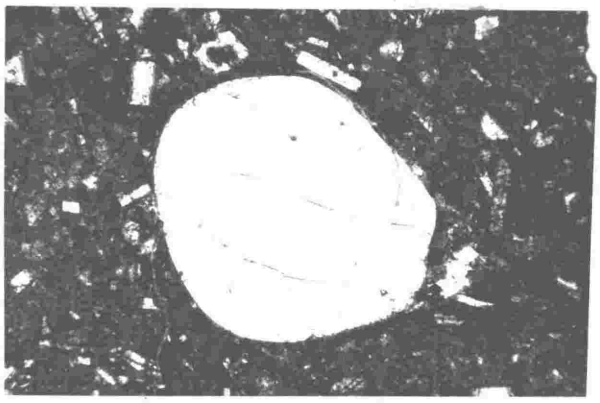

Plate 25. - Resorped quartz, crossed polarisers. Photomicrograph, x 28.

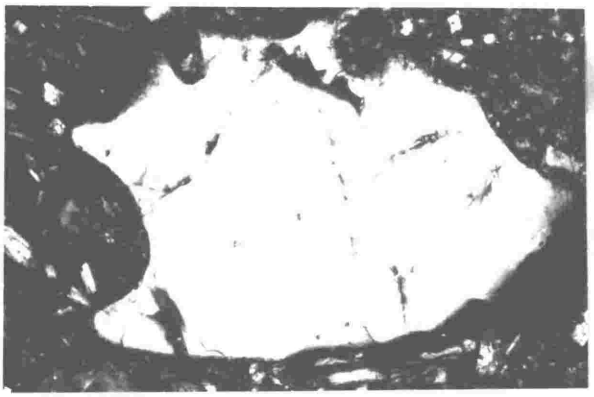

Plate 26. - Resorped quartz showing embayments, crossed polarisers. Photomicrograph, x 37.

It is possible that the strong resorption of quartz phenocrysts indicates a xenocrystic origin for them. However, the author considers it more likely that quartz crystallised from the andesitic and dacitic magmas at depth, and has been subsequently resorped due to the drop in hydrostatic pressure caused by upward movement of the magma on its way to the surface.

Quartz also occurs as poikilitic patches in the groundmass of some samples, and in such instances it is usually closely associated with cristobalite aggregates.

Cristobalite

Cristobalite has been recognised optically in the groundmass of at least 60% of samples from the Bay of Plenty volcanics, and it probably occurs in all pilotaxitic and partially-devitrified hyalopilitic groundmasses. Cristobalite generally forms small (1-5 micron) irregular patches in the groundmass, and it can easily be recognised from plagioclase and volcanic glass by its low R.I. ($\sim$ 1.485). It probably constitutes 20-40% of holocrystalline groundmasses. Groundmass cristobalite of this type is considered to be of primary origin.

Cristobalite aggregates up to 1 mm in diameter have been observed from pilotaxitic groundmasses in samples from White Island and Manawahe. The cristobalite aggregates give the groundmass a "patchy" appearance, and are often surrounded by a darker coloured rim (formed by either a dark brown zone in volcanic glass, or by a ring of minute specks of an opaque mineral). Large aggregates of cristobalite are particularly common in the holocrystalline

groundmass of microdiorite xenoliths, although the total concentration of cristobalite in such xenoliths is generally less than that in the andesites and dacites.

The presence of cristobalite in some groundmasses was confirmed by x-ray diffraction. However, it is often impossible to confirm cristobalite by this technique since most of the groundmasses contain abundant small (1-3 micron) laths of plagioclase, which are not easily separated from the rest of the groundmass. Virtual coincidence of the major cristobalite peak (d= 4.05 Å) with a strong plagioclase peak (d = 4.03 Å) makes it difficult to be certain of cristobalite identification unless the cristobalite/plagioclase ratio is high.

Cristobalite is also found as an amygdaloidal mineral in two samples from Edgecumbe and in this instance it is likely to be of secondary origin.

Tridymite

Tridymite has only been recognised in one sample (11390), a microdioritic xenolith in a Whale Island andesite. It occurs as small stubby crystals in the groundmass and is closely associated with cristobalite.

Opaline Silica and Chalcedony

Opaline silica is found in samples from Whale Island and White Island that have undergone extensive hydrothermal alteration. Chalcedony occurs as patches in a White Island dacite (11370), it does not appear to be amygdaloidal and its mode of formation is not clear.

HORNBLENDE

Hornblende is a phyric mineral in about 30% of samples from Edgecumbe and Whale Island, but it is not found in White Island and Manawahe samples. Originally it must have occurred in many more Edgecumbe and Whale Island samples than those in which it is now found, since a large proportion of samples from these volcanoes contain pseudomorphs after hornblende. The highest modal concentration of hornblende in samples of the Bay of Plenty volcanics, 4.0%, is found in a sample (11359) from West Dome on Whale Island. The average modal concentration of hornblende in those samples containing it is about 0.5%. No samples have sufficient hornblende to result in their classification as hornblende andesites or hornblende dacites (c.f. Clark, 1960 b).

Two hornblende types are present in the Bay of Plenty volcanics, common green hornblende and lamprobolite. Both types generally show opacitised rims and are frequently in various stages of alteration to pyroxene-opaque pseudomorphs. The two hornblende types are not easily distinguished in a number of samples and it appears that, at least in some cases, green hornblende is gradually altered to lamprobolite via an intermediate type of hornblende. The optical properties of the green hornblende and lamprobolite are given in Table 16.

Very few hornblende phenocrysts are free from alteration and virtually all of them have opacitised rims. As mentioned earlier pseudomorphs after hornblende are common in many samples. They generally consist of a mixture of pyroxene and opaque minerals,

TABLE 16

OPTICAL DATA FOR AMPHIBOLES

1. Green Hornblende:

X = very pale yellow X < Y < Z
Y = yellowish-green
Z = bluish-green

$2V = 65^{\circ} - 70^{\circ}$

$Z \wedge C = 20^{\circ}$

2. Lamprobolite:

X = straw-yellow X < Y < Z
Y = reddish-brown
Z = very dark brown

$2V = \sim 80^{\circ}$

$Z \wedge C = 13^{\circ}$

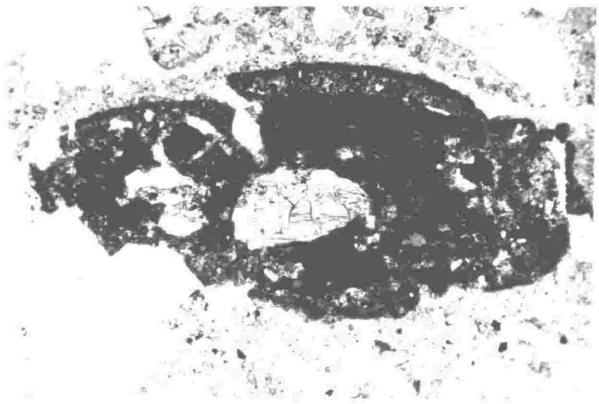

Plate 27. - Pseudomorph after hornblende. Composed mainly of pyroxene and opaques. Photomicrograph, x 30.

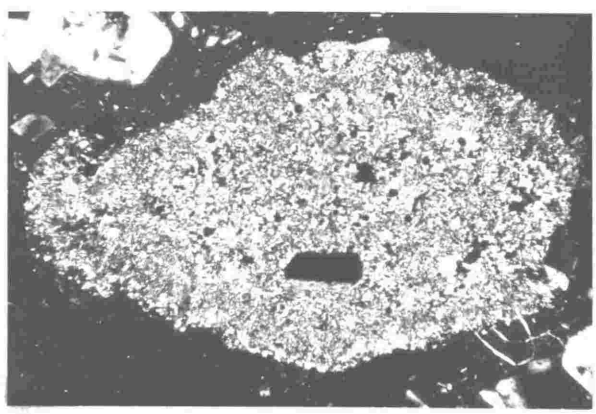

Plate 28.- Pseudomorph after hornblende consisting mainly of dendritic intergrowths of pyroxene, together with accessory opaques; crossed polarisers. Photomicrograph, x 30.

with the pyroxenes often exhibiting a "felted" texture with complex dendritic intergrowths of a number of pyroxene crystals.

BIOTITE

Biotite occurs as a phyric mineral in about 30% of samples from Edgecumbe and Whale Island, but whereas hornblende was more abundant in Whale Island samples than in Edgecumbe samples, the reverse is true for biotite. Biotite also shows substantial alteration in many samples, and many of those samples that do not contain modal biotite do contain pseudomorphs after biotite. Biotite is not generally as abundant as hornblende in those samples in which both minerals are found, and its average modal concentration is about 0.3%. Its maximum modal concentration is 2.3% in a sample (11210) from Main Dome on Edgecumbe.

Biotite has not been found in White Island samples collected by the author, but has been reported in some White Island rocks by Black (1970). Some Manawahe samples contain a few small (~ 20 micron) flakes of a yellow-brown pleochroic micaceous mineral which is tentatively identified as a variety of biotite.

There appears to be only one variety of biotite in samples of the Bay of Plenty volcanics, although it shows a variety of pleochroic schemes:

X = pale-yellowish, neutral colour.

Y = pale brownish-orange, pale red-brown, pale yellowish-green.

Z = very dark reddish-brown, very dark olive green.

The pleochroic schemes could be divided into those tending towards Z = dark green and those tending towards Z = dark brown. Such a division, however, would not have any general meaning since both

pleochroic schemes have been observed in different sections of the same crystal. Typical biotites from the Bay of Plenty volcanics have $\beta = 1.680\text{-}1.691$ and $2V = 5^{\circ}\text{-}10^{\circ}$.

Virtually all the biotite phenocrysts show opacitised rims and many are completely pseudomorphed, with pseudomorphs consisting of an opaque rim, and typically a core of pyroxenes, magnetite and felspar. Comparison of partial pseudomorphs after biotite and hornblende indicates that felspar is usually present in pseudomorphs after biotite, but is generally absent in pseudomorphs after hornblende. This difference makes it possible to decide on pseudomorph parentage in many cases where the parent crystal form is not sufficiently well-preserved to indicate which mineral has been replaced.

TITANOMAGNETITE

Titanomagnetite is a ubiquitous constituent in samples of the Bay of Plenty volcanics and occurs both as phenocrysts (0.1-0.5 mm) and as small grains in the groundmass. Its average modal concentration is about 1%, but it can be as high as 5-6% in samples which have been affected by surface oxidation (titanomagnetite is formed as an alteration product in such samples).

Titanomagnetite is also found as small (1-10 micron) poikilitic inclusions in virtually all pyroxene crystals in the Bay of Plenty volcanics. In many instances large poikilitic inclusions of titanomagnetite (up to 0.3 mm) are found in pyroxene, hornblende and plagioclase phenocrysts.

Ti contents have been determined by emission spectrography (Duncan & Taylor, 1969) and are in the range 5-8% Ti.

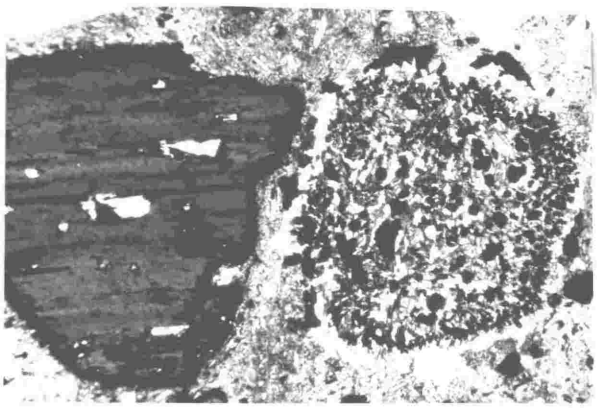

Plate 29. - Biotite (left) and a pseudomorph after biotite (right). The pseudomorph consists of pyroxene, felspar and opaques. Photomicrograph, x 35.

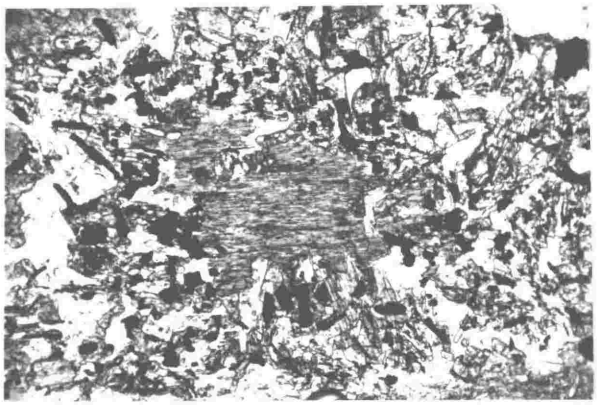

Plate 30. - Pseudomorph after biotite consisting of relict biotite (centre) surrounded by felspar, pyroxene and opaques. Photomicrograph, x 75.

ACCESSORY MINERALS

Small crystals of apatite and rutile are present as accessories in most of the rock samples. Zircon, however, has only been identified in two or three samples and is uncommon in the Bay of Plenty volcanics.

ALTERATION PRODUCTS

The minerals mainly subject to alteration in the Bay of Plenty volcanics are pyroxene, hornblende, and biotite. Hornblende and biotite in particular show opacitised rims and are frequently totally altered, with only pseudomorphs remaining (see above). Such pseudomorphs usually comprise opaques, pyroxene and minor felspar (plagioclase definitely identified, K - felspar may also be present). Pyroxenes usually alter to a brownish material which probably contains a combination of iddingsite, limonite, goethite, and magnetite. Chlorite is an occasional alteration product of biotite.

A detailed study of hydrothermal alteration on Whale Island and White Island has not been made, but the major alteration product in these areas appears to be secondary silica; in the form of opaline silica and cristobalite; which has been introduced during the leaching of the rock by hydrothermal solutions.

PETROLOGY OF ROCK SAMPLES FROM SEAMOUNTS NEAR WHITE ISLAND, BAY OF PLENTY

Accepted for publication in N.Z. Journal of Geology and Geophysics. The paper is given here in manuscript form.

PETROLOGY OF ROCK SAMPLES FROM SEAMOUNTS NEAR WHITE ISLAND, BAY OF PLENTY

A.R. Duncan,

Geology Department, Victoria University of Wellington

ABSTRACT

Descriptions of andesitic and dacitic rock samples, dredged from near the summits of five seamounts in the vicinity of White Island, are presented. Mineralogy and texture of the samples suggests that this group of seamounts may have been the source of the andesitic Loisels and Leigh pumices.

INTRODUCTION

Rock samples described in this paper were collected by the N.Z. Oceanographic Institute (cruise "Ngatoro") in the Bay of Plenty during October 1966 from seamounts between 6 and 44 km from White Island, mainly northwest and west of the island. The seamounts together with White Island are referred to as the White Island Volcanic Complex. Fig. 1 shows sample locations and bathymetry (Bathymetry by H.M.Pantin).

Sample localities were assigned station numbers * (E.630, E.636, etc.) and rock fragments from particular stations were grouped on the

---

* All station and sample numbers are those given in the N.Z.O.I. register for cruise "Ngatoro".

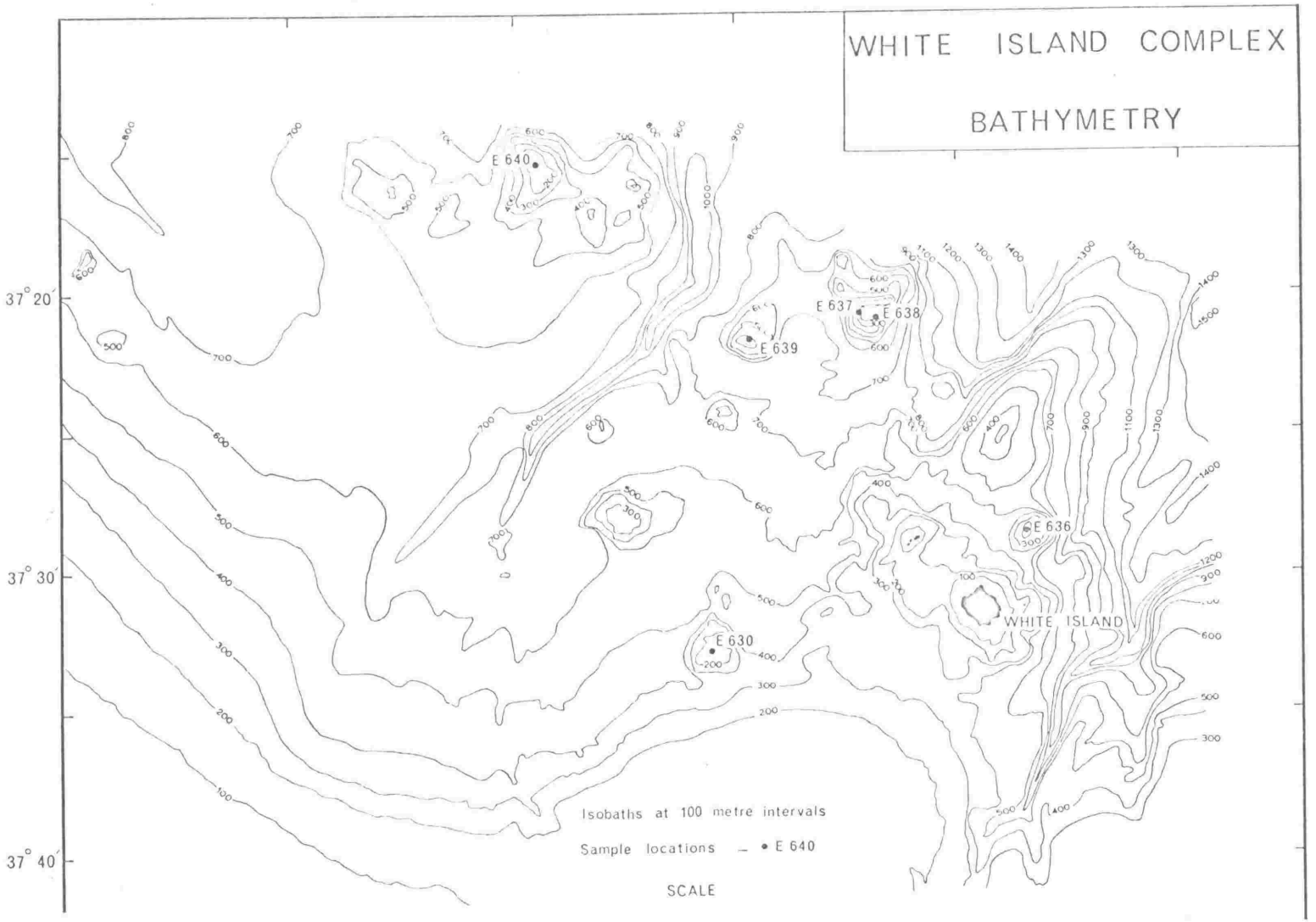
WHITE ISLAND COMPLEX
BATHYMETRY
37° 20′
37° 30′
37° 40′
E 640
E 637
E 638
E 639
E 636
E 630
WHITE ISLAND
Isobaths at 100 metre intervals
Sample locations — • E 640
SCALE

basis of colour and vesicularity, each group being given a sample number (T.1., T.1.A., etc.). Rock samples were dredged in depths of 120-500 m and dredgehauls from all localities except E.638 contained marine organisms. Many rock fragments are covered by a veneer of manganese and iron oxides and hydroxides; and a layer of calcite, containing organic remains, partially covers two pumiceous fragments (Fig. 2).

Samples sufficiently vesicular to float when dry are termed pumiceous, and the remainder are termed non-pumiceous. All the pumiceous rocks, on the evidence of the refractive indices of their colourless glass, fall within the andesite-dacite range, although a more precise identification is generally impossible (see p.[12.5]). All the non-pumiceous rocks are classified as andesitic by their phenocryst mineralogy; all are labradorite andesites according to Clark's (1960) classification.

PETROGRAPHY

Modal analyses of 11 rocks are presented in Table 1. Total groundmass content ranges from 56.5% to 95.5%. All contain phenocrystic plagioclase, magnetite and small amounts of apatite and rutile. With the exception of sample E.637 T.1, they all contain phenocrystic pyroxene.

Groundmass textures in non-pumiceous samples are generally pilotaxitic and hemicrystalline (Fig. 3); some samples show conspicuous flow texture. Sample E. 637 T.1. has unusual groundmass texture and mineralogy with considerable quartz and no ferromagnesian minerals, probably indicating deuteric or post-eruptive alteration. Sample E.638 T.2.A contains the only xenolith observed, a volcanic fragment consisting

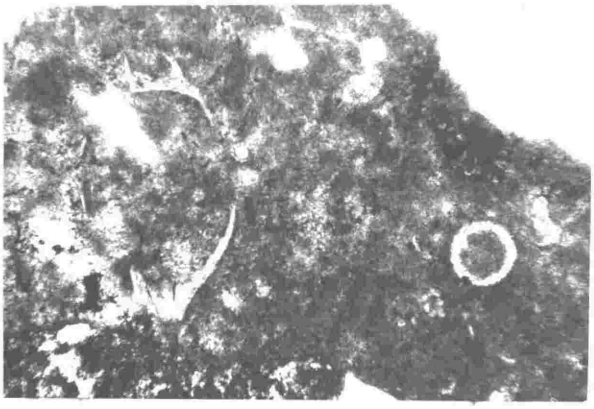

Fig. 2. - Photomicrograph showing a calcite overgrowth on sample E.637 T.1 containing organic remains. x 70.

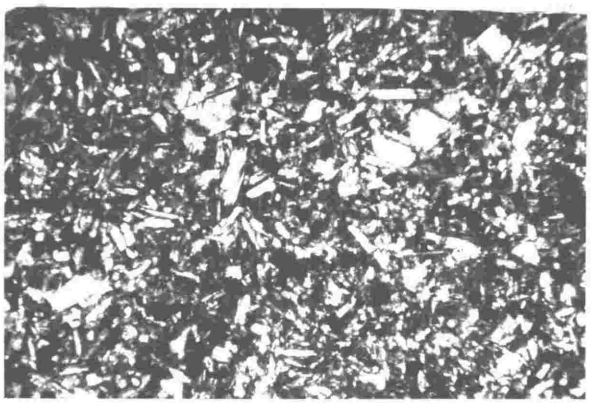

Fig. 3. - Photomicrograph illustrating typical groundmass texture of non-pumiceous seamount samples. Crossed polarisers, x 95.

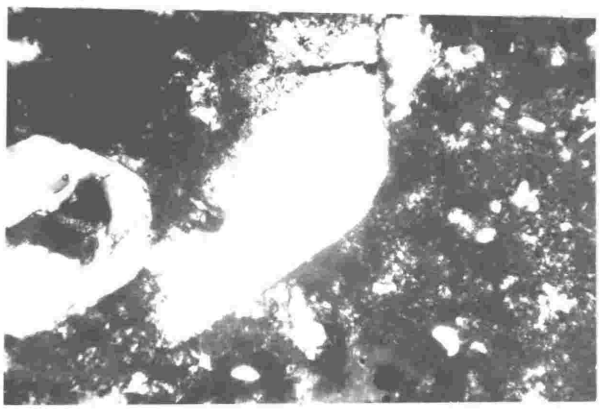

Fig. 4. - Photomicrograph of resorped quartz phenocryst in sample E.637 T.1. Crossed polarisers, x 95.

TABLE 1

MODAL ANALYSES OF BAY OF PLENTY SEAMOUNT SAMPLES

SAMPLE NO.	E.630 T.1.	E.636 T.1.	E.636 T.2.	E.637 T.1.	E.637 T.2.	E.638 T.1.A	E.638 T.1.B	E.638 T.2.A	E.638 T.2.B	E.639 T.1.	E.640 T.1.
Rock Type *	N.P.	N.P.	N.P.	N.P.	N.P.	P.	P.	P.	P.	P.	N.P.
%Groundmass	56.5	64.2	58.3	68.7	86.4	89.3	93.5	95.5	94.6	93.0	62.1
%Plagioclase	33.3	27.9	29.4	10.3	9.3	7.4	5.3	4.1	4.4	5.4	28.1
%Orthopyroxene	4.2	3.7	8.8	-	1.5	0.9	1.0	0.2	0.7	1.0	5.8
%Clinopyroxene	3.2	3.1	3.2	-	-	tr.	-	-	-	-	2.2
%Quartz	-	-	-	9.9	-	-	-	-	-	0.2	-
%Hornblende	-	-	-	-	-	1.9	-	-	-	tr.	-
%Opaques	2.8	1.1	0.3	1.1	1.2	0.5	0.2	0.2	0.3	0.4	0.5
%Zeolites	-	-	-	-	1.6	-	-	-	-	-	-
%Biotite	-	-	-	-	-	-	-	-	-	-	0.5
%Calcite	-	-	-	-	-	-	-	-	-	-	0.6
Total Crystal Content	43.5	35.8	41.7	31.3	13.6	10.7	6.5	4.5	5.4	7.0	37.9

Crystals whose maximum dimension was less than 0.05 mm were counted as groundmass. Groundmass % also includes vesicle space.

*P. - Pumiceous

N.P. - Non-pumiceous

of colourless glass, plagioclase, pyroxene, and magnetite, set in a chloritised matrix.

The optical properties of the plagioclase, pyroxene, and volcanic glass are given in Table 2.

Plagioclase

Plagioclase occurs in all sizes from crystallites up to phenocrysts with a maximum length of 4 mm. Phenocrysts are generally euhedral or subhedral. The larger phenocrysts seldom have flow alignment and are often grouped, usually with pyroxene crystals of similar size, to form glomerophenocrysts. Flow texture, when present, is usually defined by the alignment of small plagioclase crystals.

Normal and oscillatory zoning are common in the plagioclase crystals of all samples, usually the cores are normal and the rims oscillatory. Inclusions of brown glass are thought to represent material resorped due to a drop in pressure, a process suggested by Vance (1965). In the present case the drop in pressure causing resorption was apparently accompanied by a sufficiently rapid temperature drop to prevent recrystallisation. The situation thus differs to some extent from Vance's examples, in which the resorped material recrystallised to a plagioclase more sodic than that surrounding it.

The compositions of several phenocryst cores were determined for each sample by measuring the extinction angles of albite twin lamellae in sections $\perp$ a. They range from An_{39} to An_{70}, and are mostly close to An_{55}. The outer zones of some phenocrysts are as sodic as An_{20}. The phenocrysts commonly include small crystals of pyroxene, magnetite, and apatite.

TABLE 2

MINERALOGY OF BAY OF PLENTY SEAMOUNT SAMPLES

	Plagioclase Core Composition %An.			Orthopyroxene	Pyroxene	Clinopyroxene	Glass
SAMPLE NO.	No.	Range	Aver.	$2V_x$	n_y	$2V_z$	$n_{min.}$
E.630 T.1.	10	63-42	48	78^o, 80^o, 81^o	-	58^o	-
E.636 T.1.	10	60-40	49	58^o, 64^o, 54^o	-	50^o, 49^o	
E.636 T.2.	10	70-39	53	68^o, 64^o, 60^o	-	54^o, 52^o	
E.637 T.1.	10	64-40	49	-	-	-	-
E.637 T.2.	10	67-40	56	64^o, 64^o, 63^o	-	-	-
E.638 T.1.A.	10	67-42	56	68^o, 72^o, 74^o	1.695	-	1.508
E.638 T.1.B.	10	64-40	52	60^o, 58^o	1.702	-	1.511
E.638 T.2.A.	10	67-40	51	64^o, 64^o, 62^o	1.701	-	1.509
E.638 T.2.B.	8	70-42	53	66^o, 68^o	1.698	-	1.510
E.639 T.1.	10	70-42	57	62^o	1.699	-	1.510

Samples E.630 T.1., E.636 T.1., and E.636 T.2. were only available as thin sections, consequently refractive indices for the pyroxenes could not be determined.

Orthopyroxene

Orthopyroxene occurs as phenocrysts up to 2 mm long, and as crystals of groundmass size. Some phenocrysts are euhedral, but most are subhedral or anhedral. Pleochroism is usually faint with X = pale pink and Z = pale green. Inclusions of magnetite and rutile are common.

$2V_x$ ranges from 54° to 81° but the range in any one sample is not more than 10°. The range is partly due to zoning in some crystals. The refractive index for Y ranges from 1.695 to 1.702 for crystals with a range of $2V_x$ from 58° to 74°. According to 2V and refractive index variation diagram given by Deer, Howie and Zussman (1963, v.2,p.28) the orthopyroxenes are bronzite and hypersthene.

The close spatial association of orthopyroxene and clinopyroxene described by Clark (1960) for the andesites of Tongariro Subdivision is not shown by these samples.

Clinopyroxene

Since clinopyroxene phenocrysts are generally smaller than those of co-existing orthopyroxene and occur in significant amounts only in the non-pumiceous samples, which are more crystalline than the pumiceous samples, it is inferred that clinopyroxene was one of the last minerals to crystallise.

$2V_z$ ranges from 49° to 58° and thus, in the absence of refractive index determination (only thin sections were available), the clinopyroxene is classified as augite. Inclusions of magnetite are present in most phenocrysts.

Hornblende

Hornblende is present in significant quantity in sample E.638 T.1.A, and as a trace in E.639 T.1. In E.638 T.1.A it occurs as a group of

phenocrysts, most of which are subhedral and about 0.5 mm long. $2V_x$ ranges from 64° to 68°, $Z \wedge c = 20°$ and they are strongly pleochroic with X = fawn, Y = brownish-green, and Z = dark olive-green. It is most probably common hornblende. The absence of a reaction rim surrounding crystals in either sample is a conspicuous feature.

Silica Minerals

Quartz is present in two samples only, E.637 T.1. and E.639 T.1. In both, quartz phenocrysts about 0.5 mm long have rounded outlines and are resorped (Fig. 4). In E.637 T.1. the groundmass contains anhedral patches of quartz, some of which are made up of a number of quartz crystals with sutured contacts.

Cristobalite, present as scattered patches in the groundmass of E.636 T.1., the most crystalline groundmass examined, probably represents a late-crystallising phase, or a devitrification product.

Glass

Glass is rare in the non-pumiceous samples but is abundant in the pumiceous ones. Refractive indices of the colourless glass in the groundmasses of pumiceous samples, given in Table 2, range from 1.508 to 1.511. Since the refractive index measured was the lowest for the sample, the pumiceous samples are thought to be andesitic or dacitic.

Iron Oxides

An opaque mineral present in all the samples was identified as magnetite by X-ray diffraction. It is ubiquitous in the groundmass of all samples; is found as inclusions in pyroxene and plagioclase; and also as reaction rims round some pyroxene crystals in samples where

deuteric or post-eruptive alteration is considerable. Limonite is present as an alteration product.

Zeolites

Zeolites occur only in sample E.637 T.2, where they occur as amygdaloidal clusters. Individual crystals are so small that the particular zeolite mineral present could not be identified.

CONCLUSIONS

On the whole, the seamount samples cannot be distinguished mineralogically from the volcanic rocks of White and Whale Islands. However, half of the seamount samples are pumiceous, whereas no pumiceous andesite or dacite has been found on the two islands.

The Leigh and Loisels pumices were described by Wellman (1962) who suggested that their distribution indicated a source in the Bay of Plenty. The mineralogy and refractive indices of the glasses in the pumices was described as andesitic by Challis in an appendix to Wellman's (1962) paper. A summary of Challis' data for the Leigh and Loisels pumices, together with some additional data on the Loisels pumice, is presented in Table 3. Comparison of the data with that for the seamount samples in Tables 1 and 2 shows a sufficiently close correspondence to indicate that the seamounts are a possible source for the Leigh and Loisels pumices. Most of the White Island Complex lies within the area that Wellman (1962, Fig. 3) considered to contain the source of the Loisels pumice.

Part of the Loisels pumice consists of a strongly banded pumice, with bands of pale grey (dacitic) and dark grey (andesitic) pumice, the

TABLE 3

MINERALOGY OF LOISELS AND LEIGH PUMICES

LOISELS PUMICE

	%	
Groundmass	98.0	Glass $n_{min.}$ = 1.511 (Challis, 1.510)
Plagioclase	0.8	
Orthopyroxene	0.3	Orthopyroxene: $2V_x = 62^o$, $n_y = 1.699$
Clinopyroxene	0.3	
Opaques	0.6	Plagioclase core composition (%An): No. determined: 6 Range: 63-44 Average: 52
Total Crystal Content	2.0	

LEIGH PUMICE (data from Challis)

Mineralogy: Groundmass, plagioclase, orthopyroxene, clinopyroxene, magnetite.

Glass $n_{min.}$ = 1.516

darker bands containing a higher proportion of magnetite than the paler ones. Strongly banded pumice was not observed in any of the seamount samples. A pale-coloured, unbanded, dacitic pumice in the Loisels deposits at Ohui Beach was considered by Wellman (1962) to be from the same source and erupted simultaneously with the banded variety, and may be the equivalent of the pumice from E.638. The absence of banded pumice in samples from this locality may be due to the observed lesser tendency of the darker pumice varieties to become waterlogged (Wellman, pers. comm.).

Because of the distribution of the Ohui Ash and the Loisels pumice Wellman (1962) suggested that both came from the same eruptive centre. The Ohui Ash is described by Challis in Wellman (1962) as a rhyolitic ash in which green hornblende is a distinctive constituent. None of the seamount samples are rhyolitic, but two samples contain green hornblende with very similar optical properties to the hornblende in the Ohui Ash. The present very limited sampling of the White Island Complex has not yielded any material of composition sufficiently similar to the Ohui Ash to infer that its source might lie within the Complex.

ACKNOWLEDGEMENTS

The writer thanks the New Zealand Oceanographic Institute for providing the samples and thin sections for this study. Thanks are also due to Professor H.W. Wellman, Dr H.M. Pantin and Dr J.W. Brodie for their helpful and constructive criticism of the manuscript.

REFERENCES

CLARK, R.H. 1960: Petrology of the Volcanic Rocks of Tongariro Subdivision. Appendix 2., in GREGG, D.R. 1960: The Geology of Tongariro Subdivision. N.Z. Geol. Surv. Bull. n.s. 40: 107-123.

DEER, W.A.; HOWIE, R.A.; ZUSSMAN, J. 1963: Rock-forming Minerals Vol. 2, Chain Silicates. Longmans, Green, London.

VANCE, J.A. 1965: Zoning in Igneous Plagioclase: Patchy Zoning. Jour. Geol. 73: 636-651.

WELLMAN, H.W. 1962: Holocene of the North Island of New Zealand: a Coastal Reconnaissance. Trans. Roy. Soc. N.Z. 1 : 29-99.

VOLCANIC ACTIVITY ON WHITE ISLAND, BAY OF PLENTY, 1966-1969

Part 2 Tephra Eruptions - Stratigraphy and Petrography

Accepted for publication in N.Z. Journal of Geology and Geophysics. The paper is given here in manuscript form.

VOLCANIC ACTIVITY ON WHITE ISLAND, BAY OF PLENTY, 1966-1969

Part 2. Tephra Eruptions - Stratigraphy and Petrography

A.R. Duncan and C.G. Vucetich

Geology Department, Victoria University of Wellington

ABSTRACT

During the period November 1966 to April 1969, two vents within the crater of White Island have intermittently erupted approximately 1,700,000 m^3 of tephra, composed mainly of finely comminuted altered andesite. The tephra stratigraphy, grain-size distribution, and mineralogy are described.

INTRODUCTION

The western portion of the crater of White Island contains a number of vents which have been formed in the last 50 or 60 years, their names and locations are given in Fig. 1. The most recently formed vents are on the top and flanks of Crater Ridge, a 70 m high bench of andesitic blocks and debris, which was formed by a landslide from the southwestern crater wall in 1914. During the last three years vents on Crater Ridge have erupted tephra, with intermittent eruption from November 1966 to March 1967, continuous eruption from February to April 1968, and intermittent eruption from May 1968 to the time of writing (April, 1969).

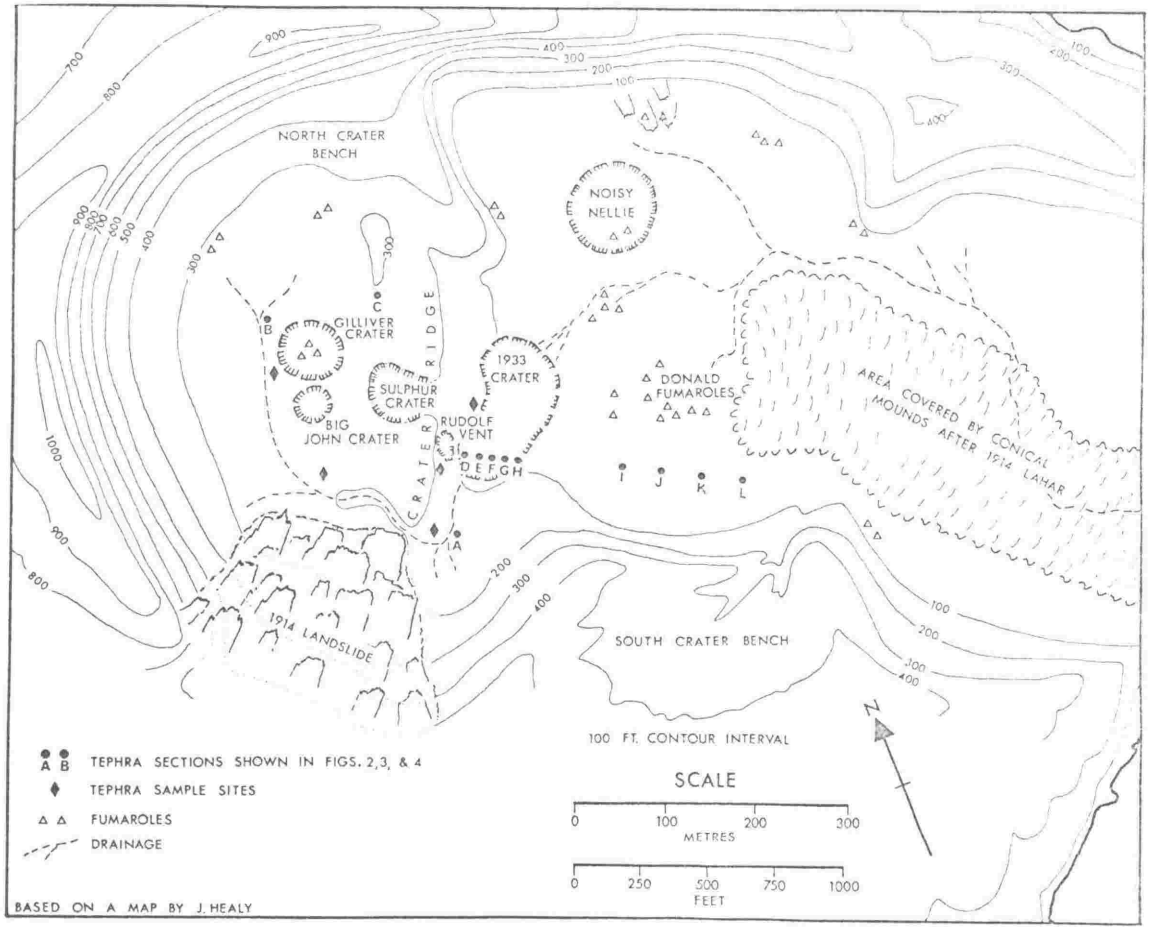

Fig. 1. - Map of the crater of White Island.
Based on an unpublished map by Mr J. Healy.

The tephra eruptions have been from two distinct vents, the second vent becoming active only after tephra eruption from the first vent had ceased. The sequential nature of eruptions from these vents has enabled the stratigraphic distinction of material erupted from them.

The chronology of the volcanic activity at White Island in the period 1966-1969 is given in part 1 of this series of papers. A brief summary of the most important events with regard to tephra eruptions is given below.

Gilliver Crater was formed in November 1966 on Crater Ridge immediately to the north of Big John Crater (see Fig. 1), and erupted tephra intermittently from November 1966 to March 1967. During mid-1967 the part of the eastern flank of Crater Ridge which forms the western wall of 1933 Crater was at high temperature over about half its area, with the rock surface at red-heat near fumarole mouths. The largest red-hot fumarole, named Rudolf by H.W. Wellman, began erupting tephra in late-January 1968. Tephra eruption from Rudolf Vent was continuous from February to April 1968, and has been intermittent since then with long periods during which only volcanic gasses (mainly steam) have been emitted.

TEPHRA, STRATIGRAPHY AND DISTRIBUTION

Most of the tephra erupted from White Island in the last three years has fallen inside the crater, and almost all tephra which fell outside the crater was removed in a matter of days by wind and rain. As the recent tephra deposits on White Island are confined to a very local area, formal stratigraphic terminology is not applied to them, and they are named for the vent from which they were erupted as Gilliver

tephra and Rudolf tephra.

If further eruptions of White Island resemble the tephra eruptions of the last few years, it will be convenient to have datum horizons from which to measure the new deposits. Hence, some sections of Gilliver and Rudolf tephras have been measured in detail. An earlier tephra erupted from Big John Crater in 1965 was observed in some sections and is also recorded.

The positions where sections were measured are shown in Fig. 1, and the sections themselves in Figs. 2 and 3. Standard sections were measured at favourable topographic sites and at distances of 50 - 150 m from the edge of the respective source vents. Due to distance from the source vent the standard sections contain few of the larger blocks which were ejected in various stages of the eruptions, but are otherwise representative. In fig. 2 the standard section for Gilliver tephra is taken as the upper portion of section A, the standard section for Big John tephra is taken as the lower portion of section A, and the standard section of Rudolf tephra as the upper portion of section C. Fig. 4 shows the Gilliver and Big John tephras in section A, together with older underlying tephras.

The sections of Fig. 3 were measured at intervals along a line from Rudolf Vent to station XII of the V.U.W. level net (see part 1 of this series of papers). Sections D to H are on the floor of 1933 Crater and the lower portion of these sections is a mixture of airfall tephra and alluvium. The upper portion of sections D to H is a reddish ash (marked 'X' in Fig. 3) which was falling at the time the sections were measured and is thought to be entirely airfall; hence variations in its

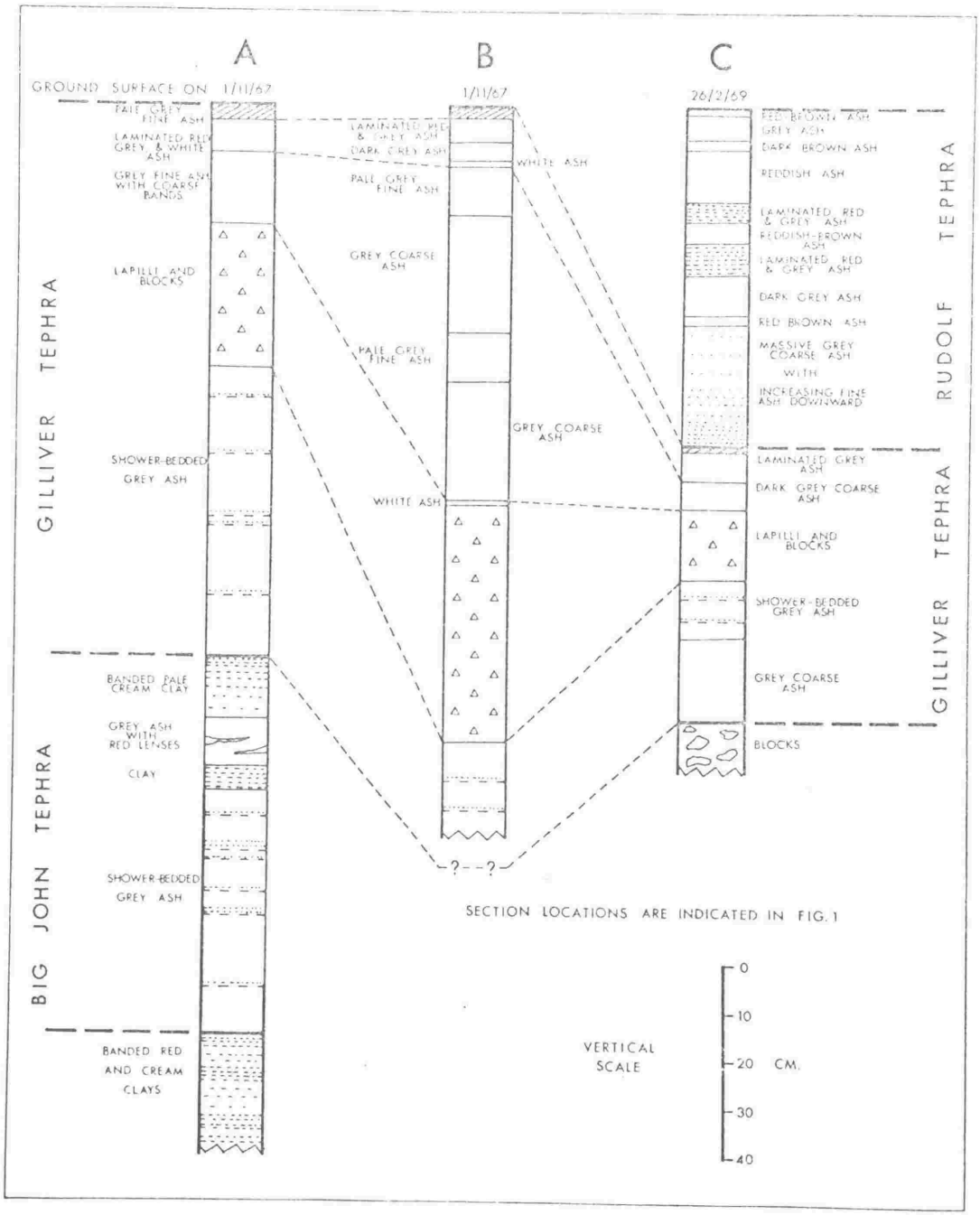

Fig. 2. - Detailed tephra sections incorporating standard sections for Big John, Gilliver and Rudolf tephras.

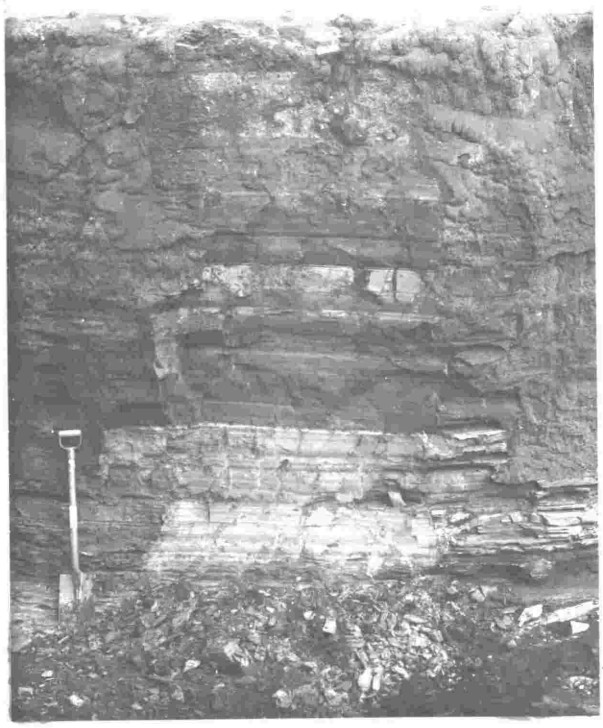

Fig. 4. - Tephra section equivalent to Section A in Fig. 2.

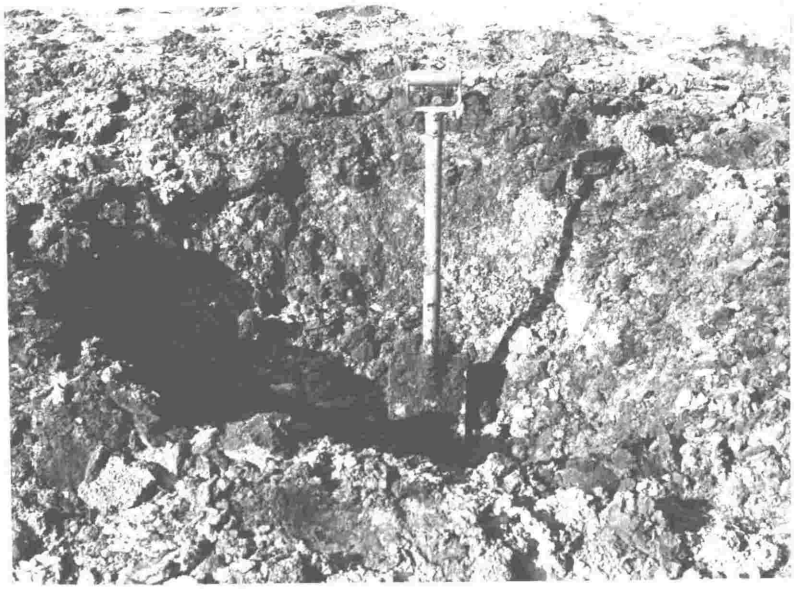

Fig. 5. - Impact crater produced by 40 kg block of andesite ejected explosively from Rudolf Vent in February 1969. Approximately 150 m away from the vent.

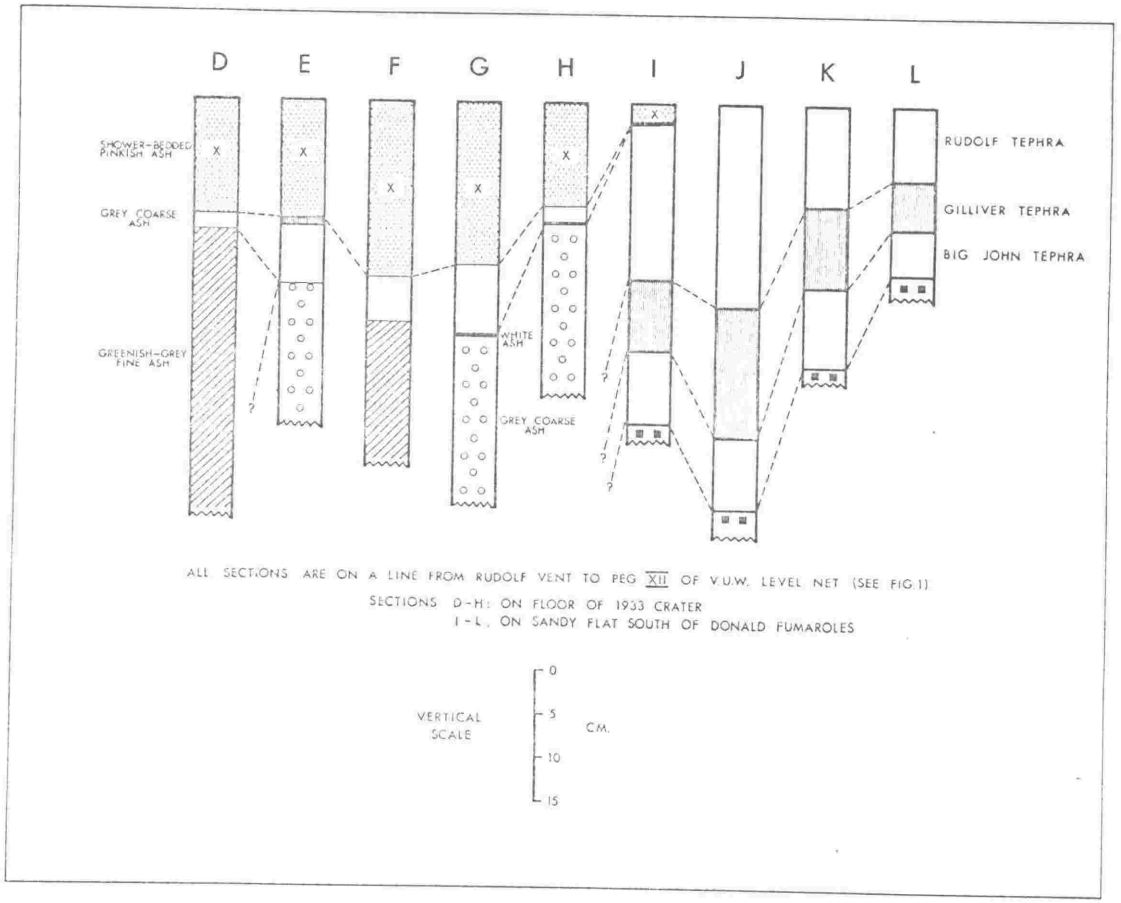

Fig. 3. - Tephra sections along a line between Rudolf Vent and Station XII of the V.U.W. level net.

thickness give an indication of the variation in ash thickness with distance from the vent. At a distance of 80 m from Rudolf Vent ash bed 'X' was 12 cm thick, it was 1 cm thick at 200 m from the vent, and 0.15 cm thick at 350 m from the vent.

Sections I to L in Fig. 3 were measured on the sandy flat area to the south of Donald Fumaroles, at sites away from run-off channels. The total thickness of the Big John, Gilliver and Rudolf tephras are exposed in each section, and variations in the thickness of these tephras are not related directly to distance from their respective vents. The measured thicknesses of tephra units in sections I to L are considered to give a reasonable indication of the true relative thicknesses of tephra erupted from the three vents; except that as the sections are closer to Rudolf Vent than to either Big John or Gilliver Craters, the relative thickness of the Rudolf tephra may be exaggerated. The average relative thickness of Rudolf tephra is 1.6 times that of Gilliver tephra, and that of Big John tephra 0.8 times that of Gilliver tephra. These thickness ratios are considered to be approximate volume ratios.

The bulk of both Gilliver and Rudolf tephras was erupted quietly, as ash-charged gas emitted at moderate velocities. Under such conditions wind direction and strength, atmospheric conditions and local wind eddies within the crater controlled the place of tephra deposition. Only one eruption of ash-size material with significant horizontal velocity has been reported. Healy (1967) states that an eruption from Gilliver Crater on 20th November, 1966 "initially sent a white cloud of ash and steam whirling horizontally along the surface of the ridge (Crater Ridge) and

flat to the west, after which the remainder of the column ascended vertically as usual". Healy considered this eruption to be of small scale nuée ardente type; however, his description also suggests close similarities to the base surge from shallow volcanic explosions, illustrated by Moore (1967).

Lapilli and blocks must have been explosively erupted, and in general these appear to have been ejected with a directional horizontal velocity component which has been the major factor controlling their distribution. Two block and lapilli eruptions from Rudolf Vent occurred in January and February 1969, and both eruptions were strongly directional with most material directed from Rudolf Vent towards the nearest part of South Crater Bench (Fig. 1). These two explosive eruptions were among the most violent that occurred on White Island in the period under study; 40 kg blocks were found 150 m from Rudolf Vent, and 5 kg blocks were found 250 m from the vent. The trajectories of the blocks at their points of impact were nearly vertical and well defined impact craters (Fig. 5) were formed.

VENT SIZES AND TEPHRA VOLUMES

Healy (1967) reported that Gilliver Crater was approximately 60 m in diameter and 120 m deep on 19th November, 1966. During 1967 and 1968 the crater showed a very gradual increase in diameter and a continual increase in the height of the vent rim during the period of its activity. When the bottom of the crater was seen, in February 1969, it was dry with a hummocky sub-horizontal surface formed by debris that had fallen from the vent walls. The main site of steam emission was at the base of the southwest vent wall, and there were also three or four

minor fumaroles in the middle of the vent floor and large caves or tunnels at the bases of the southeast and northeast vent walls. In February 1969, Gilliver Crater had an estimated diameter of 100 m and a depth also of 100 m.

At the beginning of its activity as a tephra vent, Rudolf was approximately 3 m in diameter. During the period of continuous tephra eruption from Rudolf in February-April 1968 its diameter was about 10 m. In February 1969 its depth was about 100 - 120 m and its diameter about 40 - 50 m, with part of the vent wall having collapsed, probably resulting in the block and lapilli eruptions described above.

From calculations using measured tephra sections it is considered that the volume of Gilliver tephra is about 700,000 m^3, approximately twice the volume of the vent shaft from which it was erupted. The volume of the Rudolf tephra can be estimated from average tephra thickness ratios calculated from sections I to L in Fig. 3, giving a volume of about 1,000,000 m^3. An alternative method of calculating the volume of Rudolf tephra is to use values of the weight of ash in a gas sample collected from Rudolf (A.T. Wilson, pers. comm.) and the mean gas velocity in Rudolf as derived from several measurements taken on 15th May, 1968 (D.A. Christoffel, pers. comm.). The weight of ash was found to be 0.01 g/litre of gas, the diameter of Rudolf vent was 10 m and gas emerged at an average velocity of 68 m/sec; hence the weight of ash erupted may be calculated as 54 kg/sec. Measurements made on samples of Gilliver and Rudolf tephras gave an average bulk density of 1.7 g/cm^3, allowing weights of ash to be converted to equivalent tephra volumes. The volume of ash erupted from Rudolf Vent during its period

of continuous eruption from February to April 1968 was thus calculated to be 320,000 m^3. In section C (Fig. 2) the depth of the ash layer produced in this phase of the eruption is 37% of the total depth of Rudolf tephra, and hence the total volume of Rudolf tephra calculated by this technique is 870,000 m^3. This value compares well with the value of 1,000,000 m^3 previously derived, which strongly suggests that although such estimates are not likely to be particularly accurate, they are clearly of the right order. From the average bulk density of 1.7 g/cm^3, the total mass of the Gilliver and Rudolf tephras is about 3×10^9 kg.

Recent topographic changes in the crater of White Island due to tephra burial are small, and the only areas appreciably affected are close to the active vents. Tephra cones were built up around Big John and Gilliver Craters, and Big John Crater and 1933 Crater were filled by airfall tephra and alluvium from the Gilliver and Rudolf eruptions.

GRAIN-SIZE DISTRIBUTION OF TEPHRA

Samples of Gilliver tephra were collected at three sites (see Fig. 1) during a phase of ash eruption on 27th February, 1967; they were taken from the top 5 cm and appeared homogeneous at the sample sites. Surface samples of Rudolf tephra (sites shown in Fig. 1) were collected by A.T. Wilson on 29th April, 1968, when Rudolf was in a state of continuous ash eruption. All the samples taken are considered to be representative of the ash-grade tephra erupted from Gilliver and Rudolf vents.

The size distribution of the samples was analysed by dry screening, and the size parameters and statistics are given in Table 1, with histograms of the size distributions in Fig. 6. The statistical parameters in Table 1 were derived by the graphic methods of Folk (1965) and correspond to his 'inclusive graphic' parameters. In all samples the bulk of the material is coarse ash (tephra size terminology after Fisher, 1961) but Gilliver tephra contains a much more fine ash than Rudolf tephra. The coarse ash fractions of Gilliver tephra are poorly sorted or moderately sorted and platykurtic (terminology after Folk, 1965), whereas the coarse ash fractions of Rudolf tephra are moderate or moderately well sorted and are leptokurtic or mesokurtic, suggesting, in agreement with visual observations, that the gas velocities in Rudolf Vent were markedly higher and more uniform than those in Gilliver Crater. Downdrafts were frequently observed around the rim of Gilliver Crater but were not observed during ash eruption from Rudolf Vent, which may explain the variabilityof gas velocity at Gilliver.

TEPHRA MINERALOGY

The modal mineralogy of the coarse fraction of samples was determined by grain counts on the 2.0 - 3.0 ϕ fraction of each sample, 1000 grains being counted in each sample. The modal analyses of the five samples are given in Table 2.

Grains counted as opaques include opaque minerals (titanomagnetite), extensively altered pyroxenes, and opacitised glass and groundmass material. Three types of volcanic glass are recognised:- (a) largely

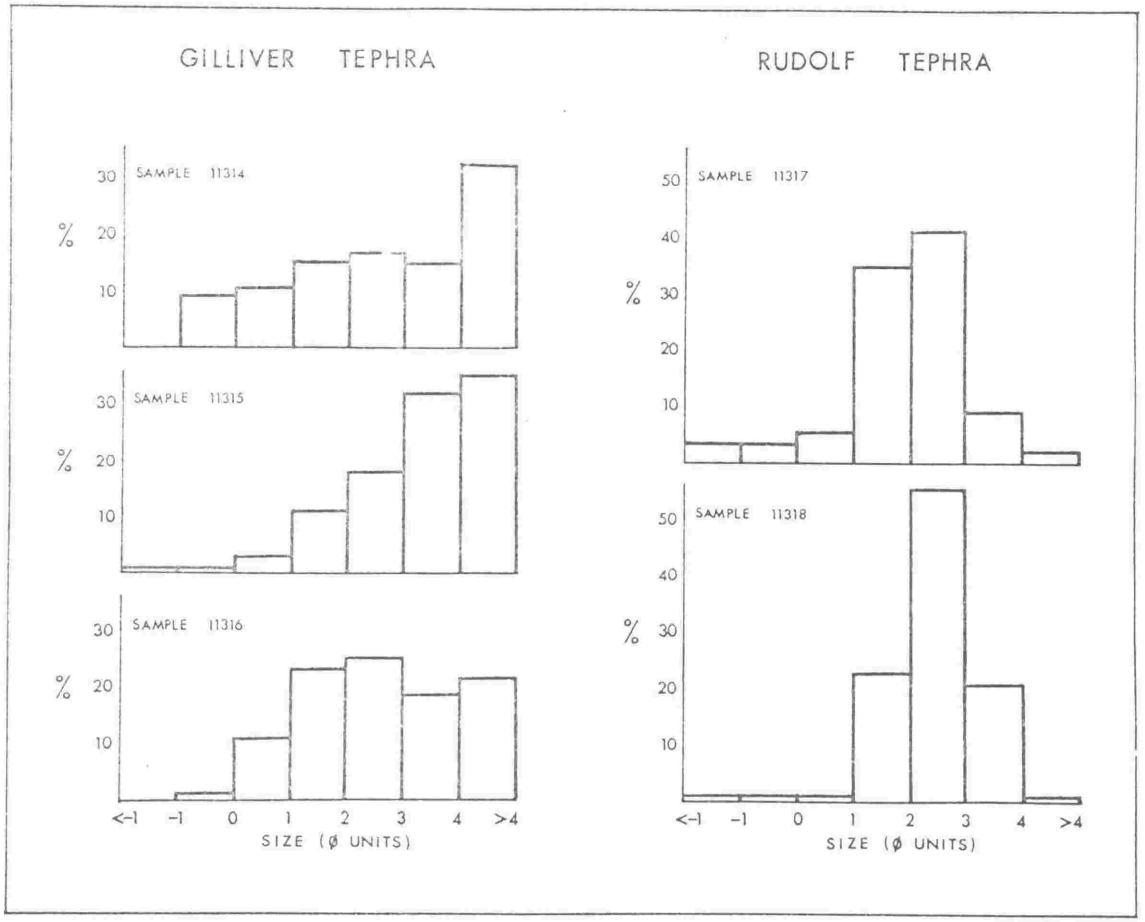

Fig. 6. - Histograms of size distributions measured on samples of Gilliver and Rudolf tephras.

TABLE 1

TEPHRA GRAIN SIZE DISTRIBUTION

			Gilliver Tephra			Rudolf Tephra	
Sample No.			11314	11315	11316	11317	11318
Lapilli		%	Nil	0.2	Nil	3.9	0.2
Coarse Ash		%	67.3	64.9	78.7	93.8	99.5
Fine Ash		%	32.7	34.9	21.3	2.3	0.3
Coarse Ash	(Median	ø	1.88	3.00	2.16	2.05	2.46
	(Mean	ø	1.78	2.79	2.14	2.03	2.49
	(Mean	mm	0.29	0.15	0.23	0.25	0.18
	(Standard Deviation	ø	1.41	0.93	1.03	0.84	0.66
	(Skewness		-0.12	-0.39	-0.04	-0.11	0.08
	(Kurtosis						

TABLE 2

MODAL ANALYSES OF TEPHRA

		Gilliver Tephra			Rudolf Tephra	
Sample No.		11314	11315	11316	11317	11318
Opaques	%	75.4	76.1	84.1	26.3	21.5
Clear Glass	%	8.8	4.5	3.8	-	-
Brown Glass	%	3.4	2.9	4.0	4.1	3.1
Pyroxene	%	6.4	8.6	4.4	57.1	62.0
Plagioclase	%	6.0	7.9	3.7	12.5	13.4

Note: Opaques include titanomagnetite, strongly altered pyroxene, and opacitised volcanic glass and groundmass material.

opacitised glass, probably from an altered andesitic groundmass, with R.I. in the range 1.521 - 1.525; (b) clear colourless glass with felspar crystallites and R.I. in the range of 1.530 - 1.532; (c) clear brown glass with crystallites and R.I. in the range 1.527 - 1.532. All three types of glass were recognised in Gilliver tephra, but only types (a) and (c) in Rudolf tephra.

The pyroxenes and plagioclase in Gilliver and Rudolf tephras are very similar. Clinopyroxene and orthopyroxene are present in both tephras with the clinopyroxene being an augite ($B = 1.693$, $2V_z = 50^\circ$) and the orthopyroxene being bronzite ($2V_x = 75^\circ$). Plagioclase in both tephras is strongly zoned and ranges from andesine to labradorite in composition.

Minor constituents in the form of lapilli sized fragments of gypsum, anhydrite, sulphur, cristobalite, and halite occur in both tephras, and are thought to be derived from the old crater floor deposits underlying Crater Ridge, which were buried in the 1914 landslide. Dr A. Ewart (pers. comm.) noted up to 30% gypsum in ash samples collected in the early stages of the Gilliver eruption. Rudolf Vent has twice erupted an unusual greenish-grey fine ash (shown in Fig. 3 at the base of columns D and F) which is a mixture of halite and an amorphous component which was identified as allophane or amorphous silica by infra-red techniques (D. Milne, pers. comm.).

The mineralogy of both tephras is essentially the same, except for the proportions of glass and minerals, and the much greater content of opacitised material in Gilliver tephra. Rudolf tephra contains six times the average crystal content of Gilliver tephra, with 60% pyroxene

and 13% plagioclase (Rudolf samples) compared with 6.5% pyroxene and 6% plagioclase (Gilliver samples).

Three factors may have influenced the size-distribution, crystal content and degree of opacitisation in Gilliver and Rudolf tephras:-

(a) The degree of alteration in the country-rock component of the tephra.

(b) The proportions of fresh magmatic material and comminuted country-rock in the tephra.

(c) The velocity of the gas stream carrying the tephra.

It is unlikely that the degree of alteration of the country-rock below Gilliver and Rudolf vents differs significantly. Consequently the difference in the degree of opacitisation in the two tephras, together with the presence of unaltered volcanic glass, is an indication of a fresh magmatic component in the tephras, with Rudolf tephra having a larger fresh component than Gilliver tephra. In view of the small proportion of unaltered material in Gilliver tephra, its fresh magmatic component is thought to be only about 10%. The higher crystal content and the unaltered condition of much of theglass and pyroxene in Rudolf tephra indicates a significantly higher proportion of fresh material, perhaps as much as 30 - 50% of the total.

The proportions of crystals to glass and the proportions of different minerals in the tephra sequence are likely to be controlled largely by factors (b) and (c) above. It would be easier to separate magma and crystals than to separate crystals from a solidified groundmass; hence a larger magmatic component would favour higher crystal contents, and the high crystal content of the Rudolf tephra samples may well be due to this effect. Higher gas velocities in

Rudolf Vent compared to those in Gilliver Crater would also favour a higher pyroxene content in the tephra since the density of the pyroxene exceeds that of andesitic glass, provided that the size distribution of crystals and glass particles is the same.

CONCLUSIONS

Surface temperatures in excess of 800° C in the crater of White Island and intermittent eruptions of tephra containing fresh volcanic glass indicate that magma probably lay at shallow depths below White Island during 1967 and 1968. Approximately 1,700,000 m^3 (about 3 x 10^9 kg) of tephra was erupted from two separate vents in the crater of White Island during the period November 1966 to April 1969. The bulk of the tephra consists of finely comminuted altered andesite; but what is considered to be a fresh magmatic component forms a significant proportion of Rudolf tephra.

ACKNOWLEDGEMENTS

The authors gratefully acknowledge the assistance of Professor R.H. Clark, Professor A.T. Wilson, Professor D.A. Christoffel and Mr R.R. Dibble in providing samples and unpublished information regarding the tephra eruptions. Transportation to the island was provided by Messrs T.G. McCracken and R.G. Butler of Whakatane, the R.N.Z.A.F. and the R.N.Z.N.

The authors are also indebted to Professor R.H. Clark and Professor H.W. Wellman for helpful criticism of the manuscript.

REFERENCES

FISHER, R.V. 1961: Proposed classification of volcaniclastic sediments and rocks. Geol. Soc. Amer. Bull. 72: 1409-1414.

FOLK, R.L. 1965: Petrology of sedimentary rocks. Hemphill's, Texas.

HEALY, J. 1967: Geological history of the Whakatane district. Whakatane Hist. Rev. 15: 9-27.

MOORE, J.G. 1967: Base surge in recent volcanic eruptions. Bull. Volcan. 30: 337-363.

EVIDENCE FOR SUBMARINE GEOTHERMAL ACTIVITY IN THE BAY OF PLENTY

A. R. DUNCAN

Geology Department, Victoria University, Wellington

and

H. M. PANTIN*

New Zealand Oceanographic Institute, DSIR, Wellington

*See footnote overleaf

Reprinted from the NEW ZEALAND JOURNAL OF MARINE AND FRESHWATER RESEARCH, *Vol. 3, No. 4, December 1969.*

EVIDENCE FOR SUBMARINE GEOTHERMAL ACTIVITY IN THE BAY OF PLENTY

A. R. DUNCAN

Geology Department, Victoria University, Wellington

and

H. M. PANTIN*

New Zealand Oceanographic Institute, DSIR, Wellington

(Received for publication 15 May 1969)

SUMMARY

Gas bubbles rising to the sea surface and unusual scattering zones on echo-sounding records provide evidence for areas of submarine geothermal activity near Whale Island and White Island.

The Taupo Volcanic Zone extends off shore in the Bay of Plenty at least as far north as White Island. Several islands in the Bay are associated with Pleistocene or Recent volcanism; and White Island, Whale Island and the Rurima Rocks (J. W. Brodie, pers. comm.) have active geothermal areas.

Two areas in which bubbles can be seen rising to the sea surface, one north and one south of Whale Island, have been brought to our attention by Mr E. G. McCracken and Mr R. G. Butler, of Whakatane. The concentration of bubbles in the sea water is low and variable; and the bubbles can only be observed in calm weather. For this reason the location and size of the bubble areas described below and shown in Fig. 1 are only approximate.

The southern bubble area is centered 2 km SSW of the eastern end of Whale Island at 37° 52.9′ S, 176° 58.7′ E, and is elongated NNE–SSW with a length of 3 km and a width of 1.5 km. The bubbles are generally a few millimetres in diameter and usually occur in groups with individual bubbles a few centimetres apart. The diameter of a bubble group is between 10 cm and 1 m, and within an area of 10 m^2 such a group appears at intervals of between 10 seconds and 2 minutes. The northern bubble area is centered 5 km NNE of the eastern end of Whale Island at 37° 48.9′ S, 177° 00.9′ E, and is 1.5 km in diameter. The rate of bubble emission in the northern area is considerably less than that in the southern area, perhaps by a factor of 10.

Because of the extremely sporadic appearance of bubbles at any one point within the bubble areas, the gas forming the bubbles was not sampled. However, because the bubble areas are close to active geothermal areas on Whale Island, we think the bubbles are probably caused by submarine geothermal activity.

---

*Now at Institute of Geological Science, Ring Road Halton, Leeds.

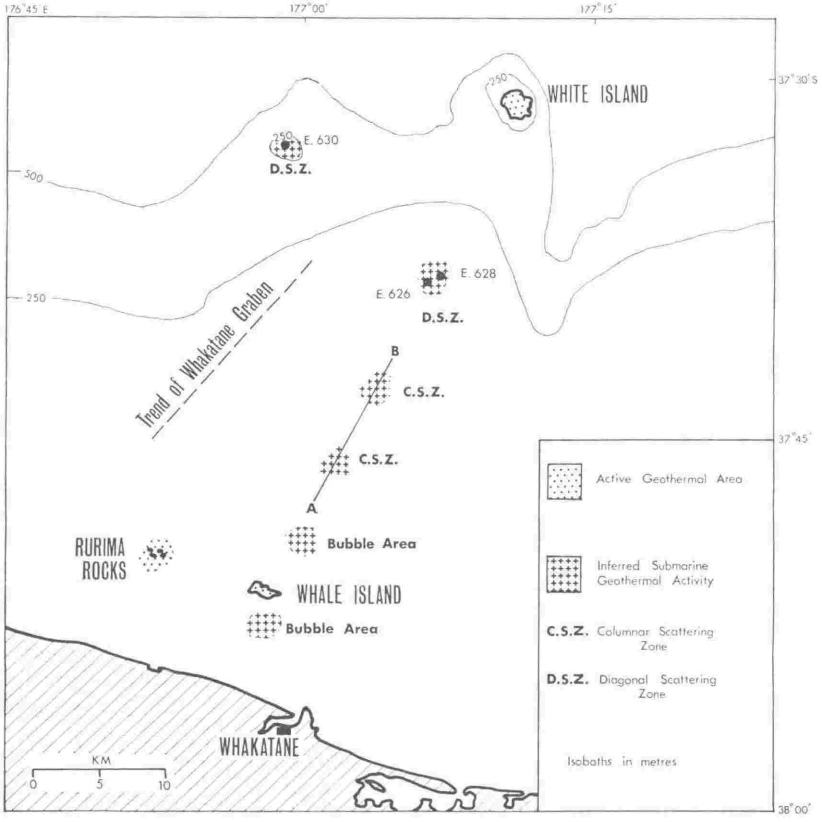

FIG. 1—Sketch map of the Bay of Plenty with generalised bathymetry showing the positions of White Island, Whale Island, Rurima Rocks, the two bubble areas, NZOI Stas E. 626, E. 628, E. 630, and track A–B for PDR record shown in Fig. 2.

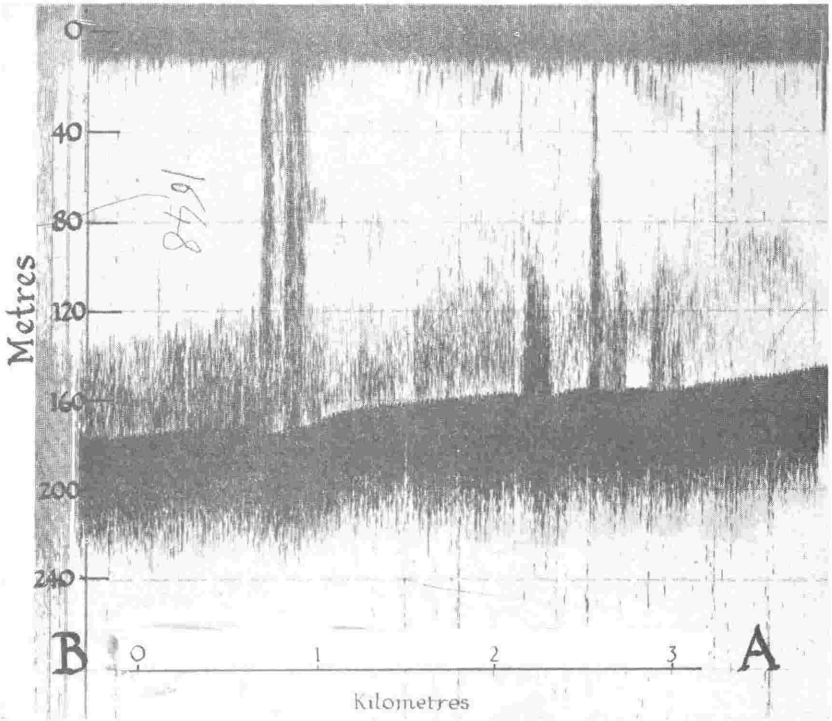

FIG. 2—PDR record for track from 37° 48.1′ S, 177° 02.0′ E to 37° 42.2′ S, 177° 06.5′ E as shown by A–B in Fig. 1.

During New Zealand Oceanographic Institute cruise *Ngatoro* in October 1966 bathymetry was determined by a Precision Depth Recorder (PDR) in the area between Whale Island and White Island and in an area to the north and west of White Island. PDR records from a track (A–B in Fig. 1) between 37° 48.1′ S, 177° 02.0′ E and 37° 42.2′ S, 177° 06.5′ E show three near-vertical bands extending from the sea floor to the surface (Fig. 2). Since these bands do not extend below the bottom echo, it is most unlikely that they represent electronic noise. It is therefore probable that the bands represent steep-sided, possibly columnar, scattering zones. The authors consider that the most likely explanation of these "columnar scattering zones" is the presence of columns of bubbles rising from submarine geothermal activity on the sea floor; such activity might also be related to the pronounced topographic depression in the sea floor below the two largest scattering bands.

PDR records at NZOI Stas E. 626 and E. 628 (11 km SSW of White Island) show a number of diffuse diagonal bands just below the trace of the outgoing pulse. A good example of these diagonal bands, from the PDR records at Sta. E. 626, is shown in Fig. 3. Diagonal bands on echo-sounding records can represent objects rising or falling through

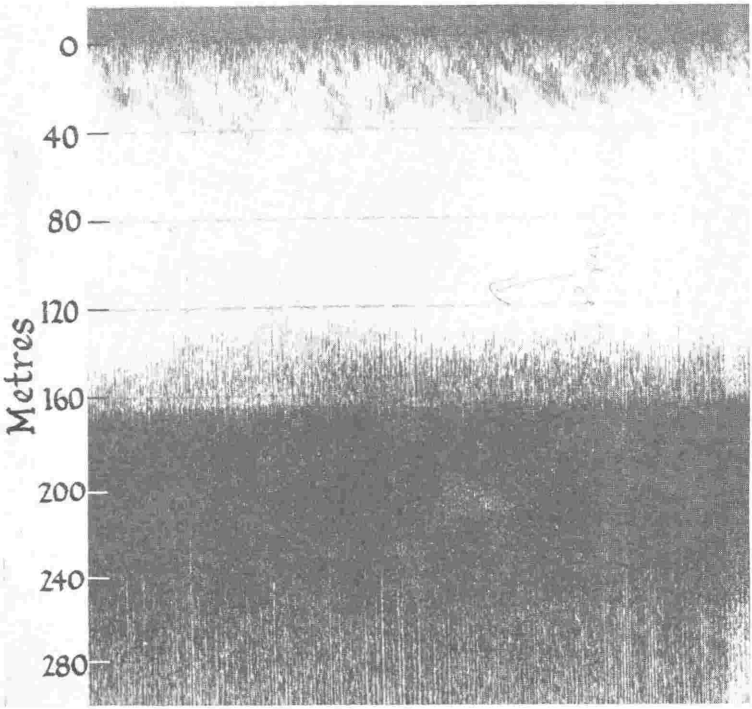

FIG. 3—PDR record from NZOI Sta. E. 626 (ship stationary).

the water; since the ship was nearly stationary when the PDR record in Fig. 3 was obtained, the horizontal axis on the record becomes a time axis for events occurring at the same position. Hence it is possible to determine that the bands shown in Fig. 3 represent objects rising through the water. McCartney and Bary (1965) have described similar, though much better defined, diagonal bands in echo-sounding records from Saanich Inlet in British Columbia, which they interpreted as being due to rising gas bubbles. It is considered that the diagonal bands shown in Fig. 3, and also seen in the PDR records from Sta. E.628, may be due to rising gas bubbles, as the direction of short-period movement of fish or plankton is likely to be more random. No surface bubble areas were observed during the ship's passage over columnar or diagonal scattering zones but the sea was too rough for reliable direct observations.

A number of seamounts occur to the north and west of White Island, and Holocene eruptions of andesitic and dacitic pumice may have taken place at some of these volcanic centres (Duncan, in prep.). Submarine geothermal activity might therefore be expected in this area. During the *Ngatoro* cruise the seamounts were crossed several times. Diagonal bands similar to those observed at Sta. E. 626 (Fig. 3) were recorded at Sta. E. 630 (on a seamount 18 km west of White Island) providing an

indication of geothermal activity. On the other hand, no columnar or diagonal scattering bands were seen on the PDR records from the other seamounts investigated, nor were surface bubble areas observed over any of the seamounts.

With the exception of the seamount at Sta. E. 630 the areas of possible submarine geothermal activity discussed above form a line parallel to the trend of the Whakatane Graben, and lie very close to a line joining Whale Island to White Island. The postulated areas of submarine geothermal activity, together with Whale Island, White Island and the Rurima Rocks thus form a marked volcanic-geothermal lineation, continuous over some 50 km.

ACKNOWLEDGMENTS

We thank Mr J. W. Brodie and Professor H. W. Wellman for discussion and helpful criticism of the manuscript.

REFERENCES

DUNCAN, A. R. (in prep.): Petrology of rock samples from seamounts near White Island, Bay of Plenty.

MCCARTNEY, B. S. and BARY, B. MCK. 1965: Echo sounding on probable gas bubbles from the bottom of Saanich Inlet, British Columbia. *Deep Sea Res. 12*: 285–94.

A. R. SHEARER, GOVERNMENT PRINTER, WELLINGTON, NEW ZEALAND—1970

PART 2

GEOCHEMISTRY OF EDGECUMBE, WHALE ISLAND, WHITE ISLAND AND MANAWAHE

GEOCHEMISTRY INTRODUCTION

Petrochemical knowledge of the volcanic rocks of the Taupo Volcanic Zone has, until quite recently, consisted of comparatively small numbers of major oxide analyses of what were considered to be representative samples of various rock types. Analyses published prior to 1958, together with a number of previously unpublished analyses, were collected and published by Steiner (1958). Clark (1960 b) gave additional analyses of the andesitic rocks of Tongariro National Park, and Ewart (1963) gave analyses of the Taupo Sub-Group tephra deposits. Additional major element analyses were published in N.Z. Geological Survey Handbook I.S. 50, edited by Thompson, Kermode and Ewart (1965).

These analyses provided valuable data on the composition of the basalts, some of the andesites, and a large number of rhyolite lavas and ignimbrites. Only three analyses of the andesites at the northeastern end of the Taupo Volcanic Zone were available, together with a further three analyses only for all the dacites in the Taupo Zone.

Taylor and White (1966) gave the first trace element analyses of rocks from the Taupo Zone - analyses of six andesites from Tongariro National Park. The amount of trace element data was rapidly increased with papers by Ewart, Taylor & Capp (1968); Taylor, Ewart & Capp (1968); Ewart & Stipp (1968); Lewis (1968 b) and Ewart & Taylor (1969).

Sufficient geochemical data was now available in the Taupo Zone for regional volcanic geochemistry to be fairly well established; and the immediate requirements were to obtain detailed data in a specific area, in order to get some idea of how this related to the overall

pattern, and to fill in some of the remaining gaps in the general data. The present author has thus made a detailed geochemical study of the andesites and dacites at the northeastern end of the Taupo Zone (the Bay of Plenty volcanics), together with additional trace and major element analyses of three basalts and a dacite elsewhere in the Taupo Zone.

New total-rock analyses for 28 elements in 44 rocks are presented, together with analyses for an additional 17 elements in 3 of the rocks.

The major aims of the present study have been: (1) to compare the geochemistry of the Bay of Plenty volcanics with other volcanic rocks in the Taupo Volcanic Zone and in other areas of the circum-pacific margin; (2) to examine differences between the geochemistry of Edgecumbe, Whale Island and White Island and suggest explanations for these differences; (3) to examine major and trace element variation trends and to determine what petrographic inferences can be made from them.

ANALYTICAL TECHNIQUES

Total-rock samples of 1 to 3 kg were crushed into pieces of about 2 cm diameter in a rock splitter with hardened steel jaws, and any apparently weathered material was discarded. The fresh material was further broken down using a large, then a small mechanical jaw-crusher, and then an agate cone-grinder. Samples were then quartered down and a 50 gm split of most samples was then ground for 10 minutes in an agate grinding vessel in a "Tema" mill, but a few sample splits were ground in a mechanical agate mortar to pass 120-mesh silk bolting cloth.

Major elements, with the exception of K and Na, were determined by x-ray fluorescence spectrography using the method of Norrish & Chappell (1967). Na and K were determined by flame photometry using both EEL and Perkin-Elmer instruments. Rb, Sr and Zr were determined by x-ray fluorescence spectrography using the methods of Norrish & Chappell (1967).

Cs and Li were determined by optical spectrography using a large Hilger (E.478) spectrograph, with Na serving as a variable internal standard, the samples being arced until the end of the alkali distillation period. The elements La, Y, Cu, Co, Ni, Sc, V, Cr, Ga, Ba and B were determined on a Jarrell-Ash Ebert (Model 71-100) grating spectrograph. Samples were mixed with twice their weight of a carbon-palladium mixture (the palladium serving as internal standard) and were arced to completion. Line intensities were read on a Jarrell-Ash microphotometer (23-100). Optical spectrographic precision is similar to that of Kolbe and Taylor (1966, Table 1.). For each sample all elements determined by optical spectrography were analysed in triplicate.

U and Th were determined by gamma-ray spectrometry using the method of Heier et al. (1965). In three samples the elements Pb, Tl, W, Hf, Yb, Tm, Er, Ho, Dy, Tb, Gd, Eu, Sm, Nd, Pr, Ce, La and Nb were determined by spark-source mass spectrometry, using the A.E.I. MS7 instrument, with Lu as an internal standard. The method used, and the precision attained have been discussed in detail by Taylor (1965 a). Further details of analytical techniques are given in Appendix 2.

As well as being determined by the methods described above, Rb, K, Sr, Ca, Zr, Ti, Mn, Fe and Mg were also determined by other analytical techniques. Comparative data and discussion is given in Appendix 2.

Primary standards used to construct spectrographic working curves were G-1 and W-1 (U.S. Geological Survey), SY-1 (Canadian Association for Applied Spectroscopy), and T-1 (Tanzania Geological Survey). In addition to the primary standards, four of the new set of U.S.G.S. standards (G-2, GSP-1, AGV-1, BCR-1) were analysed as secondary standards, and concentrations obtained from the working curves. Element concentrations adopted for the primary standards are given in Table 17, together with values for element concentrations in the secondary standards as derived from the working curves.

For major element analyses by x-ray fluorescence, concentrations were determined relative to an artificial standard F.S.22. Major element concentrations for various international rock standards, determined relative to F.S.22 by the same techniques, are given by Chappell (in press). For Rb, Sr, and Zr, analyses by x-ray fluorescence, G-1 was used as a primary standard with values taken as Rb-210 ppm,

TABLE 17A

ELEMENT CONCENTRATIONS ASSUMED FOR INTERLABORATORY GEOCHEMICAL STANDARDS

STANDARD SAMPLE	G-1	W-1	T-1	S-1	G-2	AGV-1	BCR-1	GSP-1
Mn	210	130	850	(3100)	(260)	(760)	(1350)	(325)
Ga	(23.5)	16	(20.5)	(23)	(23)	(19)	(23)	(20.5)
Cu	13	110	48	(20)	(6.1)	(55)	(25.5)	(30)
Y	13	26	(21)	450	(10.3)	(22)	(42)	(26)
Ni	-	75	11	44	-	(18)	(12.5)	(7)
Co	-	50	13.4	18	-	(15)	(41)	(7)
Sc	2.8	34	14	14	(3.5)	(13)	(28)	(6)
Cr	-	120	24	55	-	(11)	(13.5)	(12)
La	100	-	-	(160)	(117)	(31)	(20)	(175)
V	14	245	91	(76)	(45)	(120)	(320)	(54)
Ba	1060	180	(630)	(342)	(1820)	(1200)	(720)	(1230)

Notes: (S-1 Nickel + 20ppm. Zr correction)
(GSP-1 Nickel + 3 ppm. Zr correction)

All figures in brackets are intercepts read off the working curves and were not used to construct the curves.

TABLE 17B

ELEMENT CONCENTRATIONS ASSUMED FOR INTERLABORATORY GEOCHEMICAL STANDARDS - ALKALI ELEMENTS

STANDARD SAMPLE	G-1	W-1	T-1	S-1	G-2	GR	AGV-1	BCR-1	GSP-1	KOS-1	EU-2
Li	24	10	(10)	110	(32)	(49)	-	-	(31)	-	-
Cs	-	-	-	1.3	-	(9.6)	-	-	-	6.5	10.3
Li/Na	9.76	6.49	(3.67)	44.1	(10.4)	(17.6)	-	-	(14.2)	-	-
Cs/Na	-	-	-	0.52	-	2.48	-	-	-	3.87	4.31

Note: All figures in brackets are intercepts read off the working curves and were not used to construct the curves.

Sr-247 ppm, and Zr-210 ppm. Standard solutions used in flame photometric determinations were prepared from 'Analar' grade Na and K sulphates; Na and K analyses of the rock standards SY-1, T-1, G-2, AGV-1, GSP-1, and BCR-1 relative to the standard solutions are given in Table 18. Gamma-ray spectrometric determinations of U and Th were made relative to the U and Th standards supplied by the U.S. Atomic Energy Commission; AGV-1 and BCR-1 were analysed as additional checks and the values are given in Table 19.

TABLE 18

FLAME-PHOTOMETER VALUES OBTAINED FOR STANDARDS

	Na%	Na%(mean)	K%	K%(mean)
S-1	2.693	2.720	2.215	2.244
	2.747		2.233	
G-2	3.100	3.083	3.748	3.755
	3.066		3.761	
AGV-1	3.243	3.279	2.431	2.433
	3.314		2.434	
GSP-1	2.094	2.094	4.633	4.621
	2.094		4.607	
BCR-1	2.524	2.537	1.434	1.434
	2.550		1.434	
T-1			1.026	1.027
			1.027	

TABLE 19

U AND TH ANALYSES OF STANDARDS

	U (ppm)	Th (ppm)
AGV-1	1.70	6.39
	1.95	5.73
BCR-1	1.47	5.56
	1.36	5.87

CLASSIFICATION OF ANDESITES AND DACITES

Chemical classification of the calc-alkaline association has been attempted by many authors. Chayes (1965) states that "systematists and textbook writers are in almost complete agreement that modal and normative quartz are low or lacking in andesites". However, Chayes (1965, Fig. 55) shows that many volcanic rocks which have been called andesite do contain substantial amounts of normative quartz, and that the median value for normative quartz in "andesites" is 12-14%.

A chemical definition of andesite which corresponds more closely to the actual chemistry of the rocks which are commonly called "andesite" is clearly necessary. Such a definition has been proposed by Taylor et al. (1969) and is used throughout this thesis. Taylor et al.'s classification subdivides intermediate calc-alkaline volcanics according to their SiO_2 and K_2O contents, as shown in Fig. 20.

In the Bay of Plenty volcanics the petrographic definition of the andesite/dacite boundary (presence or absence of modal quartz) corresponds reasonably with the chemical definition of the boundary (greater or less than 63% SiO_2). However, modal analyses of chemically analysed samples (Tables 4, 7, 9, 10) indicate that although all petrographic dacites are chemical dacites, many chemical dacites are petrographic andesites. It is thus apparent that the petrographic classification used, results in an underestimate of the proportion of the Bay of Plenty volcanics which are chemical dacites.

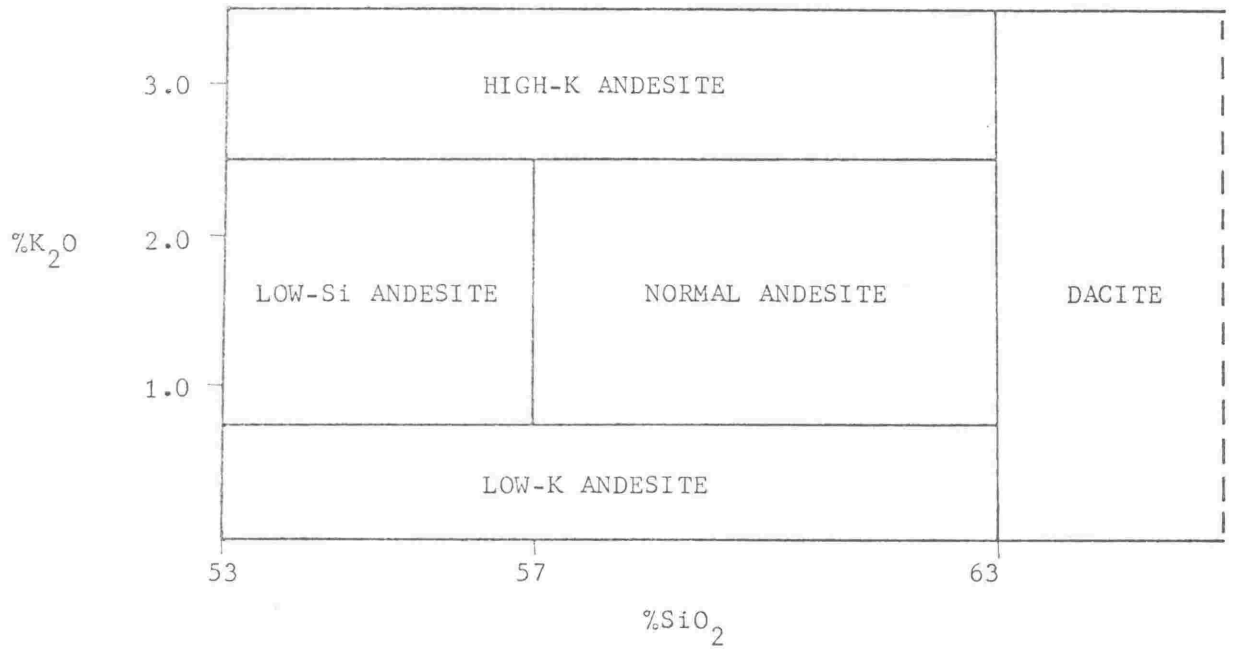

Fig. 20. - Classification of intermediate calc-alkaline volcanic rocks, based on Taylor et al. (1969), Fig. 3.

MAJOR ELEMENT ABUNDANCES

The 43 samples from Edgecumbe, Whale Island, White Island and Manawahe which have been analysed for major elements are all normal andesites or dacites. No Low-Si, Low-K or High-K varieties of andesite were found. All five xenolithic samples analysed are normal andesites, and of the non-xenolithic samples only 10% are normal andesites the remainder being dacites. Edgecumbe and White Island volcanoes contain andesites and dacites, whereas all the non-xenolithic samples analysed for Whale Island and Manawahe are dacites. Major element analyses of non-xenolithic samples are given in Tables 20, 21 and 22.

All major elements have concentrations typical of andesites and dacites. They are relatively high in Al_2O_3, most samples having in excess of 15% Al_2O_3, those having less than this amount generally contain more SiO_2 as would be expected. When compared with the circum-pacific average andesite and dacite (Taylor, 1969) FeO (total iron), CaO and MgO are higher than the averages; while Na_2O and K_2O are below the averages. Comparison of Tongariro National Park (hereafter abbreviated to TNP) andesites (Clark, 1960 b) with two Edgecumbe samples of similar SiO_2 content shows that the Edgecumbe samples contain more FeO (total iron), CaO, Na_2O and K_2O; with less MgO than their TNP counterparts.

Dacites from Edgecumbe and Whale Island have slightly less total iron, CaO, and Al_2O_3; and slightly more Na_2O and K_2O than dacites from Tauhara (Lewis, 1968 a).

The Von Wolff diagram is a convenient method of illustrating variations in major element chemistry and Fig. 21 is such a diagram

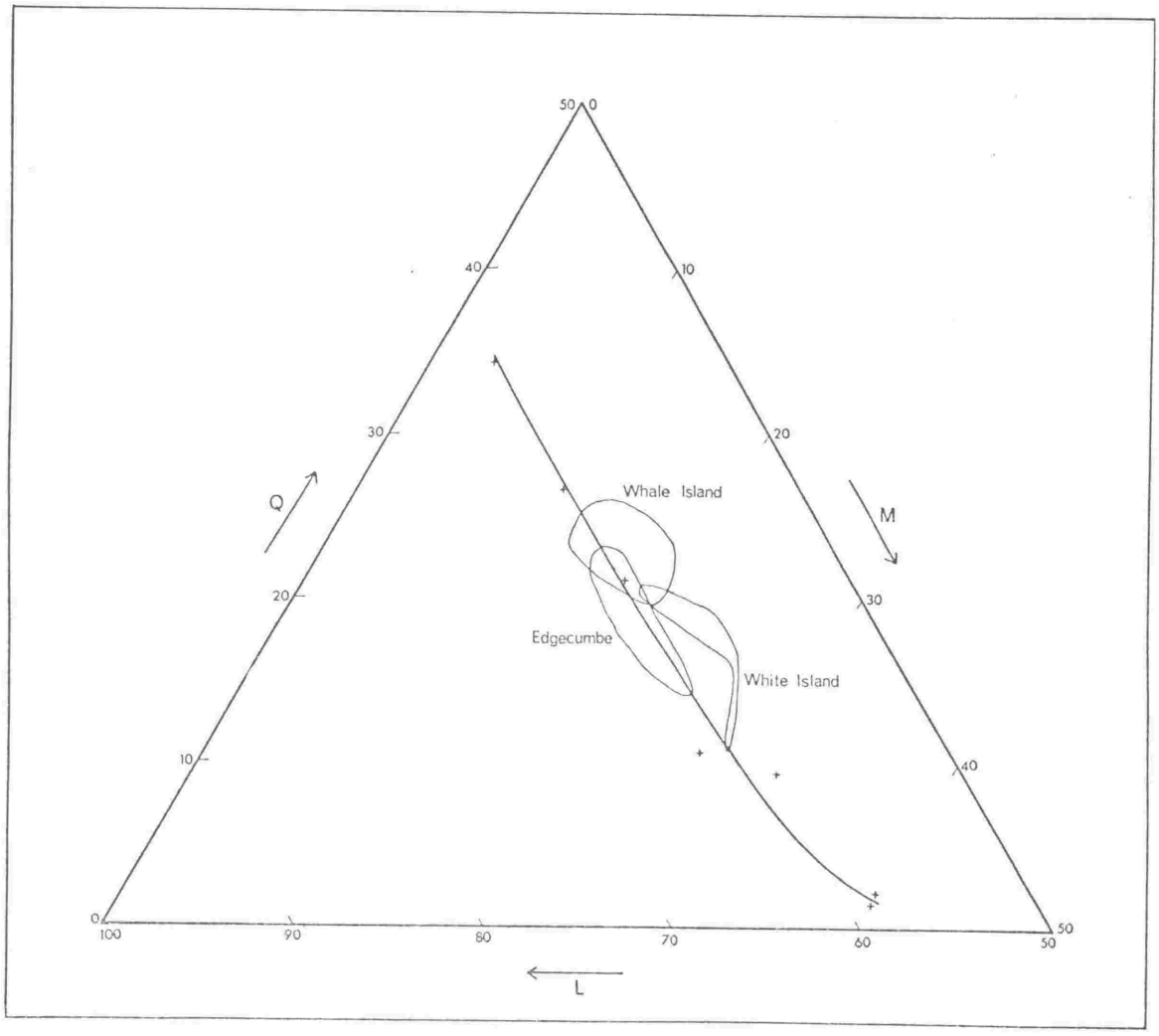

Fig. 21. - Enlarged section of a von Wolff diagram showing zones enclosing the plotted positions of analyses of non-xenolithic rocks from Edgecumbe, Whale Island and White Island. The crosses are analyses plotted by Clark (1960 b, Fig. 16). The line drawn relative to these crosses is the overall chemical trend of the Taupo Zone volcanics as shown by Clark (1960 b, Fig. 16).

TABLE 20

MAJOR ELEMENT ANALYSES - EDGECUMBE

MAJOR ELEMENTS

SAMPLE	11205	11206	11207	11208	11210	11211	11212	11213	11214	11215	11216	11217
SiO_2	60.64	59.27	65.51	59.82	64.50	64.69	65.42	63.30	62.99	62.95	61.10	64.86
TiO_2	0.69	0.73	0.68	0.70	0.57	0.57	0.57	0.76	0.68	0.68	0.74	0.61
Al_2O_3	16.20	17.14	15.59	16.67	15.52	15.89	15.55	16.54	16.25	16.23	16.40	15.91
*FeO	5.52	6.50	5.19	6.36	4.97	4.91	4.75	5.59	5.70	5.65	6.25	5.11
CaO	5.16	7.52	4.77	6.95	5.22	5.34	5.03	5.68	6.10	5.92	6.53	5.31
MgO	1.78	3.59	1.66	3.55	2.38	2.14	2.21	1.84	2.54	2.51	2.93	2.05
Na_2O	3.25	2.68	3.45	2.94	3.09	3.18	3.22	3.18	3.10	3.03	2.90	3.15
K_2O	2.01	1.43	2.30	1.55	2.01	1.92	2.03	1.94	1.77	1.75	1.65	1.90
P_2O_5	0.14	0.12	0.15	0.13	0.11	0.10	0.10	0.16	0.12	0.12	0.13	0.11
TOTAL	95.39	98.98	99.30	98.67	98.37	98.74	98.88	98.99	99.25	98.84	98.63	99.01

MAJOR ELEMENTS RECALCULATED FOR Σ = 100%

SAMPLE	11205	11206	11207	11208	11210	11211	11212	11213	11214	11215	11216	11217
SiO_2	63.57	59.88	65.97	60.63	65.57	65.51	66.16	63.95	63.47	63.69	61.95	65.51
TiO_2	0.72	0.74	0.68	0.71	0.58	0.58	0.58	0.77	0.69	0.69	0.75	0.62
Al_2O_3	16.98	17.32	15.70	16.89	15.78	16.09	15.73	16.71	16.37	16.42	16.63	16.07
*FeO	5.79	6.57	5.23	6.45	5.05	4.97	4.80	5.65	5.74	5.72	6.34	5.16
CaO	5.41	7.60	4.80	7.04	5.31	5.41	5.09	5.74	6.15	5.99	6.62	5.36
MgO	1.87	3.63	1.67	3.60	2.42	2.17	2.24	1.86	2.56	2.54	2.97	2.07
Na_2O	3.41	2.71	3.47	2.98	3.14	3.22	3.26	3.21	3.12	3.07	2.94	3.18
K_2O	2.11	1.44	2.32	1.57	2.04	1.94	2.05	1.96	1.78	1.77	1.67	1.92
P_2O_5	0.15	0.12	0.15	0.13	0.11	0.10	0.10	0.16	0.12	0.12	0.13	0.11

C.I.P.W. NORMATIVE COMPOSITIONS

SAMPLE	11205	11206	11207	11208	11210	11211	11212	11213	11214	11215	11216	11217
Q	18.45	14.42	22.03	14.45	22.44	22.45	23.15	20.25	19.32	20.01	17.30	22.80
OR	12.47	8.51	13.71	9.28	12.06	11.46	12.12	11.58	10.52	10.46	9.87	11.35
AB	28.86	22.93	29.36	25.22	26.57	27.25	27.59	27.16	26.40	25.98	24.88	26.91
AN	24.79	30.84	20.41	28.07	22.94	23.72	22.23	25.40	25.41	25.80	27.25	23.91
DI	0.98	5.09	2.12	5.03	2.29	2.10	2.02	1.80	3.66	2.68	4.02	1.70
HY	11.77	15.56	9.74	15.32	11.35	10.67	10.58	11.01	12.11	12.52	14.00	10.92
[a]MT	1.20	1.20	1.20	1.20	1.20	1.20	1.20	1.20	1.20	1.20	1.20	1.20
TL	1.37	1.41	1.29	1.35	1.10	1.10	1.10	1.46	1.31	1.31	1.42	1.18
AP	0.33	0.26	0.33	0.28	0.24	0.22	0.22	0.35	0.26	0.26	0.28	0.24

* Total Iron shown as FeO.
All values are in percent.

a Normative magnetite (MT) calculated assuming 0.83% Fe_2O_3 in each sample.

TABLE 21

MAJOR ELEMENT ANALYSES - WHALE ISLAND

MAJOR ELEMENTS

SAMPLE	11219	11220	11221	11222	11224	11225	11226	11227	11230	11231	11234	11235	11236	11237	11238	11239
SiO_2	66.54	66.64	65.52	62.76	65.93	63.89	62.74	63.95	65.13	63.66	62.05	62.44	63.11	61.80	62.97	62.81
TiO_2	0.49	0.49	0.48	0.56	0.58	0.55	0.58	0.56	0.50	0.57	0.54	0.55	0.54	0.55	0.54	0.57
Al_2O_3	15.36	14.94	15.09	15.93	15.54	15.94	15.76	15.95	15.16	15.33	15.60	15.81	15.70	15.60	16.01	16.08
*FeO	4.43	4.73	4.56	5.37	4.60	5.29	5.34	5.13	4.72	4.37	5.32	5.21	4.98	5.11	5.14	5.35
CaO	5.22	4.99	5.17	5.91	4.36	6.19	6.23	6.03	5.49	4.67	6.08	6.15	5.94	6.13	6.00	6.23
MgO	2.16	2.37	2.30	3.14	1.69	2.80	2.83	2.64	2.41	1.59	2.85	2.71	2.48	2.57	2.70	2.92
Na_2O	3.05	2.89	2.89	2.41	3.10	2.79	2.90	2.84	3.13	3.13	2.63	2.84	3.00	2.94	2.84	2.19
K_2O	2.11	2.11	2.01	1.61	2.12	1.70	1.71	1.79	2.07	2.22	1.77	1.72	1.87	1.75	1.76	1.72
P_2O_5	0.09	0.09	0.09	0.11	0.10	0.11	0.10	0.09	0.09	0.10	0.10	0.09	0.10	0.09	0.10	0.09
TOTAL	99.45	99.25	98.11	97.80	98.02	99.26	98.19	98.98	98.70	95.64	96.94	97.52	97.72	96.54	98.06	97.96

MAJOR ELEMENTS RECALCULATED FOR Σ = 100%

SAMPLE	11219	11220	11221	11222	11224	11225	11226	11227	11230	11231	11234	11235	11236	11237	11238	11239
SiO_2	66.91	67.14	66.78	64.17	67.26	64.37	63.90	64.61	65.99	66.56	64.01	64.03	64.58	64.01	64.22	64.12
TiO_2	0.49	0.49	0.49	0.57	0.59	0.55	0.59	0.57	0.51	0.60	0.56	0.56	0.55	0.57	0.55	0.58
Al_2O_3	15.44	15.05	15.38	16.29	15.85	16.06	16.05	16.11	15.36	16.03	16.09	16.22	16.07	16.16	16.33	16.41
*FeO	4.45	4.77	4.65	5.49	4.69	5.33	5.44	5.18	4.78	4.57	5.49	5.34	5.10	5.29	5.24	5.46
CaO	5.25	5.03	5.27	6.04	4.45	6.24	6.35	6.09	5.56	4.88	6.27	6.31	6.08	6.35	6.12	6.36
MgO	2.17	2.39	2.34	3.21	1.72	2.82	2.88	2.67	2.44	1.66	2.94	2.78	2.54	2.66	2.75	2.98
Na_2O	3.07	2.91	2.95	2.46	3.16	2.81	2.95	2.87	3.17	3.27	2.72	2.91	3.07	3.05	2.90	2.24
K_2O	2.12	2.13	2.05	1.65	2.16	1.71	1.74	1.81	2.10	2.32	1.83	1.76	1.91	1.81	1.79	1.76
P_2O_5	0.09	0.09	0.09	0.11	0.10	0.11	0.10	0.09	0.09	0.10	0.10	0.09	0.10	0.09	0.10	0.09

C.I.P.W. NORMATIVE COMPOSITIONS

SAMPLE	11219	11220	11221	11222	11224	11225	11226	11227	11230	11231	11234	11235	11236	11237	11238	11239
Q	24.92	25.76	25.18	22.94	26.14	21.87	20.35	21.98	22.62	23.77	21.20	20.75	20.96	20.12	21.17	21.34
OR	12.51	12.59	12.12	9.75	12.77	10.11	10.28	10.70	12.41	13.71	10.81	10.40	11.29	10.70	10.58	10.40
AB	25.98	24.62	24.96	20.82	26.74	23.78	24.96	24.29	26.82	27.67	23.02	24.62	25.98	25.81	24.54	18.96
AN	22.09	21.71	22.67	28.51	21.49	26.16	25.41	25.73	21.48	22.21	26.29	26.00	24.41	25.06	26.26	29.52
DI	2.84	2.25	2.44	0.65	-	3.44	4.55	3.27	4.61	1.18	3.50	3.95	4.26	4.90	2.91	1.24
HY	9.48	10.91	10.49	14.98	10.05	12.36	12.09	11.74	9.87	9.07	12.91	12.01	10.81	11.13	12.28	14.04
†MT	1.20	1.20	1.20	1.20	1.20	1.20	1.20	1.20	1.20	1.20	1.20	1.20	1.20	1.20	1.20	1.20
IL	0.93	0.93	0.93	1.08	1.12	1.04	1.12	1.08	0.97	1.14	1.06	1.06	1.04	1.08	1.04	1.10
AP	0.20	0.20	0.20	0.24	0.22	0.24	0.22	0.20	0.20	0.22	0.22	0.20	0.22	0.20	0.22	0.20
C	-	-	-	-	0.44	-	-	-	-	-	-	-	-	-	-	-

* Total Iron shown as FeO.

All values are in percent.

† Normative magnetite (MT) calculated assuming 0.83% Fe_2O_3 in each sample.

TABLE 22

MAJOR ELEMENT ANALYSES - WHITE ISLAND AND MANAWAHE

MAJOR ELEMENTS

SAMPLE	11240	11241	11242	11243	11244	11245	11246	11247	11248	11249
SiO_2	63.05	62.44	63.43	64.37	63.33	62.88	55.70	65.13	63.82	63.20
TiO_2	0.72	0.74	0.75	0.73	0.71	0.70	0.59	0.59	0.59	0.56
Al_2O_3	14.65	14.57	14.43	15.18	14.63	14.37	16.68	16.18	15.89	14.08
*FeO	5.71	5.90	5.90	5.02	5.52	5.49	6.88	5.05	5.18	4.72
CaO	5.57	5.80	5.91	4.76	5.42	5.50	8.21	4.50	4.38	4.12
MgO	3.42	3.52	3.84	3.12	3.12	3.58	3.80	1.46	1.43	1.37
Na_2O	3.26	3.13	3.24	3.10	3.14	2.98	2.70	3.57	3.53	3.48
K_2O	2.12	2.13	2.17	2.35	2.28	2.14	1.10	2.31	2.32	2.35
P_2O_5	0.12	0.11	0.12	0.11	0.11	0.10	0.08	0.14	0.13	0.14
TOTAL	98.63	98.34	99.81	98.74	98.26	97.74	95.74	98.93	97.27	94.02

MAJOR ELEMENTS RECALCULATED FOR Σ = 100%

SAMPLE	11240	11241	11242	11243	11244	11245	11246	11247	11248	11249
SiO_2	63.93	63.49	63.57	65.19	64.45	64.33	58.18	65.83	65.61	67.22
TiO_2	0.73	0.75	0.75	0.74	0.72	0.72	0.62	0.60	0.61	0.60
Al_2O_3	14.85	14.82	14.46	15.37	14.89	14.76	17.42	16.36	16.34	14.96
*FeO	5.79	6.00	5.91	5.08	5.62	5.62	7.19	5.10	5.33	5.02
CaO	5.65	5.90	5.92	4.82	5.52	5.63	8.58	4.55	4.50	4.38
MgO	3.47	3.58	3.85	3.16	3.18	3.66	3.97	1.48	1.47	1.46
Na_2O	3.31	3.18	3.25	3.14	3.20	3.05	2.82	3.61	3.63	3.70
K_2O	2.15	2.17	2.17	2.38	2.32	2.19	1.15	2.33	2.39	2.50
P_2O_5	0.12	0.11	0.12	0.11	0.11	0.10	0.09	0.14	0.13	0.15

C.I.P.W. NORMATIVE COMPOSITIONS

SAMPLE	11240	11241	11242	11243	11244	11245	11246	11247	11248	11249
Q	17.72	17.29	16.91	20.76	18.95	19.19	10.86	21.39	26.52	22.92
OR	12.77	12.82	12.82	14.07	13.71	12.94	6.80	13.77	14.12	14.77
AB	28.01	26.91	27.50	26.57	27.08	25.81	23.86	30.55	22.26	31.31
AN	19.28	19.76	16.46	20.82	19.41	20.12	31.48	21.56	21.56	16.88
DI	6.62	7.31	8.38	2.01	6.04	5.93	8.75	0.16	-	1.44
HY	12.94	13.23	13.22	13.09	12.17	13.47	15.91	10.10	10.55	8.28
+MT	1.20	1.20	1.20	1.20	1.20	1.20	1.20	1.20	1.20	1.20
IL	1.39	1.42	1.42	1.41	1.37	1.37	1.18	1.14	1.16	1.14
AP	0.26	0.24	0.26	0.24	0.24	0.22	0.20	0.31	0.28	0.33
C	-	-	-	-	-	-	-	-	1.53	-

* Total Iron shown as FeO.

+ Normative magnetite (MT) calculated assuming 0.83% Fe_2O_3 in each sample.

All values are in percent.

on which are plotted some of the analyses given by Clark (1960 b) of other volcanic rocks in the Taupo Volcanic Zone, together with analyses of the Bay of Plenty volcanics. Fig. 21 shows that the Bay of Plenty volcanics almost completely fill a chemical gap between the TNP andesites and the Tauhara dacite.

A detailed discussion of major element variation trends for the Bay of Plenty volcanics, together with a comparison of the chemistry of the individual volcanoes is given in later sections.

TRACE ELEMENT ABUNDANCES

The trace element analyses are presented in Tables 23, 24 and 25 using the style of tabulation proposed by Taylor & White (1966). Table 26 contains analyses by spark-source mass spectrometer for a number of additional elements in three samples. Elements are placed in sections within the tables according to their geochemical affinities which are largely controlled by size (ionic radius), valency (charge) and bond type (ionic-covalent-metallic). Within each section the arrangement is in order of decreasing ionic radius. Elements may occur in more than one section, reflecting dual geochemical behaviour, however the amount of duplication is small. Major elements are included in the sections where comparison with the trace element abundances is desirable, concentrations being expressed as percent element (not percent oxide).

Comparisons between trace element abundances in the Bay of Plenty volcanics and trace element abundances in other Taupo Zone volcanics can be made by reference to Table 33. Comparisons between the Taupo Zone andesites and dacites (including the Bay of Plenty volcanics) and other western-pacific andesites and dacites, are made using analyses in the following papers: Taylor & White (1966); Ewart, Taylor & Capp (1968); Ewart & Stipp (1968); Lewis (1968 a, b); Taylor et al. (1969), Taylor (1969); Gill (in press).

Taupo Zone andesites and dacites are generally similar to other andesite and dacites on the western pacific margin except that they are anomalously high in Rb, Tl, Th, and U, and have higher Rb/Sr and Th/U ratios compared to other western pacific andesites and dacites.

TABLE 23

TRACE ELEMENT ANALYSES - EDGECUMBE

All values are in p.p.m. unless otherwise indicated.
n.d. = not detected. - = not determined.

SECTION 1. LARGE CATIONS

SAMPLE	11205	11206	11207	11208	11210	11211	11212	11213	11214	11215	11216	11217
Cs^{+}	0.7	1.3	2.0	2.9	2.3	2.4	1.8	1.0	2.5	1.2	1.5	1.5
Rb^{+}	70	50	77	54	70	68	72	66	62	61	58	67
Ba^{2+}	620	455	595	455	520	600	610	525	480	470	440	580
$\%K^{+}$	1.67	1.19	1.91	1.29	1.67	1.59	1.69	1.61	1.47	1.45	1.37	1.58
Sr^{2+}	274	254	262	248	223	231	220	280	247	258	256	248
$\%Ca^{2+}$	3.69	5.37	3.41	4.97	3.73	3.82	3.60	4.06	4.36	4.23	4.67	3.80
$\%Na^{+}$	2.41	1.99	2.56	2.18	2.29	2.36	2.39	2.36	2.30	2.25	2.15	2.34
K/Rb	240	238	249	237	239	235	236	245	238	236	235	237
K/Cs $\times 10^{-4}$	2.39	0.92	0.96	0.44	0.73	0.66	0.94	1.61	0.59	1.21	0.91	1.05
Rb/Cs	99.6	38.5	38.4	18.8	30.4	28.3	39.8	65.7	24.7	51.2	38.9	44.5
Ba/Rb	8.90	9.08	7.75	8.36	7.43	8.85	8.51	7.99	7.77	7.65	7.55	8.68
Ba/Sr	2.26	1.79	2.27	1.83	2.33	2.60	2.77	1.88	1.94	1.82	1.72	2.34
Rb/Sr	0.254	0.197	0.293	0.220	0.314	0.294	0.326	0.234	0.250	0.237	0.228	0.269

SECTION 2. RARE EARTHS

Y^{3+}	22	20	24	18	16	16	16	22	16	19	21	18

SECTION 3. LARGE HIGHLY CHARGED CATIONS

Th^{4+}	-	5.14	-	-	-	-	-	6.56	-	5.90	5.54	6.78
U^{4+}	-	1.14	-	-	-	-	-	1.59	-	1.45	1.35	1.78
Zr^{4+}	129	92	139	93	104	104	105	124	108	109	110	110
$\%Ti^{4+}$	0.413	0.438	0.408	0.417	0.342	0.340	0.341	0.453	0.407	0.408	0.441	0.363
Th/U	-	4.50	-	-	-	-	-	4.12	-	4.08	4.11	3.79

TABLE 23 (continued)

All values are in p.p.m. unless otherwise indicated.
n.d. = not detected. - = not determined.

SECTION 4. FERROMAGNESIAN ELEMENTS

SAMPLE	11205	11206	11207	11208	11210	11211	11212	11213	11214	11215	11216	11217
Mn^{2+}	940	1050	930	1020	870	850	830	990	940	920	1050	880
%*Fe^{2+}	4.29	5.05	4.04	4.94	3.87	3.81	3.70	4.34	4.43	4.39	4.86	3.98
Cu^{2+}	15	33	9.4	16	14	16	14	13	14	15	22	16
Co^{2+}	12	17	9.5	15	13	12	11	11	13	13	16	12
Ni^{2+}	5.1	7.3	n.d.	6.4	8.4	7.4	6.5	n.d.	11	10	7.4	6.8
Li^{+}	21	18	34	21	24	24	27	24	29	27	23	25
Mg^{2+}	1.07	2.16	1.01	3.04	1.44	1.29	1.33	1.11	1.53	1.52	1.77	1.24
Ni/Co	0.43	0.43	-	0.44	0.66	0.60	0.58	-	0.84	0.79	0.46	0.58
Sc^{3+}	21	23	17	21	17	17	16	20	17	19	24	18
V^{3+}	145	190	80	150	120	130	120	135	130	140	165	125
%Ti^{4+}	0.413	0.438	0.408	0.417	0.342	0.340	0.341	0.453	0.407	0.408	0.441	0.363
Cr^{3+}	9.9	44	~2	35	26	27	21	7.3	33	31	33	24
Ga^{3+}	19	19	18	17	15	17	16	20	16	18	17	16
%Al^{3+}	8.57	9.07	8.25	8.82	8.21	8.41	8.23	8.75	8.60	8.59	9.68	8.42
Cr/V	0.077	0.228	0.025	0.230	0.214	0.207	0.179	0.054	0.253	0.221	0.197	0.187
Al/Ga $\times 10^{-4}$	0.461	0.472	0.464	0.525	0.537	0.501	0.524	0.444	0.531	0.477	0.520	0.533

SECTION 5. SMALL CATIONS

%Al^{3+}	8.57	9.07	8.25	8.82	8.21	8.41	8.23	8.75	8.60	8.59	8.68	8.42
%Si^{4+}	28.33	27.69	30.58	27.95	30.13	30.22	30.57	29.57	29.43	29.41	28.55	30.30
B^{3+}	14	13	21	14	15	17	19	18	16	18	16	13

SECTION 6. CHALCOPHILE ELEMENTS

%*Fe^{2+}	4.29	5.05	4.04	4.94	3.87	3.81	3.70	4.34	4.43	4.39	4.86	3.98
Cu^{2+}	15	33	9.4	16	14	16	14	13	14	15	22	16
Co^{2+}	12	17	9.5	15	13	12	11	11	13	13	16	12
Ni^{2+}	5.1	7.3	n.d.	6.4	8.4	7.4	6.5	n.d.	11	10	7.4	6.8
Ga^{3+}	19	19	18	17	15	17	16	20	16	18	17	16

* Total Iron shown as Fe^{2+}.

TABLE 24

TRACE ELEMENT ANALYSES - WHALE ISLAND

All values are in p.p.m. unless otherwise indicated.
n.d. = not detected. - = not determined.

SECTION 1. LARGE CATIONS																		
SAMPLE	11218	11219	11220	11221	11222	11224	11225	11226	11227	11230	11231	11233	11234	11235	11236	11237	11238	11239
Cs^{+}	1.3	1.0	0.9	0.7	1.5	n.d.	2.0	1.2	1.3	n.d.	2.7	n.d.	1.4	2.3	3.1	1.5	1.9	2.0
Rb^{+}	68	71	70	69	59	77	62	63	61	71	78	30	58	60	63	61	63	61
Ba^{2+}	770	900	780	790	740	860	635	690	645	940	810	635	675	695	625	670	605	580
$\%K^{+}$	1.67	1.75	1.75	1.67	1.34	1.76	1.41	1.42	1.49	1.72	1.84	1.17	1.47	1.43	1.55	1.45	1.46	1.43
Sr^{2+}	220	206	207	209	220	211	235	236	235	213	214	256	214	235	229	234	238	239
$\%Ca^{2+}$	4.48	3.73	3.56	3.70	4.23	3.11	4.43	4.45	4.31	3.93	3.34	4.88	4.35	4.40	4.25	4.38	4.29	4.45
$\%Na^{+}$	2.31	2.26	2.14	2.14	1.79	2.30	2.07	2.15	2.11	2.32	2.32	2.03	1.95	2.11	2.20	2.18	2.11	2.09
K/Rb	247	245	249	241	226	228	228	227	244	244	235	395	252	240	245	240	231	234
K/Cs $\times 10^{-4}$	1.28	1.75	1.94	2.39	0.89	-	0.71	1.18	1.15	-	0.68	-	1.05	0.62	0.50	0.97	0.77	0.72
Rb/Cs	52.0	71.3	78.1	99.1	39.5	-	30.9	52.1	47.0	-	29.0	-	41.6	26.0	20.4	40.3	33.3	30.6
Ba/Rb	11.4	12.6	11.1	11.4	12.5	11.1	10.3	11.0	10.6	13.3	10.4	21.5	11.6	11.6	9.89	11.1	9.57	9.48
Ba/Sr	3.50	4.37	3.77	3.78	3.36	4.08	2.70	2.92	2.74	4.41	3.79	2.48	3.15	2.96	2.73	2.86	2.54	2.43
Rb/Sr	0.307	0.346	0.340	0.331	0.269	0.366	0.263	0.264	0.260	0.330	0.365	0.116	0.272	0.254	0.276	0.259	0.265	0.257
SECTION 2. RARE EARTHS																		
Y^{3+}	17	18	14	16	19	16	14	19	16	17	19	19	17	16	16	17	16	17
SECTION 3. LARGE HIGHLY CHARGED CATIONS																		
Th^{4+}	5.88	6.18	-	-	-	-	-	-	5.20	6.50	7.25	4.66	6.03	5.57	5.72	5.31	5.64	5.29
U^{4+}	1.39	1.49	-	-	-	-	-	-	1.29	1.47	1.80	1.24	1.33	1.39	1.39	1.44	1.27	1.34
Zr^{4+}	95	104	109	108	107	128	107	98	95	102	122	97	99	98	92	90	93	96
$\%Ti^{4+}$	0.336	0.295	0.295	0.290	0.336	0.345	0.330	0.346	0.338	0.299	0.340	0.402	0.323	0.329	0.323	0.329	0.321	0.339
Th/U	4.22	4.16	-	-	-	-	-	-	4.04	4.42	4.02	3.76	4.55	4.00	4.11	3.69	4.43	3.95

TABLE 24 (continued)

All values are in p.p.m. unless otherwise indicated.

n.d. = not detected. - = not determined.

SECTION 4. FERROMAGNESIAN ELEMENTS

SAMPLE	11218	11219	11220	11221	11222	11224	11225	11226	11227	11230	11231	11233	11234	11235	11236	11237	11238	11239
Mn^{2+}	950	810	840	860	910	800	940	910	880	880	800	940	920	900	880	910	890	960
%*Fe^{2+}	4.47	3.44	3.68	3.54	4.17	3.58	4.11	4.15	3.99	3.67	3.40	4.67	4.14	4.05	3.87	3.97	3.99	4.16
Cu^{2+}	18	15	22	16	15	13	13	21	23	16	10	15	14	18	18	20	14	14
Co^{2+}	15	11	12	13	15	9.5	13	14	14	11	8.9	15	14	13	12	13	12	14
Ni^{2+}	9.4	6.4	12	7.0	8.5	n.d.	6.2	10	8.9	7.4	n.d.	n.d.	5.6	5.4	6.3	6.3	6.2	6.5
Li^{+}	21	22	24	19	17	29	15	18	18	25	21	31	19	19	20	20	20	19
%Mg^{2+}	1.97	1.30	1.43	1.39	1.89	1.02	1.69	1.71	1.59	1.46	0.96	2.10	1.72	1.64	1.50	1.55	1.63	1.76
Ni/Co	0.64	0.56	0.97	0.54	0.55	-	0.49	0.73	0.63	0.66	-	-	0.41	0.40	0.53	0.47	0.51	0.47
Sc^{3+}	15	17	17	12	21	18	18	22	20	19	15	24	14	19	17	13	17	19
V^{3+}	135	125	110	105	140	115	130	170	140	120	115	105	135	140	120	125	125	135
%Ti^{4+}	0.336	0.295	0.295	0.290	0.336	0.345	0.330	0.346	0.338	0.299	0.340	0.402	0.323	0.329	0.323	0.329	0.321	0.339
Cr^{3+}	38	27	38	33	44	114	18	38	32	30	~2	21	31	20	24	27	27	33
Ga^{3+}	16	17	14	14	16	15	13	17	16	18	16	15	13	16	14	13	16	13
%Al^{3+}		8.13	7.91	7.98	8.43	8.22	8.43	8.34	8.44	8.02	8.11		8.25	8.37	8.30	8.25	8.46	8.51
Cr/V	0.289	0.214	0.346	0.308	0.312	0.991	0.138	0.219	0.231	0.251	0.017	0.197	0.235	0.139	0.196	0.215	0.212	0.246
Al/Ga $\times 10^{-4}$		0.475	0.553	0.582	0.537	0.559	0.639	0.485	0.534	0.451	0.510		0.630	0.530	0.610	0.640	0.542	0.635

SECTION 5. SMALL CATIONS

%Al^{3+}		8.13	7.91	7.98	8.43	8.22	8.43	8.34	8.44	8.02	8.11		8.25	8.37	8.30	8.25	8.46	8.51
%Si^{4+}		31.09	31.13	30.63	29.32	30.80	29.85	29.31	29.88	30.43	29.74		28.99	29.17	29.48	28.87	29.42	29.35
B^{3+}	15	20	19	18	15	18	17	17	16	16	27	<10	20	17	20	19	18	19

SECTION 6. CHALCOPHILE ELEMENTS

%*Fe^{2+}	4.47	3.44	3.68	3.54	4.17	3.58	4.11	4.15	3.99	3.67	3.40	4.67	4.14	4.05	3.87	3.97	3.99	4.16
Cu^{2+}	18	15	22	16	15	13	13	21	23	16	10	15	14	18	18	20	14	14
Co^{2+}	15	11	12	13	15	9.5	13	14	14	11	8.9	15	14	13	12	13	12	14
Ni^{2+}	9.4	6.4	12	7.0	8.5	n.d.	6.2	10	8.9	7.4	n.d.	n.d.	5.6	5.4	6.3	6.3	6.2	6.5
Ga^{3+}	16	17	14	14	16	15	13	17	16	18	16	15	13	16	14	13	16	13

* Total iron shown as Fe^{2+}.

TABLE 25

TRACE ELEMENT ANALYSES - WHITE ISLAND AND MANAWAHE

SECTION 1. LARGE CATIONS										
SAMPLE	11240	11241	11242	11243	11244	11245	11246	11247	11248	11249
Cs^{+}	0.5	3.8	2.2	n.d.	n.d.	3.8	n.d.	n.d.	n.d.	3.1
Rb^{+}	71	72	74	78	75	74	40	79	79	83
Ba^{2+}	950	775	920	910	905	940	940	620	635	655
$\%K^{+}$	1.77	1.77	1.79	1.95	1.89	1.74	0.91	1.92	1.93	1.95
Sr^{2+}	181	176	183	163	172	169	215	221	220	212
$\%Ca^{2+}$	3.99	4.14	4.22	3.40	3.87	3.93	5.87	3.22	3.13	2.95
$\%Na^{+}$	2.42	2.32	2.40	2.30	2.33	2.21	2.00	2.65	2.62	2.58
K/Rb	250	247	242	251	253	235	227	245	244	235
K/Ca $\times 10^{-4}$	3.54	0.47	0.81	-	-	0.46	-	-	-	0.63
Rb/Cs	142	18.9	33.6	-	-	19.5	-	-	-	26.8
Ba/Rb	13.4	10.8	12.4	11.7	12.1	12.7	23.4	7.90	7.99	7.89
Ba/Sr	5.25	4.40	5.03	5.58	5.26	5.56	4.37	2.81	2.88	3.09
Rb/Sr	0.392	0.408	0.405	0.476	0.433	0.439	0.187	0.355	0.360	0.391
SECTION 2. RARE EARTHS										
Y^{3+}	22	24	30	30	33	26	24	36	39	30
SECTION 3. LARGE HIGHLY CHARGED CATIONS										
Th^{4+}	7.57	-	6.33	6.45	6.46	6.45	3.98	8.19	7.49	-
U^{4+}	1.47	-	1.50	1.36	1.71	1.63	0.78	1.77	1.70	-
Zr^{4+}	146	147	148	155	154	148	79	157	155	159
$\%Ti^{4+}$	0.430	0.441	0.448	0.436	0.428	0.418	0.349	0.356	0.353	0.333
Th/U	5.17	-	4.23	4.75	3.78	3.97	5.12	4.62	4.40	-

All values are in p.p.m. unless otherwise indicated.

n.d. = not detected. - = not determined.

TABLE 25 (continued)

SECTION 4. FERROMAGNESIAN ELEMENTS

SAMPLE	11240	11241	11242	11243	11244	11245	11246	11247	11248	11249
Mn^{2+}	830	880	880	670	710	820	1020	810	700	700
%*Fe^{2+}	4.44	4.59	4.58	3.90	4.29	4.27	5.35	3.93	4.03	3.67
Cu^{2+}	41	76	74	82	92	65	31	12	19	12
Co^{2+}	19	18	20	21	23	19	25	10	11	10
Ni^{2+}	41	53	54	45	46	52	14	n.d.	n.d.	n.d.
Li	18	16	18	21	28	21	5.2	24	30	42
%Mg^{2+}	2.05	2.12	2.31	1.88	1.88	2.16	2.29	0.88	0.86	0.83
Ni/Co	2.16	2.96	2.68	2.18	2.04	2.79	0.56	-	-	-
Sc^{3+}	17	19	25	14	14	24	23	17	19	17
V^{3+}	185	165	215	175	170	170	185	100	115	85
%Ti^{4+}	0.430	0.441	0.448	0.436	0.428	0.418	0.349	0.356	0.353	0.333
Cr^{3+}	115	104	127	101	114	120	35	2	2	2
Ga^{3+}	17	15	16	14	14	17	17	16	16	18
%Al^{3+}	7.75	7.71	7.63	8.03	7.74	7.60	8.82	8.56	8.41	7.45
Cr/V	0.628	0.627	0.585	0.584	0.675	0.698	0.188	0.020	0.017	0.023
Al/Ga $x10^{-4}$	0.453	0.514	0.468	0.586	0.538	0.439	0.528	0.538	0.526	0.414

SECTION 5. SMALL CATIONS

%Al^{3+}	7.75	7.71	7.63	8.03	7.74	7.60	8.82	8.56	8.41	7.45
%Si^{4+}	29.45	29.17	29.64	30.07	29.59	29.38	26.03	30.43	29.82	29.53
B^{3+}	32	31	37	30	21	35	20	9.9	9.5	11

SECTION 6. CHALCOPHILE ELEMENTS

%*Fe^{2+}	4.44	4.59	4.58	3.90	4.29	4.27	5.35	3.93	4.03	3.67
Cu^{2+}	41	76	74	82	92	65	31	12	19	12
Co^{2+}	19	18	20	21	23	19	25	10	11	10
Ni^{2+}	41	53	54	45	46	52	14	n.d.	n.d.	n.d.
Ga^{3+}	17	15	16	14	14	17	17	16	16	18

All values are in p.p.m. unless otherwise indicated.

n.d. = not detected. - = not determined.

* Total Iron shown as Fe^{2+}.

TABLE 26

ADDITIONAL TRACE ELEMENTS DETERMINED IN SELECTED SAMPLES BY SPARK-SOURCE MASS SPECTROMETRY

SAMPLE NO.	11217	11242	11246
Pb^{2+}	3.0	12	2.4
Tl^{+}	0.10	0.20	0.10
W^{6+}	1.0	3.3	1.5
Hf^{4+}	1.6	3.4	1.8
La^{3+}	47	28	17
Ce^{3+}	74	55	32
Pr^{3+}	10	8.6	5.0
Nd^{3+}	43	17	21
Sm^{3+}	6.7	4.4	5.3
Eu^{3+}	0.80	1.3	1.5
Gd^{3+}	2.9	4.6	5.6
Tb^{3+}	0.50	0.81	1.0
Dy^{3+}	2.8	4.5	5.5
Ho^{3+}	0.53	0.80	0.94
Er^{3+}	1.7	2.7	3.2
Tm^{3+}	0.22	0.36	0.43
Yb^{3+}	1.5	2.4	2.6
Nb^{5+}	7	9	4
Rb/Tl	670	370	400
Zr/Hf	68.8	43.5	43.9

All values are in p.p.m.

Analyst: M.J. Kaye.

The only presently known exceptions are three andesites from Fiji, (Taylor et al., 1969; Gill, in press) which although they have Th and U abundances lower than Taupo Zone andesites, have comparable Th/U ratios to those in Taupo Zone volcanics.

Three possible explanations for this regional geochemical anomaly are:- (a) lateral inhomogeneity in the upper mantle resulting in a primary basaltic or andesitic magma beneath New Zealand having chemical characteristics unlike those in other parts of the circum-pacific margin; (b) fractional crystallisation of either a primary basaltic or andesitic magma, since all four anomalous elements are typically concentrated by such a process; (c) contamination of the primary magma with "typical" upper crustal material which has higher contents of the anomalous elements than are generally found in andesites and dacites. The second and third possibilities have been considered for andesites in general by many authors, recently Taylor & White (1965, 1966), Taylor (1968, 1969) and Taylor et al. (1969) who concluded that neither process is applicable in general on geological (basalt-andesite volume problem, lack of "typical upper crust" in such areas as the Saipan and Aleutian Arcs) or geochemical grounds (high K/Rb, K/Cs, Ba/Rb, Eu/Gd, and V/Ni ratios, low Rb/Sr, Ba/Sr and Ni/Co ratios, low abundances of Cs, Rb, Tl, Ba, Th, U, Zr, and Hf in andesites).

The four elements which are anomalously high in abundance in Taupo Zone andesites and dacites are elements whose typically low concentrations in most andesites are considered by Taylor and his co-authors to be evidence against fractional crystallisation or crustal contamination as genetic processes for andesites. Consequently, these two genetic processes must be considered for the Taupo Zone in a regional context, and cannot be dismissed on general grounds.

EDGECUMBE AND WHALE ISLAND GEOCHEMISTRY

Analyses of a number of samples from the same volcanic unit (Main Dome - Edgecumbe) shows that for most elements the variation between samples is less than the limits of analytical error, and for the remaining elements the range of variation is extremely small (see Appendix 3). For samples of known relative age there is no overall chemical variation with time shown by the rocks of either Edgecumbe or Whale Island, however a cyclic chemical variation could have been operative. In view of the comparatively large number of elements analysed and the significant chemical differences between many samples, rocks from the same volcano which have very similar abundances of all the elements analysed are thought to have been erupted at about the same time. The geochemical data can thus be used for stratigraphic correlation, but not to determine relative stratigraphic order.

A comparison of the geochemistry of analysed samples with their petrography and geological relationships is given in Appendix 3.

The mean chemical compositions of Whale Island and Edgecumbe rocks are shown in Table 27, which includes figures for major and trace elements, together with some element ratios. Table 27 also includes standard deviations and values of the statistical parameters "F" and "Student's 't'". The parameter "F" is the ratio of the squares of the standard deviations for the element distributions in Edgecumbe and Whale Island rocks, and is used to determine whether there is any significant difference in the variances of the two distributions. Student's 't' is a parameter used to test for

TABLE 27

COMPARISON OF EDGECUMBE AND WHALE ISLAND ANALYSES

OXIDE or ELEMENT	EDGECUMBE		WHALE ISLAND		F	t
	Mean	S.D.	Mean	S.D.		
$\%SiO_2$	63.95	2.18	64.91	1.21	3.25	1.98
$\%TiO_2$	0.66	0.06	0.54	0.03	3.39	5.98
$\%Al_2O_3$	16.42	0.52	15.93	0.43	1.51	2.56
%FeO	5.65	0.64	5.16	0.36	3.10	2.46
%CaO	5.10	0.84	5.95	0.46	3.30	0.18
%MgO	2.60	0.61	2.68	0.28	4.63	0.45
$\%Na_2O$	3.10	0.19	2.86	0.25	1.66	2.55
$\%K_2O$	1.32	0.22	1.86	0.16	1.85	0.52
$\%P_2O_5$	0.11	0.01	0.09	0.01	3.52	5.11
[1]C.I.	30.96	4.05	30.84	2.73	2.19	0.09
[2]D.I.	56.43	5.81	57.55	3.53	2.71	0.60
Rb	63.2	7.25	63.7	4.56	2.52	0.22
Ba	523	72.23	712	107.1	2.20	4.93
Sr	246	16.76	225	12.75	1.73	3.51
K/Rb	237	1.66	239	8.41	25.59	0.81
Ba/Rb	8.27	0.62	11.1	1.14	3.37	7.45
Ba/Sr	2.14	0.37	3.19	0.65	3.07	4.75
Rb/Sr	0.25	0.04	0.28	0.03	1.44	1.66
Y	18.0	2.27	16.5	1.40	2.63	2.05
Zr	106	10.25	99.8	6.35	2.60	1.99
Mn	934	81.09	893	39.78	2.60	1.99
Cu	17.3	5.69	17.0	3.22	3.11	0.15
Co	13.2	1.88	13.0	1.18	2.54	0.46
Ni	7.6	1.73	7.3	1.82	1.10	0.43
Li	23.9	3.29	19.5	2.66	1.53	3.60
Ni/Co	0.58	0.14	0.56	0.14	1.00	0.24
Sc	19.4	2.80	17.4	2.85	1.04	1.72
V	142	23.10	130	15.70	2.16	1.51
Cr	28.2	9.09	30.0	7.23	1.58	0.55
Ga	16.9	1.29	14.9	1.69	1.70	3.11
Cr/V	0.19	0.04	0.23	0.05	1.51	1.51
B	15.4	2.14	17.8	1.56	1.87	3.20

[1] Crystallisation Index (Poldervaart & Parker, 1964)

[2] Differentiation Index (Thornton & Tuttle, 1960)

All analyses are in p.p.m. unless otherwise indicated.

12 Edgecumbe samples
16 Whale Island samples

significant difference between the means of the two distributions. Both statistical parameters are only strictly applicable to normal distributions but in view of the restricted range of composition, the author considers the assumption of a normal distribution for these samples to be justified. For a larger number of samples the normality of the distribution could reasonably be tested.

The major element compositions of the two volcanoes are extremely similar, with Whale Island being slightly more acidic. The only major elements showing significantly different abundances in the two volcanoes are Ti and P, both of which are higher in Edgecumbe than in Whale Island. The trace elements Sr, Li and Ga are significantly higher, and the elements Ba and B significantly lower in Edgecumbe than in Whale Island. The element ratios Ba/Rb and Ba/Sr are significantly higher in Whale Island, and the ratio Fe/Co significantly higher in Edgecumbe.

If a common parental magma for Edgecumbe and Whale Island is postulated, then fractional crystallisation cannot explain the overall average differences between the analysed extrusive products of these volcanoes. Accordingly it is suggested that either the magma supplied to each of these two volcanoes is not of common parentage, or that during transit to the surface processes other than crystal fractionation (e.g. crustal assimilation, wall rock reaction) have been operative. In view of this possibility of assimilation or wall rock reaction, it is significant that the concentration of Sr, Li, Ga and Ba in N.Z. marginal facies greywackes (Ewart, Taylor & Capp, 1968) is such that the differences between Whale Island and Edgecumbe average compositions could be accounted for by contaminating a magma of Whale

Island composition with a small amount of greywacke, to produce a magma of Edgecumbe composition. The concentration of other elements analysed in the marginal facies greywacke is compatible with this suggestion.

Correlation of Modal and Chemical Analyses

In view of the general similarity in both modal petrography and chemistry between Edgecumbe and Whale Island samples, a bivariate correlation matrix for modal analyses, major elements and some trace elements and element ratios was computed. The lack of strong correlation between any modal mineral and any element or ratio of elements is the most striking feature of this matrix. For minor modal constituents it is possibly explained by the probable inaccuracies of the modal analyses (discussed on p.26), but for major constituents, in particular the proportions of groundmass and plagioclase, it cannot be explained in this way. The most important inference is that the high Al_2O_3 content of these representatives of the calc-alkaline association is clearly not due to the accumulation of plagioclase in the magma, as has been suggested by some authors. Additional evidence against significant plagioclase accumulation is given in the section on trace element variations.

WHITE ISLAND GEOCHEMISTRY

The seven analysed samples from White Island fall into two clear groups. One group is represented by a single analysed sample (11246) from an outcrop at the base of Troup Head and the other group by all other analysed samples which are from various locations on the Central Cone, which is the youngest portion of the island. The Troup Head

sample is from either a tholoid or coulée underlying lavas and pyroclastics from the Central Cone, and is thought to have been erupted from an eastern vent whose activity may have preceded the formation of Central Cone, possibly coinciding with activity from the Western Cone. The Troup Head sample is an andesite with 58% SiO_2, whereas all the Central Cone samples are chemically dacitic, averaging 64% SiO_2.

Table 28 contains the analyses of the Troup Head andesite, the average of the Central Cone dacites, and the average of all non-xenolithic Edgecumbe and Whale Island samples together with their standard deviations.

The Troup Head andesite is a more basic rock than any analysed non-xenolithic sample from Edgecumbe or Whale Island, but it compares very closely in both major and trace element chemistry with many circum-pacific andesites, except with regard to the elements Ba, Sr, Th, and U. In common with the other Bay of Plenty volcanics the Troup Head andesite is high in Ba and low in Sr, however Ba is far higher than in any other N.Z. andesite (940 ppm compared to c. 250 ppm in TNP andesites of similar major element composition). The Troup Head andesite also shows unusually high Th and U contents and a high Th/U ratio.

The Central Cone dacites have unusual major and trace element compositions and are unlike any other N.Z. or circum-pacific dacite for which analyses were available to the author. When compared with the average major element composition of Edgecumbe and Whale Island dacites, the Central Cone dacites are notable for their low Al_2O_3 and high MgO and K_2O content. The low Al_2O_3 and high MgO contents

TABLE 28

COMPARISON OF WHITE ISLAND, EDGECUMBE AND WHALE ISLAND ANALYSES

	WHITE ISLAND		EDGECUMBE & WHALE ISLAND	
	Troup Head Andesite	Central Cone Dacites*	Mean**	S.D.
MAJOR ELEMENTS (%)				
SiO_2	58.18	64.02	64.39	2.15
TiO_2	0.62	0.73	0.62	0.11
Al_2O_3	17.42	14.81	16.14	0.54
[1]FeO	7.19	5.67	5.41	0.74
CaO	8.58	5.79	5.86	0.77
MgO	3.97	3.47	2.54	0.53
Na_2O	2.82	3.18	3.03	0.22
K_2O	1.15	2.22	1.90	0.22
P_2O_5	0.09	0.11	0.11	0.02
LARGE CATIONS				
Cs^+	n.d.	1.7	1.7	0.7
Rb^+	40.1	73.8	65.1	6.8
Ba^+	940	900	640	136
$\%K^+$	0.91	1.82	1.55	0.17
Sr^{2+}	215	174	235	20.2
$\%Ca^{2+}$	5.87	3.93	4.09	0.50
$\%Na^+$	2.00	2.33	2.21	0.16
K/Rb	227	247	240	5.8
Ba/Rb	23.4	12.2	10.2	1.8
Ba/Sr	4.37	5.17	2.76	0.85
Rb/Sr	0.187	0.424	0.265	0.04
RARE EARTHS				
Y^{3+}	24.2	27	18	2.4
LARGE HIGHLY CHARGED CATIONS				
Th^{4+}	3.98	6.7	5.9	0.6
U^{4+}	0.78	1.5	1.4	0.2
Zr^{4+}	79	150	105	12.4
Th/U	5.12	4.47	4.14	0.27
FERROMAGNESIAN ELEMENTS				
Mn^{2+}	1020	800	910	67
$\%Fe^{2+}$	5.35	4.35	4.06	0.42
Cu^{2+}	31	72	16	4.5
Co^{2+}	25	20	12	2.9
Ni^{2+}	14	49	6.4	3.1
Li^+	5.2	20	22	4.4
$\%Mg^{2+}$	2.29	2.07	1.53	0.41
Ni/Co	0.563	2.45	0.53	0.11
Sc^{3+}	23	19	18	2.8
V^{3+}	185	180	130	21
Cr^{3+}	35	115	30	19.3
$\%Ti^{4+}$	0.349	0.434	0.355	0.05
Ga^{3+}	17	16	16	1.9
$\%Al^{3+}$	8.82	7.74	8.38	0.26
Cr/V	0.188	0.639	0.221	0.041
Al/Ga $\times 10^{-4}$	0.528	0.484	0.536	0.058
V/Ni	13.2	3.67	20.3	4.63
SMALL CATIONS				
$\%Si^{4+}$	26.03	29.55	29.65	0.89
B^{3+}	19.5	31	17.5	2.8

* Mean of 6 analyses.

[1] Total Iron shown as FeO.

** Mean of 26 analyses.

All values are in p.p.m. unless otherwise indicated.

n.d. = not detected.

relative to their SiO_2 content also distinguishes them from other circum-pacific dacites. Trace element comparisons between Central Cone dacites and dacites from Edgecumbe and Whale Island show the former to be higher in Ba and Rb, and lower in Sr; with markedly higher Ba/Sr and Rb/Sr ratios. Fig. 22 shows histograms of the Ba and Sr distributions in Edgecumbe, Whale Island, and White Island rocks. Zr is the only large highly-charged cation to show relative enrichment in the Central Cone dacites. Many of the ferromagnesian trace elements, in particular Cu, Co, Ni, V and Cr are anomalously high in the Central Cone dacites. Comparative histograms of the Ni, Co, Cr and Cu distributions are shown in Figs. 23 and 24. Cu, Ni and Cr in Central Cone dacites are higher than in many high-alumina basalts, and most andesites. In addition the Ni/Co ratio (2.45) and the V/Ni ratio (3.67) are quite different from the values usually found in calc-alkaline volcanics (Ni/Co~0.5, V/Ni$\sim$10). Hence although the Central Cone dacites show concentration of the large cations and large highly-charged cations consistent with a derivation by fractional crystallisation from a more basic parental magma; the strong concentration of many ferromagnesian trace elements is incompatible with such a derivation. There are two other major possible processes; the first, an unlikely one, that these dacites are direct mantle melts, and thus have unusual compositions. The second possibility is that a normal dacite or andesite has been contaminated with material which has unusually high Cu, Co, Ni, V, and Cr, but has a major element composition approximately in the andesite-dacite range. The author considers that direct mantle derivation is unlikely, because of the very large concentration factors that would be required for many of the large

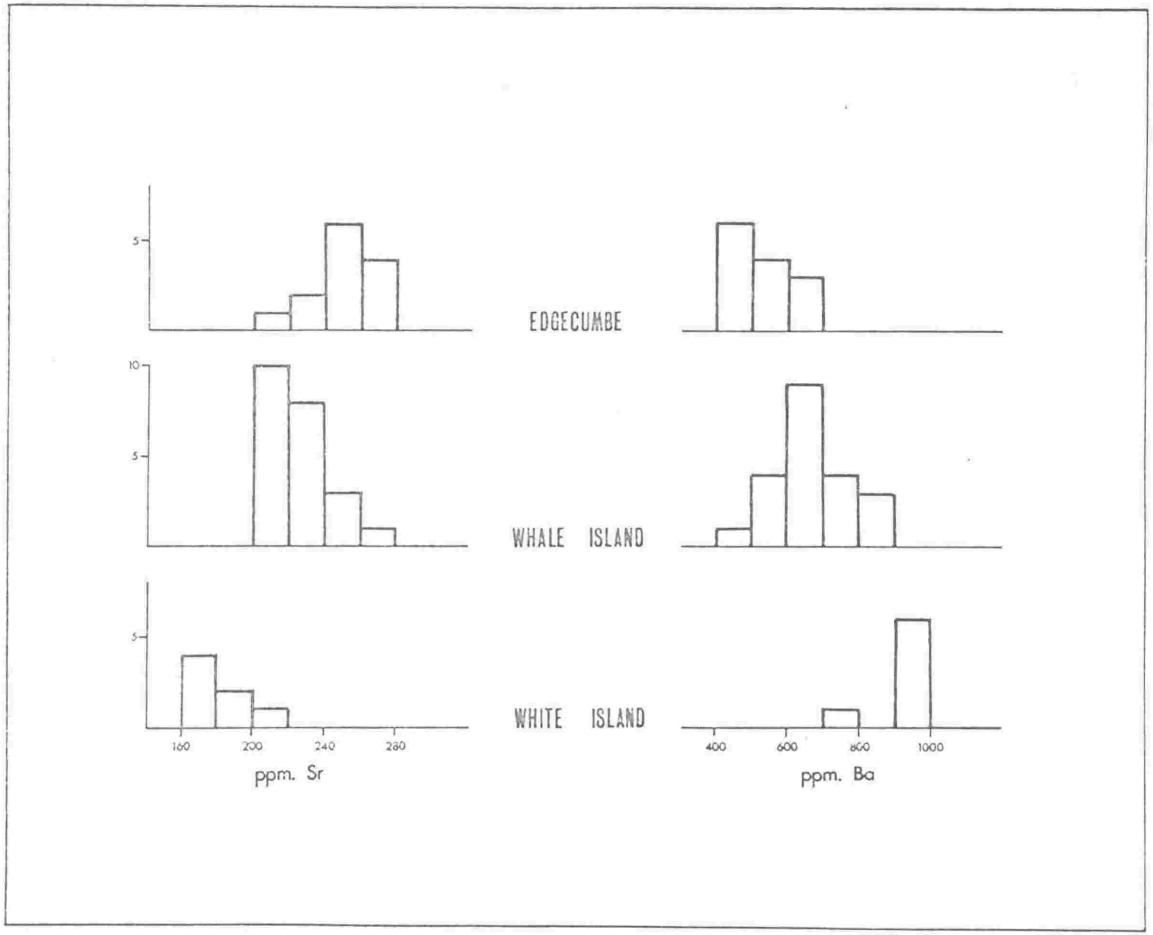

Fig. 22. - Histograms of Strontium and Ba distributions in samples from Edgecumbe, Whale Island and White Island.

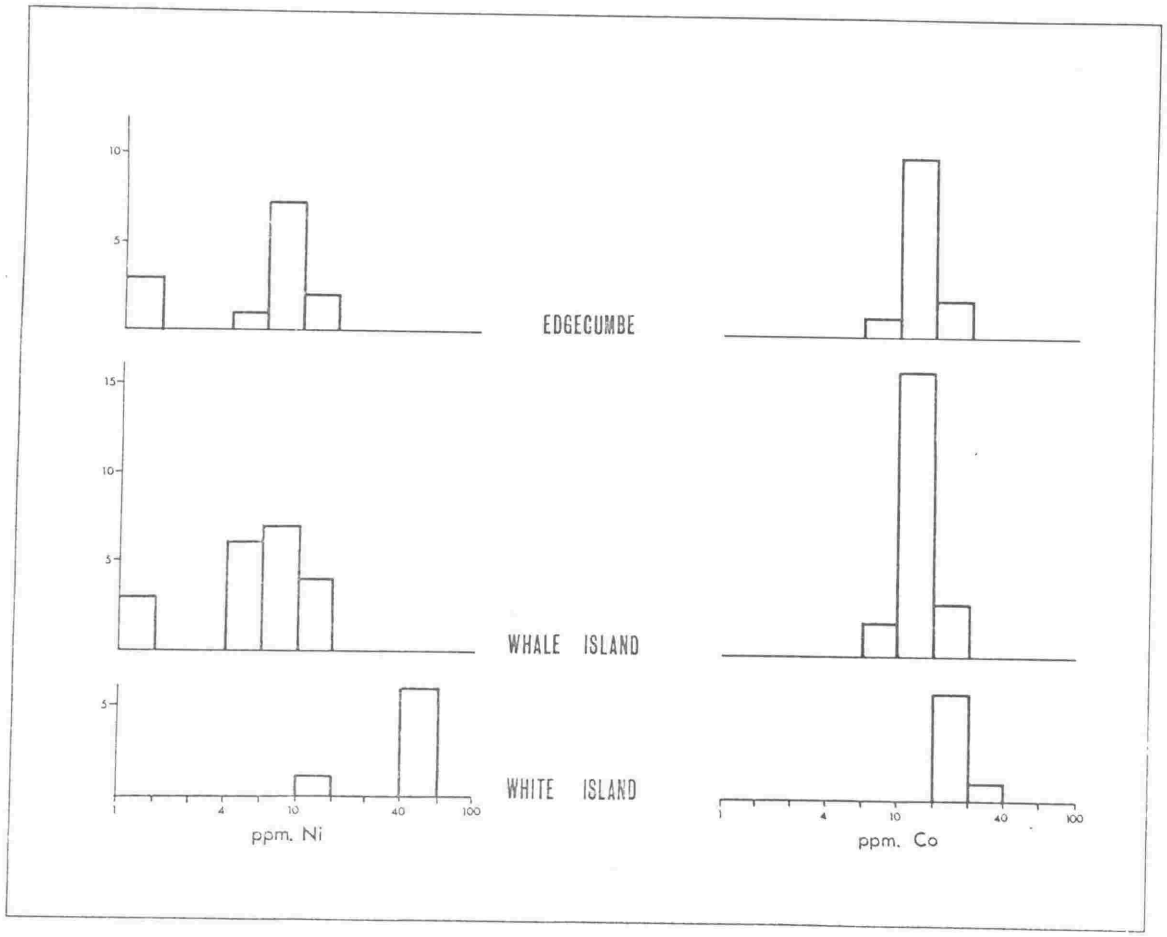

Fig. 23. - Histograms of Nickel and Cobalt distributions in samples from Edgecumbe, Whale Island and White Island.

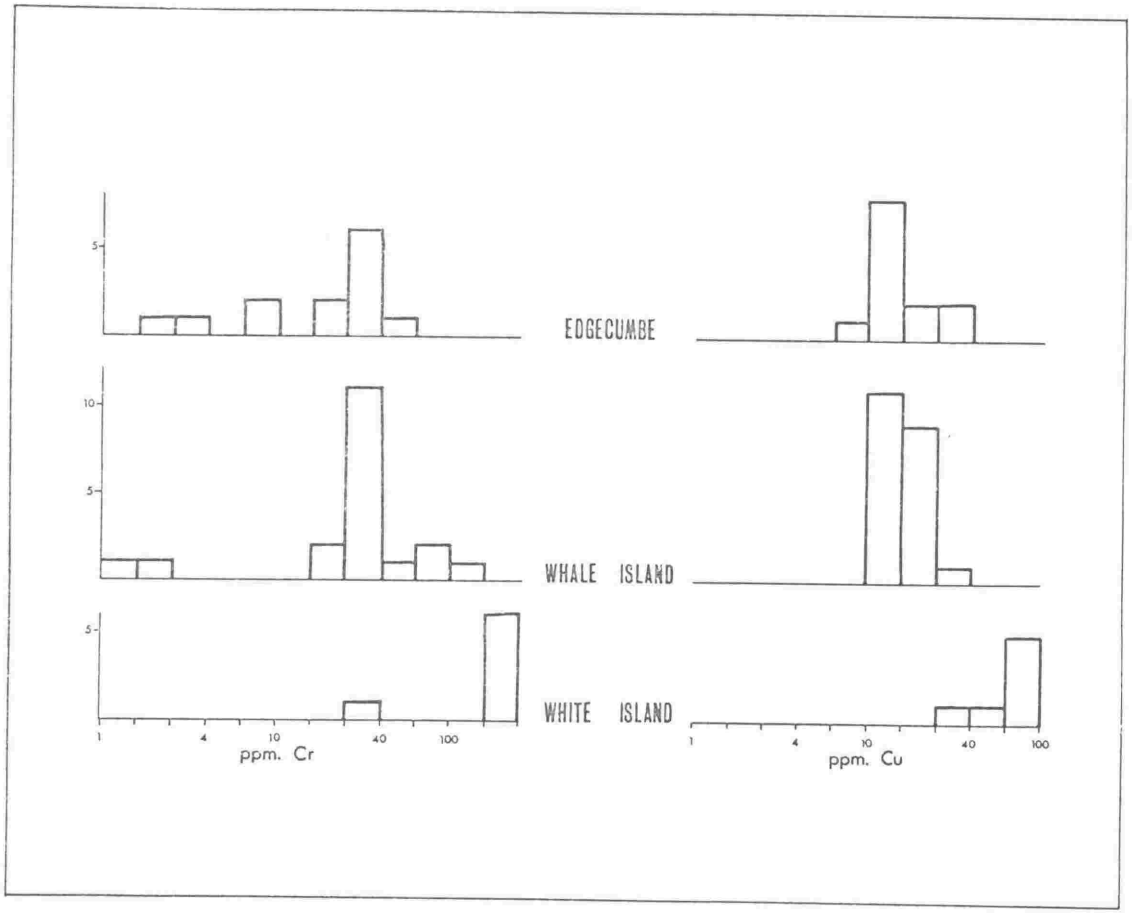

Fig. 24. - Histograms of Chromium and Copper distributions in samples from Edgecumbe, Whale Island and White Island.

cations or large highly-charged cations during the partial melting process or during subsequent wall-rock reaction.

What type of material would be a suitable contaminant? The combination of fairly acidic major element composition, and a relatively high content of ferromagnesian trace elements is unusual in igneous rocks, but is much more common in sedimentary rocks. Analyses of trace elements in N.Z. shales or mudstones, likely to be present on the continental shelf near White Island have not been made. However analyses of shales, argillites and greywackes, some from N.Z. (Ewart, Taylor & Capp, 1968) and others from North America and Europe (Shaw, 1954; Weber & Middleton, 1961;) have compositions which approximately match the theoretical contaminant. Additional evidence that marine sediments may be involved in the contamination of White Island magmas was obtained from analysis of boron in Edgecumbe, Whale Island and White Island samples, the results of which are expressed as a histogram in Fig. 25. B is twice as high in Central Cone dacites as in Edgecumbe and Whale Island rocks, and is markedly higher than the values for B in other N.Z. volcanic rocks reported by Ellis & Sewell (1963). The significance of high B concentrations in Central Cone dacites is that B is an element which is concentrated in marine sediments (e.g. compilation of data by Turekian & Wedepohl, 1961; Taylor, 1965 b) and has been used for the determination of paleosalinity of shales (Degens et al., 1957, 1958). Anomalously high B contents, together with the other evidence discussed above, suggests that the Central Cone magma was contaminated by marine sediments.

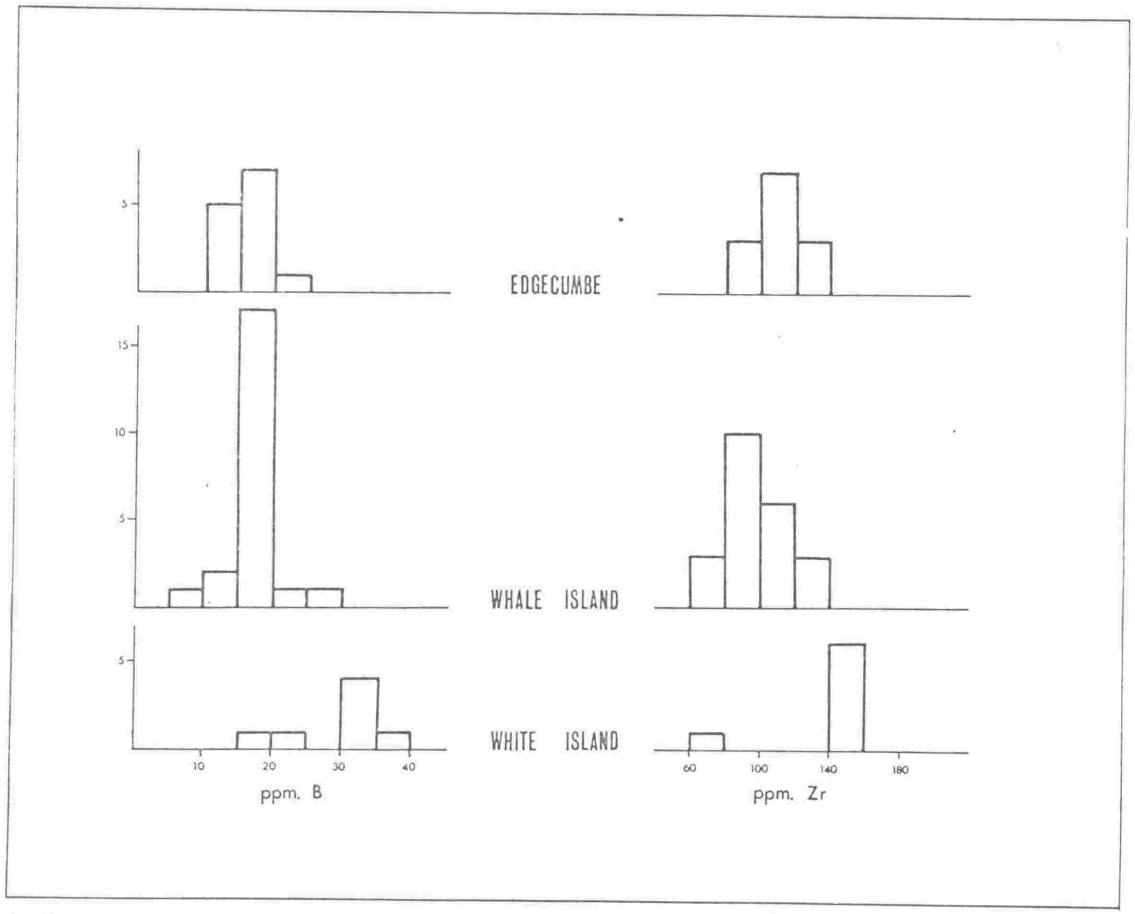

Fig. 25. - Histograms of Boron and Zirconium distributions in samples from Edgecumbe, Whale Island and White Island.

Halite, anhydrite and gypsum (all are evaporation products of seawater) occurred in significant quantities in ash erupted from White Island in 1968 and 1969. Oxygen isotope data obtained by Stewart & Hulston (pers. comm.) indicates that a significant proportion of the steam output of White Island during the 1968 eruptions from Rudolf vent consisted of seawater. The Cl^- content of a White Island rock sample (Ellis & Sewell, 1963) is more than twice that in any other N.Z. andesite or dacite, and a sample of Central Cone dacite has ten times the I^- content of an Edgecumbe dacite.

It seems therefore, that there is a strong possibility that both marine sediments and seawater have contaminated the parental magma for the Central Cone of White Island, giving rise to dacites with unusual trace element chemistry. The parental magma is of unknown composition, but it was probably andesitic or dacitic.

MANAWAHE GEOCHEMISTRY

All three analysed samples from Manawahe are dacites of very similar composition, and they all show significant differences from the other Bay of Plenty volcanics with regard to a number of elements. In particular, Manawahe samples are high in the elements, Y, Th, U, Zr and Li; and low in the elements Mg, Ni, Cr, B and the Cr/V ratio, when compared to the other Bay of Plenty volcanics.

MAJOR ELEMENT VARIATIONS

Major element variations in the Bay of Plenty volcanics have been studied from two aspects; (1) whether their chemistry fits into the basalt-andesite-dacite-rhyolite variation trend for the volcanics of the Taupo Zone, as determined by Steiner (1958) and Clark (1960 b); and (2) to determine the process of variation within the Bay of Plenty volcanics.

Both Steiner (1958, Fig. 18) and Clark (1960 b, Figs. 13 and 14) illustrated the variation pattern of the major oxides using Harker diagrams, in addition, Steiner used an AFM ternary diagram and Clark a von Wolff ternary diagram to illustrate the overall chemical trend. Harker diagrams for the Bay of Plenty volcanics together with their RMA (reduced major axis) regression lines, are given in Figs. 26, and 27, (RMA regressions are for non-xenolithic samples). Clark's (1960 b) Harker diagram curves for the Taupo Zone volcanics are shown on the Bay of Plenty diagrams by dotted lines. For most elements the Bay of Plenty volcanics lie close to Clark's curves the largest discrepancies being for CaO, FeO (total iron) and Na_2O, in which the Bay of Plenty volcanics are slightly, but consistently higher in CaO and FeO, and lower in Na_2O. Another feature is the substantially greater spread of points for the oxides Al_2O_3 and MgO in the Bay of Plenty volcanics than in the rest of the Taupo Zone volcanics. The Bay of Plenty xenolithic accumulates do not show marked displacement from the Al_2O_3 and FeO variation curves, such as that shown by the TNP basic (accumulative) andesites from Clark's (1960 b, Fig. 14) curves; thus inferring that marked enrichment in

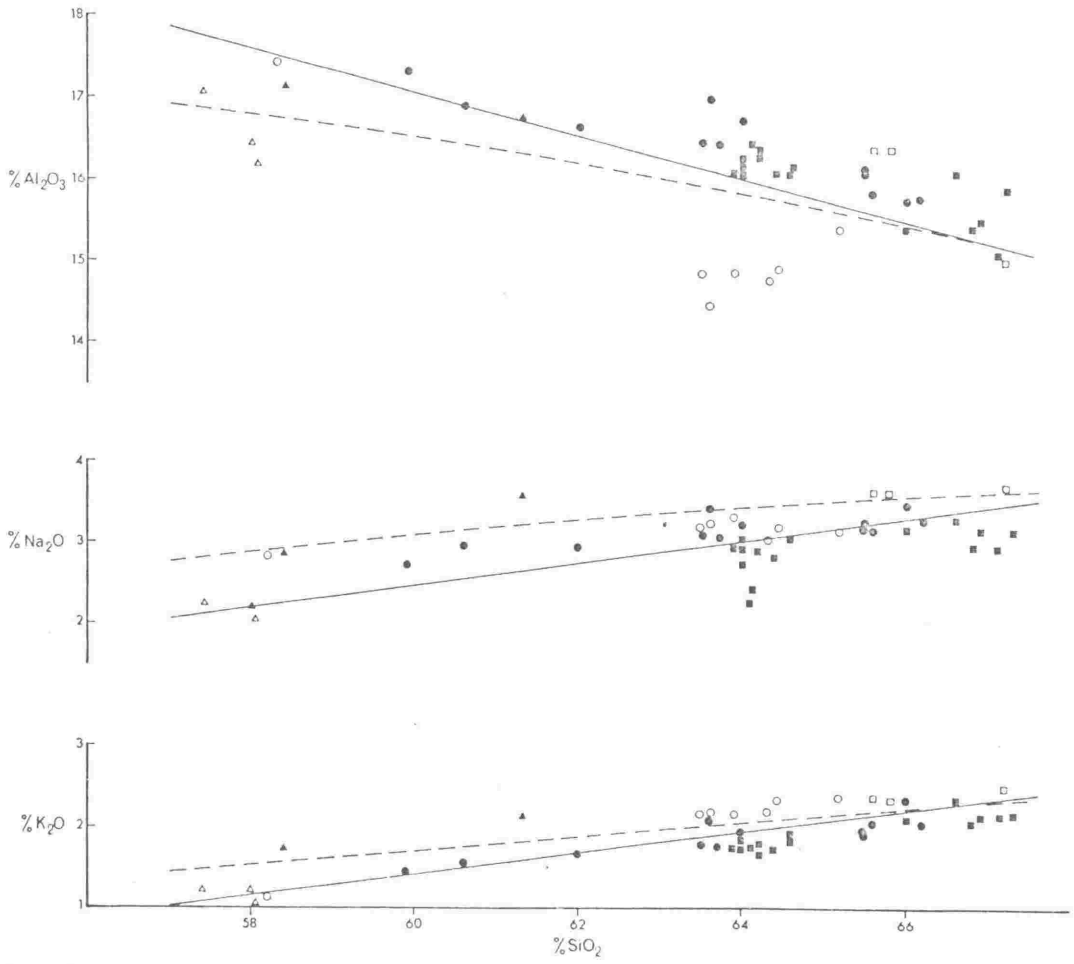

Fig. 26. - Harker diagram for the Bay of Plenty volcanics. Solid lines are RMA regression lines fitted to non-xenolithic samples of the Bay of Plenty volcanics, dotted lines are the overall trends for Taupo Zone volcanics taken from Clark (1960 b, Fig. 13). Symbols are identified below:

- ● Edgecumbe non-xenolithic samples
- ■ Whale Island non-xenolithic samples
- ○ White Island samples
- □ Manawahe samples
- △ Type IA xenoliths
- ▲ Type IB and Group II xenoliths.

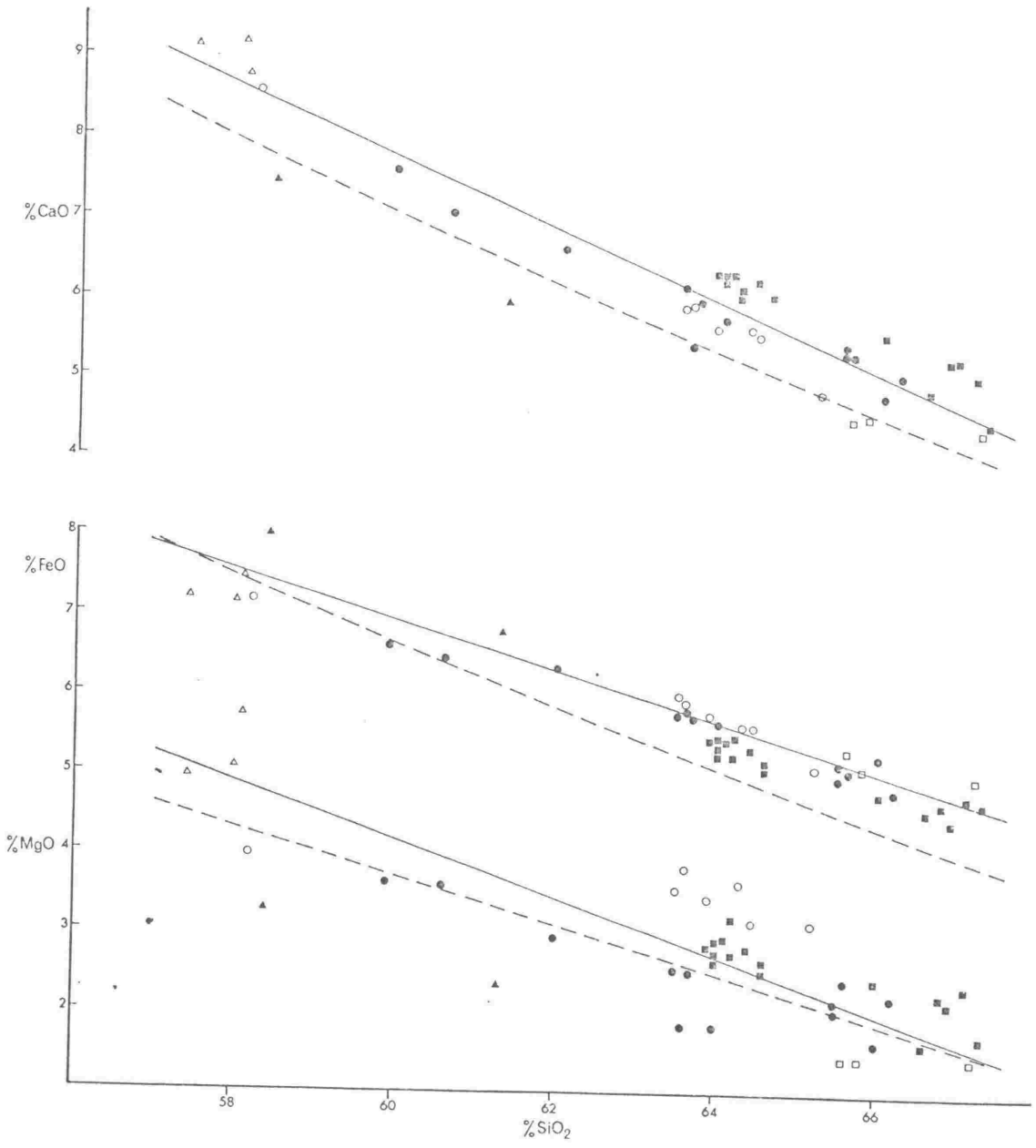

Fig. 27. - Harker diagram for the Bay of Plenty volcanics. Solid lines are RMA regression lines fitted to non-xenolithic samples of the Bay of Plenty volcanics, dotted lines are the overall trends for Taupo Zone volcanics taken from Clark (1960 b, Fig. 13). Symbols are the same as those in Fig. 26.

pyroxene relative to felspar has not occurred in the Bay of Plenty xenoliths.

Analyses of the Bay of Plenty volcanics fall close to the trend line for the Taupo Zone volcanics shown in Clark's (1960 b, Fig. 16) von Wolff diagram (see Fig. 28). As on the Harker diagrams the Bay of Plenty volcanics show greater scatter about the trend than was shown by previously published analyses, but they do not show any marked divergence from the overall trend. The same argument applies to comparisons with Steiner's (1958, Figs. 18, 20) diagrams, addition of samples for the Bay of Plenty volcanics broadens the variation trends due to greater scatter but does not otherwise affect their general validity. In summary of this aspect of the major element variations it is thus apparently still correct to say that a petrochemical relationship exists between the analysed volcanic rocks of the Taupo Zone, as was suggested by previous authors. However, in view of the scatter of the analyses from the Bay of Plenty samples it is now uncertain as to whether Clark's (1960 b) description of this petrochemical relationship as "intimate" still holds true.

Molar ratio variation diagrams (as proposed by Pearce, 1968) for the Bay of Plenty volcanics, using K_2O as the reference oxide; are given in Fig. 29. These diagrams permit direct testing of various differentiation theories, but in view of the uncertainties in compositions and amounts of pyroxenes, plagioclase and titanomagnetite in possible cumulates, the overall compositional variation of the Bay of Plenty volcanics could not be tested against a crystal fractionation theory. However, the only phenocryst minerals which contain appreciable

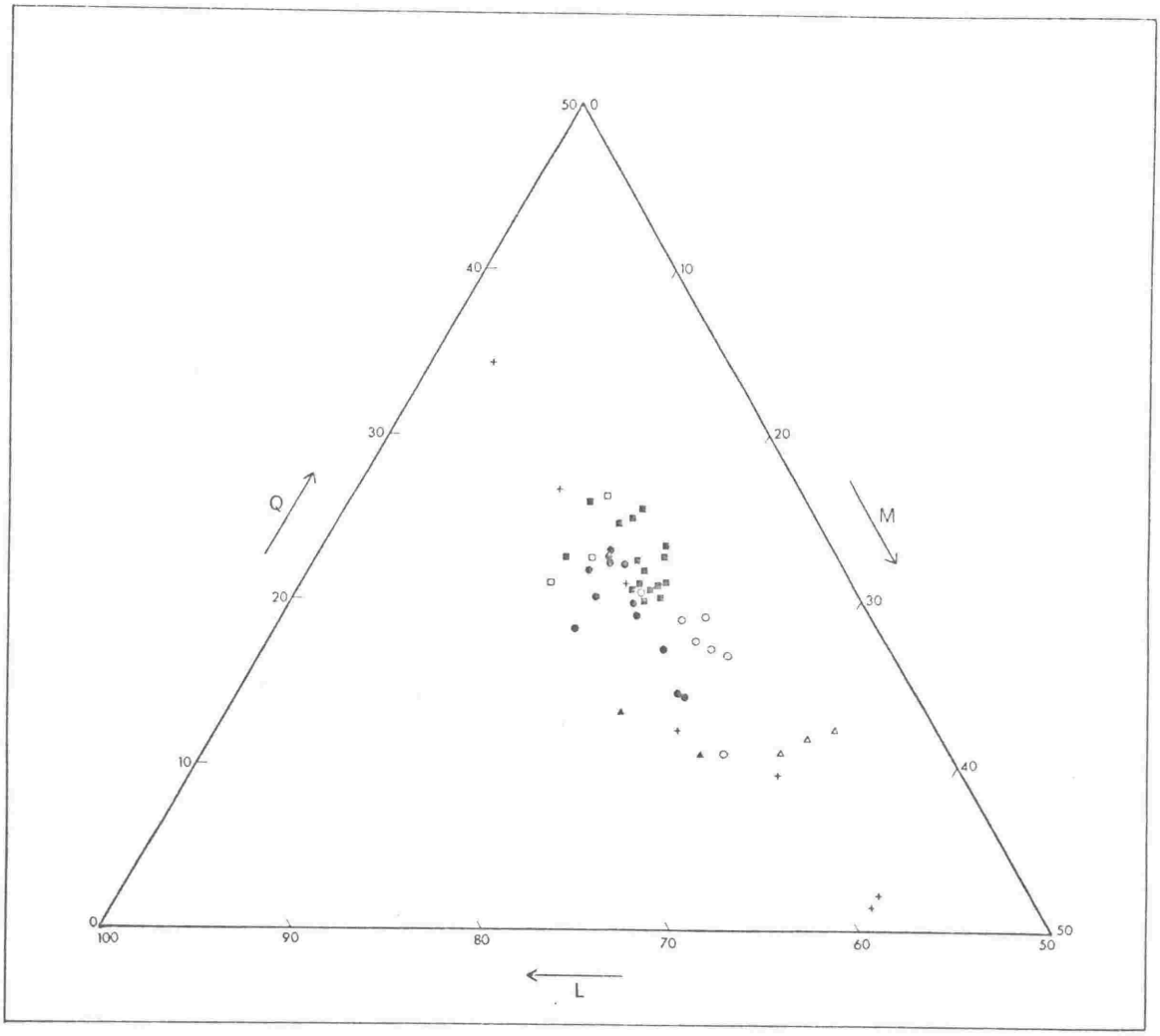

Fig. 28. - Enlarged section of a von Wolff diagram on which are plotted the major element analyses of the Bay of Plenty volcanics (data from Tables 20, 21, 22, 35, 52). Crosses represent analyses from Clark (1960 b, Fig. 16). Other symbols are detailed below:

- ● Edgecumbe non-xenolithic samples
- ■ Whale Island non-xenolithic samples
- ○ White Island samples
- □ Manawahe samples
- △ Type IA xenoliths
- ▲ Type IB and Group II xenoliths

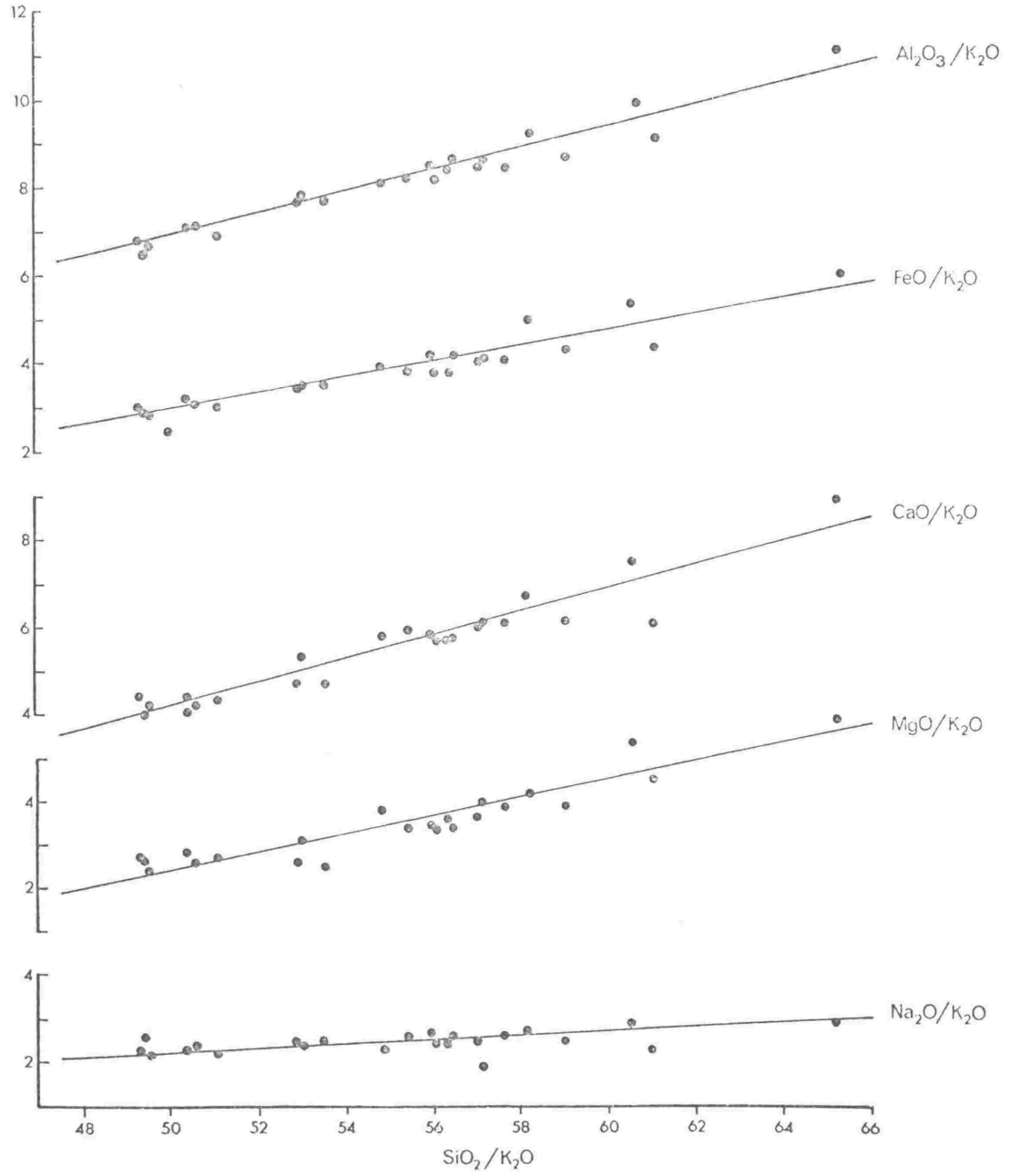

Fig. 29. - Molar ratio variation diagrams of Edgecumbe and Whale Island samples, with RMA regression lines fitted to each set of points. K_2O is used as reference oxide.

Na_2O and Al_2O_3 are plagioclase, biotite and hornblende. The two latter minerals are very late crystallising in these rocks, and are most unlikely to have been significantly fractionated from the magma. Thus it is possible to test if the relative slopes of the Al_2O_3/K_2O and Na_2O/K_2O variation trends against SiO_2/K_2O are consistent with crystal fractionation and removal of plagioclase.

The slopes of the Al_2O_3/K_2O and Na_2O/K_2O trends versus SiO_2/K_2O were calculated for plagioclase subtraction (using the calculation technique shown by Pearce, 1968) and are given in Fig. 30 together with the observed trends for the Bay of Plenty volcanics. Plagioclase compositions of An_{48} and An_{35} were used and it can be seen from Fig. 30 that although the Al_2O_3/K_2O v. SiO_2/K_2O for subtraction of An_{35} plagioclase fits the slope of the corresponding curve for the Bay of Plenty volcanics, neither the An_{35} or the An_{48} plagioclase Na_2O/K_2O v. SiO_2/K_2O calculated trend fits the slope of the Bay of Plenty curve. This comparison of slopes is valid regardless of what initial composition (within the range of analysed samples) is chosen as a starting composition, since for a molar ratio variation diagram only the position of a line and not its slope is affected by the starting composition.

Molar ratio variation diagrams thus show that the major element variation within the Bay of Plenty volcanics was not due to crystal fractionation alone. Additional processes must therefore be invoked to explain the differentiation. Possibilities are contamination of the magma, either by wall-rock assimilation or mixing of magmas; or volatile transfer of alkalies within a magma chamber.

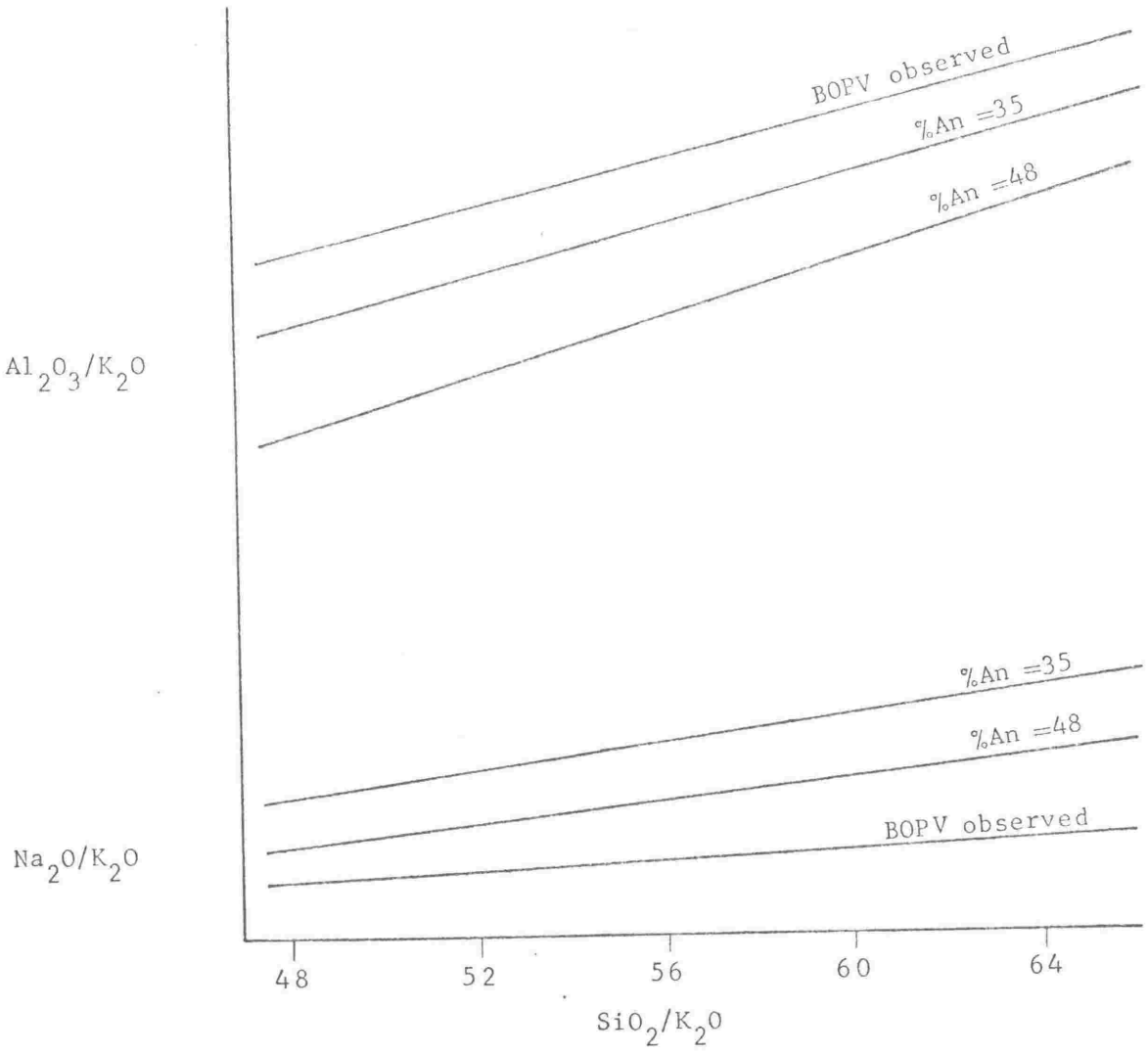

Fig. 30. - Molar ratio variation diagram. Comparison of the slopes of the observed trend-lines for Na_2O/K_2O v. SiO_2/K_2O and Al_2O_3/K_2O v. SiO_2/K_2O in the Bay of Plenty volcanics (BOPV) with the slopes of trend-lines calculated for the subtraction of An_{35} and An_{48} plagioclase from a Bay of Plenty andesite composition.

K_2O - SiO_2 Variations

The relationship between K_2O and SiO_2 in many circum-pacific andesites has been described by Dickinson and Hatherton (e.g. Dickinson & Hatherton, 1967; Dickinson, 1968; Hatherton & Dickinson, 1968; Hatherton 1968, 1969). Dickinson & Hatherton consider that for any one andesite volcano a straight-line variation relationship exists between K_2O and SiO_2, permitting the estimation of a K_2O % corresponding to a particular SiO_2 %. They estimate the K_2O % at 55% and 60% SiO_2, designating the estimates K_{55} and K_{60} respectively. They conclude (Dickinson & Hatherton, 1967) that specific K_{55} and/or K_{60} values can be obtained for any particular volcano, and that such values show a systematic variation with the depth to the Benioff seismic zone beneath the volcano. Higher values of K_{55} and K_{60} are associated with greater depths to the seismic zone, from this correlation it is inferred (Hatherton, 1969) that the K_2O - SiO_2 relationship in andesites is governed either by partial melting processes which vary with depth in the mantle, or by processes which are affected by the path length traversed by the magma during its passage through the mantle.

As a test of this hypothesis Hatherton & Dikcinson (1968) compared the K_{60} values for the Taupo Volcanic Zone with depths to the Benioff zone at two points, under Tongariro National Park and under White Island. Using chemical analyses from Steiner's compilation (1958) they calculated the K_{60} values to be 1.45% for the TNP andesites and 2.1% for the White Island andesites. The difference in K_{60} was inferred (from Dickinson & Hatherton, 1967, Fig. 3) to represent a difference of 60 km in the depth to the Benioff zone beneath the

two volcanoes, a difference which is in agreement with the seismic cross-sections of Hamilton & Gale (1968).

The present author has two specific objections to the values derived by Dickinson & Hatherton (1968). Firstly, the graph (Hatherton & Dickinson, 1968, Fig. 3) from which the K_{60} and K_{55} values for the TNP andesites were estimated also uses points for basalts from K-Trig, Tarawera and Rotoatua, an Edgecumbe andesite, and dacites from Tauhara and Waiotapu, to define the trend-line from which the K_{55} and K_{60} estimates for TNP were made. If only the analyses for the TNP andesites are taken into account then the K_{60} value for TNP is increased from $\sim$ 1.45% (Hatherton & Dickinson, 1968) to 1.73% (using an RMA regression line to calculate the K_{60} value). Furthermore, if three other analyses for TNP given by Steiner (1958) and excluded by Hatherton & Dickinson (no reason given) are included in the calculation then the K_{60} value for TNP is increased still further to 1.80%. Secondly, since only two analyses of White Island were available to Dickinson & Hatherton it was not possible for them to determine the true K_2O - SiO_2 trend for this volcano. They therefore found it necessary to infer that the K_2O - SiO_2 trends for White Island and selected Taupo Zone rocks from other areas were parallel, in order to derive an estimate for K_{60} for White Island; such an estimate is clearly uncertain.

A more stringent test of Hatherton & Dickinson's hypothesis may now be made using the additional analyses available for the Bay of Plenty volcanics. Values of K_{60} for the Bay of Plenty volcanics were calculated from RMA regression lines (fitted to non-xenolithic samples) and are as follows: Edgecumbe - 1.49%, Whale Island - 1.14% and

White Island - 1.50% (includes analyses from Steiner, 1958). It is thus apparent that on the basis of presently available data the Bay of Plenty volcanoes have lower K_{60} values than the TNP andesites (K_{60} taken as 1.80%) and are at variance with Hatherton & Dickinson's (1968) hypothesis with respect to the Taupo Zone.

Hatherton & Dickinson (1968) also inferred, as a consequence of the apparent validity of their hypothesis for the Taupo Zone, that andesites in this area could not have suffered any crustal contamination or hybridisation. Such an inference is no longer justified.

TRACE ELEMENT VARIATIONS

In the following discussion the relative behaviour of pairs of elements in the Bay of Plenty volcanics is generally determined by reference to the bivariate correlation matrices (Tables 29, 30, 31) given in the map folder. In general the distributions of elements in Whale Island and Edgecumbe rocks was not significantly different (Table 27) and the value of the quoted correlation coefficient (r) was obtained from the combined data. For elements which show significantly different distributions in samples from Edgecumbe and Whale Island, the correlation coefficients for each volcano are quoted separately as r_E and r_W. White Island trace element abundances are significantly different from Whale Island and Edgecumbe abundances and could not be combined with them for statistical analysis, there are also too few White Island samples to enable a meaningful separate statistical treatment to be made.

Since the trend of calc-alkaline differentiation is one of SiO_2 enrichment the hypothesis of crystal fractionation can be tested using SiO_2 variation as the main reference parameter. The differentiation index (Thornton & Tuttle, 1960) and crystallisation index (Poldervaart & Parker, 1964) are also used as fractionation parameters in part of the following discussion.

1. Large Cations

The ions Cs^+ and Rb^+ substitue only for K^+ in the common silicate minerals. Cs^+ tends to be concentrated in later-crystallising K-bearing minerals on account of the size (ionic radius) difference between K^+ and Cs^+. In the Bay of Plenty volcanics K-bearing phases crystallise only at a late stage and it would therefore be anticipated that Rb and Cs would be concentrated in more acid members of the suite, this is supported by the strong positive correlation ($r = 0.883$) for Rb against SiO_2. The Cs abundances, however, show considerable scatter, and variations in abundance are thought to be unreliably established, due to the very small difference between the analysed abundances of Cs and the detection limit for this element by the technique used for its determination.

Ba^{2+} substitutes only for K^+ among the common cations and generally concentrates in early-forming K-minerals, resulting in Ba decrease during fractionation. The opposite trend is shown by the Bay of Plenty volcanics (relative to SiO_2, $r_E = 0.747$, $r_W = 0.753$), supporting the petrological evidence that a K-bearing mineral has not crystallised at an early stage.

Sr^{2+} is intermediate in size between K^+ and Ca^{2+} and exhibits complex geochemical behaviour. Its substitution for K and Ca in

various minerals is controlled very strongly by the mineral structure, thus it substitutes comparatively readily for Ca and K in felspars, but very little for Ca in pyroxenes or for K in micas. In the Bay of Plenty volcanics Sr will be principally concentrated in plagioclase. The relative concentrations of Sr in plagioclase and in augite are shown by analyses (Ewart & Taylor, 1969) of augite and plagioclase from Edgecumbe which contain 17 and 465 ppm Sr respectively. Fractional crystallisation of plagioclase would thus cause depletion of Sr in the remaining magma, resulting in a strong negative correlation between SiO_2 and Sr. Such a negative correlation is observed for both Edgecumbe and Whale Island ($r_E = -0.571$, $r_W = -0.820$). The possibility of plagioclase fractionation is considered further in the section on rare earth elements.

Apart from the variations in the abundances of the elements themselves, the variation in element ratios has long been considered a particularly useful indication of crystal fractionation. The K/Rb ratio is of special interest since these two elements are considered to show an extremely high coherence in geochemical processes, thus any changes in their ratio are considered to be of very high geochemical significance. For the Bay of Plenty volcanics the K-Rb coherence is extremely high, their correlation coefficient being 0.967 (for 26 samples). The K/Rb ratio for the Bay of Plenty volcanics does not show any significant correlation with SiO_2 ($r = 0.284$), or with the crystallisation index ($r = -0.357$) and differentiation index ($r = 0.338$).

The lack of a fractionating K-bearing phase is further substantiated by the increase in the Ba/Rb and Ba/Sr ratios with increasing SiO_2, however neither ratio shows strong correlation with SiO_2.

2. Rare Earths

During crystal fractionation the rare earth elements (REE) as a whole, are generally enriched with additional concentration of the larger and lighter REE relative to the smaller REE taking place simultaneously (Haskin & Frey, 1966; Haskin et al., 1966). The most striking feature of all rare-earth distribution patterns is the alternating high and low abundances ("zig-zag") of the even and odd atomic number REE (controlled by the Oddo-Harkins rule). In order to overcome this "zig-zag effect" it is customary to normalise an REE distribution by dividing individual REE abundances by the abundance of the same element in another sample. Two REE distributions, a composite sample of North American shales (Haskin et al., 1966, Table 28) and an average chondritic meteorite (Haskin et al., 1966, Table 8) are generally used as reference patterns and are used here to normalise the REE distribution patterns for the three analysed samples from the Bay of Plenty volcanics. The average chondritic pattern is considered to represent unfractionated primitive material, and the composite North American Shale (hereafter abbreviated to NAS) is considered to represent fractionated upper-crustal material.

Three samples (11217, 11242, 11246) were analysed for REE by spark-source mass spectrometry, and the abundances are given in Table 26. The analyses are normalised according to the procedure described above and the normalised results are plotted against ionic radii in Figs. 31 and 32.

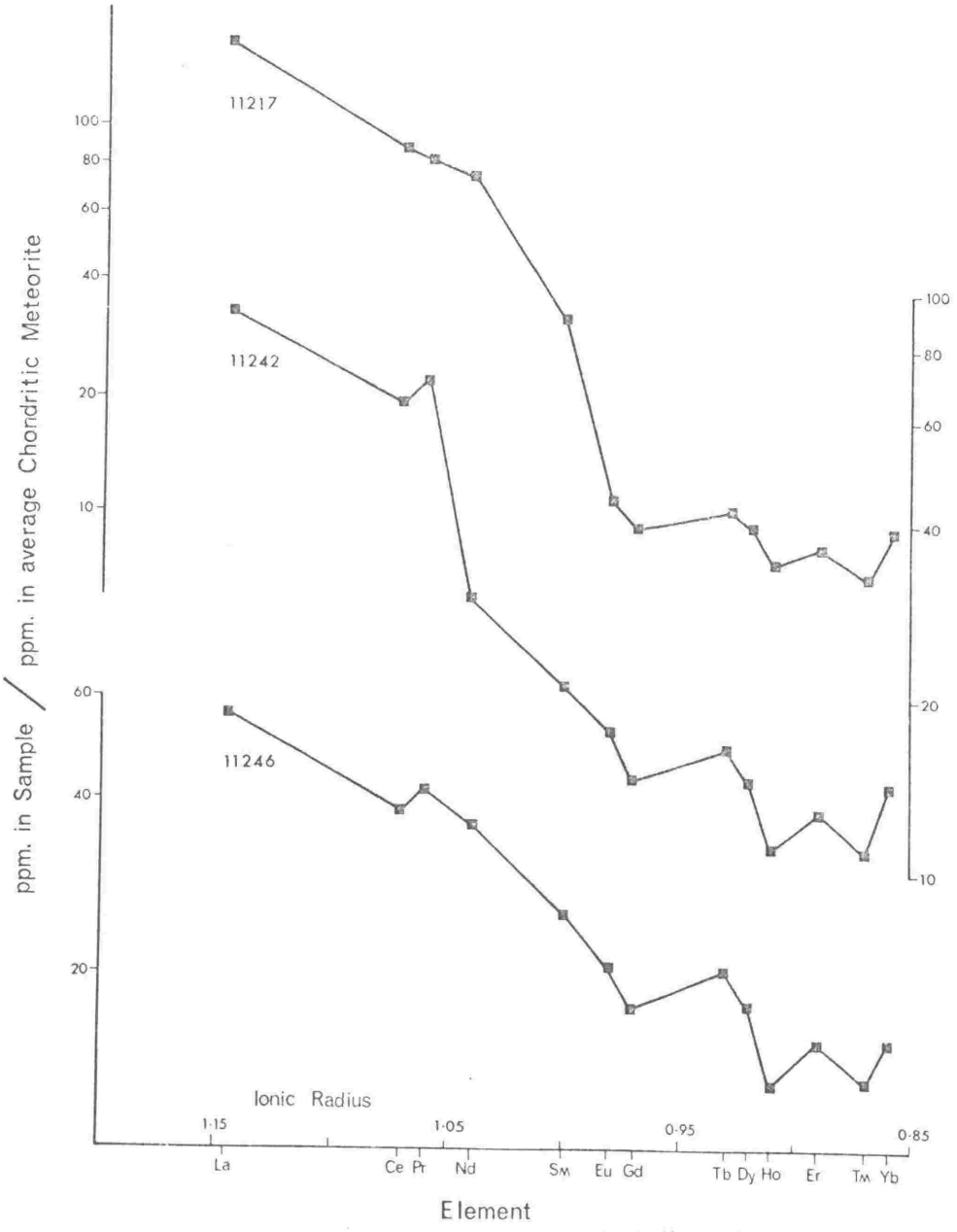

Fig. 31. - Rare earth variation patterns for an andesite from White Island (11246), a dacite from White Island (11242), and a dacite from Edgecumbe (11217). The pattern has been constructed by dividing the individual REE abundances in each sample (data from Table 26) by the corresponding element abundances in the average chondritic meteorite (Haskin et al., 1966, Table 8). The scales on the left of the diagram refer to samples 11217 and 11246, the scale on the right of the diagram refers to sample 11242.

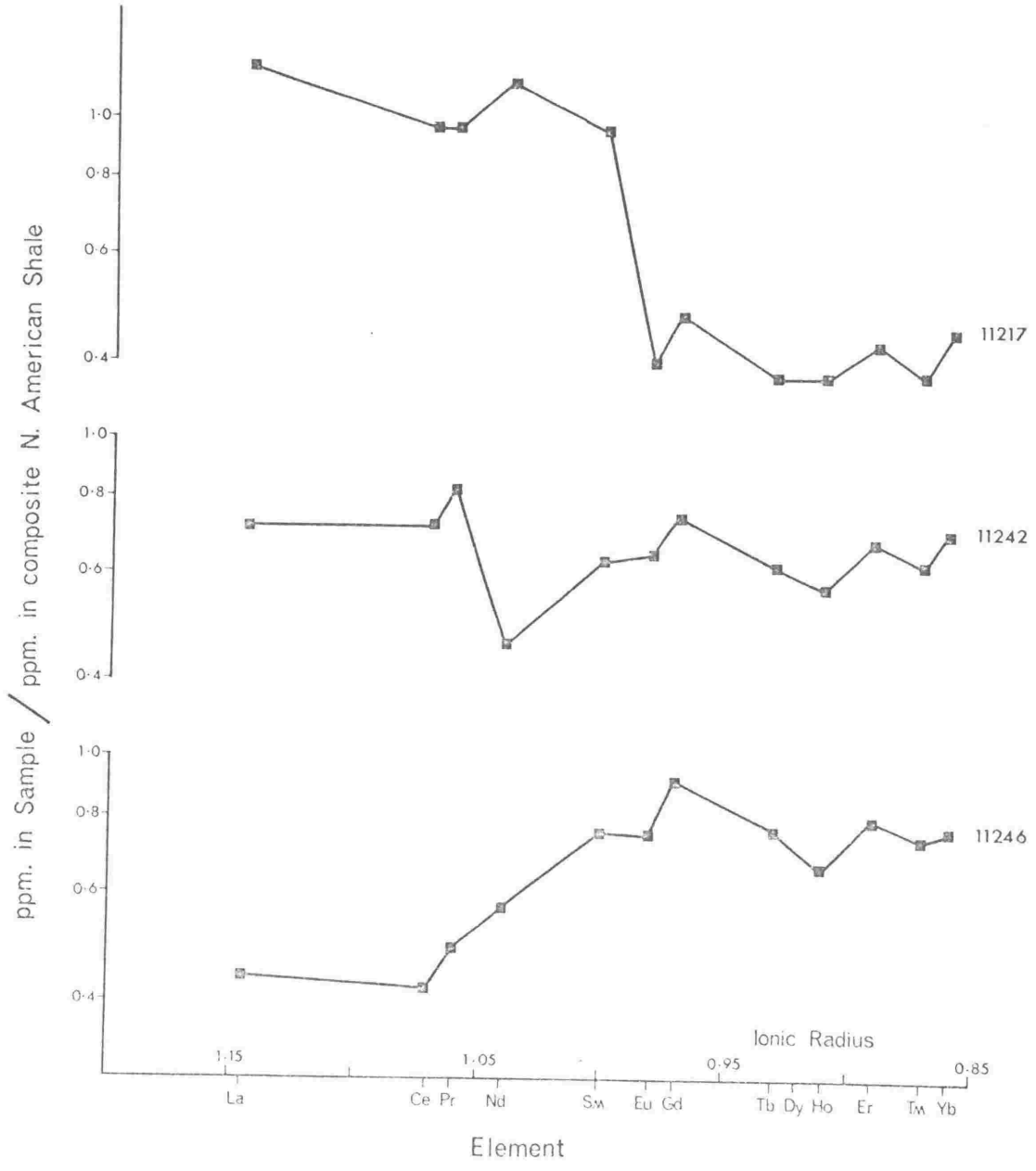

Fig. 32. - Rare earth variation patterns for the same samples as shown in Fig. 31. The pattern has been constructed by dividing the individual REE abundances in each sample (data from Table 26) by the corresponding element abundances in the composite North American Shale (Haskin et al., 1966, Table 28).

Total REE content in the Bay of Plenty samples is intermediate between the chondritic average and the NAS value, but is much closer to the latter. Compared to the chondritic average, all the Bay of Plenty samples are strongly fractionated with enrichment of the light REE (La-Sm) relative to the heavy REE (Eu-Yb). Sample 11246 (White Island andesite) is less fractionated than the NAS, sample 11242 (White Island dacite) is comparable to the NAS, and sample 11218 (Edgecumbe dacite) is more fractionated than the NAS.

The relative REE patterns of the White Island andesite (11246) and dacite (11242) are consistent either with the dacite having been derived from the andesite by crystal fractionation, or with the andesite having been contaminated with typical upper-crustal material. The Edgecumbe dacite (11218) shows a more strongly fractionated REE pattern than any andesite or rhyolite previously analysed from the Taupo Volcanic Zone (Ewart, Taylor & Capp, 1968, Fig. 16). This dacite has either undergone more crystal fractionation than the rhyolites or andesites of the Taupo Zone, or has been contaminated with material which has not significantly contaminated the rhyolites or andesites.

Depletion in Eu, generally expressed as a Eu/Gd ratio, is not evident in the Bay of Plenty samples. Ewart, Taylor & Capp (1968) and Taylor, Ewart & Capp (1968) have shown Eu depletion to be minor in the Taupo Zone rhyolites and to be marked in the Snowy Mountain leucogranites. In both cases they ascribed it to crystal fractionation of plagioclase (Eu^{2+} probably substituting for K^{+}; Taylor, 1965 b).

It thus seems unlikely that significant plagioclase fractionation has contributed to the compositional variation of the Bay of Plenty volcanics.

3. Large Highly Charged Cations

The elements Zr, Th and U generally tend to form ionic complexes (Ringwood, 1955), which being large relative to $(SiO_4)^{4-}$ tend to be concentrated in residual fractions during fractional crystallisation.

Zr in the Bay of Plenty volcanics shows weak correlation with SiO_2 ($r = 0.261$), but shows slightly stronger correlation with the crystallisation index ($r = -0.476$) and differentiation index ($r = 0.417$). A somewhat stronger correlation with SiO_2 is shown by Th ($r = 0.564$) and U ($r = 0.565$) but the Th/U ratio shows no significant correlation ($r = 0.195$) with SiO_2.

Th and U show no evidence of removal by crystal fractionation and are probably concentrated in the residual liquid if this process is operative.

4. Ferromagnesian Elements

Mn^{2+} has a very similar ionic radius to Fe^{2+} and would be expected to substitute readily for it, thus the separation of Fe-bearing phases from the magma would result in a drop of Mn in the residual liquid. Burns & Fyfe (1964) have shown that by subtraction of the crystal field stabilisation energies (CFSE) for tetrahedral sites (in the magma) from CFSE for octahedral sites (in the crystal) a value for the "site preference energy" for an octahedral site may be obtained for any transition metal. Comparison of the octahedral site preference energies of Fe^{2+}, Mn^{2+}, and Fe^{3+}, Mn^{3+} shows that Fe^{2+} will tend to be concentrated in the crystalline phase relative to Mn^{2+}, and the

reverse is expected for the trivalent ions. Thus a substantial variation in the Fe/Mn ratio is unlikely. With FeO (total iron) showing a strong negative correlation ($r = -0.964$) with SiO_2, the similar correlation shown by Mn^{2+} ($r = -0.936$) is as expected.

Cu^{2+} is similar in size to Fe^{2+}, and Cu^{+} is similar in size to Na^{+}; Taylor (1966) thus suggests that Cu could be found in many of the common silicate minerals. However, as the Cu-O bond is markedly covalent the Cu content of any silicate mineral is unlikely to be high, furthermore the susceptibility of Cu^{2+} to Jahn-Teller distortion (Orgel, 1960; Burns & Fyfe, 1967) results in a preference for the more-deformable sites in a magma rather than the less-deformable sites in a crystal. For these reasons Cu^{2+} is generally expected to concentrate in residual liquids and crystallise in late-stage minerals, particularly in sulphides. In the Bay of Plenty volcanics Cu^{2+} does not show the expected behaviour, having a weak, but definitely negative correlation with SiO_2 ($r = -0.449$) and similar weak correlations with the differentiation and crystallisation indices ($r = 0.452$ and -0.430 respectively). The deviation from predicted behaviour indicates that if the Cu^{2+} variation pattern is to be explained by crystal fractionation then a sulphide or spinel phase containing Cu must have separated from the magma.

Co^{2+} and Ni^{2+} are intermediate in size between Fe^{2+} and Mg^{2+} but in general both substitute more for Fe^{2+} than for Mg^{2+}, also Ni^{2+} is preferentially enriched relative to Co^{2+} in early crystallising Fe minerals. The predicted order of uptake in crystalline phases is the same when the relative octahedral site preference energies are

considered. On this basis it is predicted that crystal fractionation of ferromagnesian minerals, particularly of olivine and/or of orthopyroxene will result in rapid depletion of Ni and Co in the residual liquid, and a simultaneous drop in the Ni/Co ratio. The Co^{2+} abundances in the Bay of Plenty volcanics show a reasonably strong negative correlation with SiO_2 ($r = -0.757$), but Ni and the Ni/Co ratio do not show the expected correlations with SiO_2 ($r = 0.121$ and 0.430 respectively). The correlation of Ni against SiO_2 is non-significant, and that of Ni/Co against SiO_2 is significant only at a low confidence level. Analyses of an augite and hypersthene from Edgecumbe (Ewart & Taylor, 1969) show Ni contents of 17 and 23 ppm respectively, compared with 7.3 ppm Ni in the total rock (Ewart, Taylor & Capp, 1968). Clearly if separation of augite or hypersthene had taken place during crystal fractionation, a marked drop in total rock Ni would have resulted.

The lack of agreement between the observed SiO_2-Ni and SiO_2-Ni/Co trends and the predicted trends (predicted both from empirical observations and from theoretical considerations) strongly suggests that if augite and/or hypersthene have been removed from the magma to any significant extent due to crystal fractionation, then Ni^{2+} must have been added to the residual liquid by some other process.

Li^+ is very much smaller than the other alkali ions (ionic radius - 0.68 Å) and is generally thought to substitute for Mg^{2+} (Taylor, 1965 b) in ferromagnesian minerals. It tends to concentrate in the late-stage ferromagnesian minerals and will thereby tend to increase during crystal fractionation, except during separation of

late-crystallising ferromagnesian minerals. A trend of increasing Li^+ during differentiation is shown by the Bay of Plenty volcanics where the correlation of Li^+ with SiO_2 is positive ($r = 0.601$), and fairly strong correlation is also shown with the crystallisation index ($r = -0.708$) and differentiation index ($r = 0.697$). Li^+ shows enrichment in Type IB xenoliths which are thought to contain more late-stage pyroxene crystals than any other rock sample.

Sc^{3+} substitutes for Fe^{2+} and little Sc enrichment is observed until the final stages of crystallisation when strong Sc enrichment in residual fractions may occur, possibly due to complex formation in the presence of excess anions (Ringwood, 1955). Sc^{3+} in the Bay of Plenty volcanics shows a negative correlation with SiO_2 ($r = -0.622$) and consequent Sc depletion during differentiation, but the rate of depletion is comparable with that shown by total iron. Analyses of augite and hypersthene from Edgecumbe (Ewart & Taylor, 1969) show 205 and 85 ppm Sc, thus fractionation of these pyroxenes would cause a much greaterchange in the Fe/Sc ratio of the residual liquid than is actually shown by the variation trend of the Bay of Plenty volcanics.

V^{3+} substitutes mainly for Fe^{3+} and generally shows a steady depletion during fractionation provided minerals containing Fe^{3+} are separating from the magma. Such a steady decrease is shown by the Bay of Plenty volcanics with a V-SiO_2 correlation coefficient of -0.832 and a decrease from 183 ppm V at 65% SiO_2 to 128 ppm V at 60% SiO_2 (values calculated from RMA regression equation). Such a decrease could be explained by crystal fractionation of pyroxenes, principally augite which contains substantially more V^{3+} than

coexisting hypersthene (Ewart & Taylor, 1969). The data in Duncan & Taylor (1968, Table 1) on the trace element composition of titanomagnetites in the Bay of Plenty volcanics shows that this mineral contains very high concentrations of V^{3+} (4500-8000 ppm) and thus the trend of V depletion could be produced by separation of extremely small quantities of titanomagnetite. Conversely the difference between the initial and final abundances of V in the Bay of Plenty volcanics severely limits the amount of titanomagnetite which can have separated from them (Duncan & Taylor, 1968; Taylor et al., 1969).

Cr^{3+} is virtually identical in size to Fe^{3+} and shows a much larger octahedral site preference energy (Burns & Fyfe, 1964) which leads to its preferential concentration in early-crystallising ferromagnesian minerals and its rapid depletion in residual liquids. The pattern of Cr^{3+} variation in the Bay of Plenty volcanics is certainly not a simple one of rapid depletion due to crystal fractionation. Cr^{3+} shows a very considerable fluctuation in abundance (relative deviation of 67%) and does not show any marked correlation with SiO_2 ($r = -0.267$), crystallisation index ($r = 0.470$), or differentiation index ($r = -0.451$). Pyroxenes in Edgecumbe andesite show concentration factors (relative to the total rock) of 7 for Cr in augites and 2 for Cr in hypersthene. Fractionation of pyroxene from Bay of Plenty volcanic magmas would thus be expected to produce a much more rational pattern of Cr variation than has been observed. In view of the extreme variance shown by Cr small amounts of chromite are possibly being added to or removed from the magma, either by fractional crystallisation or by contamination.

The geochemistry of Ga^{3+} is complex, with substitution for Al^{3+}, Fe^{3+}, and entry into Zn sulphide (Taylor, 1965 b). In the Bay of Plenty volcanics it shows a slight negative correlation with SiO_2 ($r = -0.354$), but the total variation is only very small.

Additional information on the expected trace element variation patterns for the Bay of Plenty volcanics if crystal fractionation is operative, is obtained from a suite of Whale Island dacites, sampled from the bedded volcanic breccia deposits which are considered to have formed entirely from the central spine of the island (see p.). This suite of samples shows a complementary relationship between the modal percentages of plagioclase and pyroxene (Fig. 33) from which it is inferred that all the samples are from the same extrusive magmatic unit, in which modal variations are a product of crystal fractionation within this single unit. Within this suite the ratio Cr/V shows a strong positive correlation with pyroxene content, and the ratio Sc/Y a strong negative correlation with pyroxene content (see Fig. 33). It can thus be inferred that if pyroxene fractionation is an important process in the differentiation of the Bay of Plenty volcanics as a whole, then Cr/V will show a strong negative, and Sc/Y a strong positive correlation with SiO_2. The observed correlation coefficients for Cr/V - SiO_2 are $r = 0.229$ and for Sc/Y - SiO_2 are $r = -0.263$. The variation of these ratios is thus additional evidence against the hypothesis that crystal fractionation of pyroxene has played an important part in the development of chemical variation trends in the Bay of Plenty volcanics.

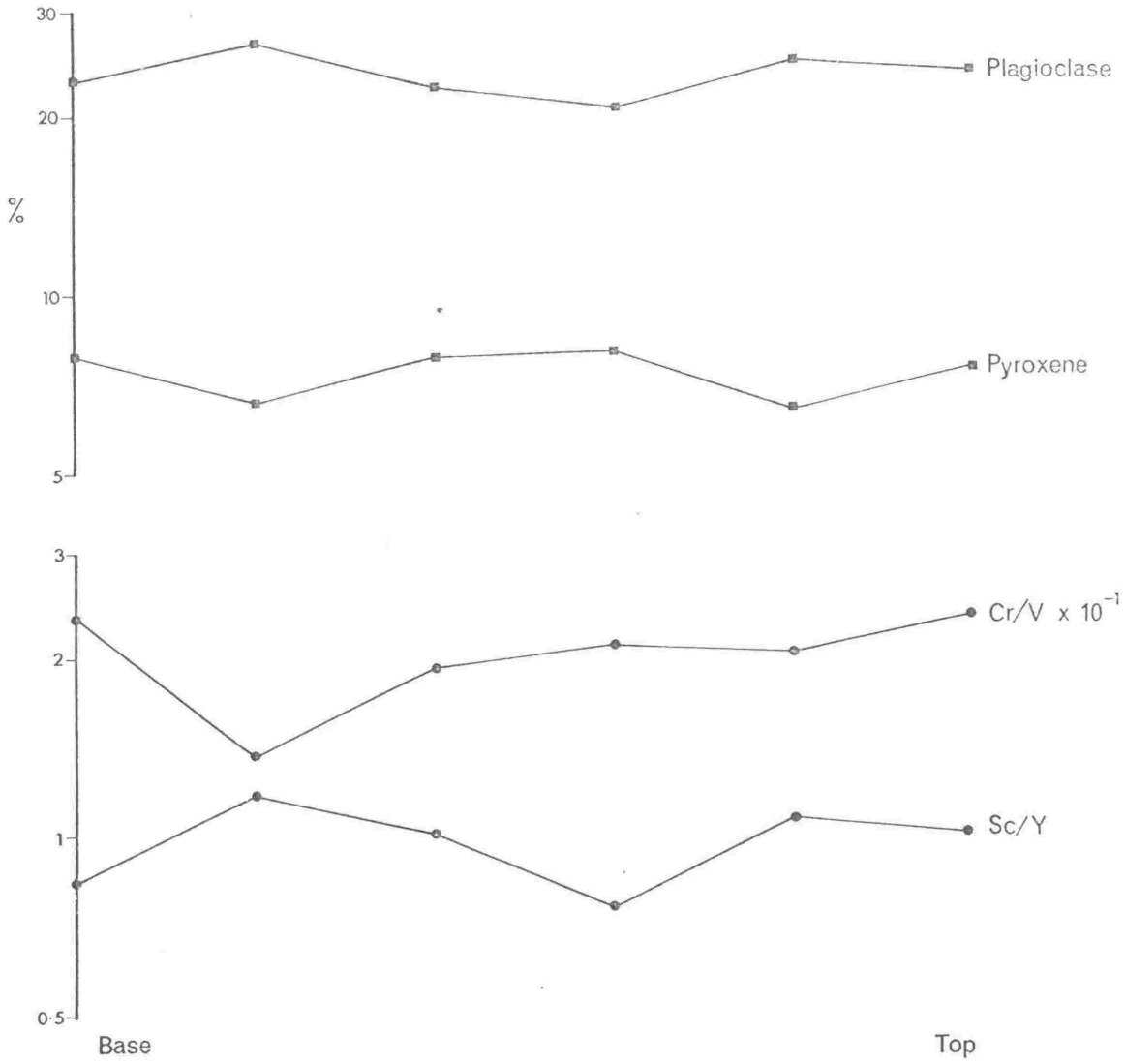

Fig. 33. - Variation patterns of modal plagioclase and pyroxene, and the Cr/V and Sc/Y ratios in a suite of six rock samples from the bedded volcanic breccia exposed in a cliff section on the northern face of Central Cone, Whale Island. The samples are plotted in stratigraphic sequence and the bottom and top of the section are indicated.

PETROGENETIC INFERENCES FROM MAJOR AND TRACE ELEMENT VARIATIONS

Although many features of the major and trace element variation patterns for the Bay of Plenty volcanics are compatible with fractional crystallisation (see previous section), certain chemical features are incompatible with the separation of significant quantities of any of the phenocrystic minerals, these are detailed below.

Separation of plagioclase in significant amounts is precluded by the rare earth distribution patterns which do not show any depletion in Eu, nor are Eu/Gd ratios at all depressed. Evidence from the molar ratio variation diagrams for Al_2O_3 and Na_2O variations strongly suggests that although plagioclase is the only phenocrystic mineral to contain significant quantities of these elements, fractionation of plagioclase does not explain the observed variation pattern. From petrological evidence it is most unlikely that hornblende or biotite has been an early crystallising phase which could have participated to any extent in crystal fractionation, this being substantiated by the variation trends of Ba and the ratios Ba/Rb and Ba/Sr. Significant pyroxene fractionation is precluded by the variation trends of Ni, Sc, Cr and the ratios Ni/Co, Cr/V and Sc/Y.

The possibility of chemical variations in the Bay of Plenty volcanics being caused by contamination of the parental magma with a particular material can be assessed by comparing the abundance trends, element by element, with abundances in possible contaminants. Such an approach is obviously restricted due to the present lack of trace element data for any possible contaminants other than the

"marginal facies" Triassic-Jurassic greywackes and argillites (Ewart, Taylor & Capp, 1968), and the various volcanic rock types of the Taupo Zone.

For the purposes of this comparison the chemical variation trends are represented by the element abundances in the Bay of Plenty volcanics at SiO_2 concentrations of 60% and 65%, calculated from the RMA regression equations. The calculated trends (Table 32) are then compared with analytical data for the "marginal facies" greywacke (mean of analyses for samples 32 & 33, Ewart, Taylor & Capp, 1968) and argillite (Ewart, Taylor & Capp, 1968; sample 34), and a calculated 60:40 mix of greywacke:argillite using the same analyses. It is apparent from Table 32 that neither greywacke, argillite, nor any mixture of them could have produced the observed variation trends, for the elements Ti, Al, P, Sr, Y, Cu, Cr and Ga, by contamination of the Bay of Plenty parental magma (assuming this to be similar in composition to the most basic Edgecumbe andesites). Contamination by greywacke alone would in addition fail to produce the trends for Si, Fe, Mg, K, Rb, Ba and Co.

Ewart & Stipp (1968) and Ewart, Taylor & Capp (1968) have suggested that the rhyolitic material of the Taupo Volcanic Zone may have been produced by partial melting of the "marginal facies" greywacke-argillite. Assuming 50% melting, the composition of the residual material has been calculated and is given in Table 32. The residual greywacke-argillite composition cannot be used as a contaminant to produce the trends observed for the elements Si, Ti, Al, Fe, Mg, P, Rb, Ba, Sr, Y, Cu, Co, Sc, V, Cr and Ga.

TABLE 32

CHEMICAL VARIATION TRENDS IN THE BAY OF PLENTY VOLCANICS AND ANALYSES OF SOME POSSIBLE CONTAMINANTS

	EDGECUMBE & WHALE ISLAND		1	2	3	4	5
$\%SiO_2$	60.00	65.00	63.99	68.41	65.77	56.22	75.32
$\%TiO_2$	0.79	0.57	0.81	0.65	0.75	1.25	0.25
$\%Al_2O_3$	18.04	15.86	16.05	16.65	16.31	19.27	13.35
%FeO	6.72	5.18	6.11	3.50	5.07	8.39	1.75
%CaO	7.53	5.74	4.03	1.59	3.04	4.52	1.56
%MgO	3.73	2.49	2.82	1.45	2.26	4.25	0.27
$\%Na_2O$	2.34	3.05	4.43	3.28	3.97	3.80	4.14
$\%K_2O$	1.39	1.92	1.57	4.32	2.68	2.05	3.31
$\%P_2O_5$	0.14	0.10	0.18	0.14	0.17	0.29	0.05
Rb	49.5	65.5	44	140	82	56	108
Ba	307	680	350	930	580	290	870
Sr	277	227	380	230	320	516	124
Y	22	16	20	28	23	21	25
Zr	81	106	210	205	208	256	160
Cu	27.8	15.6	42	32	38	70	6
Co	16.8	12.6	15	7.7	12	24	n.d.
Ni	3.1	8.1	16	14	15	30	n.d.
Li	12.5	22.7	30	35	32	29	35
Sc	25.5	17.2	16	12	15	25	5
V	183	128	110	75	95	181	9
Cr	48.7	26.4	26	26	27	52	2
Ga	20.2	15.1	23	24	24	32	16
B	11.6	17.6	30	80	50	76	24

1. "Marginal Facies" Greywacke: (Ewart, Taylor & Capp; 1968).
2. "Marginal Facies" Argillite: (Ewart, Taylor & Capp; 1968).
3. Greywacke:Argillite in 60:40 proportions.
4. Residual greywacke-argillite after 50% melting to produce rhyolite (5).
5. Average Taupo Zone Rhyolite (Ewart, Taylor & Capp; 1968).

NOTES

(1) Element and oxide concentrations in Edgecumbe and Whale Island rocks at SiO_2% of 60 and 65 were calculated from the RMA regression equations.

(2) All values are in p.p.m. unless otherwise indicated.

If magmatic materials are also considered among the possible contaminants, then rhyolitic magma is obviously the most probable, since rhyolitic rocks are by far the most abundant in the Taupo Zone. Comparison of element abundances in the average Taupo Zone rhyolitic eruptive (Ewart, Taylor & Capp, 1968) given in Table 32 with the variation trends for elements in the Bay of Plenty volcanics shows excellent correspondence. If average rhyolitic material is a contaminant of the parental Bay of Plenty magma, all trace element trends are qualitatively explained with the exception of Ni. Since Ni shows a very low correlation with SiO_2 ($r = 0.121$) the Ni variation trend is considered to be unreliable.

It is concluded that if the chemical variation trends in the Bay of Plenty volcanics were produced by contamination of the parental magma with upper crustal material then it could not have had the composition of "marginal facies" greywacke, argillite, or a greywacke-argillite combination. Nor is the residual material left after the partial melting of greywacke-argillite to produce rhyolite a suitable contaminant. However the average Taupo Zone rhyolite is qualitatively suitable for explaining the trace element and major element variations of the Bay of Plenty volcanics by a contamination process.

Although it is certainly possible that magmatic mixing takes place, the author considers it more probable that material of this composition is produced immediately in contact with the andesitic magma as the partial melting product of the wall-rocks surrounding the magma chamber. It is suggested that this partial melt, which has the same composition as a rhyolite, is assimilated directly into the

andesitic magma and is unlikely to have existed as a discrete rhyolitic magma at this locality. If these views are correct then important inferences concerning the location of the crustal magma chambers underlying Edgecumbe and Whale Island volcanoes can be made. Not only must they lie within the same rock formation which has suffered partial melting on a regional scale to produce rhyolitic magmas, but they must also lie in a position within this body at which rhyolitic magmas have not been previously generated. Since the Edgecumbe and Whale Island volcanoes are younger than large volumes of rhyolitic eruptives in the same locality, it is inferred that the andesitic and dacitic magma chambers are at a greater or lesser depth in the crust than the zone of partial melting from which rhyolite has been produced.

Since the variation trends in both Whale Island and Edgecumbe suites are extremely similar, and could both be explained by assimilation of identical material, the overall difference between the trace element abundances in the two volcanoes (Table 27) must be due to slightly different compositions of the parental magma for each volcano. The differences in the abundances of Sr, Li, Ga, and Ba in the two volcanoes could be explained by contamination of a Whale Island parental magma composition with greywacke to produce the appropriate parental magma composition for Edgecumbe. It is suggested that initially the parental magma for both volcanoes was the same composition, with the Whale Island parental magma being emplaced in the upper crust at a temperature such that only partial melting of the wall-rock took place, giving rise to the chemical variation pattern observed.

The Edgecumbe parental magma is postulated to have been emplaced at slightly higher temperature so that almost total melting of the wall-rock, possibly greywacke, modified its composition at an early stage. Subsequent partial melting and assimilation of wall-rock material at a lesser depth (the partial melt being of rhyolitic composition) would result in chemical variation trends identical to those shown by the Whale Island suite.

The hypothesis that the chemical variation of the Edgecumbe and Whale Island volcanic suites is produced by assimilation of the low melting point components of the wall-rock also provides a suitable mechanism for producing the cyclic chemical variations which have been suggested in an earlier section (p. 32). Each pulse of andesitic magma rising from depth will assimilate wall-rock material during its "holding time" in the upper crust, and later eruptions from this pulse of magma will be more contaminated than early eruptions from it. Successive pulses of magma will show similar patterns of upper crustal contamination, and provided they do not occupy the sites of previous "magma chambers" a cyclic pattern of variation will be produced for the volcano as a whole.

Chemical variation trends for White Island rocks have been extensively discussed in a previous section (p. 179) and the conclusion drawn that the trends are due more to contamination or assimilation than to crystal fractionation. However it should be emphasised that the material responsible for contamination of White Island magmas must be of very different composition to that which has been assimilated by the Edgecumbe and Whale Island magmas.

THE ORIGIN OF ANDESITE

The calc-alkaline association consists of four main rock types, each of which may have a complex history of crystallisation, as well as being related in its origin to that of the association as a whole. Several different hypotheses of origin have been suggested, and it is unlikely that any single hypothesis will satisfy all the features shown by rocks of the calc-alkaline association in different areas.

The hypotheses that have been proposed to explain the origin of andesites fall into five main groups, these are:

(1) Fractional crystallisation of basaltic magma.

(2) Melting of lower crustal material.

(3) Mixing of magmas.

(4) Contamination of basaltic magma with sialic crust.

(5) Partial melting in the upper mantle.

Details of many of the hypotheses and objections to certain of them have been given by Green & Ringwood (1968), Kuno ((1968), Osborn (1969) and Taylor (1969).

The occurrence of regional geochemical anomalies in andesite composition, such as the high Rb, Tl, Th, U abundances and high Rb/Sr and Th/U ratios in Taupo Zone andesites, is evidence that local factors affect calc-alkaline genetic processes. Thus, as no hypothesis is likely to be of general applicability, all hypotheses must be tested in specifically local context.

Origin of Andesite in the Taupo Volcanic Zone

Osborn (1969) suggested that andesite and alpine peridotite are complementary products of fractionating olivine basalt magma under conditions of constant moderate oxygen pressure. Osborn's petrogenetic model, based on a great deal of experimental work (Osborn, 1959, 1962; Roeder & Osborn, 1966 a, b; Osborn, 1969), implies that titanomagnetite crystallises early and is fractionated continuously, thus being incorporated into the accumulative alpine peridotite. However, Challis & Lauder (1966, Table 2) consider that the characteristic opaque mineral found in alpine peridotites of tholeiitic parentage is chromite, not titanomagnetite. Fractionation of basalt to produce an alpine peridotite with chromite as the opaque mineral would not be affected by the geochemical restrictions on titanomagnetite separation discussed by Duncan & Taylor (1968). Indeed, removal of chromite from the parental magma of most andesites is strongly suggested by the generally low, but extremely variable, Cr abundance in andesites. In the Taupo Zone the marked compositional 'gap' between basalts and andesites (Clark, 1960 b), and the small amount of basalt at the surface make it unlikely that andesite has been derived by fractionation of basalt. Sr isotope determinations by Ewart & Stipp (1968) indicate that the andesites could not have formed by fractional crystallisation of basalt with the same Sr^{86}/Sr^{87} ratios as those of analysed Taupo Zone basalts.

Since the composition of the lower crust in the New Zealand region is unknown, the validity of a lower crustal melting hypothesis for the origin of the Taupo Zone andesites cannot be tested.

Basalt and rhyolite are the only two magmas in the Taupo Zone which could be mixed together to produce andesite or dacite. A theoretical mixture of the average Taupo Zone rhyolite and the K-Trig basalt (mixing proportions calculated to give best fit for major elements, data from Ewart, Taylor & Capp, 1968) is compared to TNP andesite in Fig. 34, which shows the relative trace element compositions of the andesite and the mixture. The element abundances in TNP andesite are plotted along a 45° diagonal line and where the two compositions are equivalent the element abundance in the mixture will also fall on this line. Increasing distance between the plotted point for an element abundance in the basalt-rhyolite mixture and the diagonal line indicates increasing disparity in composition between the mixture and the TNP andesite. Elements showing considerable disparity in composition are Ba, Zr, Cr, Cu and Y.

The only non-volcanic sialic materials in the Taupo Zone for which trace element analyses are available are "marginal facies" greywacke and argillite (Ewart, Taylor & Capp, 1968). Fig. 35 is a comparison diagram for the compositions of TNP andesite and a theoretical basalt-greywacke-argillite mixture (mixing proportions calculated to give best fit for major elements). Substantial disparity between the two compositions is shown by abundances of the elements Sr, Zr, Cr and La.

Two possible methods of producing andesite by partial melting of the upper mantle have been suggested by Green & Ringwood (1966, 1968). The first hypothesis requires the partial melting of quartz eclogite at about 150 km depth, this process is unlikely to be operable due to the relative Ni, Co and V abundances in eclogitic garnets and pyroxenes,

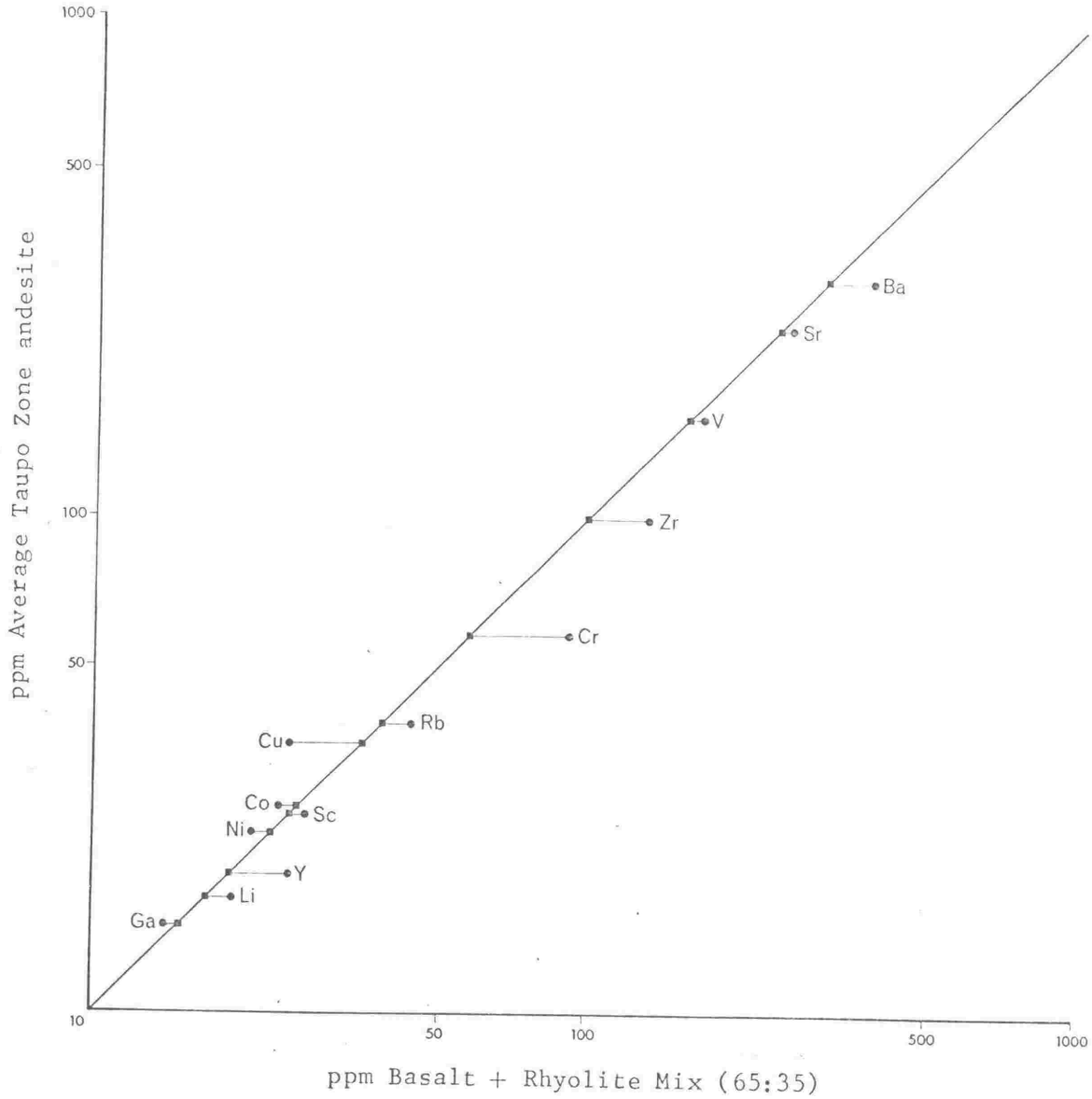

Fig. 34. - Comparison of trace element abundances in average Taupo Zone andesite (calculated from data in Table 33) and in a calculated rhyolite/basalt mix (data from Table 33). The mixing ratio was chosen to give the best fit for the major element data. Points representing the andesite abundances fall on the 45° diagonal line, points representing element abundances in the mixture generally fall off the line and are joined to the corresponding element abundance in the andesite by tie-lines. Increasing length of the tie-line indicates increasing disparity in composition between the andesite and the mixture.

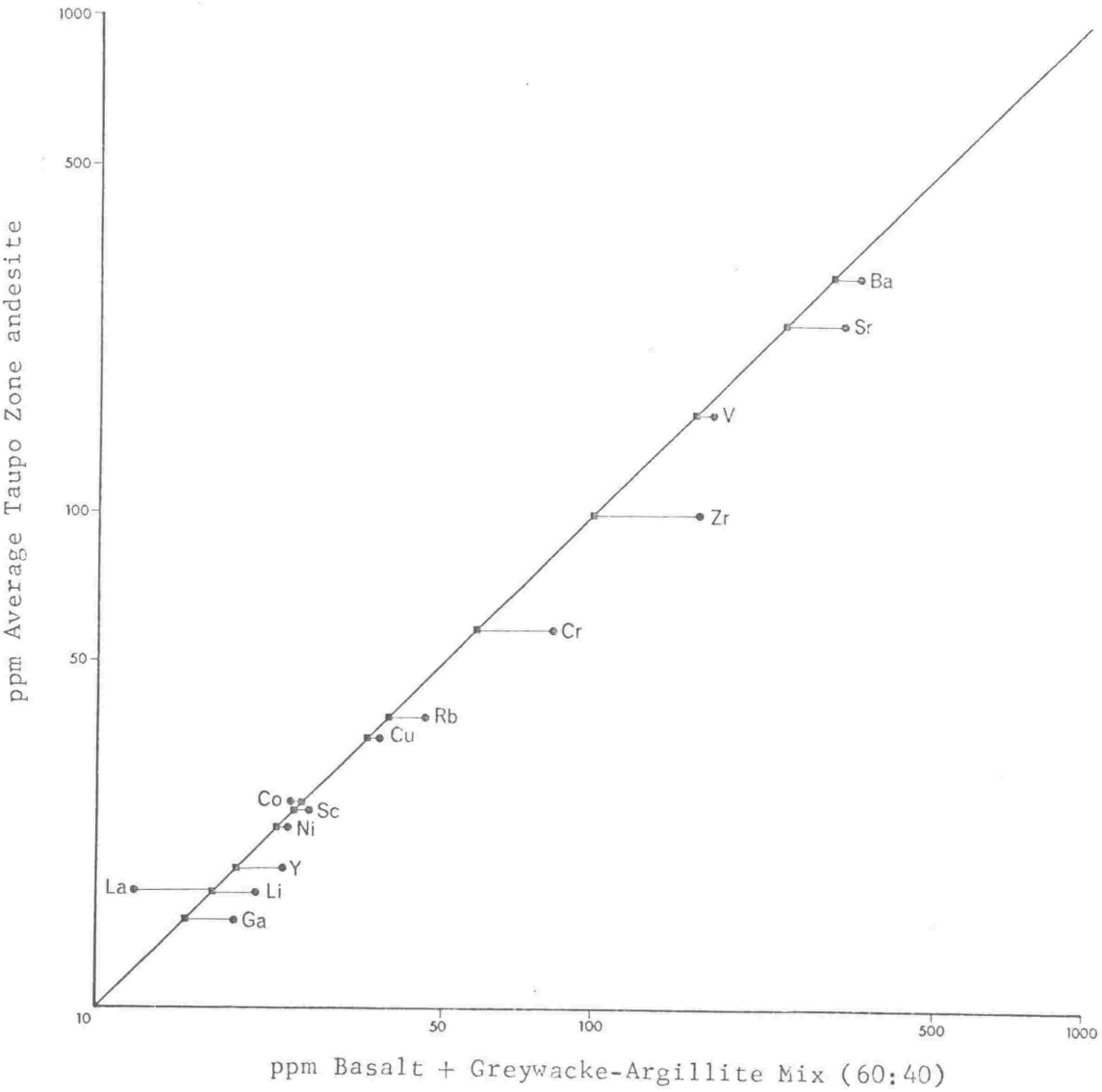

Fig. 35. - Comparison of trace element abundances in average Taupo Zone andesite and in a calculated basalt/greywacke-argillite mix (data from Table 33). Plotting technique is the same as that used in Fig. 34.

together with the Ni/Co and V/Ni ratios in andesites (see Taylor et al., 1969). Green & Ringwood's second hypothesis suggests that andesites are formed at depths of 30-40 km by partial melting of wet basaltic material or amphibolite, this process appears to be consistent with andesite geochemistry.

It can therefore be concluded that the origin of andesite in the Taupo Zone is not clearly defined, since at least two or three different hypotheses appear to be consistent with the available data.
The hypotheses which appear the least likely in the Taupo Zone are those involving fractional crystallisation of basaltic magma, or the mixing of magmas, to produce an andesite. The hypothesis preferred by the author is that Taupo Zone andesites were formed by partial melting of the upper mantle or lower crust at a depth of 30-40 km, under hydrous conditions. Such a process is consistent with Taylor's (1969) requirements for a two-stage genetic process to explain andesite geochemistry.

PETROGENESIS OF TAUPO ZONE VOLCANIC ROCKS

All available major and trace element analyses of Taupo Zone volcanic rocks are given in reduced form (analyses of some rock types are averaged) in Table 33, together with analyses of "marginal facies" greywacke and argillite for comparison. All writers since Steiner (1958) and Clark (1960), except for Schofield (1968), have agreed on the existence of separate basaltic and rhyolitic parent magmas in the Taupo Zone. Two compositional "gaps" exist in the Taupo Zone basalt-andesite-dacite-rhyolite suite. The first gap, an absence of analysed rocks containing between about 52% and 56% SiO_2 (except for low-Si andesites of accumulative origin) was recognised by Clark (1960 b); and the second gap, a very small number of analysed rocks containing between about 68% and 71.5% SiO_2 was recognised by Steiner (1958).

There are no discontinuities in the trace element variation trends corresponding to the compositional gap between basalt and andesite (52-56% SiO_2). There are, however, a number of discontinuities in trace element variation trends corresponding to the dacite-rhyolite gap (68-71.5% SiO_2). In particular the variation trends of Sr, total REE, Sn, Nb, Mn, Li, Sc, V, B, Tl and the ratios Ba/Sr, Rb/Sr, Zr/Hf and Rb/Tl all show abrupt changes in slope, or reverse in slope, between 68% and 71.5% SiO_2.

Clark's (1960) suggestion that Taupo Zone andesites formed by a fractionating basalt assimilating heated acidic material of rhyolitic composition now appears unlikely, since trace element analyses by Ewart, Taylor & Capp (1968) indicate that a basalt-rhyolite

IDENTIFICATION OF ANALYSIS NUMBERS AND SOURCES OF DATA FOR TABLE 33

1. K-Trig Basalt - Ewart, Taylor & Capp (1968), analysis No. 31, TiO_2 from Grange (1937).

2. Ongaroto Basalt - Sr, Rb, U, Th and K from Ewart & Stipp (1968). Other elements are new analysis - Analysts: M.J. Kaye (major elements), A.R. Duncan (trace elements).

3. Orakeikorako Basalt - Sr, Rb, U, Th and K from Ewart & Stipp (1968). Other elements are new analysis - Analysts: M.J. Kaye (major elements), A.R. Duncan (trace elements).

4. Karangahape Low-Si Andesite - Sr, Rb, U, Th and K from Ewart & Stipp (1968). Other elements are new analysis - Analysts: M.J. Kaye (major elements), A.R. Duncan (trace elements).

5. Average Tongariro National Park Low-Si Andesite - average of 4 analyses (samples L, 152, H, K) from Taylor & White (1966).

6. Average Tongariro National Park Labradorite/Labradorite-Pyroxene Andesite - average of 2 analyses (samples 1954, 136) from Taylor & White (1966).

7. Tama Lakes Hornblende Andesite - Ewart, Taylor & Capp (1968) analysis No. 29R.

8. Average Edgecumbe and Whale Island Dacite - average of 28 analyses of Edgecumbe and Whale Island samples, data from Tables 20, 21, 23, 24 and 26. Analysts: A.R. Duncan, (elements in Table 26 determined by M.J. Kaye).

9. Average White Island Dacite - average of 6 analyses of samples from the Central Cone, data from Tables 22, 25, 26. Analysts: A.R. Duncan, (elements in Table 26 determined by M.J. Kaye).

10. Average Manawahe Dacite - average of 3 analyses of Manawahe samples, data from Tables 22 and 25. Analyst: A.R. Duncan.

11. Tauhara Dacite - Sr, Rb, Th, U, K from Ewart & Stipp (1968). Other elements are new analysis - Analysts: M.J. Kaye (major elements), A.R. Duncan (trace elements).

12. Maungaongaonga Dacite - Ewart, Taylor & Capp (1968), analysis No. 27.

13. Average Taupo Zone Rhyolitic Eruptive - average of 26 analyses of ignimbrites and rhyolite lavas by Ewart, Taylor & Capp (1968), analysis No. 35.

14. "Marginal Facies" Greywacke - average of analyses No.'s 32 and 33 in Ewart, Taylor & Capp (1968).

15. "Marginal Facies" Argillite - Ewart, Taylor & Capp (1968), analysis No. 34.

16. 60:40 Greywacke-Argillite - a calculated 60:40 mixture of greywacke: argillite using analyses 14 and 15 in this table.

TABLE 33

ANALYSES OF TAUPO ZONE VOLCANIC AND SEDIMENTARY ROCKS

SECTION 1. MAJOR ELEMENTS ↓															
ANALYSIS NO.	1.	2.	3.	4.	5.	6.	7.	8.	9.	10.	11.	12.	13.	14.	15.	16.
SiO_2	51.03	51.28	49.32	56.67	56.48	59.73	59.79	64.39	64.02	65.41	67.76	67.60	75.32	63.99	68.41	65.77
TiO_2	1.17	1.06	1.16	0.58	0.53	0.58	0.52	0.62	0.73	0.59	0.37	0.71	0.25	0.81	0.65	0.75
Al_2O_3	16.71	15.51	17.43	13.71	14.94	16.87	17.34	16.14	14.81	15.70	14.70	15.35	13.35	16.05	16.65	16.31
*FeO	10.22	8.94	8.97	7.10	7.86	7.21	6.15	5.41	5.67	5.10	3.84	4.36	1.75	6.11	3.50	5.07
CaO	10.81	10.80	11.77	9.93	9.04	7.46	6.56	5.86	5.79	5.62	4.78	3.41	1.56	4.03	1.59	3.04
MgO	6.39	9.04	7.91	8.47	8.15	4.69	5.30	2.54	3.47	1.46	2.58	1.34	0.27	2.82	1.45	2.26
Na_2O	3.07	2.54	2.85	2.48	2.22	2.27	3.33	3.03	3.18	3.60	3.62	4.61	4.14	4.43	3.28	3.97
K_2O	0.41	0.57	0.36	0.91	0.71	1.14	0.91	1.90	2.22	2.37	2.18	2.41	3.31	1.57	4.32	2.68
P_2O_5	0.19	0.25	0.20	0.12	0.07	0.03	0.09	0.11	0.11	0.14	0.10	0.20	0.05	0.18	0.14	0.17
SECTION 2. LARGE CATIONS																
Cs^+	n.d.	n.d.	n.d.	n.d.	1.2	1.5	0.7	1.6	1.7	1.0	1.9	1.1	3.3	0.9	9.4	4.2
Rb^+	9.6	11	3.9	24	19	40	25	65	74	80	63	73	108	44	139	82
Tl^+	n.d.	-	-	-	0.43	0.33	0.55	0.10	0.20	-	-	0.5	1.1	-	-	-
Ba^{2+}	115	145	105	205	200	245	280	640	900	640	450	680	870	350	930	580
$\%K^+$	0.33	0.45	0.27	0.71	0.59	0.95	0.75	1.55	1.82	1.93	1.77	1.99	2.70	1.25	3.49	2.15
Pb^{2+}	1.7	-	-	-	6.0	8.6	10.6	3.0	12	-	-	11	18	-	-	-
Sr^{2+}	328	308	338	508	400	250	232	235	174	218	315	242	124	382	227	320
$\%Ca^{2+}$	7.58	7.72	8.41	7.10	6.45	5.32	4.65	4.09	3.93	3.10	3.42	2.43	1.09	2.77	1.11	2.10
$\%Na^+$	2.23	1.88	2.11	1.84	1.65	1.68	2.45	2.21	2.33	2.62	2.69	3.41	3.02	3.17	2.37	2.85
K/Rb	344	429	692	297	311	238	306	240	247	241	280	270	250	283	251	270
Rb/Tl	-	-	-	-	44	121	45	670	370	-	-	-	98	-	-	-
Ba/Rb	12.0	13.8	27.4	8.54	10.5	6.13	11.4	10.2	12.2	7.98	7.15	9.28	8.06	7.94	6.69	7.44
Ba/Sr	0.35	0.48	0.32	0.40	0.50	0.98	1.21	2.76	5.17	2.94	1.43	2.81	7.02	0.92	4.10	1.81
Rb/Sr	0.029	0.034	0.012	0.047	0.048	0.160	0.106	0.265	0.424	0.368	0.201	0.303	0.871	0.115	0.612	0.256
SECTION 3. RARE EARTHS																
La^{3+}	n.d.	n.d.	n.d.	n.d.	12	18	12	47	28	n.d.	n.d.	16	26	12	31	24
Ce^{3+}	19	-	-	-	25	30.5	16.7	74	55	-	-	-	43.5	-	-	-
Pr^{3+}	4.1	-	-	-	2.3	3.2	2.62	10	8.6	-	-	-	6.4	-	-	-
Nd^{3+}	20	-	-	-	6.2	11.5	7.9	43	17	-	-	-	18.2	-	-	-
Sm^{3+}	4.0	-	-	-	1.6	2.4	1.95	6.7	4.4	-	-	-	5.5	-	-	-
Eu^{3+}	1.3	-	-	-	0.57	0.74	0.55	0.80	1.3	-	-	-	1.0	-	-	-
Gd^{3+}	4.0	-	-	-	2.0	2.7	1.73	2.9	4.6	-	-	-	4.3	-	-	-
Tb^{3+}	0.8	-	-	-	0.40	0.56	0.41	0.50	0.81	-	-	-	1.15	-	-	-
Ho^{3+}	1.2	-	-	-	0.58	0.71	0.57	0.53	0.80	-	-	-	1.4	-	-	-
Er^{3+}	4.2	-	-	-	1.5	2.2	1.43	1.7	2.7	-	-	-	3.9	-	-	-
Tm^{3+}	0.56	-	-	-	0.24	0.30	0.18	0.22	0.36	-	-	-	0.46	-	-	-
Yb^{3+}	2.7	-	-	-	1.4	1.9	1.38	1.5	2.4	-	-	-	3.55	-	-	-
Y^{3+}	25	23	23	16	15	21	13	18	27	35	17	31	25	20	28	23

TABLE 33 (continued)

SECTION 4. LARGE HIGHLY CHARGED CATIONS

ANALYSIS NO.	1.	2.	3.	4.	5.	6.	7.	8.	9.	10.	11.	12.	13.	14.	15.	16.
Th^{4+}	1.07	1.23	0.63	3.20	2.7	3.9	4.01	5.9	6.7	7.84	7.88	8.27	11.5	-	-	-
U^{4+}	0.18	0.33	0.13	0.75	0.7	1.0	0.77	1.4	1.5	1.73	1.93	1.70	2.56	-	-	-
Zr^{4+}	120	83	78	80	95	105	88	105	150	157	143	215	160	210	205	208
Hf^{4+}	2.55	-	-	-	2.1	2.6	1.6	1.6	3.4	-	-	4.6	4.5	-	-	-
Sn^{4+}	0.54	-	-	-	0.55	0.60	0.33	-	-	-	-	1.65	1.3	-	-	-
Nb^{5+}	4.0	-	-	-	3.5	4.3	2.7	7	9	-	-	6.1	5.6	-	-	-
$\%Ti^{4+}$	0.690	0.635	0.695	0.348	0.320	0.350	0.312	0.355	0.434	0.347	0.222	0.426	0.150	0.468	0.378	0.432
Mo^{6+}	1.7	-	-	-	0.49	0.64	1.0	-	-	-	-	2.0	2.6	-	-	-
Th/U	6.08	3.73	4.85	4.26	3.86	3.90	5.18	4.14	4.47	4.53	4.08	4.87	4.49	-	-	-
Zr/Hf	-	-	-	-	45.2	40.4	55.0	68.8	43.5	-	-	46.7	35.6	-	-	-
SECTION 5.	FERROMAGNESIAN ELEMENTS															
Mn^{2+}	1470	1320	1290	1060	1070	1020	390	910	800	730	670	770	390	850	390	670
$\%^{*}Fe^{2+}$	7.80	6.95	6.97	5.52	6.10	5.59	4.74	4.06	4.35	3.88	2.98	3.38	1.34	4.58	2.65	3.81
Cu^{2+}	35	43	44	49	90	35	51	16	72	15	23	3.0	6.0	42	32	38
Co^{2+}	37	39	40	37	41	29	25	12	20	11	11	4.6	n.d.	15	7.7	12
Ni^{2+}	32	116	65	73	60	28	31	6.4	49	n.d.	43	2.8	n.d.	16	14	15
Li^{+}	10	4.3	3.6	6.5	10	11	24	22	20	32	17	10	35	30	35	32
$\%Mg^{2+}$	3.78	5.45	4.77	5.11	4.91	2.82	3.17	1.53	2.07	0.86	1.56	0.81	0.16	1.64	0.85	1.32
Ni/Co	0.86	2.99	1.63	1.95	1.46	0.97	1.24	0.53	2.45	-	3.77	0.61	-	1.07	1.82	1.26
Sc^{3+}	39	28	29	29	36	27	21	18	19	18	13	11	4.7	16	12	15
V^{3+}	255	225	220	150	170	160	140	130	180	100	80	26	8.5	110	75	95
$\%Ti^{4+}$	0.690	0.635	0.695	0.348	0.320	0.350	0.312	0.355	0.434	0.347	0.222	0.426	0.150	0.468	0.378	0.432
Cr^{3+}	140	400	85	380	280	75	49	30	115	2	56	0.9	1.7	27	26	27
Ga^{3+}	13	12	13	12	15	14	16	16	16	17	14	25	16	23	24	24
$\%Al^{3+}$	8.68	8.21	9.22	7.25	7.89	8.90	9.10	8.38	7.74	8.14	7.78	8.10	6.95	8.18	8.57	8.34
Cr/V	0.55	2	0.383	2.48	1.65	0.469	0.350	0.221	0.639	0.020	0.695	0.035	0.200	0.245	0.347	0.284
Al/Ga $\times 10^{-4}$	0.668	0.684	0.709	0.604	0.527	0.636	0.569	0.536	0.484	0.478	0.556	0.324	0.434	0.356	0.357	0.348
V/Ni	7.97	1.94	3.38	2.05	2.83	5.71	4.52	20.3	3.67	-	1.86	9.29	-	6.88	5.36	6.25

TABLE 33 (continued)

SECTION 6. SMALL CATIONS															
ANALYSIS NO.	1.	2.	3.	4.	5.	6.	7.	8.	9.	10.	11.	12.	13.	14.	15.	16.
%Al^{3+}	8.68	8.21	9.22	7.25	7.89	8.90	9.10	8.38	7.74	8.14	7.78	8.10	6.95	8.18	8.57	8.34
Ge^{4+}	-	-	-	-	0.70	0.72	-	-	-	-	-	-	-	-	-	-
%Si^{4+}	23.4	23.96	23.04	26.48	26.34	27.82	27.7	29.65	29.55	29.93	31.66	31.5	34.6	28.8	31.1	29.7
B^{3+}	9.9	n.d.	n.d.	5	-	11	-	18	31	10	8.7	-	24	30	80	-
SECTION 7. CHALCOPHILE ELEMENTS																
Tl^{+}	n.d.	-	-	-	0.43	0.33	0.55	0.10	0.20	-	-	0.5	1.1	-	-	-
Ag^{+}	-	-	-	-	0.14	0.07	-	-	-	-	-	-	-	-	-	-
Pb^{2+}	1.7	-	-	-	6.0	8.6	10.6	3.0	12	-	-	11	18	-	-	-
Cd^{2+}	-	-	-	-	2.5	1.13	-	-	-	-	-	-	-	-	-	-
Bi^{3+}	n.d.	-	-	-	-	0.12	n.d.	-	-	-	-	1.0	-	-	-	-
In^{3+}	n.d.	-	-	-	0.20	0.16	0.08	-	-	-	-	0.05	0.08	-	-	-
Sb^{3+}	1.0	-	-	-	0.32	0.25	n.d.	-	-	-	-	1.0	0.43	-	-	-
%*Fe^{2+}	7.80	6.95	6.97	5.52	6.10	5.59	4.74	4.06	4.35	3.88	2.98	3.38	1.34	4.58	2.65	3.81
Cu^{2+}	35	43	44	49	90	35	51	16	72	15	23	3.0	6.0	42	32	38
Co^{2+}	37	39	40	37	41	29	25	12	20	11	11	4.6	n.d.	15	7.7	12.1
Sn^{4+}	0.54	-	-	-	0.55	0.60	0.33	-	-	-	-	1.65	1.3	-	-	-
Ni^{2+}	32	116	65	73	60	28	31	6.4	49	n.d.	43	2.8	n.d.	16	14	15
Mo^{6+}	1.7	-	-	-	0.49	0.64	1.0	-	-	-	-	2.0	2.6	-	-	-
As^{3+}	-	-	-	-	2.5	2.7	-	-	-	-	-	-	-	-	-	-
Ga^{3+}	13	12	13	12	15	14	16	16	16	17	14	25	16	23	24	24
Ge^{4+}	-	-	-	-	0.70	0.72	-	-	-	-	-	-	-	-	-	-

* Total Iron shown as Fe^{2+}.

All values are in p.p.m. unless otherwise indicated.

n.d. = not detected. - = not determined.

mix would not have the appropriate trace element composition (Fig. 34). Steiner's (1958) hypothesis that andesite has been produced by basalt assimilating acid-gneiss basement has been considered by Ewart & Stipp (1968), who concluded that the xenoliths in the 1954 Ngauruhoe lavas, on which Steiner's hypothesis is based, are more likely to represent superficial tertiary sediments than basement material. Possible assimilation of "marginal-facies" greywacke-argillite by basaltic magma to produce andesite, as suggested by Ewart & Stipp (1968), does not seem consistent with presently available trace element data (Fig. 35). Thus andesite may also be a separate parent magma in the Taupo Volcanic Zone.

Schofield's (1968) hypothesis that basalt and rhyolite in the Taupo Zone have been derived by fractional crystallisation of a parental andesitic magma is inconsistent with isotopic and trace element data (Ewart & Stipp, 1968; Ewart, Taylor & Capp, 1968; Ewart & Taylor, 1969;) and data in the present thesis.

Basalt

The Taupo Zone basalts have mantle type Sr^{87}/Sr^{86} ratios, with a very small range of 0.7042 - 0.7043 (Ewart & Stipp). The K-Trig, Tarawera and Orakeikorako basalts are high-Al varieties by Kuno's (1960) definition, but the Ongaroto basalt is not a high-Al variety. There are significant differences in certain element abundances and element ratios between the different basalts (Table 33: Al, Fe, Mg, Rb, Th, U, Zr, Ni, Li, Cr, K/Rb, Ba/Rb, Rb/Sr, Th/U, Ni/Co, Cr/V, V/Ni) particularly between the Ongaroto basalt and the K-Trig and

Orakeikorako basalts. The low Ni, Cr, Co, and Cu abundances which were considered by Taylor (1969) to be characteristic of high-Al basalts are shown by the K-Trig and Orakeikorako basalts; the Ongaroto basalt, however, has much higher Ni and Cr but has Co and Cu abundances similar to those in the K-Trig basalt.

It is concluded that all the Taupo Zone basalts are derived from the mantle, but that at least two chemically distinctive basalt types, with different petrogenetic histories, are present.

Andesite and Dacite

Arguments in favour of a separate parent andesite magma, and various genetic hypotheses for it, have been discussed previously. Low-Si andesites of accumulative origin were reported from TNP by Clark (1960 b). A low-Si andesite cropping out at Karangahape has a major and trace element composition extremely similar to that of the TNP low-Si andesites (Table 33). However the Karangahape low-Si andesite has an anomalously low Sr^{87}/Sr^{86} ratio (0.7043), significantly lower than most other andesitic ratios (0.7053 - 0.7063) reported by Ewart & Stipp (1968), which suggests that it is not a crystal accumulate formed from an andesitic magma. Titiraupenga andesite (Ewart & Stipp, 1968) also has an anomalously low Sr^{87}/Sr^{86} ratio (0.7046), and its mineralogy strongly suggest that it may be a low-Si type (no chemical analysis is available). These anomalies should be further investigated by future work.

The trace element composition of dacites is more variable than that of any other volcanic rock type in the Taupo Zone (Table 33), suggesting that the dacites may have originated by more than one process. The Bay

of Plenty dacites have probably been formed by an andesitic magma assimilating upper crustal material. Other genetic processes suggested for Taupo Zone dacites are fractional crystallisation of andesite (Steiner, 1958) and partial melting of greywacke-argillite (Ewart & Stipp, 1968).

Rhyolite

A crustal melting hypothesis for the origin of the Taupo Zone rhyolites is generally accepted (Steiner, 1958; Clark 1960 a, b; Healy, 1964; Ewart, 1966; Ewart & Stipp, 1968). The crustal material of most suitable major element, trace element, and isotopic composition is considered to be "marginal facies" greywacke-argillite (Ewart & Stipp, 1968; Ewart, Taylor & Capp, 1968).

SUMMARY

1. Major element compositions of Bay of Plenty volcanics are typical of the calc-alkaline association. Most samples range in composition from andesite to dacite, with the majority being dacites, and are intermediate in composition between the TNP andesites and the Tauhara dacites.

2. The Bay of Plenty volcanics and other Taupo Zone andesites and dacites are generally higher in Rb, Tl, Th, and U, with higher Rb/Sr and Th/U ratios than other western pacific andesites and dacites.

3. Edgecumbe and Whale Island samples differ significantly in abundances of the elements Ti, P, Sr, Li, Ga, Ba, and B, and in the ratios Ba/Rb, Ba/Sr, and Fe/Co. If the two volcanoes had a common parent magma these differences could not be the result of fractional crystallisation processes.

4. White Island analyses fall into two distinct groups, the Troup Head andesite and the Central Cone dacites. Central Cone dacites have very unusual trace element compositions, particularly for the elements Ba, Sr, Zr, Cu, Co, Ni, V, Cr and the ratios Ni/Co, V/Ni, Ba/Sr and Ba/Rb. Their unusual composition precludes derivation by fractional crystallisation of the Troup Head andesitic magma. The anomalous concentrations of the elements detailed above together with unusually high B, Cl and I content, suggests that they may have formed by contamination of andesitic magma with marine sediments and seawater.

5. Major element analyses of the Bay of Plenty volcanics follow the same variation trend as the rest of the Taupo volcanics, but show a wider scatter about the trend.

6. Major element variation trends for Edgecumbe and Whale Island cannot be entirely explained by fractional crystallisation, since the Al_2O_3 and Na_2O trends cannot be explained by plagioclase fractionation, even though this is the only phenocryst mineral containing appreciable amounts of these oxides.

7. Trace element variation trends for Edgecumbe and Whale Island cannot be explained by crystal fractionation involving separation of plagioclase, augite, hypersthene, biotite or hornblende from the parent magma.

8. Variation trends for Edgecumbe and Whale Island are consistent with assimilation of material with the composition of average Taupo Zone rhyolite into an andesitic parent magma. It is considered that this process is more likely to be one of wall-rock partial melting and assimilation than one of magmatic mixing.

9. Present knowledge of the geochemistry of Taupo Zone volcanic rocks particularly the recognition of compositional gaps between 52% and 56% SiO_2 and between 68% and 71.5% SiO_2, suggests the presence of three parent magmas: basalt, andesite and rhyolite.

10. Two types of basalt are present in the Taupo Zone, a high-Al basalt (definition by Kuno, 1960) and a tholeiitic basalt. Both types are considered to be of mantle origin (Ewart & Stipp, 1968) but their detailed petrogenetic history must clearly be different.

11. The composition of Taupo Zone andesites is incompatible with their formation by mixing of Taupo Zone basalt and rhyolite; or by

contamination of a basalt with "marginal facies" greywacke-argillite. It is considered that the most likely origin for Taupo Zone andesites is by partial melting of the upper mantle or lower crust (Green & Ringwood, 1968).

12. Taupo Zone dacites show extremely variable trace element compositions, suggesting that they may have been formed by more than one process. The variation trends of the Bay of Plenty dacites suggest that they were formed by contamination of an andesitic magma with upper crustal material.

13. All available information suggests that Taupo Zone rhyolites were formed by partial melting of upper crustal material. Ewart & Stipp (1968) and Ewart, Taylor & Capp (1968) suggest that the most likely such material is "marginal facies" greywacke-argillite.

Contr. Mineral. and Petrol. 20, 30—33 (1968)

Trace Element Analyses of Magnetites from Andesitic and Dacitic Lavas from Bay of Plenty, New Zealand

A. R. Duncan

Geology Department, Victoria University of Wellington, P. O. Box 196, Wellington, New Zealand

S. R. Taylor

Department of Geophysics and Geochemistry, Australian National University, P. O. Box 4, Canberra, A. C. T. 2601, Australia

Received July 22, 1968

Abstract. Five magnetites from andesitic and dacitic lavas from the volcanoes Edgecumbe, Whale Island, and White Island were separated, and analysed for Mg, Ti, Cu, V, Ni, Co, Mn, and Cr. The vanadium contents provide difficulties for OSBORN's (1962) hypothesis for the origin of calc-alkaline volcanic rocks.

Introduction

The volcanoes Edgecumbe, Whale Island and White Island are in the Bay of Plenty region in New Zealand (E. Long. 176°—178°, S. Lat. 37°30′—38°30′). They are 40 km apart and lie on the flanks of the northeast trending Whakatane Graben and its seaward extension, the White Island Trench.

Total-rock analyses of 40 andesitic and dacitic lavas from the volcanoes (DUNCAN, unpublished data) show a variation in SiO_2 from 58—67%, and typical calc-alkaline major element chemistry. The trace element chemistry of magnetite was investigated because of it's importance for hypotheses of the origin of the calc-alkaline volcanic association.

Analytical Methods

Total-rock samples were broken down in large and small jaw crushers, then ground in an agate cone-grinder, and finally in an agate grinding vessel on a "Tema" mill. Magnetite was extracted by hand magnet, with the sample and the magnet immersed in acetone. Magnetite concentrates were purified by repeated separations under acetone, the final concentrates being at least 98% pure. The elements Mg, V, Ti, Cu, Ni, Co, Mn, and Cr were determined on a Jarrell-Ash Ebert grating spectrograph. Samples were mixed with twice their weight of a carbon-palladium mixture, the palladium acting as an internal standard, and were arced to completion. Johnson-Matthey "Specpure" oxides of the elements listed above were mixed in a base of "Specpure" Fe_2O_3, and a set of standards obtained by successive dilution with additional "Specpure" Fe_2O_3. Two previously analysed magnetites from the Skaergaard Intrusion (VINCENT *et al.*, 1957) were re-analysed and found to plot on the working curves obtained from successive dilutions of the standard mix.

All samples and standards were analysed in triplicate. The lines Mg 2783, V 3185, Ti 3262, Cu 3274, Ni 3414, Pd 3421, Co 3453, Mn 4034, and Cr 4254 were read. The analytical precision, expressed as relative deviation, was $\pm$ 5%.

Discussion of Analytical Data

Analyses of the five magnetites are given in Table 1, and analyses of the total-rock samples from which three of the magnetites were separated are given in Table 2.

Osborn (1962) and Roeder and Osborn (1966a, 1966b) have proposed that if basalt is crystallising under conditions of constant moderate oxygen pressure, early crystallisation of magnetite will result. They have further suggested that the crystallisation would be followed by early separation of magnetite preventing iron enrichment of the magma and permitting the formation of the calc-alkaline suite by crystal fractionation.

The octahedral site preference energies (Burns and Fyfe, 1964) of divalent ferromagnesian trace elements, Ni and Co, exceed the site preference energy of Fe^{2+}, and similarly the site preference energies of trivalent ferromagnesian trace elements Cr, Mn, V, and Ti exceed that of Fe^{3+}. Consequently the proportion of ferromagnesian trace elements is greatest in the early-crystallising and least in the late crystallising magnetite. Thus the concentrations of Ni, Co, Cr, V, and Ti in the magnetites analysed will be less than in magnetite which may have crystallised from the magma at an earlier time.

The loss of magnetites having the compositions shown in Table 1 will strongly deplete the magma in vanadium. For example if magnetite representing 1% by

Table 1. *Analyses of Magnetites*

Sample:	11,206	11,250	11,215	11,228	11,251
Mg-%	1.33	1.24	1.72	1.28	1.11
V-%	0.63	0.60	0.55	0.45	0.80
Ti-%	7.2	6.6	7.2	5.1	6.9
Cu	150	120	100	60	270
Ni	63	60	61	64	320
Co	160	160	160	210	230
Mn	2,800	2,800	2,900	2,700	2,500
Cr	170	360	370	47	1,100

All concentrations are in ppm unless otherwise indicated.

weight of the magma were removed this would result in a decrease of 60 ppm vanadium in the remaining total-rock; and so on in proportion. The amount of vanadium which could be removed from a fractionating basaltic parental magma to produce an andesite is severely restricted by the vanadium content in andesites relative to that in basalts, shown in Fig. 1 (after Taylor, 1968). If it is assumed after Osborn (1962) that andesite is formed from basalt by fractional crystallisation, including early crystallisation and removal of magnetite; and using Taylor's (1968) values for the vanadium content of average high-Al basalt and average andesite, the maximum amount of magnetite which could have been removed is 2%.

Since the removal of 2% magnetite from the basalt would result in a reduction in total iron (expressed as FeO) of less than 2%, it cannot explain the observed 4% difference in iron between the high-Al basalt and the andesite. Furthermore, since Osborn advocated separation of magnetite in order to counteract the trend of absolute iron enrichment, his hypothesis requires a separation of more

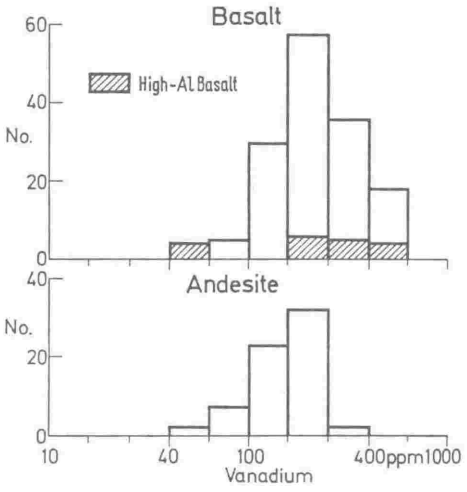

Fig. 1. Vanadium content of basalts and andesites

Table 2. *Total-Rock analyses*

Sample	11,206	11,215	11,228
SiO_2	59.88	63.69	58.05
TiO_2	0.74	0.69	0.64
Al_2O_3	17.32	16.42	16.18
FeO	6.57	5.72	7.46
CaO	7.60	5.99	8.76
MgO	3.63	2.54	5.73
Na_2O	2.71	3.07	2.06
K_2O	1.44	1.77	1.05
P_2O_5	0.12	0.12	0.08
	Total iron expressed as FeO		
V	192	140	160
Cu	32	15	25
Ni	7.3	10	16
Co	17	13	21
Mn	1,050	920	1,120
Cr	44	31	64

All trace element concentrations are in ppm.
Sample 11,228 is a xenolith in a dacitic lava from Whale Island.

Sample Locations:

11,206 = Mt. Edgecumbe, western flow units
11,250 = Mt. Edgecumbe, base of main cone, North side
11,215 = Mt. Edgecumbe, base of main cone, North side
11,228 = Whale Island, cognate xenolith from flow on top of main cone
11,251 = White Island, South shore.

than 4% magnetite; the vanadium data makes this most unlikely. Ferromagnesian silicate minerals generally contain more vanadium than the magma from which they crystallise, consequently removal of these together with magnetite will not counteract the trend of vanadium depletion due to the magnetite separation.

Taking the Taupo Volcanic Zone, New Zealand as a specific area in which to test Osborn's hypothesis, the same conclusion is reached. The difference in vanadium content between the K-Trig high-Al basalt (EWART *et al.*, 1968) and the average composition of Edgecumbe, Whale Island and White Island rocks from which the magnetite samples were separated, is 120 ppm. The difference in vanadium content infers the separation of a maximum of 2% magnetite, which is insufficient to explain the 3.74% difference in total iron content. Further trace element analyses of magnetites from calc-alkaline volcanic rocks will provide a more general and conclusive test of OSBORN's hypothesis.

The extreme variability of chromium in the magnetites is noteworthy. Since magnetite can be easily separated in a high state of purity from volcanic material, it is suggested that the chromium content of magnetites may be a useful tool in the stratigraphic correlation of products of a single eruption.

References

BURNS, R. G., and W. S. FYFE: Site preference energy and selective uptake of transition-metal ions from a magma. Science **144**, 1001—1003 (1964).

EWART, A., S. R. TAYLOR, and A. C. CAPP: Trace and minor element geochemistry of the Rhyolitic Volcanic Rocks, Central North Island, New Zealand. Total rock and residual liquid data. Contr. Mineral. and Petrol. **18**, 76—104 (1968).

OSBORN, E. F.: Reaction series for subalkaline igneous rocks based on different oxygen pressure conditions. Am. Mineralogist **47**, 211—226 (1962).

ROEDER, P. L., and E. F. OSBORN: Fractional crystallisation trends in the system Mg_2SiO_4—$CaAl_2Si_2O_8$—FeO—Fe_2O_3—SiO_2 over the range of oxygen partial pressures of 10^{-11} to $10^{-0.7}$ atm. Bull. volcanol. **29**, 659—668 (1966a).

— — Experimental data for the system MgO—FeO—Fe_2O_3—$CaAl_2Si_2O_8$—SiO_2 and their petrological implications. Am. J. Sci. **264**, 428—480 (1966b).

TAYLOR, S. R.: Trace element chemistry of andesites and associated calc-alkaline rocks. In press (1968).

VINCENT, E. A., J. B. WRIGHT, R. CHEVALLIER, and S. MATTHIEU: Heating experiments on some natural magnetites. Mineral. Mag. **31**, 624—655 (1957).

Dr. S. R. TAYLOR
Dept. of Geophysics and Geochemistry
Australian National University, P. O. Box 4
Canberra, A. C. T. 2601, Australia

Universitätsdruckerei H. Stürtz AG Würzburg
Printed in Germany

Geochimica et Cosmochimica Acta, 1969, Vol. 33, pp. 275 to 286. Pergamon Press. Printed in Northern Ireland

Genetic significance of Co, Cr, Ni, Sc and V content of andesites

S. R. Taylor and Maureen Kaye
Department of Geophysics and Geochemistry, Australian National University, Canberra

A. J. R. White
Department of Geology, Australian National University, Canberra

A. R. Duncan
Department of Geology, Victoria University of Wellington, New Zealand

and

A. Ewart
Department of Geology, University of Queensland, Brisbane, Australia

(*Received* 13 *August* 1968; *accepted in revised form* 19 *September* 1968)

Abstract—The vanadium content of calc-alkaline andesites averages 175 ppm and is similar to that observed in basalts (average 200 ppm). The average nickel content of andesites is about 18 ppm, which is much lower than the nickel contents of alkali or tholeiitic basalts (average 120 ppm) but is similar to concentrations observed in high-Al basalts (average 25 ppm). The Ni/Co ratios of calc-alkaline andesites and high-Al basalts are less than one, in contrast to ratios of greater than two in alkali and tholeiitic basalts.

The data are difficult to explain by previous hypotheses for the origin of andesite magma, that involve (1) removal of magnetite (2) mixing or assimilation of basic, or acid material, or deep-sea sediments, (3) partial melting of quartz eclogite at high pressures and (4) fractional crystallisation from a parent high-Al basalt, under low pressures. A two-stage process of partial melting from pyrolite is consistent with the ferromagnesian trace element abundances.

Introduction

The calc-alkaline andesites, typically occurring in orogenic regions, are often considered to be intermediate in composition between the common basic and acidic rocks. Although they contain an average of about 60% SiO_2 and appropriate amounts of other major constituents, except potassium, the abundances of many trace elements (Taylor, 1968a, b; Taylor and White, 1965, 1966) do not show this intermediate character. This paper is concerned with the abundances of the ferromagnesian trace elements (Ni, Co, V, Sc and Cr) in calc-alkaline andesites and their significance for theories of the origin of andesite magma.

Element Abundances

Andesitic rocks of similar major element chemistry occur in the orogenic zones along the western margin of the Pacific Ocean. They occur in regions of thick (New Zealand, Japan), intermediate (Fiji) and thin crust (Marianas, Aleutians) alike. Rocks for which there are reliable chemical data occur in New Zealand, Fiji, Bougainville, Saipan, Japan, Kurile Islands, Kamchatka and the Aleutian Islands. Table 1 compares the average major element composition and Ni, Co, Cr, V and Sc contents

Table 1. Major element and ferromagnesian trace element composition of basaltic and calc-alkaline rocks. Data from Taylor (1968b)

%	Alkali and tholeiitic basalt	High-Al basalt	Low Si andesite	Low K andesite	Andesite	High K andesite
SiO_2	49·2	51·7	54·9	57·3	59·5	60·8
Al_2O_3	15·7	16·9	17·5	17·4	17·2	16·8
FeO	11·2	10·4	8·2	7·3	6·1	5·1
MgO	8·7	6·5	4·7	3·5	3·4	2·2
CaO	10·8	11·0	8·5	8·7	7·0	5·6
Na_2O	2·3	3·1	3·4	2·6	3·7	4·1
K_2O	1·0	0·4	1·1	0·7	1·6	3·3
TiO_2	1·8	—	0·8	0·6	0·7	0·8
ppm						
Ni	120	25	28	15	18	3
Co	50	40	28	20	24	13
Cr	130	40	85	44	56	3
V	200	250	200	195	175	160
Sc	40	40	31	31	30	20
Ni/Co	2·4	0·63	1·0	0·75	0·75	0·23
V/Ni	1·7	10·0	8·0	13	9·7	53

of these calc-alkaline andesites (from Taylor, 1968b) with data for high-Al basalts and for alkali and tholeiitic basalts. With the exception of Cr in andesites, frequency distribution of the ferromagnesian trace elements is lognormal (Figs. 1 and 2). The frequency diagrams are plotted on logarithmic co-ordinates to cover the wide ranges in composition and to display lower concentration levels adequately.

The data in Table 1 and these diagrams illustrate the low abundance of nickel in andesites (18 ppm average) and high-Al basalts (25 ppm average) in comparison to alkali and tholeiitic basalts which average 120 ppm (Fig. 1). In contrast, the concentrations of vanadium show only minor differences in all these rock types (Fig. 2). Both cobalt and scandium are slightly lower in andesites compared to basalts. A wider scatter exists for the chromium data with both andesites and high-Al basalts showing similar frequency distributions, with lower values than those observed for alkali and tholeiitic basalts. Greater contrasts are shown by the element ratios. Ni/Co ratios (Table 1) are less than one in andesites and high-Al basalts, but exceed two in alkali + tholeiitic basalts. V/Ni ratios show the reverse relationship being greater than 8 in high-Al basalt and andesites, but much lower (about 2) in alkali and tholeiitic basalts.

Relation of Andesites to High-Al Basalts

Similarities in the Ni/Co and V/Ni ratios and in the absolute abundances of the ferromagnesian elements in calc-alkaline andesites and high-Al basalts are noteworthy. These data make it difficult to derive andesites from high-Al basalts by fractional crystallisation processes that involve removal of olivine, orthopyroxene or

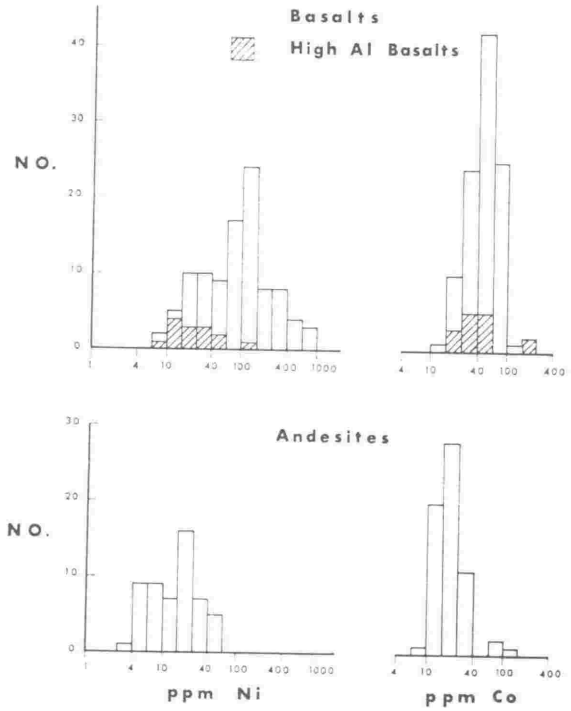

Fig. 1. Frequency diagram of the distribution of nickel and cobalt in andesites, basalts and high-Al basalts. Note that the nickel content of andesites is much lower than that of average basalts but is similar to the high-Al basalt values.

Sources of data for Figs. 1 and 2.

Data for Ni, Co and Cr in basalts are from the compilation by TUREKIAN and CARR (1960). Values for V and Sc are from NESTERENKO *et al.* (1964), NOCKOLDS and ALLEN (1954, 1956) and TUREKIAN (1963). Data for these elements in andesites are from TAYLOR and WHITE (1966 and unpublished data), TAYLOR and BLAKE (1968) MARKHININ and SAPOZHNIKOVA (1962), COATS (1952, 1959), COATS *et al.* (1961), DREWES *et al.* (1961), LEWIS *et al.* (1960), NELSON (1959), POWERS *et al.* (1960), NOCKOLDS and ALLEN (1953).

clinopyroxene. This is because these minerals contain abundant octahedral lattice sites which Ni especially will preferentially enter thereby leading to depletion of Ni in the derivative andesitic magma.

FRACTIONAL CRYSTALLISATION INVOLVING REMOVAL OF MAGNETITE

OSBORN (1962) proposed that early crystallisation and removal of magnetite would lead to the observed lack of enrichment of iron in the calc-alkaline association, if these are a sequence of rocks derived from a basic parent by fractionation. Spinel structures readily accommodate the ferromagnesian trace elements as is shown by the occurrence of chromite ($Fe^{2+}Cr_2O_4$), trevorite ($NiFe^{3+}{}_2O_4$), jacobsite ($MnFe^{3+}{}_2O_4$) as well as magnetite ($Fe^{2+}Fe^{3+}{}_2O_4$). Vanadium is stabilised in octahedral sites by ligand fields, and is abundant in magnetites.

Magnetites from andesites and dacites from Mt. Edgecumbe, New Zealand,

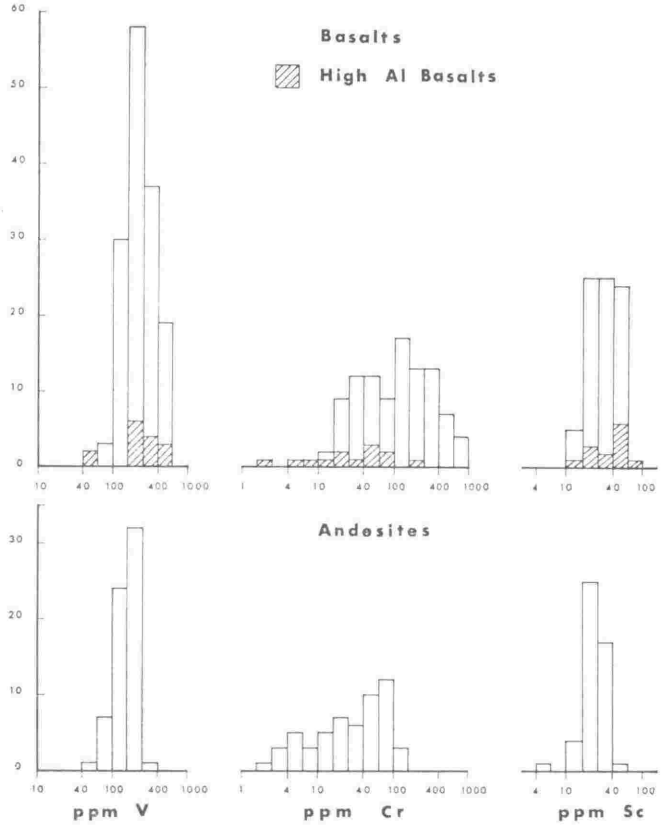

Fig. 2. Frequency diagram of the distribution of vanadium, chromium and scandium in basalts, high-Al basalts and andesites. Note the similar distribution of Cr in high-Al basalt and andesite. The V and Sc contents of andesites are similar to the levels in basaltic rocks.

contain from 0·45 to 0·80% vanadium and average 0·60 per cent (Duncan and Taylor, 1968). Crystallisation and removal of magnetites of this vanadium content will strongly deplete the magma in vanadium. Removal of one per cent of magnetite will result in an average decrease of 60 ppm V in the magma; similarly removal of 2% magnetite will cause a decrease of 120 ppm. However the similarity of vanadium contents in andesites and basalts severely restricts the amount of magnetite which could be removed from parental basaltic magma to produce andesite and this restricts the maximum amount of magnetite which could separate from the basalt to less than 2 per cent. Because the removal of this amount of magnetite from the basaltic magma would reduce total iron by less than 2%, it therefore cannot account for the observed differences in iron of 4% between high-Al basalts and andesites.

Mixing Hypotheses

Simple bulk mixing of basic and acid material could produce the major element composition of andesites, except for potassium, but not the trace element compositions (Taylor, 1968a, b). Low Ni and high V contents present special problems for

such mixing. If a high-Al basalt was one parent, the similarities in Ni and V contents between andesites and this class of basalt do not allow much dilution by the acid component, which would typically contain very low concentrations (<10 ppm) of both these elements (TAYLOR, 1968a). If either alkali or tholeiitic basalts were the basic parents, the low Ni values in andesites would require >70% granitic material in the mixture. However, vanadium contents of andesites are so similar to those of basalts (Table 1 and Fig. 2) that no large-scale dilution with acid material could have occurred.

INCORPORATION OF SEA FLOOR SEDIMENTS

It is possible that movement of the oceanic crust down the dipping seismic zone beneath island arcs followed by partial melting could produce calc-alkaline rocks.

The average amounts of ferromagnesian trace elements of the deep sea clays, which might contribute at least some material to such a process are:

Ni	225 ppm	
Co	74 ppm	
Cr	90 ppm	(TUREKIAN and WEDEPOHL, 1961)
V	120 ppm	
Sc	19 ppm	

Addition of this material would add substantial amounts of nickel with a low V/Ni ratio of about 0·5. However the V/Ni ratio in andesites (about 10) differs from that in deep sea clays by a factor of 20 so that mechanisms to equalise these ratios are necessary. If andesites are produced by this mechanism, it is clear that the involvement of deep sea clays is negligible.

DERIVATION OF CALC-ALKALINE ROCKS FROM ECLOGITES

GREEN and RINGWOOD (1966) have shown that, at 25–40 kbar and in the absence of water, andesite is the low melting fraction of quartz eclogite with a composition "similar to basalts found associated with the calc-alkaline series" (p. 307). They conclude that fractional crystallization of basalt or partial melting of quartz eclogite at depths of 100–140 km could produce andesite, leaving behind a residuum of about 30% clinopyroxene and 20% garnet. Under wet conditions the same process would produce a dacite and a residuum of 33% clinopyroxene and 26% garnet. They cite the occasional presence of almandine-pyrope garnets in the intermediate and acid calc-alkaline rocks in support of the hypothesis of deep seated origin (GREEN and RINGWOOD, 1968b).

Ferromagnesian trace elements in garnets and clinopyroxenes of high temperature eclogites and in garnets of calc-alkaline rocks have been determined in order to test these hypotheses.

Analytical methods for garnet and clinopyroxene

A Jarrell Ash (Model 71-100) grating spectrograph with a 15,000 lines/in. grating in the 1st order, giving a dispersion of 5·2 Å/mm, was used. The arc was focussed on the slit using a 450 mm cylindrical quartz lens. The slit width was 10 μ. A seven step sector (2:1) ratio was used. Two Ilford N-30 plates covered the wavelength range 2450–4950 Å.

One part of sample was mixed with 2 parts of National Carbon Co SP–2 graphite powder which contained 0·04% $(NH_3)_4Pd(NO_3)_2$ (Johnson Matthey Specpure). Using a 10 A d.c. arc

and anode excitation the samples were arced to completion. Anodes were National Carbon Co. L4261 (SPK) preformed electrodes and cathodes were National Carbon Co. L3863 1/8 in. carbon rods.

The following lines were read using a Jarrell Ash Microphotometer (Model 23-100) with a slit width of 7 μ and drive rate of 0·5 mm/min: Pd 3421 Internal standard, Ni 3414 and 3391, Co 3453, Cr 4254 and 4344, V 4379 and Sc 4246. A computer programme was used to obtain relative line intensities. Thanks are due to M. Cook, A.N.U. Psychology Dept., for help with the programme. Working curves were constructed using the values for the international inter-laboratory standards given in Table 2 and the accuracy of the results is dependent on these values. The precision of the determinations expressed as relative deviation is $\pm 5\%$.

Table 2. Working curves were constructed using the following values for the International Geochemical Standards. (All data in ppm)

	G-1	W-1	S-1	G-2	GSP-1	AGV-1	PCC-1	DTS-1	BCR-1
Ni	1·2	75	—	3	8	16	2400	2400	11
Co	2·5	50	19	4·9	6·2	14	105	132	44
Cr	22	120	55	8·2	10	11	2800	4200	13
V	14	240	—	42	50	113	31	—	360
Sc	2·8	34	15	3·4	5·9	12	9	3	32

Cobalt and nickel. Nickel is low in the garnets of eclogites compared with the pyroxenes (Table 3). This nickel distribution relationship was also found by Turekian (1963) in coexisting garnet and pyroxene from eclogites.

The Ni/Co ratio is low in the garnets (0·25–2·3) and high in the co-existing pyroxenes (6·8–22·2). The distribution coefficient (calculated according to Banno and Matsui, 1965) for the exchange reaction

$$Ni_{px} + Co_{ga} \rightleftharpoons Co_{px} + Ni_{ga}$$

is $K'_{Tpx} = \ln (Ni/Co)ga - \ln (Ni/Co)px$. The high temperature eclogite data, plotted on a logarithmic scale (Fig. 3) to produce a straight line with a 45° slope, give a K′ value of 0.11: A Norwegian orthopyroxene-bearing eclogite has a low distribution coefficient consistent with a low temperature origin.

Garnets from some calc-alkaline rocks (Table 4) (see also Green and Ringwood, 1968b) are lower in nickel than eclogite garnets. Cobalt is slightly lower. Nickel, cobalt and the Ni/Co ratio (0·54) in the Lipari garnet are comparable with those in andesites.

Vanadium and nickel. Like nickel, vanadium also enters pyroxene in preference to garnet (Table 3) so that the partition of V and Ni between co-existing pyroxenes and garnets from eclogites is close to unity (K′ = 0·80: Fig. 3). V/Ni ratios are much lower both in garnets (<3·6) and pyroxenes (<1) compared with calc-alkaline rocks (>8) but resemble those in alkali and tholeiitic basalts (~2). The V/Ni ratios in calc-alkaline garnets, although difficult to evaluate (for all except the Lipari sample) because of low nickel content, are comparable with the rocks in which they occur.

Origin of Calc-Alkaline Garnets

The major and trace element chemistry of the garnets from the calc-alkaline rocks (Table 4) is distinctly different from that of the eclogitic garnets. In particular, Ni and Cr are very much lower in the calc-alkaline garnets. They also have generally lower Ni/Co and higher V/Ni ratios than the garnets from eclogites. It is clear that

Table 3. Data for co-existing pyroxenes and garnets from eclogites. (All data in ppm.) Analyst M. Kaye

	R396		R392		RV4		E4*		E16*		T263		
	Ga	Cpx	Ga	Cpx	Ga	Cpx	Ga	Cpx	Ga	Cpx	Ga	Cpx	Opx
Ni	75	400	47	210	54	280	30	300	140	1000	24	790	1800
Co	72	38	56	31	67	48	13	30	65	45	71	43	120
Cr	1600	2500	1000	1300	530	740	750	1200	820	1300	1400	2000	160
V	55	200	59	200	190	370	50	450	80	450	70	420	34
Sc	58	17	60	19	51	22	40	20	75	10·0	33	21	1
Ni/Co	1·04	10	0·8	6·8	0·80	5·8	2·3	10·0	2·2	22·2	0·25	18·4	15
V/Ni	0·73	0·5	1·3	0·9	3·6	1·3	1·7	1·5	0·57	0·45	3·9	0·53	0·02
Garnet components and properties													
Gr + And	18·9		17·3		8·3		18·1		13·6		8·1		
Sp	0·3		0·5		0·7		0·7		0·5		0·6		
Py	62·3		63·8		62·2		44·6		57·0		51·6		
Al	18·4		18·4		29·2		36·6		28·5		39·6		
Refractive index ±0·002	1·738		1·739		1·752		1·761		1·753		1·751		

Sample localities

R396: Fassaite eclogite with small amounts of plagioclase. Inclusion in Delegate breccia pipe, N.S.W. Australia (Lovering and White, 1969).

R392: Fassaite eclogite. Inclusion in Delegate breccia pipe, N.S.W. Australia (Lovering and White, 1969).

RV4: From eclogite inclusion, Roberts Victor Mine, Orange Free State, South Africa. (Coll. S. R. Taylor).

E4, E16: Eclogite inclusion, kimberlite pipe, Basutoland (Nixon *et al.*, 1963).

T263: from eclogite, Almeklovsaeter, Almeklovdalen, Sunnmore, Norway (provided by H. Neumann).

* Analyst: J. M. Rooke.

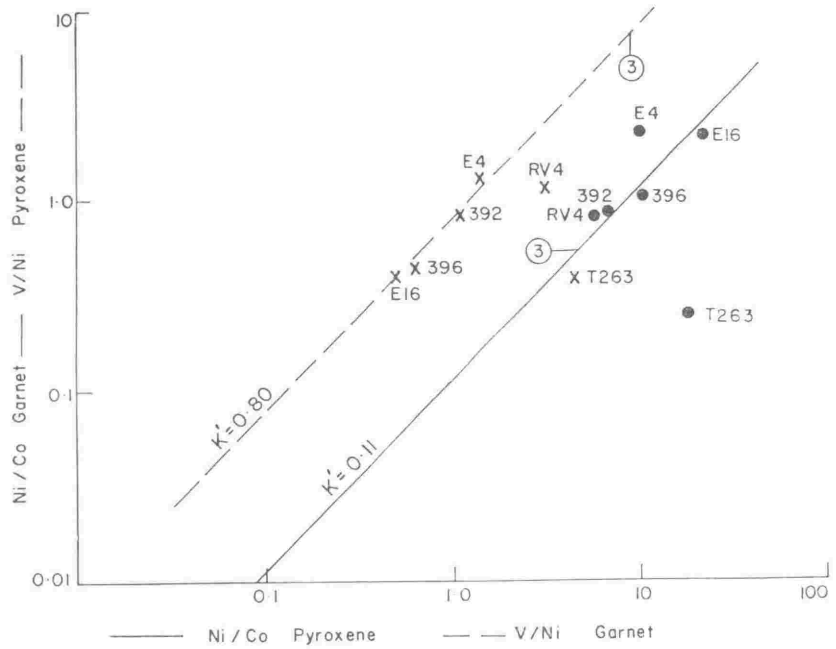

Fig. 3. The distribution of V and Ni (crosses) and Ni and Co (circles) between co-existing garnet and clinopyroxene from eclogites. Data are from Table 2. K′ for V/Ni (dashed line) and for Ni/Co (full line) are the lines of best fit with a slope of 45°, for four of the high temperature eclogites. The Norwegian eclogite (T-263) contains orthopyroxene, and is probably a low-temperature variety; K′ is significantly lower for each element pair.

the garnets in these calc-alkaline rocks are not residual garnets from an eclogitic parent, but their compositions are consistent with the chemistry of the enclosing calc-alkaline rock. These trace element data support the view of Green and Ringwood (1968b) that the garnets in calc-alkaline rocks have crystallised from the calc-alkaline magma.

Partial Melting of Eclogite

Because garnet is the liquidus phase of andesite at pressures >23 kbar (Green and Ringwood, 1968a), partial melting in which the residual phases do not equilibrate with the melt would lead to a high Ni/Co ratio in the magma, since pyroxene rich in nickel will melt first.

If the andesite or dacite melt comes to equilibrium with the residual garnet and pyroxene, nickel, vanadium and chromium will be partitioned between residual phases and melt and the distribution of these elements should strongly favour the residual phases for crystal-chemical reasons. This could account for the low nickel content of andesites, but not for the high vanadium.

It is clearly very difficult to derive andesitic liquids with low Ni/Co ratios and high V/Ni ratios from melting of eclogitic garnets and pyroxenes. Any melt derived from an eclogite parent will have high Ni/Co and low V/Ni ratios if non-equilibrium melting took place, or low vanadium contents if equilibrium partial melting occurred.

Table 4. Trace element composition of garnets from some calc-alkaline rocks. (All data in ppm). Analyst: M. Kaye

	1	2	3	4
Ni	<3	<3	25	<2
Co	43	39	47	20
Cr	180	130	370	27
V	100	83	260	91
Sc	220	180	150	79
Ni/Co	<0·07	<0·08	0·54	<0·10
V/Ni	>33·3	>27·7	10·4	>45·5
Garnet components				
Grossular	2·8	3·0	3·2	5·5
Spessartine	2·7	2·3	2·9	0·95
Pyrope	22·4	17·2	17·7	12·1
Almandine	71·5	78·0	75·7	81·4
Refractive index	±0·002			
	1·801	1·802	1·796	1·805

Sample localities
1: Mt. Painter Porphyry (Dacite), Mt. Painter, A.C.T., Australia.
2: Mt. Painter Porphyry (Dacite), Coppins Crossing, A.C.T., Australia.
3: Garnet–cordierite andesite, Fuardo, Lipari, Tyrrhenian Sea, Italy. Krantz Specimen No. 225. (Maccarrone, 1963).
4: From Rhyolite, Rakaia Gorge, New Zealand (provided by D. Gregg, Canterbury Museum).

Multistage Processes for Origin of Calc-Alkaline Rocks

Ni, Co, Cr and V preferentially enter octahedral co-ordination sites because of ligand field effects (Burns and Fyfe, 1964). There is an abundance of such sites in minerals (notably hypersthene and clinopyroxene) crystallising from andesite magma, and high concentrations of the ferromagnesian trace elements would be expected in them, if these elements are present. Removal of olivine would deplete the magma in Ni and Co, which are typically concentrated in the mineral, and enrich the residual melt in V, Sc and Cr, which enter olivine only in limited amounts, due to valency difficulties. Olivine andesites of accumulative origin, although observed (Clark, 1960) are rare and sporadic in occurrence, and cannot account for the rather uniform depletion of nickel in andesites. Accordingly we conclude that the low contents of Ni (<20 ppm), chromium, low Ni/Co ratios (<1) and high vanadium contents are primary features of andesite magma.

These values are very different from those predicted in primitive upper mantle material or in melts derived therefrom. Most of the nickel and cobalt in the upper mantle will be contained in olivines, orthopyroxenes and clinopyroxenes. Based on the nickel content and Ni/Co ratios of peridotites, and using the pyrolite model of Ringwood (1962), values of the order of 1000–2000 ppm Ni and 100–200 ppm Co

with Ni/Co ratios about 10 may be anticipated. Alkali and tholeiitic basalts, derived from this material average about 120 ppm Ni and 50 ppm Co (Ni/Co $\sim$ 2·4). If we take these values as representative of partition occurring between melt and residue, then it is difficult to produce melts with nickel contents of 20 ppm, and occasionally as low as 1–2 ppm.

The effect of high water content on the distribution ratio is unknown, but it would need to change the distribution factor for Ni between melt and residual pyrolite by 1–2 orders of magnitude. The chromium content provides another example. The distinction between the behaviour of Cr and V, both trivalent cations. is consistent with the presence of Cr in a separate minor phase (e.g. chromite) in the mantle, where it is probably in the range 1000–5000 ppm. It is difficult to produce melts with Cr contents of a few parts per million in a single stage of partial melting from such material.

Accordingly we postulate that the material from which andesites were derived by partial melting was already depleted in nickel and chromium relative to concentrations expected in the normal mantle compositions. Thus the ferromagnesian trace element data are consistent with derivation by at least two stages of partial melting from the mantle as suggested by Taylor and White (1965, 1966), Green and Ringwood (1966, 1968a) and Taylor (1968a, b). Similar arguments apply to the genesis of the high-Al basalts associated with the calc-alkaline andesites.

Summary and Conclusions

Calc-alkaline andesites of the circum-Pacific type typically contain low amounts of nickel ($<$30 ppm), low Ni/Co ratios ($<$1), high V contents ($>$150 ppm) high V/Ni ratios ($>$8), and low but variable Cr contents. These elements show similar absolute and relative abundances in high-Al basalts. Alkali and tholeiitic basalts show similar V and Sc contents to andesites but contain much higher Ni, Co and Cr contents. (Ni/Co $>$ 2, V/Ni $<$ 2).

The significance of these observations for theories of the genesis of andesites are:

(a) Similar nickel contents of high-Al basalt and andesite preclude derivation of the latter from the former by fractional crystallisation.

(b) Origin of calc-alkaline rocks from basaltic magmas by fractionation involving removal of magnetite will deplete the derived magmas in vanadium. This origin is precluded by the similarity in vanadium contents of basalts and andesites.

(c) Addition of alkali or tholeiitic basalt to granitic mineral would provide too much nickel and too little vanadium. Mixing of high-Al basalt and acid material does not provide enough Ni.

(d) Deep-sea clays have V/Ni ratios of 0·5 and Ni/Co ratios of 3. Only very limited addition of such material can be tolerated without affecting the Ni/Co and V/Ni ratios of andesites.

(e) Dry melting of eclogite at 25–40 kbar will not produce a melt with the appropriate Ni/Co and V/Ni ratios. Garnets in calc-alkaline rocks have a distinctly different trace element composition from those in eclogites.

(f) The Ni and Cr contents and Ni/Co ratios are too low to be derived in a single stage from pyrolite, but are consistent with two stages of partial melting from the upper mantle.

References

Banno S. and Matsui Y. (1965) Eclogite types and partition of Mg, Fe, and Mn between clinopyroxene and garnet. *Proc. Japan Acad.* **41,** 716–721.

Burns R. and Fyfe W. S. (1964) Site preference energy and selective uptake of transition-metal ions from a magma. *Science* **144,** 1001–1003.

Clark R. H. (1960) Appendix in Gregg D. R. The geology of the Tongariro subdivision, *N.Z. Geol. Surv. Bull.* 40.

Coats R. R. (1952) Magmatic differentiation in Tertiary and Quaternary volcanic rocks from Adak and Kanaga Islands, Aleutian Islands, Alaska. *Bull. Geol. Soc. Amer.* **63,** 485–514.

Coats R. R. (1959) Geologic reconnaissance of Semisopochnoi Island, Western Aleutian Islands, Alaska. *U.S. Geol. Surv. Bull.* **1028-0,** 477–517.

Coats R. R., Nelson W. H., Lewis R. Q. and Powers H. A. (1961) Geologic reconnaissance of Kiska Island, Aleutian Islands, Alaska. *U.S. Geol. Surv. Bull.* **1028-R,** 563–581.

Drewes H., Frazer G. D., Snyder G. L. and Barnett H. F. (1961) Geology of Unalaska Island and adjacent insular shelf, Aleutian Islands, Alaska. *U.S. Geol. Surv. Bull.* **1028-S,** 583–676.

Duncan A. R. and Taylor S. R. (1968) Trace element analyses of magnetites from andesitic and dacitic lavas from Bay of Plenty, New Zealand. *Contrib. Mineral Petrol.* **20,** 30–33.

Green T. H. and Ringwood A. E. (1966) Origin of the calc-alkaline igneous rock suite. *Earth Planet. Sci. Lett.* **1,** 307–316.

Green T. H. and Ringwood A. E. (1968a) Genesis of the calc-alkaline igneous rock suite. *Contrib. Mineral Petrol* **18,** 105–162.

Green, T. H. and Ringwood A. E. (1968b) Origin of garnet phenocrysts in calc-alkaline rocks *Contrib. Mineral Petrol.* **18,** 163–174.

Lewis R. Q., Nelson W. H. and Powers H. A. (1960) Geology of Rat Island, Aleutian Islands, Alaska. *U.S. Geol. Surv. Bull.* **1028-Q,** 555–562.

Lovering J. F. and White A. J. R. (1969) Granulitic and eclogitic inclusions from basic pipes at Delegate, Australia. *Contrib. Mineral Petrol.* in press.

Maccarrone E. (1963) Aspetti geochimico-petrografico di alcuni esemplari di andesite granato-cordieritifera dell'Isola di Lipari. *Period. Min.* **32,** 277–302.

Markhinin E. K. and Sapozhnikova A. M. (1962) Content of Ni, Co, Cr, V and Cu in volcanic rocks of Kamchatka and the Kurile Islands. *Geochem.* 427–432 (English translation).

Nelson W. H. (1959) Geology of Segula, Davidof and Khvostof Islands, Alaska. *U.S. Geol. Surv. Bull.* **1028-K,** 257–266.

Nesterenko G. V., Avilova N. S. and Smirnova N. P. (1964) Rare elements in the traps of the Siberian platform. *Geochem. Int.* **I,** 970–976.

Nixon P. H., Knorring O. von and Rooke J. M. (1963) Kimberlites from and associated inclusions of Basutoland: a mineralogical and chemical study. *Amer. Mineral.* **48,** 1090–1132.

Nockolds S. R. and Allen R. (1953) The geochemistry of some igneous rock series. *Geochim. Cosmochim. Acta* **4,** 105–142.

Nockolds S. R. and Allen R. (1954) The geochemistry of some igneous rock series: Part II. *Geochim Cosmochim. Acta* **5,** 245–285.

Nockolds S. R. and Allen R. (1956) The geochemistry of some igneous rock series–III. *Geochim. Cosmochim. Acta* **9,** 34–77.

Osborn E. F. (1962) Reaction series for sub-alkaline igneous rocks based on different oxygen pressure conditions. *Amer. Mineral.* **47,** 211–226.

Powers H. A., Coats R. R. and Nelson W. H. (1960) Geology and submarine physiography of Amchitka Island, Alaska. *U.S. Geol. Surv. Bull.* **1028-P,** 521–551.

Ringwood A. E. (1962) A model for the upper mantle. *J. Geophys. Res.* **67,** 857–866.

Taylor S. R. (1968a) Geochemistry of andesites. *Proc. IAGC Symposium on Origin and Distribution of the Elements.* Section V. Pergamon.

Taylor S. R. (1968b) Trace element chemistry of andesites and associated calc-alkaline rocks. *Proc. Symposium on Andesites,* Univ. Oregon. A.G.U. Monograph, in press.

Taylor S. R. and Blake D. H. (1968) Trace element chemistry of calc-alkaline rocks from Bougainville, Saipan and Fiji. In preparation.

Taylor S. R. and White A. J. R. (1965) Geochemistry of andesites and the growth of continents. *Nature* **208,** 271–273.

Taylor S. R. and White A. J. R. (1966) Trace element abundances in andesites. *Bull. Volcanol.* **29,** 177–194.

Turekian K. K. (1963) The chromium and nickel distribution in basaltic rocks and eclogites. *Geochim. Cosmochim. Acta* **27,** 835–846.

Turekian K. K. and Carr M. H. (1960) The geochemistries of chromium, cobalt and nickel. *Int. Geol. Congress 21st Session (Norden)* **1,** 14–26.

Turekian K. K. and Wedepohl K. H. (1961) Distribution of the elements in some major units of the Earth's crust. *Bull. Geol. Soc. Amer.* **72,** 175–192.

PART 3

XENOLITH PETROGRAPHY AND GEOCHEMISTRY

XENOLITH PETROGRAPHY

Xenoliths large enough to be seen in hand specimen are quite common in both Edgecumbe and Whale Island rocks, but are rare in White Island and Manawahe rocks. Such large xenoliths (some are up to 4 kg in mass) probably occur with equal frequency in both Edgecumbe and Whale Island rocks, but are more frequently found at Whale Island since they are particularly conspicuous in rounded and abraded beach boulders.

The large xenoliths are predominantly of two types, one being porphyritic microdiorite and the other altered andesite and dacite. Porphyritic microdiorites, here termed Group I xenoliths, contain typical andesitic and dacitic phenocrystic minerals, of an assemblage closely related to the host lava. Thus pyroxene-plagioclase microdiorites are found in lavas whose phenocrystic minerals are pyroxene and plagioclase, and those microdiorites containing hornblende and/or biotite are usually found in a host lava with the same phenocrystic mineralogy. Modal analyses of 4 Group I xenoliths are given in Table 34, and it can be seen that they are very similar to non-xenolithic samples (Tables 4, 7, 9, 10) except that they contain a lower groundmass content and a slightly higher pyroxene/plagioclase ratio. The discontinuous groundmass texture in Group I xenoliths is usually hyalopilitic, although patches of groundmass with pilotaxitic or intersertal texture are common in many such xenoliths. The crystalline portions of the xenolith groundmass often contain well-developed patches of cristobalite, but the overall cristobalite content of the xenolithic groundmasses is lower than the critobalite content of

TABLE 34

MODAL ANALYSES OF XENOLITHS

		GROUP I				GROUP II
	SAMPLE NO.	11209	11223	11228	11229	11232
Groundmass		34.0	26.3	35.0	41.3	90.1
Plagioclase		40.6	49.1	39.6	37.5	8.4
Orthopyroxene		7.0	6.0	7.5	5.1	0.7
Clinopyroxene		7.7	11.9	14.6	9.6	0.4
Quartz		4.7	3.5	-	2.5	-
Hornblende		2.4	-	-	0.3	0.1
Opaques		3.6	3.2	3.3	3.7	0.3

non-xenolithic groundmasses. Plagioclase compositions in Group I xenoliths are similar to those of plagioclase in the host lavas, but pyroxene compositions in the xenoliths show slightly higher Mg/Fe ratios (see Appendix 1) than pyroxenes in the host lavas. Contacts between xenolith and host lava are usually sharp, and no reaction between the two is apparent; some large phenocrysts "bridge" the boundary. Group I xenoliths are thought to be cognate orthocumulates (cumulate terminology as defined by Wager, Brown & Wadsworth; 1960), the cumulus minerals representing all the phenocrystic minerals in the magma at the time of xenolith formation.

Fragments of andesite and dacite included as xenoliths in younger lavas are quite common and are here termed Group II xenoliths. In most cases the xenolithic fragments are altered to the extent that the groundmass is cloudy in appearance and the pyroxenes are partially opacitised. A particularly good example of Group II xenoliths is composite sample 11232, a collection of rounded xenoliths of dacite from the border zone of East Dome on Whale Island (modal analysis given in Table 34).

Apart from the large xenoliths, there are many small xenoliths and aggregates of minerals found in the Bay of Plenty volcanics. Most of the mineral aggregates, consisting of varying proportions of plagioclase, pyroxene and titanomagnetite, are clearly glomerophenocrysts. However, one particular mineral aggregate which consists largely of small equant plagioclase crystals with minor interstitial cristobalite and pyroxene (typical examples may be seen in samples 11211, 11326, 11212), may be of xenolithic origin.

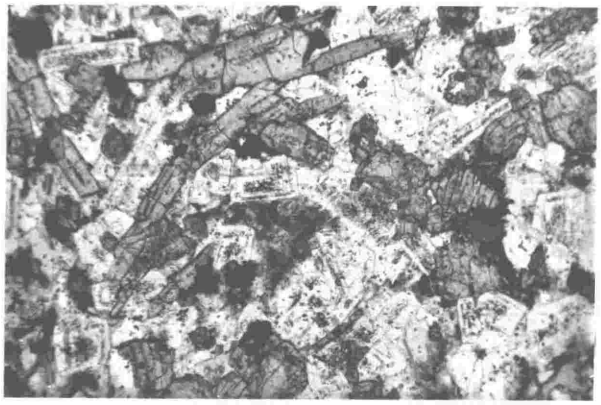

Plate 31. - Porphyritic microdiorite xenolith consisting mainly of pyroxene and plagioclase, with accessory opaques (sample 11390). Photomicrograph, x 20.

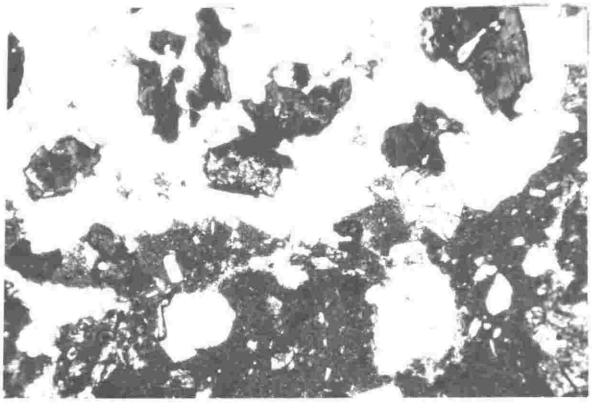

Plate 32. - Contact between microdiorite xenolith and host dacite (sample 11220), dacite (lower part of photograph) has a darker coloured groundmass. Photomicrograph, x 20.

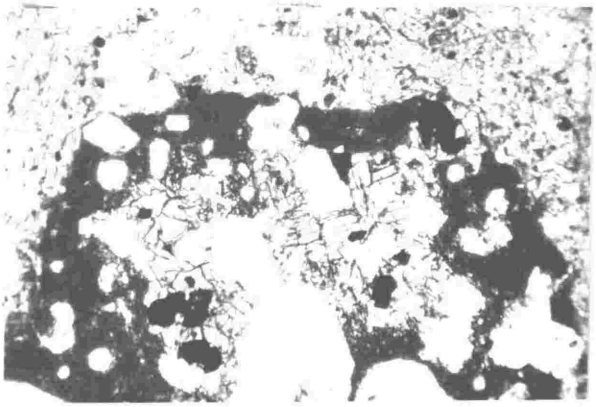

Plate 33. - Andesite xenolith (dark coloured) in a dacitic host rock (sample 11356). Photomicrograph, x 20.

The plagioclase in these aggregates is seldom twinned and is generally more anorthitic than plagioclase in the host lava, with core compositions up to An_{92}. The author considers these aggregates to be plagioclase adcumulates which crystallised at an early stage in the crystallisation history of the magma. However the lack of twinning in the plagioclase and the texture of the aggregates (hypidiomorphic-granular/granoblastic) is similar to that in some hornfelses, and it is possible that these plagioclase aggregates may be xenolithic.

A number of xenoliths of more exotic composition were found in Edgecumbe and Whale Island lavas, these are detailed below. In no instance was there any obvious reaction between the xenolith and the host lava, and xenolith/lava interfaces are generally sharp.

(A) Ignimbrite - one xenolith, thought to be of Matahina ignimbrite found in a lava from Main Dome, Edgecumbe.

(B) Cordierite-Sillimanite Rock - presumably a thermally metamorphosed argillaceous sediment, found in sample 11225 from Central Cone, Whale Island.

(C) Siliceous hornfels - mainly quartz crystals showing sutured contacts, also contains about 10% plagioclase and pyroxene, together with minor sphene. Found in sample 11391, a beach boulder from the west coast of Whale Island.

(D) Re-crystallised siliceous siltstone - composed predominantly of fine siliceous material which has been extensively re-crystallised into patches of quartz with sutured contacts. Found in sample 11392 from the west coast of Whale Island.

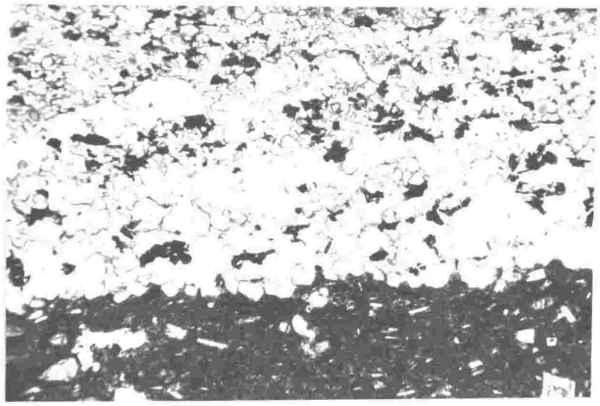

Plate 34. - Siliceous hornfels xenolith (top) in contact with host dacite (bottom). Sample 11391. Photomicrograph, x 80.

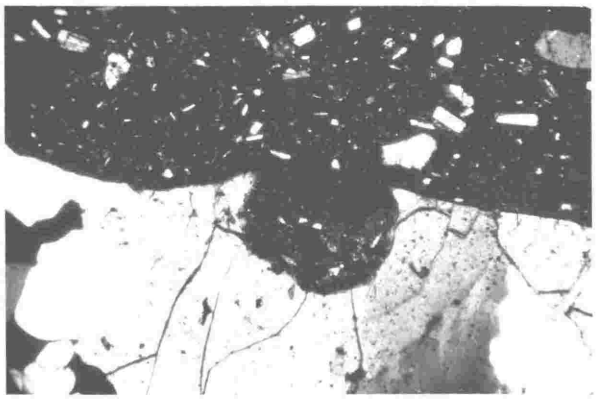

Plate 35. - Resorption at contact between quartzite xenolith (bottom) and host dacite (sample 11393), crossed polarisers. Photomicrograph, x 30.

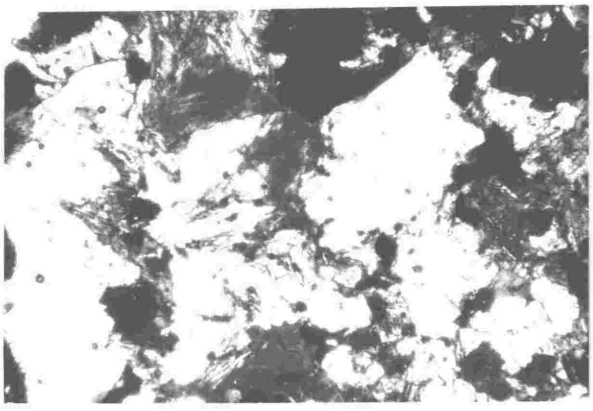

Plate 36. - Sillimanite-cordierite xenolith in sample 11225, crossed polarisers. Photomicrograph, x 25.

(E) Quartzite - a very pure quartzite found in sample 11393, a beach boulder from the west coast of Whale Island.

(F) Anorthosite - consists predominantly of calcic plagioclase with minor amounts of a dark green spinel, rutile and kyanite, and is probably of metamorphic origin. Found in sample 11391, a beach boulder from the west coast of Whale Island.

XENOLITH GEOCHEMISTRY

Five xenoliths were analysed, four from Whale Island and one from Edgecumbe, and their major and trace element chemistry, together with the average analysis and standard deviation of Edgecumbe and Whale Island non-xenolithic samples, is given in Tables 35 and 36. Group I xenoliths are subdivided on the basis of their relative chemistry into types IA and IB of which type IA is the more basic.

Type IA xenoliths have major element compositions typical of many circum-pacific andesites, and are very similar in composition to the labradorite-pyroxene andesites of TNP (Clark, 1960). They are, however, substantially more basic than the Bay of Plenty andesites and dacites in which they are found. The Type IA xenoliths have about 1% less SiO_2, and are slightly higher in CaO and MgO than the TNP andesites. In contrast they have higher SiO_2 and Al_2O_3, and much lower MgO than the TNP basic andesites which Clark (1960 b) considered to be of accumulative origin. Clark showed that the TNP basic andesites were enriched in olivine and pyroxene, relative to other phenocrystic minerals, a compositional difference which is reflected in their displacement towards the "M" apex on a von Wolff ternary diagram. The Bay of Plenty Type IA xenoliths plot much nearer to the field of the normal (non-accumulative) TNP andesites (Fig. 28). This supports the evidence from modal analyses that the Type IA xenoliths show only slight concentration of pyroxene relative to plagioclase when compared to non-xenolithic samples.

Type IB xenoliths (sample 11209) have very similar major element compositions to Type IA xenoliths, but are slightly lower in CaO and

TABLE 35

MAJOR ELEMENT ANALYSES OF XENOLITHIC SAMPLES

SAMPLE NO.	11223	11228	11229	11209	11232	NON-XENOLITHIC MEAN	S.D.
SiO_2	57.41	58.05	58.00	58.36	61.29	64.37	1.78
TiO_2	0.67	0.64	0.61	0.96	0.97	0.60	0.08
Al_2O_3	17.09	16.18	16.44	17.12	16.74	16.14	0.53
FeO	7.20	7.46	7.15	8.00	6.79	5.37	0.55
CaO	9.11	8.76	9.19	7.48	5.95	5.97	0.64
MgO	4.96	5.73	5.09	3.29	2.37	2.65	0.44
Na_2O	2.25	2.06	2.20	2.89	3.58	2.96	0.25
K_2O	1.22	1.05	1.21	1.74	2.16	1.85	0.19
P_2O_5	0.09	0.08	0.11	0.15	0.15	0.11	0.02

TABLE 36

TRACE ELEMENT ANALYSES OF XENOLITHS

SAMPLE NO.	11223	11228	11229	11209	11232	NON-XENOLITHIC MEAN	S.D.
LARGE CATIONS							
Rb^{+}	38.7	35.8	39.6	58.6	69.9	65.1	6.8
Ba^{2+}	540	455	500	475	575	643	136
$\%K^{+}$	1.00	0.85	0.99	1.43	1.65	1.55	0.17
Sr^{2+}	262	205	255	276	251	235	20.2
$\%Ca^{2+}$	6.38	6.09	6.48	5.28	3.92	4.09	0.50
$\%Na^{+}$	1.63	1.48	1.61	2.12	2.45	2.21	0.16
K/Rb	258	237	250	244	236	240	5.8
Ba/Rb	14.0	12.7	12.6	8.11	8.23	10.2	1.8
Ba/Sr	2.06	2.22	1.96	1.72	2.29	2.76	0.85
Rb/Sr	0.148	0.174	0.155	0.213	0.278	0.265	0.04
RARE EARTHS							
Y^{3+}	20.7	14.4	16.7	25.7	24.1	17.6	2.4
LARGE HIGHLY CHARGED CATIONS							
Th^{4+}	3.02	3.52	3.37	-	7.20	5.9	0.6
U^{4+}	0.79	0.70	0.78	-	1.57	1.4	0.2
Zr^{4+}	63	72	68	83	127	106	12.4
Th/U	3.85	5.03	4.32	-	4.59	4.14	0.27
FERROMAGNESIAN ELEMENTS							
Mn^{2+}	1154	1125	1084	1190	1022	906	67
$\%^{*}Fe^{2+}$	5.48	5.65	5.49	6.15	4.86	4.06	0.42
Cu^{2+}	20.8	24.9	28.9	15	11.8	16.3	4.5
Co^{2+}	18.8	21.3	23.6	14.6	11.9	12.2	2.9
Ni^{2+}	14.3	16.4	15.9	n.d.	n.d.	6.4	3.1
Li^{+}	15.5	21.2	15.9	25.7	17.1	22.2	4.4
$\%Mg^{2+}$	2.93	3.37	3.03	1.96	1.32	1.53	0.41
Ni/Co	0.76	0.77	0.67	-	-	0.53	0.11
Sc^{3+}	26.2	23.6	26.8	27.4	22.3	18.1	2.8
V^{3+}	193	160	193	192	182	132	21
$\%Ti^{4+}$	0.394	0.371	0.360	0.572	0.535	0.355	0.05
Cr^{3+}	71	64	71	3	1	29.6	19.8
Ga^{3+}	19.2	14.8	14.0	22.3	17.4	15.9	1.9
$\%Al^{3+}$	8.86	8.60	8.59	8.95	8.16	8.38	0.26
Cr/V	0.368	0.400	0.368	0.0156	0.0054	0.221	0.041
Al/Ga $\times 10^{-4}$	0.461	0.581	0.614	0.402	0.469	0.536	0.058
SMALL CATIONS							
$\%Si^{4+}$	26.28	26.40	26.75	26.95	26.38	29.65	0.89
B^{3+}	16.0	11.5	11.2	15.9	21.6	17.5	2.8

* Total Iron shown as Fe^{2+}.

All values are in p.p.m. unless otherwise indicated.

n.d. = not detected. - = not determined.

MgO, and higher in Na_2O and K_2O. Sample 11209 plots in the TNP andesite field on a von Wolff diagram (Fig. 28).

Type IA xenoliths are somewhat low in large cations and large highly charged cations relative to non-xenolithic samples of the Bay of Plenty volcanics, and are high in the ferromagnesian trace elements with the exception of Li. The element ratios Ba/Rb, Ni/Co and Cr/V are higher, and the ratios Ba/Sr and Rb/Sr are lower, in Type IA xenoliths than in non-xenolithic samples. These differences are consistent with the Type IA xenoliths being accumulates of the phenocrystic minerals in the Bay of Plenty andesite and dacite magmas. The xenoliths are therefore considered to be accumulates formed during the main stages of magma crystallisation, probably prior to any eruptions from the magma body in which they were formed. They do not show the compositional difference from non-xenolithic samples that would be expected if differential crystal settling had occurred to an appreciable extent.

As discussed above, the major element chemistry and modal analyses of Type IA and Type IB xenoliths are very similar, however substantial differences in trace element chemistry necessitates their division. The Type IB xenoliths are low in Ba and Zr, and have lower Ba/Sr ratios than non-xenolithic samples, but are not otherwise depleted in the other large cations and the other large highly-charged cations, and are slightly enriched in the element Y. They differ markedly from Type IA xenoliths in having lower Ni and Cr than non-xenolithic samples, and very low Cr/V ratios. Also, whereas Type IA xenoliths were lower in Li relative to non-xenolithic samples, Type IB xenoliths are slightly

higher. Thus although the modal mineralogy and major element analysis of a Type IB xenolith suggest an accumulative origin similar to that proposed for the Type IA xenoliths, the trace element data is incompatible with such an origin. The very low Ni (< 1 ppm) and Cr (3 ppm) in a rock containing 15% pyroxene strongly suggests that the pyroxene crystallised very late in the cooling history of the magma body in which the xenoliths formed. High Li, as shown in this xenolith type, is also considered to be a late-stage feature in the crystallisation history of ferromagnesian minerals (Taylor, 1965 b). It is therefore suggested that Type IB xenoliths may represent very late stage crystal accumulates from which the siliceous matrix material has been partially removed possibly by "filter-pressing", to give rise to the comparatively basic major element composition.

Trace element geochemistry is thus able to distinguish between the products of two different processes whose starting points are apparently the same, and whose final products are very similar in both petrography and major element chemistry.

Group II xenoliths contain 61% SiO_2, and have more acidic major element chemistry than Group I xenoliths. Except that they contain more Na_2O and K_2O, their major element chemistry is similar to andesites from Edgecumbe (11206, 11216). Their trace element chemistry, compared to Edgecumbe andesites, shows enrichment in the large cations and large highly-charged cations, and depletion in the ferromagnesian trace elements, particularly Ni (< 1 ppm) and Cr (1 ppm) with extremely low Cr/V ratios (0.0054). They are slightly higher in V. The chemistry of the analysed Group II xenoliths thus suggests that they have been

incorporated into the dacite in which they were found after their fractional crystallisation from a more basic magma. Their petrography is consistent with this hypothesis, and their texture is generally similar to eruptive andesites, suggesting that the magma from which the xenoliths formed crystallised at or near the surface.

PART 4

APPENDICES

APPENDIX 1.

Table 37, on the following pages, includes the complete set of electron microprobe analyses of pyroxenes made by the author, and Dr D.R. Wood.

Where analysis numbers are bracketed together, analyses are from different parts of the same crystal. Where two analyses only are bracketed together, the first analysis is of the core of the crystal, and the second analysis is of its rim. Where more than two analyses are bracketed together, they are from crystals showing bands of different composition, in which the position of the bands is not clearly related to crystal morphology.

The analyses in Table 37 were presented as ternary diagram plots in Figs. 18 and 19.

TABLE 37

ELECTRON MICROPROBE ANALYSES OF PYROXENES

SAMPLE NO. 11209, EDGECUMBE DIORITIC XENOLITH

ANALYSIS NO.	FeO (%)	MgO (%)	CaO (%)	ATOMIC PERCENT Fe	Mg	Ca	Mg/Fe RATIO
1	19.35	21.08	0.83	33.37	64.79	1.84	0.85
2	24.58	15.42	0.59	46.53	52.03	1.44	0.49
3	16.70	24.49	1.05	27.07	70.74	2.19	1.14
4	28.98	14.67	0.49	51.97	46.89	1.14	0.39
5	17.30	22.70	1.14	29.21	68.33	2.46	1.02
6	25.97	16.23	0.50	46.77	52.08	1.15	0.48
7	16.40	25.79	1.05	25.74	72.15	2.11	1.22
8	18.08	27.07	1.30	26.59	70.96	2.46	1.16
9	18.95	26.06	1.12	28.35	69.50	2.15	1.07
10	28.18	17.70	0.63	46.55	52.11	1.34	0.49
11	19.95	21.88	1.08	33.07	64.64	2.29	0.85
12	22.67	18.70	1.08	39.50	58.09	2.40	0.64
13	15.25	24.02	1.17	25.60	71.88	2.52	1.22
14	24.00	16.67	0.58	44.07	54.57	1.36	0.54

SAMPLE NO. 11221, WHALE ISLAND DACITE

ANALYSIS NO.	FeO (%)	MgO (%)	CaO (%)	ATOMIC PERCENT Fe	Mg	Ca	Mg/Fe RATIO
1	26.72	16.29	0.48	47.41	51.51	1.09	0.47
2	25.90	14.84	0.43	48.96	50.00	1.04	0.44
3	29.39	15.34	0.56	51.15	47.60	1.25	0.41
4	24.55	16.98	0.73	43.98	54.22	1.79	0.54
5	16.37	23.91	0.89	27.22	70.87	1.90	1.13
6	24.34	15.73	0.63	45.77	52.71	1.52	0.50
7	26.82	15.90	1.05	47.47	50.15	2.38	0.46
8	25.57	15.51	0.57	47.40	51.24	1.36	0.47
9	28.54	13.96	0.49	52.80	46.03	1.17	0.38
10	27.20	16.47	0.52	47.54	51.29	1.17	0.47
11	29.28	14.59	0.45	52.42	46.55	1.03	0.39
12	28.96	14.75	0.57	51.72	46.96	1.31	0.40
13	22.53	19.14	0.78	39.08	59.18	1.74	0.66
14	14.36	26.58	1.60	22.51	74.27	3.22	1.44
15	19.00	21.93	1.27	31.82	65.45	2.73	0.90
16	15.76	24.51	1.20	25.84	71.64	2.52	1.21
17	23.02	19.60	0.80	39.03	59.23	1.74	0.66
18	16.09	26.42	1.53	24.69	72.29	3.01	1.27
19	14.97	26.81	1.87	22.98	73.35	3.67	1.39
20	27.94	16.92	0.84	47.22	50.96	1.81	0.47

TABLE 37 (continued)

SAMPLE NO. 11223, WHALE ISLAND DIORITIC XENOLITH

ANALYSIS NO.	FeO (%)	MgO (%)	CaO (%)	ATOMIC PERCENT Fe	Mg	Ca	Mg/Fe RATIO
1	15.00	23.60	1.04	25.69	72.02	2.29	1.22
2	19.62	20.19	0.87	34.59	63.44	1.97	0.70
3	13.93	26.31	1.01	22.43	75.49	2.08	1.47
4	14.48	26.21	1.07	23.14	74.66	2.20	1.40
5	6.09	16.73	15.06	11.03	54.02	34.95	2.13
6	8.28	12.79	14.49	16.67	45.93	37.40	1.20
7	6.67	17.81	14.40	11.73	55.83	32.44	2.07
8	8.24	18.91	10.27	14.95	61.16	23.88	1.78
9	5.46	14.80	15.19	10.64	51.43	37.93	2.11
10	8.13	13.12	14.65	16.17	46.51	37.33	1.25

SAMPLE NO. 11224, WHALE ISLAND DACITE

ANALYSIS NO.	FeO (%)	MgO (%)	CaO (%)	ATOMIC PERCENT Fe	Mg	Ca	Mg/Fe RATIO
1	16.72	25.73	0.67	26.35	72.30	1.35	1.19
2	15.76	26.90	0.91	24.29	73.92	1.79	1.32
3	27.80	15.98	0.85	48.45	49.66	1.89	0.45
4	28.10	14.96	0.66	50.53	47.95	1.51	0.41
5	27.3	14.79	0.71	50.06	48.28	1.66	0.42
6	23.20	13.93	0.74	53.12	45.16	1.72	0.37
7	21.65	19.90	0.89	37.17	60.89	1.95	0.71
8	27.27	14.85	0.99	49.58	48.12	2.31	0.42
9	30.00	14.54	0.74	52.76	45.58	1.67	0.38
10	29.84	14.57	0.60	52.74	45.91	1.35	0.38
11	28.98	15.29	0.50	50.96	47.92	1.12	0.41
12	29.11	15.01	0.45	51.56	47.41	1.03	0.40
13	30.66	13.29	0.59	55.64	42.93	1.38	0.34
14	30.71	14.25	0.69	53.88	44.56	1.56	0.36
15	12.35	30.41	0.98	18.22	79.93	1.85	1.91
16	20.86	21.20	1.20	34.65	62.79	2.56	0.79
17	23.46	19.13	0.89	39.96	58.09	1.95	0.63
18	13.18	28.40	0.84	20.31	78.03	1.66	1.67
19	26.91	15.53	1.29	47.84	49.22	2.94	0.45
20	29.01	13.57	0.87	53.41	44.54	2.05	0.36
21	14.12	10.13	12.83	29.03	37.15	33.82	0.56
22	13.20	11.05	12.81	26.76	39.95	33.29	0.65
23	11.45	12.43	13.17	22.69	43.89	33.42	0.84
24	11.89	11.55	13.42	23.95	41.45	34.61	0.75

TABLE 37 (continued)

SAMPLE NO. 11252, EDGECUMBE ANDESITE

ANALYSIS NO.	FeO (%)	MgO (%)	CaO (%)	ATOMIC PERCENT Fe	Mg	Ca	Mg/Fe RATIO
1	19.13	22.20	1.06	31.85	65.89	2.26	0.90
2	19.33	22.32	0.95	32.03	65.94	2.03	0.90
3	19.55	22.69	0.98	31.92	66.03	2.05	0.90
4	18.90	21.09	1.03	32.69	65.02	2.29	0.87
5	19.32	22.87	1.10	31.41	66.29	2.30	0.92
6	19.14	21.33	0.97	32.77	65.10	2.13	0.86
7	16.92	26.53	1.05	25.80	72.13	2.06	1.22
8	18.35	25.60	1.03	28.10	69.88	2.02	1.08
9	17.72	28.06	1.14	25.61	72.28	2.11	1.23
10	17.82	23.21	1.01	29.46	68.39	2.15	1.01
11	18.35	20.85	1.01	32.31	65.41	2.27	0.88
12	18.61	20.38	1.13	33.01	64.42	2.57	0.85
13	21.01	19.13	1.11	37.17	60.32	2.52	0.71
14	19.84	20.80	1.17	33.96	63.48	2.56	0.81
15	16.66	23.96	0.96	27.49	70.48	2.03	1.12
16	20.37	20.91	0.97	34.59	63.30	2.11	0.80
17	19.99	20.93	1.17	34.00	63.44	2.56	0.81
18	20.33	20.46	1.08	34.94	62.68	2.38	0.78
19	8.17	15.17	13.07	15.72	52.05	32.23	1.44
20	7.69	14.79	13.42	15.00	51.45	33.55	1.49
21	9.30	15.63	15.51	16.31	48.84	34.85	1.30
22	6.07	15.82	13.77	11.70	54.33	33.97	2.02
23	10.16	13.97	13.15	19.57	47.98	32.45	1.07
24	9.35	13.29	13.09	18.78	47.56	33.66	1.10
25	9.19	14.76	13.50	17.41	49.83	32.76	1.25
26	9.07	14.29	13.67	17.42	48.92	33.65	1.22
27	10.32	14.82	14.20	18.79	48.08	33.12	1.11

Note: Analyses bracketed together are from the same crystal, where there are two analyses bracketed the first analysis is of the core of the crystal, and the second analysis is of its rim.

APPENDIX 2

ANALYTICAL TECHNIQUES

Analytical techniques have been discussed previously (p. 154), and additional details only are given here. Operating conditions and analytical lines for those elements determined by optical emission spectrography are given in Tables 38 and 39. Operating conditions for elements determined by x-ray fluorescence spectrography are given in Table 40.

The elements Zr and B were determined by optical emission spectrography, but not using the precise technique described by Ahrens and Taylor (1961). Accordingly a brief description of the techniques used for these two elements is given below.

Zirconium

Zr was determined spectrographically with the conditions as given in Table 38. However, when the working curves were plotted it was found that a straight line could be drawn through the standards used, with the exception of the basalts W-1 and BCR-1, which gave anomalously high results. These anomalous results are considered due to interference on the Zr 3438.23 analysis line by the Fe 3438.31 line. This interference has been previously noted in meteorite analyses at levels of more than 20% Fe, but has not previously been considered significant at the 10-15% Fe level.

To overcome this interference a correction technique was devised by Mrs M.J. Kaye, in which the Zr working curve is drawn through points for the granite standards G-1 and G-2 and values

read off. These values are then corrected by subtracting a Zr figure according to the Fe concentration of the sample. Zr correction values are obtained from a graph of Δ Zr against %Fe, which appears to be linear within the range of the standards used. A comparison of Zr analyses for the Bay of Plenty volcanics is given in Table 41, which contains the Zr concentrations read off the original working curve, the Zr concentrations obtained by the interference correction technique just described, and Zr concentrations determined by x-ray fluorescence analyses (which is probably the most accurate of the 3 determinations). It is clear that values obtained from the original working curve are high compared to the other two sets of values.

Boron

Boron was determined spectrographically with the conditions as given in Table 38. Quantitative determination of Boron by emission spectrography at normal concentration levels (5-50 ppm) in silicate rocks suffers from two problems, the estimation of background at the Boron line (2497.73 Å) and interference by SiO bands. A trace of optical density across the spectrographic plate of the standard granite G-1 ($\sim$1.5 ppm B), from 2496.25 Å to 2500 Å (Fig. 36), shows that the combination of background and SiO band interference on the B 2497.13 analysis line is equivalent to background plus SiO band intensity at 2498.17 Å, density at the latter wavelength was therefore treated as background for all B determinations, thus eliminating the effect of SiO band interference. A similar trace for a typical sample from the Bay of Plenty volcanics is also given in Fig. 36.

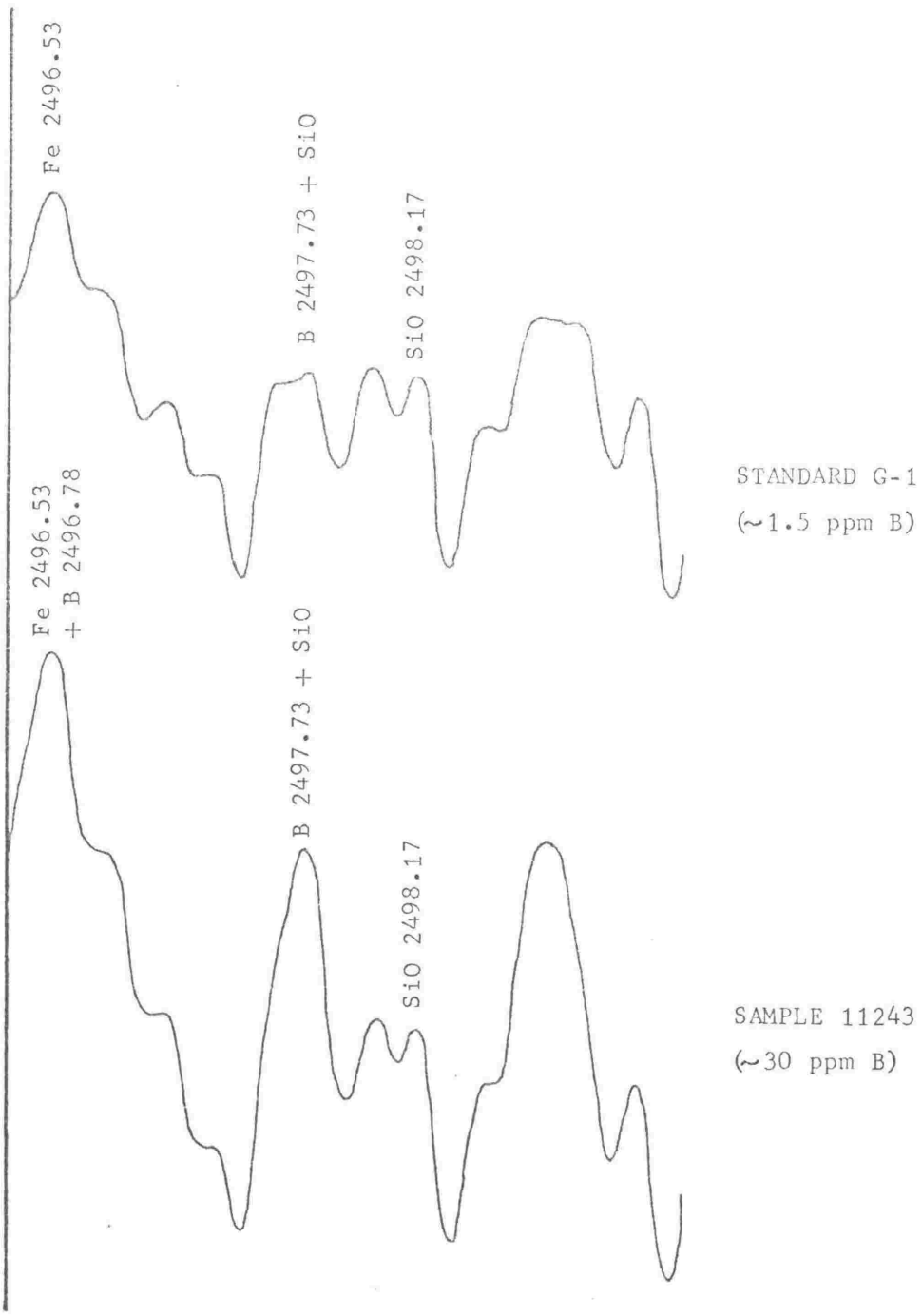

Fig. 36. - Optical density traces across a spectrographic plate using scanning densitometer (Jarrell-Ash 23-100). Wavelength range 2496.25 - 2500 Å. Background and SiO band intensity read at 2498.17 Å, and subtracted from B 2497.73 analysis line.

TABLE 38

ANALYSES USING JARRELL-ASH EBERT (71-100)

GRATING SPECTROGRAPH

Conditions

D.C. Arc, anode excitation

Optical System - 100 mm cylindrical Quartz lens, vertical image focused on slit.

Step sector rotating - 7 steps, logarithmic.

Slit Width = 10 μ

Slit Height = 10½ mm

Wave length range = 2450 - 4950 Å

Current = 10 amp.

Anode = L. 4261 SPK

Cathode = L. 113 SP ⅛" rod.

Plates = Ilford N30, emulsion 8133A +7

Developer = Kodak D19, 4 mins.

Fixer = Kodak rapid liquid fixer, 4 mins.

Analytical lines

Internal Standard = Pd 3421

B 2497.7, Mg 2783, Mn 2801, Fe 2929, Ga 2943, Ca 3158, Ti 3262, Cu 3274, Y 3327, Ni 3414, Zr 3438, Co 3453, Sc 4246, Cr 4254, La 4333, V 4379, Sr 4607, Ba 4934

TABLE 39

ANALYSES USING LARGE HILGER (E. 478) SPECTROGRAPH

Conditions

D.C. Arc, anode excitation

Optical System - glass optics in spectrograph, F. 958 glass lens focused on slit.

Step sector rotating - 7 steps, logarithmic but steps 6 and 7 were half masked to convert them to steps 7 and 8.

Slit Width = 10 μ

Slit Height = 11 mm

Current = 6 amp.

Anode = L. 4260 SPK

Cathode = L. 113 SP ⅛" rod.

Plates = Kodak 1-N, emulsion 1 NB3D6

Developer = Kodak D19, 4 mins.

Fixer = Kodak rapid liquid fixer, 4 mins.

Analytical lines

Internal Standard = Na 5682

Rb 7947, Li 8126, Cs 8521.

TABLE 40

OPERATING CONDITIONS FOR X-RAY FLUORESCENCE SPECTROGRAPH

ELEMENT ANALYSED	CRYSTAL	TUBE ANODE	kV	mA	COUNTING TIME (Secs)
Mg	ADP	Cr	55	36	200
Al	PE	Cr	55	36	100
Si	PE	Cr	55	36	100
P	GE	Cr	55	36	100
K	LiF	Cr	50	20	40
Ca	LiF	Cr	50	20	40
Ti	LiF	Cr	50	20	40
Mn	LiF	W	55	36	40
Fe	LiF	W	55	36	40
Rb	LiF	Mo	60	32	200(Pk)
					100(Bk)
Sr	LiF	Mo	60	32	200(Pk)
					100(Bk)
Zr	LiF	W	55	36	200(Pk)
					100(Bk)

TABLE 41

COMPARISON OF Zr CONCENTRATIONS DETERMINED BY DIFFERENT TECHNIQUES

	EMISSION SPECTROGRAPHIC		X.R.F.		EMISSION SPECTROGRAPHIC		X.R.F.
SAMPLE NO.	Uncorrected Zr (ppm)	Corrected Zr (ppm)	Zr (ppm)	SAMPLE NO.	Uncorrected Zr (ppm)	Corrected Zr (ppm)	Zr (ppm)
11205	196	148	129	11228	132	65	72
11206	158	98	92	11229	124	59	68
11207	204	167	139	11230	167	124	102
11208	147	95	93	11231	146	115	122
11209	157	82	83	11232	197	146	127
11210	151	107	104	11233	145	84	97
11211	150	105	104	11234	154	118	99
11212	144	104	105	11235	149	106	98
11213	180	133	124	11236	139	95	92
11214	143	96	108	11237	139	92	90
11215	159	109	109	11238	138	96	93
11216	168	110	110	11239	133	89	96
11217	147	103	110	11240	217	168	146
11218	147	99	95	11241	202	156	147
11219	145	105	104	11242	204	159	148
11220	147	105	109	11243	219	184	155
11221	137	98	108	11244	216	177	154
11222	158	100	107	11245	190	159	148
11223	146	73	63	11246	159	91	79
11224	179	141	128	11247	189	153	157
11225	140	98	107	11248	199	159	155
11226	146	92	98	11249	190	157	159
11227	148	101	95				

APPENDIX 3

COMPARISON OF ANALYSES FOR ELEMENTS THAT HAVE BEEN ANALYSED BY MORE THAN ONE METHOD

Table 17 contained the concentrations assumed for interlaboratory standard samples that were used to draw spectrographic working curves for elements usually determined by emission spectrography. Some elements whose analyses in Tables 20, 21, 22, 23, 24 and 25 were made by x-ray fluorescence or flame photometry, were also determined by emission spectrography and the concentrations for these elements in the interlaboratory standards are given in Table 42.

Analyses of the elements Rb, Sr, K, Ca, Zr, Ti, Mn, Fe and Mg in the Bay of Plenty volcanics by various analytical methods are given in Table 43, and the average differences between analytical methods are given in Table 44.

Average differences between concentrations determined by emission spectrography and concentrations determined by x-ray fluorescence are less than the estimated precision of the emission spectrographic results ($\pm$ 10%) .

Analyses of K by flame photometry and x-ray fluorescence differ by very small amounts only (average of + 0.5% relative), less than the estimated precision of the flame photometer results ($\pm$ 1%).

TABLE 42

ELEMENT CONCENTRATIONS ASSUMED FOR INTERLABORATORY GEOCHEMICAL STANDARDS

STANDARD SAMPLE	G-1	W-1	T-1	S-1	G-2	AGV-1	BCR-1	GSP-1
%Mg	0.247	3.99	(1.35)	2.45	0.46	0.90	2.20	0.57
%Fe	1.37	7.80	4.22	5.85	(2.05)	4.70	9.30	3.11
%Ca	0.99	7.84	3.72	7.22	(1.37)	3.50	4.98	1.45
Ti	1550	6400	3600	2900	2900	6300	13600	4000
Zr	210	90	180	2500	(282)	(219)	(185)	(495)
Sr	(280)	175	400	260	(470)	(530)	(320)	(240)

TABLE 42A

ELEMENT CONCENTRATIONS ASSUMED FOR INTERLABORATORY GEOCHEMICAL STANDARDS - ALKALI ELEMENTS

STANDARD SAMPLE	G-1	W-1	T-1	S-1	G-2	GR	AGV-1	BCR-1	GSP-1	KOS-1	EU-2
%K	4.52	0.53	1.02	2.24	3.70	3.74	2.37	1.40	4.57	2.96	3.97
%Na	2.46	1.54	3.26	2.49	3.04	2.82	3.15	2.44	2.08	1.68	2.39
Rb	220	22	(30)	147	(163)	(210)	(68)	(38)	(260)	-	-
Rb/Na	89.4	14.29	(9.42)	59.04	(51.8)	(76.2)	(21.2)	(15.6)	(124)		

Note: All figures in brackets are intercepts read off the working curves and were not used to construct the curves.

TABLE 43

COMPARISON OF ANALYSES BY DIFFERENT ANALYTICAL TECHNIQUES

SAMPLE NO.	Rb		%K			Sr		%Ca		Zr		%Ti		Mn		%Fe		%Mg	
	1.*	2.*	2.	3.*	4.*	1.	2.	1.	2.	1.	2.	1.	2.	1.	2.	1.	2.	1.	2.
11205	59	69.7	1.67	1.67	-	276	274	3.77	3.69	148	129	0.455	0.413	1020	937	4.99	4.29	1.45	1.07
11206	42	50.1	1.22	1.19	1.25	255	254	5.4	5.37	98	92	0.471	0.438	1030	1053	5.43	5.05	2.26	2.16
11207	78	76.8	1.90	1.91	-	236	262	3.12	3.41	167	139	0.393	0.408	845	932	4.19	4.04	1.11	1.01
11208	52	54.4	1.32	1.29	-	260	248	5.4	4.97	95	93	0.403	0.417	875	1020	4.80	4.94	1.95	3.04
11209	61	58.6	1.42	1.43	-	192	276	5.6	5.28	82	83	0.559	0.572	1360	1190	6.37	6.15	1.88	1.96
11210	66	70.0	1.72	1.67	-	211	223	3.71	3.73	107	104	0.358	0.342	843	867	4.29	3.87	1.62	1.44
11211	59	67.8	1.61	1.59	-	256	231	4.15	3.82	105	104	0.353	0.340	810	852	4.33	3.81	1.39	1.29
11212	70	71.7	1.72	1.69	-	237	220	3.72	3.60	104	105	0.343	0.341	787	829	3.99	3.70	1.30	1.33
11213	50	65.7	1.64	1.61	1.73	282	280	4.19	4.06	133	124	0.448	0.453	888	991	4.72	4.34	1.21	1.11
11214	68	61.8	1.48	1.47	-	232	247	4.37	4.36	96	108	0.416	0.407	818	937	4.39	4.43	1.64	1.53
11215	54	61.4	1.48	1.45	1.56	236	258	3.97	4.23	109	109	0.406	0.408	822	922	4.71	4.39	1.54	1.52
11216	55	58.3	1.39	1.37	1.41	265	256	5.1	4.67	110	110	0.456	0.441	1070	1045	5.39	4.86	2.59	1.77
11217	59	66.8	1.60	1.58	1.69	288	248	4.03	3.80	103	110	0.380	0.363	860	880	4.41	3.98	1.37	1.24
11218	54	67.6	-	1.67	1.71	242	220	4.48	-	99	95	0.336	-	947	-	4.47	-	1.47	-
11219	56	71.3	1.77	1.75	1.74	163	206	3.88	3.73	105	104	0.309	0.295	888	805	4.07	3.44	1.36	1.30
11220	61	70.3	1.74	1.75	-	220	207	3.69	3.56	105	107	0.308	0.295	825	844	3.87	3.68	1.52	1.43
11221	54	69.4	1.68	1.67	-	235	209	4.09	3.70	98	108	0.287	0.290	758	855	3.78	3.54	1.38	1.39
11222	54	59.3	1.35	1.34	-	268	220	4.60	4.23	100	107	0.334	0.336	840	914	4.60	4.17	2.07	1.89
11223	29	38.7	1.06	1.00	1.05	187	262	6.3	6.38	73	63	0.405	0.394	1240	1154	6.16	5.48	3.36	2.93
11224	82	77.2	1.78	1.76	-	245	211	3.07	3.11	141	128	0.362	0.345	802	798	3.90	3.58	1.01	1.02
11225	46	61.8	1.42	1.41	-	231	235	4.12	4.43	98	107	0.315	0.330	748	937	4.12	4.11	1.82	1.84
11226	50	62.3	1.42	1.42	-	321	236	4.84	4.45	92	98	0.377	0.346	1030	914	4.88	4.15	2.90	1.71
11227	43	61.1	1.52	1.49	1.52	245	235	4.55	4.31	101	95	0.369	0.338	913	883	4.52	3.99	1.95	1.59
11228	30	33.8	0.86	0.85	0.87	212	205	5.8	6.09	65	72	0.359	0.371	993	1125	5.58	5.65	3.39	3.37
11229	31	39.6	1.05	0.99	1.05	235	255	6.6	6.48	59	68	0.393	0.360	1060	1084	5.86	5.49	3.27	3.05
11230	61	70.5	1.70	1.72	1.78	138	213	4.51	3.93	124	102	0.338	0.299	957	880	4.27	3.67	1.65	1.46
11231	72	78.2	1.82	1.84	1.90	245	214	3.41	3.34	115	122	0.324	0.340	665	798	3.30	3.40	0.87	0.96
11232	54	69.9	1.56	1.65	1.71	255	251	4.12	3.92	146	127	0.576	0.535	978	1022	5.23	4.86	1.34	1.32
11233	36	29.6	-	1.17	1.23	242	256	4.81	-	84	97	0.402	-	940	-	4.67	-	2.10	-
11234	50	58.3	1.43	1.47	1.57	224	214	4.44	4.35	118	99	0.349	0.323	823	922	4.36	4.14	1.74	1.72
11235	57	59.7	1.42	1.43	1.43	276	235	4.36	4.40	106	98	0.329	0.329	837	898	4.36	4.05	1.71	1.64
11236	52	63.2	1.52	1.55	1.56	233	229	4.47	4.25	95	92	0.345	0.323	785	863	4.09	3.87	1.60	1.53
11237	47	60.5	1.47	1.45	1.52	244	234	4.92	4.38	92	90	0.343	0.329	840	914	4.16	3.97	1.66	1.52
11238	51	63.2	1.45	1.46	1.50	233	238	4.27	4.29	96	93	0.333	0.321	847	891	4.03	3.93	1.73	1.63
11239	51	61.2	1.44	1.43	1.46	234	239	4.34	4.45	89	96	0.362	0.339	917	960	4.39	4.16	1.96	1.76
11240	67	70.8	1.82	1.77	2.03	236	181	4.78	3.99	168	146	0.473	0.430	917	828	5.07	4.44	2.50	2.05
11241	68	71.8	1.77	1.77	-	191	176	4.22	4.14	156	147	0.461	0.441	867	883	4.82	4.54	2.14	2.12
11242	76	73.9	1.80	1.79	1.80	227	183	4.24	4.22	159	146	0.475	0.448	1030	883	4.95	4.58	2.46	2.21
11243	52	77.7	1.99	1.95	1.89	195	163	3.73	3.40	185	155	0.453	0.436	690	674	4.47	3.90	1.43	1.45
11244	91	74.7	1.87	1.89	1.88	211	172	4.68	3.87	177	154	0.447	0.428	797	712	4.52	4.29	2.39	1.91
11245	94	74.1	1.78	1.74	1.82	217	169	4.18	3.93	159	148	0.440	0.418	937	821	4.45	4.27	2.61	2.16
11246	47	40.1	0.95	0.91	1.01	245	215	7.1	5.87	91	79	0.383	0.349	1013	1022	5.87	5.35	2.62	2.24
11247	82	78.5	1.87	1.92	1.98	208	221	3.06	3.22	153	157	0.375	0.356	732	805	3.88	3.93	0.86	0.88
11248	77	79.2	1.90	1.93	1.95	247	220	3.15	3.13	159	155	0.378	0.353	712	697	4.22	4.03	1.02	0.86
11249	109	83.0	1.93	1.95	-	226	212	3.12	2.95	157	159	0.368	0.333	753	697	3.83	3.67	0.95	0.83

* Numbers denote analytical method.

1. - Optical Spectrograph
2. - X-ray Fluorescence Spectrograph
3. - Flame Photometer
4. - Gamma-ray Spectrograph.

TABLE 44

AVERAGE DIFFERENCES BETWEEN ANALYTICAL METHODS

The values listed below are the average differences between the concentration of a particular element determined by emission spectrography and the concentration of that element determined by X.R.F., expressed as a percentage of the mean X.R.F. concentration. A + sign indicates that the average emission spectrographic concentration is greater than the average X.R.F. concentration, a - sign indicates the converse.

Element	Average Difference
Rb	7.7% -
Sr	3.4% +
Ca	4.1% +
Zr	3.9% +
Ti	2.1% +
Mn	1.9% -
Fe	7.2% +
Mg	7.9% +

Analyses for K by different methods are compared to the flame photometry concentration in a similar way to that above, the values are:

K (X.R.F.)	0.5%	+
K (γ - ray spec.)	3.4%	+

APPENDIX 4

STATISTICAL TECHNIQUES USED IN THE TREATMENT OF PETROGRAPHIC AND GEOCHEMICAL DATA

F - TEST

An F-test was applied to pairs of distributions to determine if the two distributions in question had significantly different standard deviations. Unless the two distributions have standard deviations which are not significantly different, a further procedure to test whether or not the means of the two distributions differ is invalid. The equations used are:

$$F = \frac{s_1^2}{s_2^2} \quad \text{where} \quad s_1^2 > s_2^2$$

and: $$s_1^2 = \sum \frac{(X_1-\bar{X}_1)^2}{N_1-1} \qquad s_2^2 = \sum \frac{(X_2-\bar{X}_2)^2}{N_2-1}$$

where X_1 denotes values from the first distribution and X_2 from the second distribution; $\bar{X}_1$ is the mean of the first distribution and $\bar{X}_2$ is the mean of the second distribution; N_1 and N_2 are the number of values in each distribution. The significance level of F was determined from tables by Arkin & Colton (1963).

STUDENT'S t - TEST

To determine whether or not two distributions had significantly different means, a "student's t-test" was applied, assuming the null hypothesis, H: $U_1=U_2$ (where U_1 is mean of one distribution, and U_2 is mean of other distribution). A value 't' was calculated from the

following formulae and its value compared to the value of t at a particular significance level, as given by Arkin & Colton (1963).

$$t = \frac{\left|\bar{X}_1 - \bar{X}_2\right|}{S_p \sqrt{((N_1 \cdot N_2)/(N_1+N_2))}}$$

$$\text{where} \quad S_p = \frac{(S_1 \cdot (\bar{X}_1 - 1)) + (S_2 \cdot (\bar{X}_2 - 1))}{(N_1+N_2-2)}$$

Symbols used are the same as for the F-test equations, and S_p is the pooled standard deviation for the two distributions.

CORRELATION COEFFICIENT

The correlation coefficient is used in two ways in this thesis, the first is as a measure of the covariance between pairs of variables which comprise a bivariate distribution, the second is as a measure of the closeness of fit of a regression line. The value of the correlation coefficient (r) is calculated according to the formulae below.

$$r = \frac{N \cdot \Sigma xy - \Sigma x \cdot \Sigma y}{\sqrt{(N \cdot \Sigma x - (\Sigma x)^2)(N \cdot \Sigma y - (\Sigma y)^2)}}$$

The value of r must lie between +1 and -1, and the higher its absolute value, the better is the degreee of correlation. If the sign of r is positive then variable x increases as the variable y increases, if r is negative then one variable increases as the other decreases. Significance levels for r can be obtained from tables by Arkin & Colton (1963).

REDUCED MAJOR AXIS REGRESSION LINE

The disadvantage of using a least squares technique to fit regression lines to chemical and petrological data is the necessity to assume that one of the variables is independent and the other variable is dependent. Such a dependent/independent relationship is seldom inherent in geochemical and petrological data, and an arbitrary choice is often required. However, the reduced major axis technique for regression analysis treats both variables as independent and is used throughout this thesis. Taking the equation for a straight line as: $y = a+bx$, then for a reduced major axis regression line the values of a and b are calculated from the equations below:

$$b = \frac{S_y}{S_x}$$ (the sign of b is determined from the sign of the correlation coefficient)

$$a = \bar{y} - b\bar{x}$$

Where S_y and S_x are the standard deviations of y and x, and $\bar{x}$ and $\bar{y}$ are the means of y and x.

COMPUTER PROGRAMMES

Computer programmes written by the author for the calculation of the mean, standard deviation, relative deviation, correlation matrix, F matrix and t matrix are given on the next 8 pages.

Programming language - Card ALGOL 3.

```
UGSTAT 2A, CORRELATION MATRIX;
'BEGIN''COMMENT' THIS PROGRAMME WILL CALCULATE A CORRELATION MATRIX FOR
                 UP TO 50 ELEMENTS;
      'INTEGER' A,B;
      'SWITCH' SS:=START;
START;'READ' A,B;
      'COMMENT' DATA CARD 1 - A,B WHERE A=NO. OF SAMPLES AND B=NO. OF
                ELEMENTS;
      'COMMENT' DATA CARD 2 - JOB TITLE AS STRING;
      'COMMENT' DATA CARD 3 - ELEMENTS INPUT AS STRINGS IN SAME ORDER
                AS SAMPLE DATA, EACH STRING SHOULD BE 4 SPACES, USE AS
                MANY CARDS AS NEEDED;
      'COMMENT' MAIN DATA INPUT WITH CONCENTRATIONS OF ALL ELEMENTS IN
                ONE SAMPLE FOLLOWED BY CONCENTRATIONS OF ALL ELEMENTS
                IN NEXT SAMPLE AND SO ON;
      'COMMENT' SAMPLE NUMBERS MAY BE PUNCHED ON DATA CARDS IN COLUMNS
                73-80, THEY WILL BE IGNORED BY THE COMPUTER;
      'COMMENT' SIZE LIMITS ARE AS FOLLOWS: B MUST BE<51, THE MAXIMUM
                VALUE OF A IS LIMITED SUCH THAT (A+7)*(3+1)<2000;
      'BEGIN''INTEGER' M,X,I,J,N,Q;
            'REAL' RA,RB,RC;
            'COMMENT' "CBS" ; ALLOCATION OF ARRAYS TO BACKING STORE;
            'REAL''ARRAY' DATA (/1:A+1,1:B+1/),SUM,SQSUM,SUMXY,MEAN,
            SD,RD(/1:B+1/);
            'REAL''ARRAY' R(/1:B+1,1:B+1/);
            'INTEGER''ARRAY' TITLE(/1:100/),ATITLE(/1:25/);
            'SWITCH'SW:=L1,L2,L3,L4,L5;
            'PROCEDURE' OUTPUT(P,V,S,T);
            'INTEGER' P,V,S,T;
            'BEGIN'
                  'FOR'X=1'STEP'1'UNTIL'P+1'DO''PRINT'$$L??;
                  'PRINT'$$S11??;
```

```
        M:=V;
        'FOR'X:=S'STEP'1'UNTIL'T'DO'
        'PRINT' OUTSTRING(TITLE,M),$$S5??;
        Q:=M;
        M:=1;
        'PRINT'$$L??;
        'FOR'X:=1'STEP'1'UNTIL'B'DO'
        'BEGIN''PRINT'$$L2??,$$S??,OUTSTRING(TITLE,M),$$S??;
              'FOR'J:=S'STEP'1'UNTIL'T'DO'
              'PRINT' ALIGNED (4,3),R(/X,J/);
        'END';
        'PRINT'$$L??;
'END';
LINEPRINTER;SAMELINE;
M:=1;
INSTRING(ATITLE,M);
M:=1;
'PRINT'TOPOFFORM,$$L2??,OUTSTRING(ATITLE,M),$$L4??;
M:=1;
'FOR'X:=1'STEP'1'UNTIL'B'DO'INSTRING(TITLE,M);
M:=1;
'PRINT' DIGITS(4),A,B,$$L2??;
'PRINT'$CORRELATION MATRIX?,$$L3??;
'FOR'I:=1'STEP'1'UNTIL'A'DO''FOR'J:=1'STEP'1'UNTIL'B'DO'
'READ' DATA(/I,J/);
'FOR'J:=1'STEP'1'UNTIL'B'DO'
'BEGIN' SUM(/J/):=SQSUM(/J/):=0;
        'FOR'I:=1'STEP'1'UNTIL'A'DO'
        'BEGIN'
              SUM(/J/):=SUM(/J/)'DATA(/I,J/);
              SQSUM(/J/):=SQSUM(/J/)'DATA(/I,J/)**2;
        'END';
'END';
```

```
    'FOR'J:=1'STEP'1'UNTIL'B'DO'
    'BEGIN'
        MEAN(/J/):=SUM(/J/)/A;
        SD(/J/):=SQRT((SQSUM(/J/)-((SUM(/J/)**2)/A))/(A-1));
        RD(/J/):=(SD(/J/)*100)/MEAN(/J/);
    'END';
    'FOR'X:=1'STEP'1'UNTIL'B'DO'
    'BEGIN''FOR'J:=1'STEP'1'UNTIL'B'DO'
        'BEGIN' SUMXY(/J/):=0;
            'FOR'I:=1'STEP'1'UNTIL'A'DO'
            SUMXY(/J/):=SUMXY(/J/)'DATA(I,X/)*DATA(/I,J/);
        'END';
        'FOR'J:=1'STEP'1'UNTIL'B'DO'
        'BEGIN'
            RA:=A*SUMXY(/J/)-SUM(/X/)*SUM(/J/);
            RB:=A*SQSUM(/X/)-SUM(/X/)**2;
            RC:=A*SQSUM(/J/)-SUM(/J/)**2;
            R(/X,J/):=RA/SQRT(RB*RC);
        'END';
    'END';
    'IF'B>40'THEN''GOTO'L1;
    'IF'B>30'THEN''GOTO'L2;
    'IF'B>20'THEN''GOTO'L3;
    'IF'B>10'THEN''GOTO'L4;
    OUTPUT(1,1,1,B);
    'GOTO'L5;
L1: OUTPUT(1,1,1,10);
    OUTPUT(8,Q,11,20);
    OUTPUT(8,Q,21,30);
    OUTPUT(8,Q,31,40);
    OUTPUT(8,Q,41,B);
    'GOTO'L5;
```

```
        L2: OUTPUT(1,1,1,10);
            OUTPUT(8,Q,11,20);
            OUTPUT(8,Q,21,30);
            OUTPUT(8,Q,31,B);
            'GOTO'L5;
        L3: OUTPUT(1,1,1,10);
            OUTPUT(8,Q,11,20);
            OUTPUT(8,Q,21,B);
            'GOTO'L5;
        L4: OUTPUT(1,1,1,10);
            OUTPUT(8,Q,11,B);
        L5: 'PRINT'TOPOFFORM,$$L2?ELEMENT STATISTICS?,$$L2??;
            M:=1;
            'PRINT'OUTSTRING(ATITLE,M),$$L4??,$$S21??;
            $MEAN        SD          RD?,$$L3??;
            M:=1;
            'FOR'X:=1'STEP'1'UNTIL'B'DO''PRINT'$$S10??,
            OUTSTRING(TITLE,M),ALIGNED(6,3),MEAN(/X/),RD(/X/),
            $$L2??;
      'END';
      'GOTO' START;
'END';
```

```
UGSTAT3 - CALCULATION OF F AND T TEST MATRICES;
'BEGIN'
      'COMMENT' DATA CARD 1 - A,B, WHERE A = NUMBER OF ANALYTICAL
            GROUPS, B = NUMBER OF ELEMENTS IN EACH ANALYTICAL GROUP,
            VALUE OF B MUST BE THE SAME FOR ALL GROUPS. A MUST BE<19;
      'COMMENT' DATA CARD 2 - JOB TITLE AS STRING;
      'COMMENT' DATA CARD(S)3 - NAMES OF ANALYTICAL GROUPS AS STRINGS,
            USE AS MANY CARDS AS NECESSARY;
      'COMMENT' DATA CARD(S)4 - NAMES OF ELEMENTS AS STRINGS, USE AS
            MANY CARDS AS NECESSARY;
      'COMMENT' DATA CARDS 5 - MAIN DATA BLOCK - DATA IS GIVEN GROUP BY
            GROUP, WITH GROUPS IN THE SAME ORDER AS ON DATA CARD 3,
            WITHIN EACH GROUP DATA IS GIVEN ELEMENT BY ELEMENT IN THE
            SAME ORDER AS ON DATA CARD 4,FOR EACH ELEMENT GIVE THE
            NUMBER OF ANALYSES, THE MEAN RESULT AND THE STANDARD
            DEVIATION (IN THAT ORDER);
      'COMMENT' PROGRAM OUTPUT IS IN THE FORM OF F AND T MATRICES, WITH
            ONE MATRIX FOR EACH ELEMENT;
      'COMMENT' THE VALUE OF A MUST BE <19 AND THE VALUE OF B IS DEFINED
            SUCH THAT B MUST BE <16000/(5*(A+1)**2), IF
            (5*(B+1)*(A+1)**2) IS >7800, THEN PART OF THE COMPILER IN
            THE BACKING STORE WILL BE OVERWRITTEN;
      'INTEGER' A,B,M,X;
      'INTEGER''ARRAY' TITLE(/1:25/),ATITLE,BTITLE(1:200/);
      'SWITCH' SS:=L1;
      LINEPRINTER;
      SAMELINE;
 L1:  'READ' A,B;
      M:=1;
      INSTRING(TITLE,M);
      M:=1;
      'FOR'X:=1'STEP'1'UNTIL'A'DO' INSTRING (ATITLE,M);
      M:=1;
      'FOR'X:=1'STEP'1'UNTIL'B'DO' INSTRING (BTITLE,M);
      M:=1;
```

```
'BEGIN'
      'INTEGER' I,J,K,N,C;
      'REAL' NA,NB,XA,XB,SA,SB,SP;
      'REAL''ARRARY' DATA (/1:B+1,1:A+1,1:4/);
      'COMMENT'"CBS": ALLOCATION OF ARRAYS TO BACKING STORE;
      'REAL''ARRAY' FMAT,TMAT(/1:B+1,1:A+1,1:A+1/);
      NN(/1:B+1,1:4,1:A+1,1:A+1/);
      'FOR'J:=1'STEP'1'UNTIL'A'DO''FOR'I:=1'STEP'1'UNTIL'B'DO'
      'FOR'K:=1'STEP'1'UNTIL'3'DO''READ' DATA(/I,J,K/);
      'FOR'I:=1'STEP'1'UNTIL'B'DO''FOR'J:=1'STEP'1'UNTIL'A'DO'
      'BEGIN'
            NA:=DATA(/I,J,1/);
            XA:=DATA(/I,J,2/);
            SA:=DATA(/I,J,3/);
            'FOR'K:=1'STEP'1'UNTIL'A'DO'
            'BEGIN'
                  'SWITCH' SW:=L2,L3,L4,L5;
                  'IF'J=K'THEN''GOTO'L4;
                  NB:=DATA(/I,K,1/);
                  XB:=DATA(/I,K,2/);
                  SB:=DATA(/I,K,3/);
                  FMAT(/I,J,K/):=SA**2/SB**2;
                  NN(/I,1,J,K/):=NA-1;
                  NN(/I,2,J,K/):=NB-1;
                  'GOTO''IF'FMAT(/I,J,K/) 1'THEN'L2'ELSE'L3;
            L2:   FMAT(/I,J,K/):=1/FMAT(/I,J,K/);
                  NN(/I,1,J,K/):=NB-1;
                  NN(/I,2,J,K/):=NA-1;
            L3:   SP:=((SA*(NA-1))+(SB*(NB-1)))/(NA+NB-2);
                  TMAT(/I,J,K/):=(ABS(XA-XB)/SP)*SQRT((NA*NB)
                  /(NA+NB));
                  NN(/I,3,J,K/):=NA+NB-2;
                  'GOTO'L5;
            L4:   FMAT(/I,J,K/):=TMAT(/I,J,K/):=0.0;
                  'FOR'X:=1'STEP'1'UNTIL'3'DO'
```

```
            NN(/I,X,J,K/):=0.0;
L5:  'END';
     'END';
     M:=1;
     'PRINT' TOPOFFORM,$$L2??,OUTSTRING(TITLE,M);
     M:=1;
     'PRINT' $$L4?ANALYTICAL GROUPS ARE IDENTIFIED IN THE?,
     $ TEST MATRICES BY THE FOLLOWING NUMBERS?,$$L2??;
     'FOR'X:=1'STEP'1'UNTIL'A'DO'
     'PRINT' $$S5??,DIGITS(2),X,$ - ?,OUTSTRING (ATITLE,M),
     $$L??;
     M:=1;
     'FOR'I:=1'STEP'1'UNTIL'B'DO'
     'BEGIN'
          'SWITCH' SP:=P1,P2,P3,P4;
          'PRINT' $$L6??,$F TEST MATRIX - ?,
          OUTSTRING(BTITLE,M),$$L3??;
          'IF'A>6'THEN'C:=6'ELSE'C:=A;
          N:=1;
     P1:  'FOR'J:=N'STEP'1'UNTIL'C'DO'
          'PRINT' $$S15??,DIGITS(2),J;
          'FOR'J:=1'STEP'1'UNTIL'A'DO'
          'BEGIN'
               'PRINT'$$L2??,$$S5??,DIGITS(2),J;
               'FOR'K:=N'STEP'1'UNTIL'C'DO'
               'PRINT'$$S2??,ALIGNED(2,2),FMAT(/I,J,K/),
               $ (?,DIGITS(3),SPECIAL(1),ENTIER
               (NN(/I,1,J,K/)),$,?,ENTIER(NN(/I,2,J,K/)),
               $)?;
          'END';
          'IF'C=A'THEN''GOTO'P4;
          N:='IF'C=6?THEN'7'ELSE'13;
          'IF'N=7'AND'A =12'THEN'C:=A'ELSE''GOTO'P2;
          'GOTO'P3;
     P2:  C:='IF'N=7'THEN'12'ELSE'A;
```

```
            P3: 'PRINT' $$L6??;
                'GOTO'P1;
        P4: 'END';
            'PRINT' $$L4??;
            M:=1;
            'FOR'I:=1'STEP'1'UNTIL'B'DO'
            'BEGIN'
                'SWITCH' SR:=R1,R2,R3,R4;
                'PRINT' $$L6??,$T TEST MATRIX - ?,
                OUTSTRING(BTITLE,M),$$L3??;
                C:='IF'A>7'THEN'7'ELSE'A;
                N:=1;
             R1: 'FOR'J:=N'STEP'1'UNTIL'C'DO'
                'PRINT' $$S11??,DIGITS(2),J;
                'FOR'J:=1'STEP'1'UNTIL'A'DO'
                'BEGIN'
                    'PRINT'$$L2??,$$S2??,DIGITS(2),J;
                    'FOR'K:=N'STEP'1'UNTIL'C'DO'
                    'PRINT'$$S2??,ALIGNED(2,2),TMAT(/I,J,K/),
                    $ (?,DIGITS(3),SPECIAL(1),ENTIER
                    (NN(/I,3,J,K/)),$)?;
                'END';
                'IF'C=A'THEN''GOTO'R4;
                N:='IF'C=7'THEN'8'ELSE'15;
                'IF'N=8'AND'A =14'THEN'C:=A'ELSE''GOTO'R2;
                'GOTO'R3;
             R2: C:='IF'N=8'THEN'14'ELSE'A;
             R3: 'PRINT' $$L6??;
                'GOTO'R1;
        R4: 'END';
            'PRINT' $$L??;
    'END';
    'GOTO'L1;
'END';
```

MULTIVARIATE ANALYSIS

MAJOR ELEMENTS

Binary variation diagrams using parameters such as SiO_2 (Harker diagrams) molar ratios, crystallisation index (Poldervaart & Parker, 1964), differentiation index (Thornton & Tuttle, 1960), iron ratio-albite ratio (Wager, 1956); and ternary variation diagrams such as the ACF, AFM and von Wolff diagrams although useful for illustrating chemical trends, suffer from the disadvantage that not all chemical trends can be shown by any one type of diagram. Interpretation of simple diagrams which cannot represent more than a portion of the major element chemistry is often misleading. It is with these limitations in mind that recent applications of the techniques of multivariate statistical analysis (Le Maitre, 1968; Manson, 1967; Prinz, 1967) to the problem of producing variation diagrams suitable for completely general application are particularly interesting.

The techniques of Le Maitre, Manson and Prinz - principal component and factor analyses - are described in appendices to papers by Manson (1967) and Le Maitre (1968) and are outlined below. Principal component analysis and factor analysis differ only in the mathematical manipulations used in the final stages of derivation of factor coefficients. Both provide a means of representing in two dimensional diagrams, many of the attributes of a chemical analysis located in n-dimensional space according to its oxide percentages. The representation of a major element chemical analysis in n-dimensional space can be thought of as a point defining n coordinates (the oxide

percentages) along n oxide axes. A suite of chemical analyses can thus be represented by a series of unique points in n-dimensional space, producing what Le Maitre terms a "single n-dimensional Harker diagram".

N-dimensional space can be most easily visualised if we put n = 3, although there are no mathematical limitations on the value of n. If we then consider a suite of samples analysed for three components, each sample can be represented as a point positioned relative to three orthogonal axes in 3-dimensional space, according to the values of the three components. The techniques of principal component analysis and factor analysis allow us to determine three new axes through the resulting 3-dimensional scatter diagram. The first new axis, termed the first latent vector, is that vector along which the maximum "spread" (variance) of the array is taken up. The second latent vector is the direction of the maximum "spread" of the array normal to the first latent vector, and the third latent vector is normal to both the first and second latent vectors. For the Bay of Plenty volcanics the first four latent vectors have been computed for the distribution of the major element analyses in 9-dimensional space (9 major oxides being analysed). The vector loadings for both principal component analysis and factor analysis of major elements, together with the percentage of the total variance of the nine oxide distribution which is taken up along each vector is given in Table 45. The first three vectors account for 93.7% of the total variance and the first four for 96.0%.

The analyses of the Bay of Plenty volcanics relative to these vectors are plotted in two different ways. The results of principal component analysis are plotted on what Le Maitre has termed a "principal latent vector variation diagram" (abbreviated to PLVVD), Fig. 37, and the factor analysis results are plotted on a double ternary diagram (Fig. 38) similar to that used by Prinz (1967); the calculation of the vector axis co-ordinates used for plotting is discussed below. The major element chemistry of the samples is more completely represented by these diagrams than by any of the classical variation diagrams, however, they have the disadvantage that in being projections from n-dimensional space they do not show chemical composition directly.

One particularly useful property of the PLVVD is that the composition of material that can be added to or removed from one composition to produce another, must project as a point on the straight line joining the two compositions on the PLVVD, this property can be used to test various hypotheses. For instance, if the Edgecumbe dacites were derived from the Edgecumbe andesites (samples 11206, 11208, 11216) by removal of material having the composition of Type IA xenoliths, only two of the Edgecumbe dacites (samples 11205, 11213) fall within the suite of lines joining the points representing the Edgecumbe andesites and the Type IA xenoliths (Fig.37) and thus these are the only two dacites which could have been formed by such a process. Another particularly valuable use of the PLVVD and the double-ternary factor diagrams is the ease with which the complete major element composition of individual volcanoes can be compared.

For instance the lower part of Fig. 37 shows that the Edgecumbe and Whale Island dacites are similar in composition, and both are different from the White Island dacites. The difference shows up much more clearly than on conventional variation diagrams (Figs. 26, 27 and 28). Oneparticularly frustrating aspect of a double-ternary factor diagram however is that it is almost impossible to assign precise chemical meaning to strong linear trends such as that shown in a lower section of Fig. 38. The trend is obviously significant but does not appear so clearly on any other variation diagram.

TRACE ELEMENTS

Vector loadings for principal component analysis and factor analysis of trace element data, together with the percentage of the total variance of the 16 element distribution which is taken up along each vector is given in Table 46.

The PLVVD for trace elements in the Bay of Plenty volcanics (Fig. 39) is a good example of the power of multivariate analysis in providing criteria for presentation of data for 16 trace elements (Rb, Ba, Sr, Y, Zr, Ti, Mn, Cu, Co, Ni, Li, Sc, V, Cr, Ga, B) in a readily assimilated visual form. The most striking feature of both sections of the PLVVD is the obvious difference in the trace element compositions of White Island dacites, compared to that of the other Bay of Plenty volcanics. A second feature shown by both sections of the PLVVD is that the overall trace element chemistry of the Type IB and Group II xenoliths is less similar to non-xenolithic samples, than is the case for Type IA xenoliths. A reasonable separationof analyses

Symbols used in Figs. 37, 38, 39 and 40

- ● Edgecumbe non-xenolithic samples
- ■ Whale Island non-xenolithic samples
- ○ White Island samples
- □ Manawahe samples
- △ Type IA xenoliths (11223, 11228, 11229)
- ▲ Type IB and Group II xenoliths (11209, 11232).

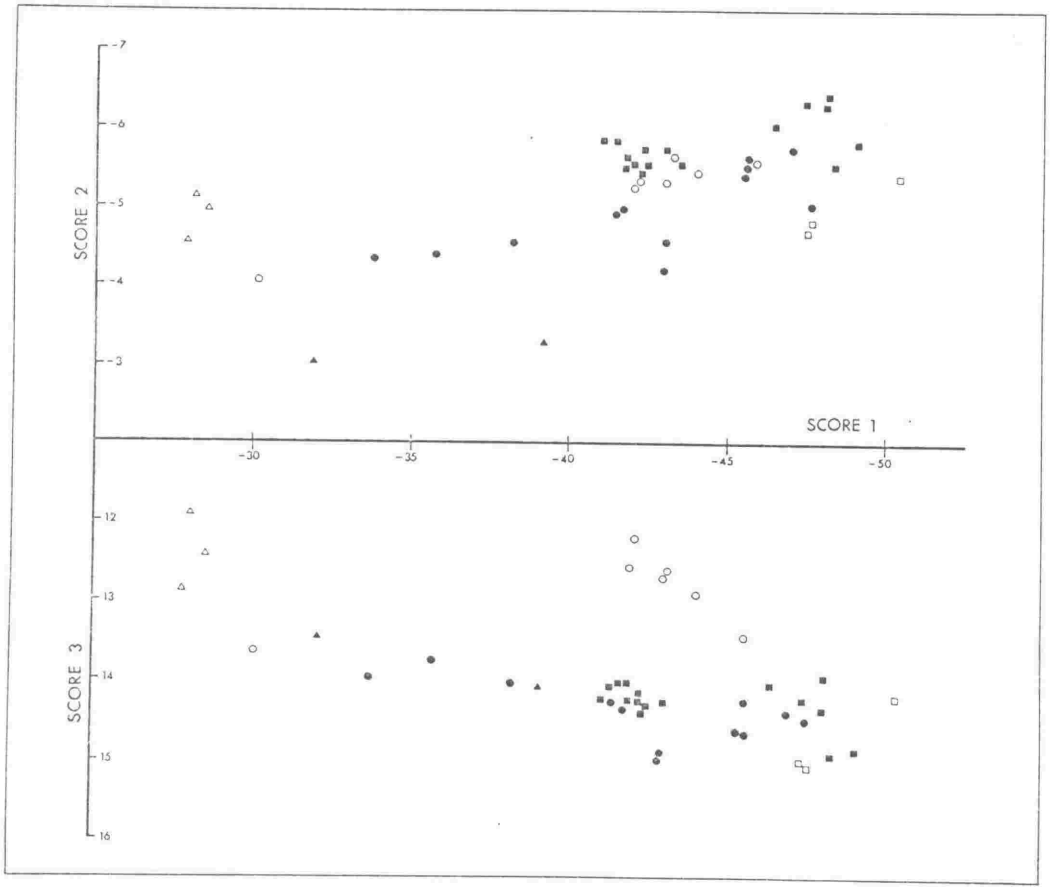

Fig. 37. - Principal latent vector variation diagram for major element analyses of the Bay of Plenty volcanics (data from Table 47). Key to symbols used is on the previous page.

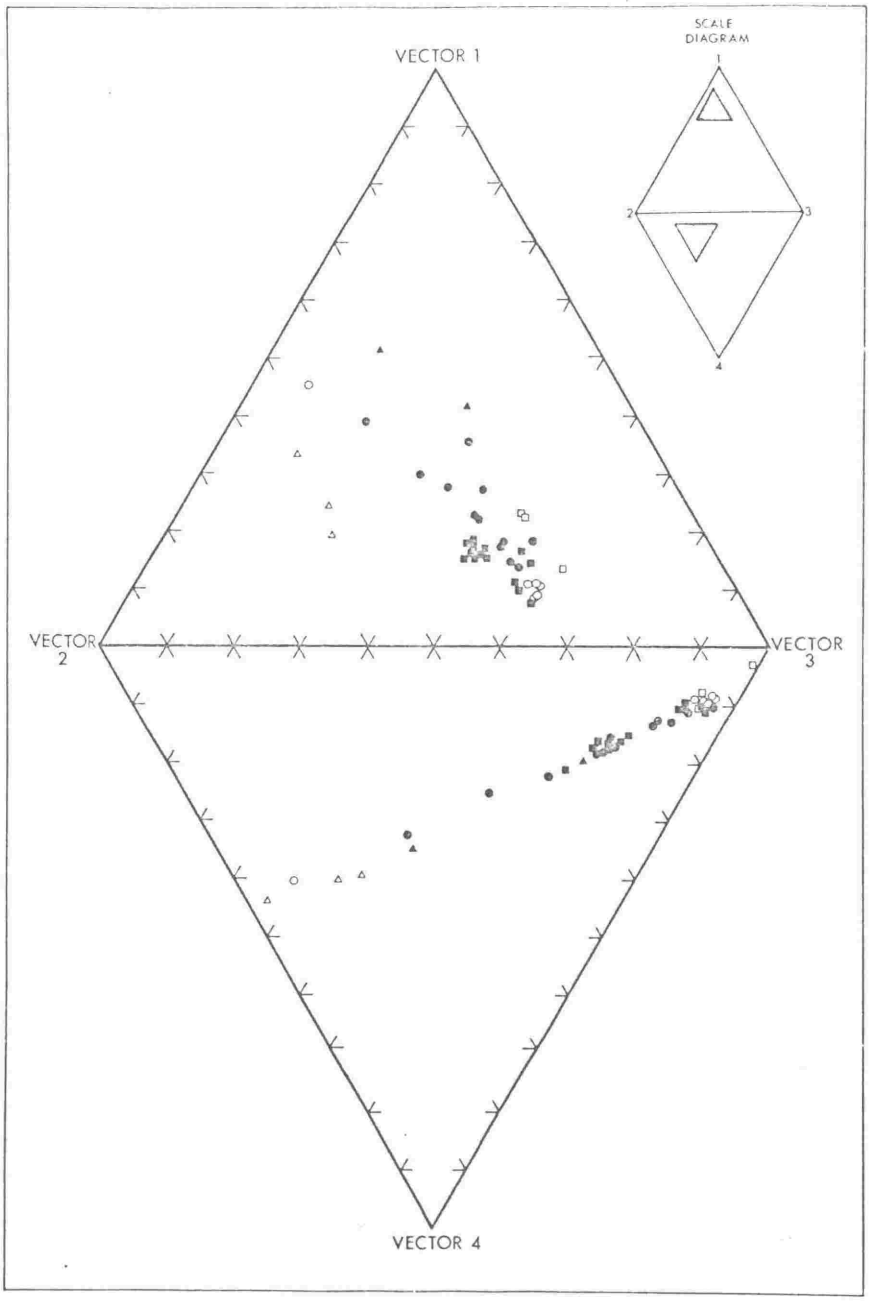

Fig. 38. - Double ternary factor analysis diagram for major element analyses of the Bay of Plenty volcanics (data from Table 48). Key to symbols used is on page preceding Fig. 37.

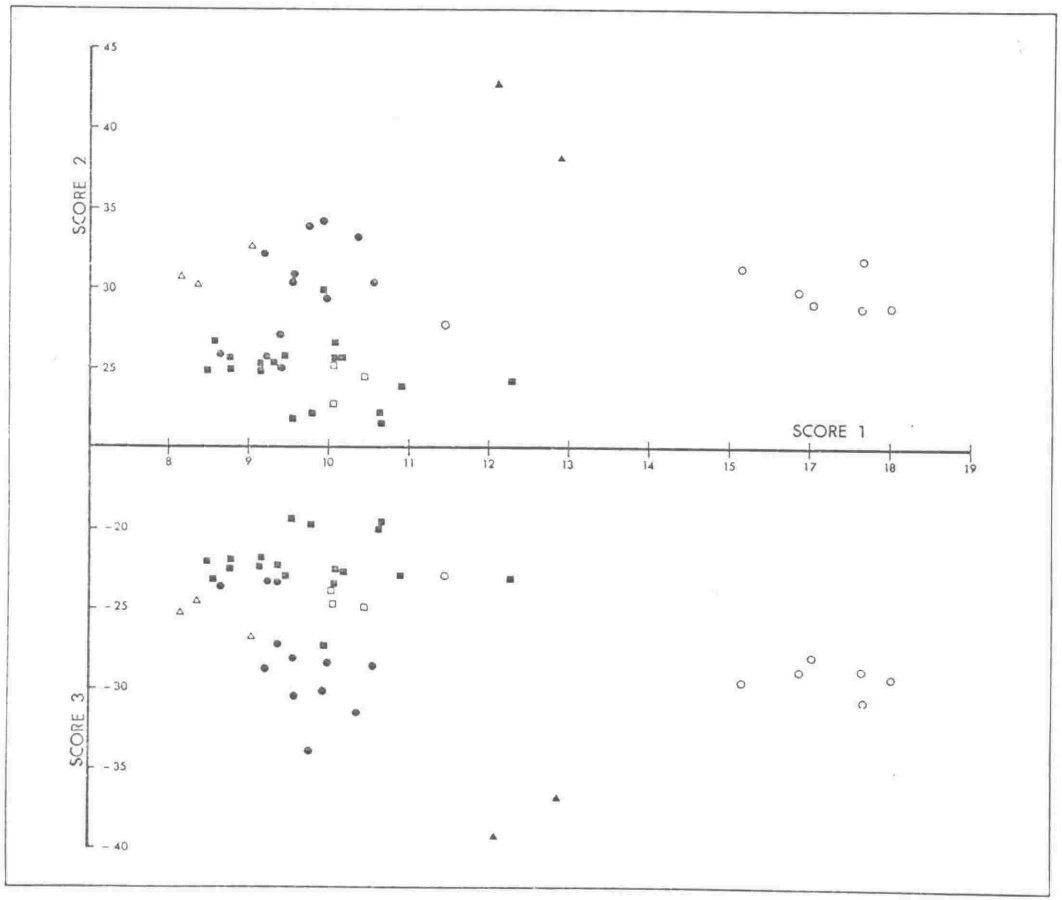

Fig. 39. - Principal latent vector variation diagram for trace element analyses of the Bay of Plenty volcanics (data from Table 47). Key to symbols used is on page preceding Fig. 37.

of Whale Island and Edgecumbe samples into two distinct groups is apparent in both sections, but is better developed in the lower section of the diagram. This division is an indication of the sensitivity of the multivariate technique to the different distributions in these two volcanoes of the elements Ba, Sr, Li, Ga, and B. The trace element geochemistry of Manawahe is intermediate between that of Edgecumbe and Whale Island, but is more similar to that of Whale Island.

Essentially the same pattern is shown by the double ternary diagram (Fig. 40) except for the relationship between Manawahe and the other Bay of Plenty volcanoes. In the double ternary diagram Manawahe is clearly different from Whale Island, Edgecumbe and White Island in its overall trace element chemistry. The two diagrams differ because they represent projections from n-dimensional space by two different techniques, and whereas four vectors are represented in the double ternary diagram, only three are represented in the PLVVD.

Most analyses of the Bay of Plenty volcanics could thus be correctly attributed to their parent volcano on the basis of their plotted positions in Figs. 39 and 40.

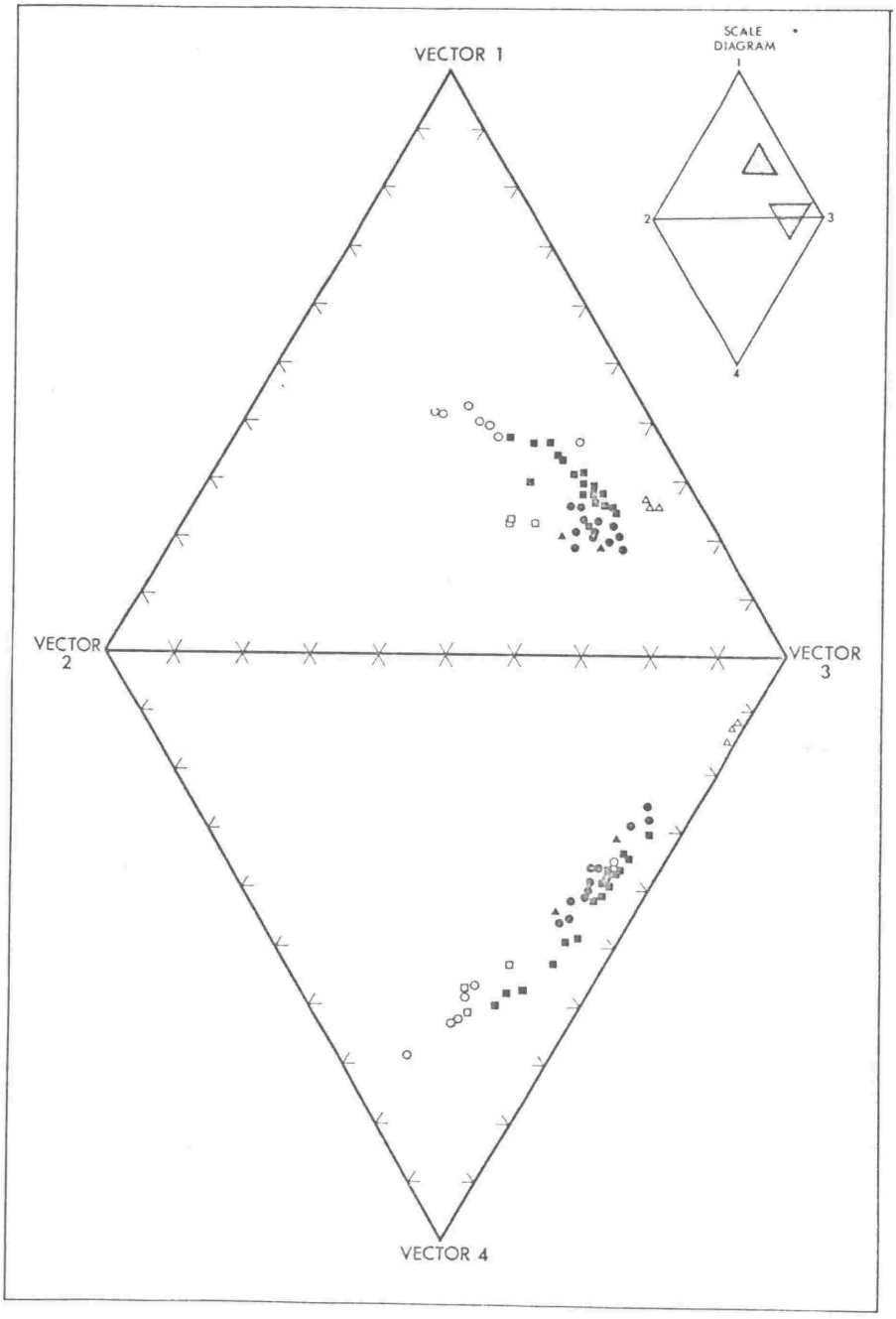

Fig. 40. - Double ternary factor analysis diagram for trace element analyses of the Bay of Plenty volcanics (data from Table 49). Key to symbols used is on page preceding Fig. 37.

TABLE 45 MULTIVARIATE STATISTICS

MAJOR ELEMENTS

Variance Taken Up By First Four Vectors

	Percentage of Total Variance	Cumulative Percentage
1	60.854	60.854
2	23.074	83.927
3	9.736	93.663
4	2.336	95.999

Principal Component Analysis - Vector Loadings

	Vector 1	Vector 2	Vector 3	Vector 4
SiO_2	-0.961	-0.205	0.090	-0.142
TiO_2	0.319	0.846	-0.325	0.022
Al_2O_3	0.613	0.267	0.711	0.168
FeO	0.887	0.382	-0.183	0.084
CaO	0.976	-0.123	-0.033	0.068
MgO	0.831	-0.238	-0.481	0.023
Na_2O	-0.763	0.544	0.003	0.228
K_2O	-0.918	0.279	-0.218	0.011
P_2O_5	-0.121	0.930	0.094	-0.212
MnO	0.902	0.147	0.181	-0.274

Factor Analysis - Vector Loadings

	Vector 1	Vector 2	Vector 3	Vector 4
SiO_2	-0.868	-0.265	-0.410	-0.049
TiO_2	0.299	0.905	0.017	0.124
Al_2O_3	0.204	0.133	0.959	-0.030
FeO	0.814	0.457	0.317	0.037
CaO	0.902	-0.054	0.390	-0.067
MgO	0.983	-0.078	-0.086	-0.015
Na_2O	-0.749	0.444	-0.184	0.372
K_2O	-0.761	0.251	-0.534	0.199
P_2O_5	-0.297	0.900	0.149	-0.119
MnO	0.687	0.202	0.516	-0.404

TABLE 46 MULTIVARIATE STATISTICS

TRACE ELEMENTS

Variance Taken Up By First Four Vectors

	Percentage of Total Variance	Cumulative Percentage
1	33.586	33.586
2	28.541	62.127
3	16.181	78.308
4	5.741	84.049

Principal Component Analysis - Vector Loadings

	Vector 1	Vector 2	Vector 3	Vector 4
Rb	0.379	-0.739	-0.381	-0.280
Ba	0.712	-0.313	0.222	-0.231
Sr	-0.521	0.503	-0.490	-0.082
Y	0.469	-0.067	-0.679	0.286
Zr	0.588	-0.517	-0.549	0.051
Ti	0.233	0.556	-0.672	-0.060
Mn	-0.451	0.827	0.055	-0.115
Cu	0.907	0.242	-0.080	0.178
Co	0.554	0.682	0.231	0.312
Ni	0.936	0.212	0.051	0.055
Li	-0.196	-0.529	-0.542	0.387
Sc	-0.093	0.829	-0.225	0.067
V	0.456	0.831	-0.040	-0.109
Cr	0.825	0.252	0.206	0.115
Ga	-0.223	0.337	-0.697	-0.342
B	0.799	0.011	0.021	-0.501

Factor Analysis - Vector Loadings

	Vector 1	Vector 2	Vector 3	Vector 4
Rb	-0.012	-0.288	0.074	-0.871
Ba	0.419	-0.146	0.108	-0.348
Sr	-0.315	-0.039	-0.599	0.259
Y	0.202	-0.929	-0.180	-0.152
Zr	0.246	-0.607	0.040	-0.646
Ti	0.394	-0.264	-0.554	-0.071
Mn	-0.056	0.361	-0.425	0.558
Cu	0.895	-0.334	0.052	-0.085
Co	0.746	-0.159	0.019	0.516
Ni	0.938	-0.160	0.077	-0.151
Li	-0.217	-0.171	-0.056	-0.212
Sc	0.210	-0.039	-0.639	0.591
V	0.654	-0.079	-0.373	0.284
Cr	0.932	0.046	0.077	0.012
Ga	-0.139	-0.086	-0.938	-0.035
B	0.677	0.064	-0.049	-0.596

CALCULATION OF VECTOR AXIS CO-ORDINATES

1. Principal Component Analysis

The author has adopted the technique used by Le Maitre (1968) and has calculated the score for a particular sample on a particular vector as the sum of the cross-products of the vector loadings for each element and the element concentrations. These values, which are plotted on the PLVVD's (Figs. 37,39) are listed in Table 47.

2. Factor Analysis

For factor analysis the element or oxide concentrations are normalised by dividing the individual element concentrations in each sample by the square root of the sum of the squares of all element concentrations in that sample. The score for a particular sample on a particular vector is then calculated as the sum of the cross-products of the vector loadings for each element and the normalised element concentrations. Vector axis scores are then grouped into sets of three vectors at a time, and the scores for each sample recalculated to percentages for plotting on a ternary diagram for each group of vectors.

TABLE 47

PRINCIPAL COMPONENT ANALYSIS - VECTOR AXIS CO-ORDINATES

	MAJOR ELEMENTS				TRACE ELEMENTS			
SAMPLE NO.	SCORE 1	SCORE 2	SCORE 3	SCORE 4	SCORE 1	SCORE 2	SCORE 3	SCORE 4
11205	-42.95	-4.20	14.99	-4.52	1053	3043	-2865	-541
11206	-33.72	-4.32	13.98	-3.85	991	3412	-3018	-523
11207	-47.55	-5.07	14.49	-5.15	998	2933	-2845	-526
11208	-35.73	-4.39	13.78	-4.01	918	3216	-2876	-508
11209	-31.85	-3.02	13.47	-3.52	1208	4261	-3937	-632
11210	-45.68	-5.66	14.25	-5.11	862	2587	-2364	-459
11211	-45.58	-5.54	14.62	-5.04	922	2551	-2339	-477
11212	-46.96	-5.76	14.40	-5.22	939	2513	-2342	-478
11213	-42.97	-4.54	14.87	-4.66	1035	3334	-3153	-550
11214	-41.45	-4.32	14.23	-4.61	953	3042	-2819	-496
11215	-41.78	-4.97	14.36	-4.66	955	3055	-2838	-496
11216	-38.23	-4.53	14.01	-4.31	974	3382	-3059	-522
11217	-45.49	-5.43	14.61	-5.05	938	2713	-2509	-488
11218	-	-	-	-	1008	2563	-2254	-522
11219	-48.03	-6.30	14.37	-5.43	1065	2150	-1961	-515
11220	-48.12	-6.44	13.95	-5.55	977	2212	-1982	-485
11221	-47.44	-6.34	14.21	-5.43	952	2185	-1944	-4[illegible]
11222	-41.38	-5.83	14.09	-4.89	1012	2560	-2265	-[illegible]
11223	-27.81	-4.54	12.86	-3.46	901	3263	-267[illegible]	-527
11224	-49.13	-5.81	14.85	-5.44	1227	2429	-2306	-522
11225	-42.31	-5.74	14.15	-4.88	874	2563	-2253	-492
11226	-41.73	-5.52	14.03	-4.76	1004	2667	-2352	-511
11227	-43.05	-5.72	14.28	-4.91	943	2582	-2304	-489
11228	-28.16	-5.14	11.91	-3.73	813	3075	-2511	-477
11229	-28.61	-4.95	12.41	-3.66	838	3027	-2452	-482
11230	-46.42	-6.04	14.03	-5.24	1063	2225	-1973	-532
11231	-48.31	-5.59	14.91	-5.26	1090	2393	-2305	-529
11232	-39.16	-3.23	14.09	-4.06	1289	3824	-3679	-622
11233	-	-	-	-	992	2985	-2743	-513
11234	-41.71	-5.64	14.02	-4.83	915	2497	-2182	-490
11235	-41.96	-5.56	14.23	-4.78	936	2522	-2236	-499
11236	-43.49	-5.59	14.31	-4.88	878	2479	-2204	-477
11237	-42.23	-5.47	14.24	-4.75	911	2529	-2232	-493
11238	-42.40	-5.57	14.36	-4.81	849	2488	-2200	-473
11239	-41.09	-5.88	14.24	-4.89	856	2665	-2321	-484
11240	-43.01	-5.32	12.72	-4.89	1587	2989	-2877	-605
11241	-41.98	-5.27	12.54	-4.82	1515	3122	-2969	-566
11242	-42.17	-5.44	12.18	-4.88	1665	3185	-3007	-610
11243	-45.68	-5.57	13.45	-5.13	1700	2872	-2732	-566
11244	-44.08	-5.43	12.93	-5.00	1663	2871	-2887	-553
11245	-43.29	-5.69	12.62	-5.03	1601	2911	-2798	-585
11246	-30.10	-4.06	13.68	-3.44	1145	2756	-2292	-580
11247	-47.69	-4.84	15.08	-5.01	1003	2515	-2484	-477
11248	-47.41	-4.68	15.00	-4.96	1046	2437	-2491	-466
11249	-50.36	-5.40	14.22	-5.44	1003	2271	-2345	-436

TABLE 48

FACTOR ANALYSIS - VECTOR AXIS CO-ORDINATES

MAJOR ELEMENTS

	FIRST TERNARY DIAGRAM			SECOND TERNARY DIAGRAM		
SAMPLE NO.	SCORE 1	SCORE 2	SCORE 3	SCORE 2	SCORE 3	SCORE 4
11205	-72.01	-15.52	-12.47	-49.44	-39.72	-10.84
11206	-72.82	-18.22	-8.96	-56.54	-27.82	-15.65
11207	-69.66	-15.25	-15.09	-45.70	-45.22	-9.08
11208	-71.96	-17.47	-10.58	-53.68	-32.51	-13.81
11209	-75.25	-16.55	-8.20	-55.98	-27.72	-16.30
11210	-68.95	-16.29	-14.76	-47.22	-42.79	-9.98
11211	-69.43	-16.32	-14.25	-47.96	-41.86	-10.18
11212	-68.81	-16.14	-15.04	-46.80	-43.61	-9.59
11213	-71.40	-15.88	-12.72	-49.31	-39.49	-11.21
11214	-70.55	-16.56	-12.89	-49.75	-38.75	-11.49
11215	-70.51	-16.55	-12.95	-49.65	-38.85	-11.50
11216	-71.43	-16.90	-11.65	-51.55	-35.54	-12.91
11217	-69.59	-16.20	-14.21	-47.79	-41.93	-10.28
11219	-68.03	-16.47	-15.51	-46.58	-43.87	-9.54
11220	-67.52	-16.44	-16.05	-45.79	-44.71	-9.50
11221	-67.90	-16.59	-15.51	-46.63	-43.58	-9.79
11222	-69.09	-17.62	-13.29	-50.04	-37.73	-12.23
11223	-72.62	-20.78	-6.60	-61.36	-19.50	-19.14
11224	-68.89	-15.83	-15.28	-46.14	-44.53	-9.33
11225	-69.16	-17.26	-13.58	-49.51	-38.94	-11.55
11226	-69.42	-17.12	-13.45	-49.58	-38.96	-11.46
11227	-69.21	-17.08	-13.71	-49.25	-39.52	-11.23
11228	-69.91	-21.01	-9.07	-57.46	-24.81	-17.74
11229	-70.89	-20.77	-8.34	-58.61	-23.53	-17.86
11230	-68.21	-16.46	-15.33	-46.78	-43.57	-9.65
11231	-69.30	-15.81	-14.89	-46.70	-43.96	-9.34
11232	-73.31	-14.91	-11.77	-49.57	-39.14	-11.28
11234	-69.24	-17.27	-13.49	-49.59	-38.73	-11.68
11235	-69.53	-17.19	-13.28	-49.91	-38.55	-11.55
11236	-69.36	-16.83	-13.81	-48.97	-40.21	-10.82
11237	-69.63	-17.01	-13.37	-49.69	-39.05	-11.27
11238	-69.57	-17.13	-13.29	-49.85	-38.68	-11.48
11239	-69.20	-17.84	-12.96	-50.59	-36.76	-12.65
11240	-68.31	-15.99	-15.70	-45.67	-44.82	-9.51
11241	-68.32	-16.14	-15.54	-45.94	-44.22	-9.84
11242	-67.74	-16.16	-16.11	-45.31	-45.17	-9.51
11243	-68.37	-15.89	-15.75	-45.59	-45.18	-9.23
11244	-68.24	-15.93	-15.83	-45.47	-45.17	-9.36
11245	-67.70	-16.33	-15.97	-45.66	-44.64	-9.69
11246	-74.04	-19.27	-6.68	-61.00	-21.16	-17.84
11247	-70.45	-15.18	-14.37	-46.70	-44.20	-9.10
11248	-70.62	-15.03	-14.36	-46.53	-44.46	-9.01
11249	-68.74	-14.91	-16.34	-43.91	-48.12	-7.96

TABLE 49

FACTOR ANALYSIS - VECTOR AXIS CO-ORDINATES

TRACE ELEMENTS

	FIRST TERNARY DIAGRAM			SECOND TERNARY DIAGRAM		
SAMPLE NO.	SCORE 1	SCORE 2	SCORE 3	SCORE 2	SCORE 3	SCORE 4
11205	33.29	-17.17	-49.54	25.56	73.75	0.69
11206	33.41	-15.97	-50.63	24.77	78.56	-3.33
11207	32.74	-17.43	-49.83	25.50	72.91	1.59
11208	33.05	-15.99	-50.96	24.57	78.32	-2.89
11209	32.62	-16.69	-50.68	25.27	76.74	-2.02
11210	33.59	-16.44	-49.97	24.86	75.58	-0.45
11211	34.05	-16.60	-49.35	25.05	74.44	0.51
11212	34.07	-16.87	-49.06	25.23	73.37	1.41
11213	32.61	-17.07	-50.32	25.39	74.82	-0.21
11214	33.15	-16.64	-50.21	25.10	75.72	-0.83
11215	33.05	-16.75	-50.20	25.23	75.60	-0.83
11216	32.98	-16.28	-50.74	24.91	77.65	-2.55
11217	33.60	-16.76	-49.64	25.19	74.61	0.20
11218	35.22	-15.97	-48.81	24.55	75.02	0.42
11219	36.29	-16.88	-46.84	25.35	70.36	4.29
11220	35.81	-16.37	-47.82	24.89	72.73	2.38
11221	35.68	-16.24	-48.08	24.70	73.14	2.17
11222	35.20	-16.20	-48.60	24.83	74.66	0.46
11223	34.09	-14.44	-51.47	23.31	83.10	-6.41
11224	36.52	-17.41	-46.07	26.03	68.86	5.09
11225	34.08	-15.83	-50.09	24.28	76.85	-1.13
11226	34.89	-16.16	-48.95	24.89	75.38	-0.27
11227	34.50	-16.24	-49.25	24.85	75.36	-0.20
11228	34.07	-14.22	-51.71	23.10	83.47	-7.06
11229	34.30	-14.33	-51.37	23.34	83.65	-6.99
11230	36.30	-16.36	-47.34	24.84	71.90	3.26
11231	34.89	-17.64	-47.46	25.84	69.51	4.64
11232	33.11	-17.58	-49.31	26.01	72.96	1.02
11233	33.44	-16.67	-49.90	25.21	75.46	-0.67
11234	34.79	-15.81	-49.40	24.37	76.19	-0.56
11235	34.55	-16.13	-49.32	24.66	75.42	-0.08
11236	34.26	-16.03	-49.71	24.49	75.96	-0.46
11237	34.49	-15.93	-49.58	24.44	76.03	-0.47
11238	34.04	-15.88	-50.08	24.33	76.70	-1.02
11239	33.94	-15.58	-50.48	24.10	77.11	-2.22
11240	37.02	-18.06	-44.92	27.04	67.26	5.70
11241	36.68	-17.82	-45.50	26.94	68.81	4.24
11242	37.34	-17.89	-44.77	27.17	67.97	4.86
11243	37.35	-19.29	-43.37	28.33	63.70	7.97
11244	37.37	-19.06	-43.57	28.23	64.53	7.23
11245	37.48	-18.11	-44.40	27.24	66.78	5.97
11246	36.29	-15.53	-48.18	24.55	76.18	-0.73
11247	33.54	-18.17	-48.28	26.42	70.19	3.39
11248	33.53	-18.95	-47.52	27.17	68.13	4.69
11249	33.61	-18.88	-47.51	26.90	67.69	5.42

APPENDIX 5

COMPARISON OF GEOCHEMISTRY WITH PETROGRAPHY AND GEOLOGY

EDGECUMBE

Before the petrochemistry of rocks from different volcanic units can be meaningfully compared it is necessary to establish that rocks taken from the same unit have very similar chemistry for the elements analysed. Such a test establishes in practical terms the sum of the absolute chemical variation within a volcanic unit, the possible errors involved in sampling such a unit and in reducing the sample to a suitable final fraction for analysis, and the precision of the analysis itself. Three samples taken from Main Dome on Edgecumbe (11210, 11211 and 11212) averaged 400 gm each, and were the smallest samples taken for geochemical analysis; hence for these samples the error due to sampling and reduction techniques can be expected to be at a maximum. The major and trace element concentrations for these samples show very small differences only (Table 50) and comparisons between volcanic units in the following discussion are made accordingly.

For Edgecumbe samples of known relative age there is no consistent chemical variation with time. Consequently the relative chemistry cannot be used to determine their time sequence. However, in view of the comparatively large number of elements analysed and the significant chemical variation shown by the volcano, rocks having very similar concentrations of all the analysed elements are considered to have been erupted at about the same time. The geochemical data can thus be used for stratigraphic correlation, but not to determine relative stratigraphic order.

TABLE 50

COMPARISON OF ANALYSES OF THREE SAMPLES FROM THE SAME VOLCANIC UNIT (MAIN DOME, EDGECUMBE)

SAMPLE	11210	11211	11212
Cs	2.3	2.4	1.8
Rb	70	68	72
Ba	520	600	610
%K	1.67	1.59	1.69
Sr	223	231	220
%Ca	3.73	3.82	3.60
%Na	2.29	2.36	2.39
Y	16	16	16
Zr	104	104	105
Mn	870	850	830
%*Fe	3.87	3.81	3.70
Cu	14	16	14
Co	13	12	11
Ni	8.4	7.4	6.5
Li	24	24	27
Mg	1.44	1.29	1.33
Sc	17	17	16
V	120	130	120
%Ti	0.342	0.340	0.341
Cr	26	27	21
Ga	15	17	16
%Al	8.21	8.41	8.23
%Si	30.13	30.22	30.57
B	15	17	19

All values are in ppm unless otherwise indicated.

* Total Iron.

Detailed sample locations for analysed samples are given in Table 51.

The northern, southern and western Base-Flows (see p. 10 and Fig. 3) are thought to have been the earliest flows of the Edgecumbe volcano. Since the western Base-Flows have more basic major element chemistry than the southern and northern Base Flows, it is clear that they were not extruded from the same magma body at the same time. The northern and southern Base Flows have extremely similar chemistry with the exception of their Ni content, Ni being not detectable (< 1 ppm) in the southern Base Flows compared to 5 ppm in the northern Base Flows; a significant difference, but as it is the only such difference it most likely indicates that the northern and southern Base Flows were extruded at similar times but not simultaneously.

Three samples from units whose correlatives elsewhere on Edgecumbe cannot be inferred geologically were analysed, one from the North Dome and two from the lahar fan. The chemistry of the North Dome sample (11208) is very similar to that of sample 11216 from flow Bb, and they are therefore considered to be correlatives. Flow Bb is considered on geological grounds to be close in age to flow Ac on the northwest ridge and hence it is considered that the basal flows on the northern and northwestern ridges and North Dome, which lies at the foot of flow Ac on the northwestern ridge were extruded at about the same time. From additional geological evidence discussed earlier (p. 14) the extrusion of North Dome thus appears to pre-date the extrusion of Main Dome. Of the two samples from the lahar fan, one of them (11215) is indistinguishable chemically from sample 11214 taken from the tholoid plugging vent 11 on the east peak of the Main Cone. The tholoid crops

TABLE 51

SAMPLE LOCATIONS FOR ANALYSED SAMPLES OF THE BAY OF PLENTY VOLCANICS

EDGECUMBE

11205	Northern Base Flows
11206	Western Base Flows
11207	Main Cone, flow Aa
11208	North Dome
11209	North Dome (xenolith)
11210	Main Dome
11211	Main Dome
11212	Main Dome
11213	Southern Base Flows
11214	East peak tholoid, plug in vent 11.
11215	Lahar fan
11216	Main Cone, flow Bb.
11217	Lahar fan

WHALE ISLAND

11218	West Dome, contact zone.
11219	West Dome
11220	West Dome, peak.
11221	West Dome, peak.
11222	Flow A
11223	Central Cone, volcanic breccia in McEwans Bay.
11224	East Dome
11225	Central Cone
11226	Central Cone
11227	Central Cone
11228	Central Cone (xenolith)
11229	Beach boulder, S.W. point (xenolith)

TABLE 51 (continued)

WHALE ISLAND (continued)

11230	Beach boulder, S.W. point (host of 11229).
11231	East Dome border zone.
11232	East Dome border zone (composite sample of xenoliths).
11233	Cone Tholoid
11234	Bottom
11235	
11236	Central Cone bedded
11237	volcanic breccia section
11238	on north face
11239	Top

WHITE ISLAND

11240	Central Cone, bay W. of Porporo.
11241	Central Cone, Otaketake.
11242	Central Cone, N.E. point.
11243	Central Cone, inside S.E. crater Wall.
11244	Central Cone, Crater Bay.
11245	Central Cone, Crater Bay.
11246	Troup Head, basal tholoid or coulée

MANAWAHE

11247	N68/120253
11248	N68/123253
11249	N68/132230

out at the apex of the fan of lahar debris, and its chemical equivalence with part of this debris supports the hypothesis already proposed on geological evidence that much of the lahar debris has been derived by the collapse of an extrusive spine of which the tholoid is a remnant. Sample 11217, also from the lahar fan is chemically different from any other Edgecumbe analysed sample, and therefore cannot be correlated by geochemical comparison.

WHALE ISLAND

All non-xenolithic samples analysed from Whale Island are dacitic in chemistry. The average Whale Island sample contains substantially more modal quartz than the average Edgecumbe sample, thus the higher average SiO_2 content of Whale Island rocks is in accord with the petrographic differences between the volcanoes.

The three main volcanic units which make up the Whale Island volcano, Central Cone, East Dome and West Dome, all show distinctive compositions. In major elements Central Cone rocks are rather more basic, with lower SiO_2, Na_2O and K_2O, and higher FeO (total iron), CaO and MgO, than rocks from East and West Domes. Similarly the trace element concentrations show the greater "basicity" of Central Cone rocks, reflected in generally lower contents of the large cations and large highly-charged cations, and higher contents of ferromagnesian trace elements than in East and West Dome rocks. The major element chemistry of East and West Dome samples is very similar except that MgO is notably lower in East Dome. Certain trace elements, however, show quite different concentrations in the two domes. East Dome is

distinctly richer in Rb, Th, U, and Zr, and is depleted in Cu, Co, Ni and Cr relative to West Dome.

The chemical, petrographic and geological evidence are consistent with the West Dome magma being derived from the Central Cone magma by fractional crystallisation. The relative chemistry of East Dome and Central Cone samples is consistent with the East Dome magma having been derived from the Central Cone magma by fractional crystallisation, such a process also being consistent with their relative ages. However as shown in Table 7, East Dome samples have the lowest modal plagioclase contents and the highest proportion of groundmass in any Whale Island samples, which is not consistent with their derivation from any other Whale Island magma whose extrusive equivalent was sampled. Additionally, the similarity of the major element chemistry of East and West Domes and the dissimilarity of their trace element chemistry strongly suggests that they were not fractionation products of the same magma body.

The close similarity between the major and trace element chemistry of sample 11222 from Flow A and the samples from the Central Cone, supports the suggestion made on the basis of geological evidence that Flow A was erupted from a parasitic vent on the western flank of the Central Cone not long after the Central Cone was formed.

The Cone Tholoid which crops out at the base of the Central Cone, and which is stratigraphically inferred to be the oldest exposed portion of the Whale Island volcano, is chemically unlike any other portion of the island. A complete major element analysis of the sample (11233) from the Cone Tholoid has not been made, but its K_2O, Na_2O, FeO (total iron), CaO and MgO contents indicate that it is the

most basic non-xenolithic rock sampled from Whale Island. Relative to other Whale Island samples it is richer in Li and Sc, and depleted in Rb, Th, U, Ni and B; it also has a markedly higher K/Rb ratio of 390. The strong enrichment in Li (31 ppm) and depletion in Ni (<1 ppm), together with the depletion of the large cations give this rock a particularly unusual composition. Its trace element composition is quite unlike any other N.Z. intermediate calc-alkaline rock whose analysis has been previously published, or any such rocks analysed by the present author.

APPENDIX 6

Co-ordinates for ACF, AFM and von Wolff Ternary Diagrams, and Differentiation Index and Crystallisation Index Values for the Bay of Plenty Volcanics (see Table 52 on following page).

TABLE 52

CO-ORDINATES FOR ACF, AFM AND VON WOLFF TERNARY DIAGRAMS, AND DIFFERENTIATION INDEX AND CRYSTALLISATION INDEX VALUES FOR THE BAY OF PLENTY VOLCANICS

SAMPLE NO.	A	C	F	A	F	M	Q	L	M	D.I.	C.I.
11205	30.87	30.43	38.70	38.87	37.83	23.29	18.42	65.97	15.59	59.66	28.24
11206	27.52	31.46	41.02	25.08	36.64	38.28	14.40	62.14	23.45	45.77	38.90
11207	29.52	30.84	39.64	42.52	35.63	21.85	22.00	63.36	14.62	64.99	23.85
11208	26.59	30.69	42.72	27.14	35.43	37.43	14.43	62.43	23.12	48.85	36.08
11209	25.56	30.74	43.70	25.74	41.97	32.28	10.82	63.20	25.97	45.48	36.19
11210	29.10	30.58	40.32	36.64	32.95	30.41	22.41	61.44	16.13	60.96	27.88
11211	30.28	31.51	38.21	38.12	33.59	28.29	22.42	62.32	15.25	61.06	28.14
11212	29.65	30.80	39.54	38.83	32.15	29.02	23.11	61.81	15.07	62.73	26.77
11213	31.00	31.68	37.32	37.78	38.20	24.02	20.23	64.00	15.76	58.88	29.06
11214	28.55	31.61	39.84	33.38	35.99	30.62	19.30	62.20	18.49	56.14	31.00
11215	29.16	30.97	39.87	33.21	36.15	30.63	19.98	62.10	17.91	56.34	31.02
11216	27.76	30.95	41.30	29.37	37.41	33.21	17.27	61.85	20.86	51.94	33.68
11217	30.52	31.15	38.33	37.81	35.11	27.08	22.76	62.03	15.19	60.94	27.98
11219	29.91	32.35	37.74	39.46	31.05	29.49	24.39	60.49	14.61	63.33	26.82
11220	28.34	30.45	40.61	36.61	32.18	31.21	25.72	58.81	15.46	62.85	26.61
11221	29.64	31.41	38.94	37.11	31.83	31.06	25.14	59.63	15.21	62.15	27.56
11222	29.92	29.19	40.90	27.50	34.21	38.28	22.91	59.98	18.10	53.41	34.29
11223	24.77	32.14	43.09	18.43	35.53	46.04	10.78	59.04	30.17	36.96	45.23
11224	30.02	29.32	37.66	41.85	33.99	24.16	26.12	61.29	12.58	65.56	24.38
11225	28.30	31.66	39.44	31.37	34.06	34.57	21.84	59.92	18.23	55.65	32.23
11226	27.92	32.06	40.02	31.77	33.88	34.35	20.32	60.53	19.13	55.49	31.99
11227	29.23	31.92	38.80	32.99	33.66	33.35	21.95	60.59	17.45	56.86	31.48
11228	23.36	30.17	46.46	15.57	34.58	49.86	12.38	55.30	32.30	38.96	45.39
11229	23.78	32.47	43.75	17.98	35.06	46.96	11.73	57.05	31.16	37.49	44.56
11230	27.69	32.60	39.71	37.61	31.39	31.00	22.59	60.60	16.80	61.75	27.33
11231	32.03	31.90	36.07	43.74	32.99	23.27	23.74	63.48	12.77	65.05	25.41
11232	26.40	30.53	43.07	35.28	39.02	25.70	13.33	66.14	20.51	56.30	28.53
11234	28.50	31.30	40.20	30.52	34.31	35.16	21.16	59.99	18.83	54.92	32.59
11235	28.69	32.72	38.59	35.16	33.11	31.73	20.72	60.90	18.37	55.67	32.18
11236	28.71	32.13	39.16	32.22	33.92	33.86	20.92	61.57	17.49	58.12	30.29
11237	28.25	32.35	38.80	33.74	33.72	32.54	20.08	61.44	18.46	56.52	31.35
11238	29.39	31.52	39.09	32.62	33.56	33.82	21.13	61.25	17.61	56.18	32.01
11239	30.60	30.59	38.81	27.48	35.46	37.06	23.50	58.76	17.73	52.80	35.08
11240	22.56	29.66	47.78	32.11	31.69	36.21	17.70	59.93	22.36	58.39	27.79
11241	22.27	29.98	47.75	30.79	32.42	36.79	17.27	59.27	23.34	56.93	28.70
11242	20.85	29.94	49.21	30.43	31.05	38.51	16.89	58.67	24.43	57.14	28.41
11243	26.38	27.49	46.13	34.55	29.78	35.67	20.73	61.35	17.91	61.30	27.06
11244	23.52	30.07	46.41	33.43	31.99	34.58	18.93	60.09	20.97	59.64	27.16
11245	23.09	29.21	47.70	30.67	30.89	38.44	19.15	58.72	22.12	57.80	28.77
11246	25.77	32.86	41.37	22.99	37.78	39.23	10.84	61.99	27.15	41.43	41.35
11247	31.90	30.03	38.07	44.75	35.45	19.80	21.37	65.75	12.87	65.60	24.11
11248	35.34	27.93	36.73	39.15	39.80	21.05	20.75	65.95	13.28	65.51	23.80
11249	27.75	31.42	40.83	46.10	34.54	19.36	22.89	62.85	14.24	68.89	20.26

PART 5

REFERENCES

AHRENS, L.H.; TAYLOR, S.R. 1961: Spectrochemical Analysis. Addison-Wesley, Reading (Mass) and London.

ARKIN, H.; COLTON, R.R. 1963: Tables for statisticians. Barnes & Noble, New York.

BLACK, PHILLIPA M. (in press): Observations on White Island volcano. Bull. Volcan.

BOTTINGA, Y.; KUDO, A.; WEILL, D. 1966: Some observations on oscillatory zoning and crystallisation of magmatic plagioclase. Am. Miner., 51: 792-806.

BURNS, R.G.; FYFE, W.S. 1964: Site preference energy and selective uptake of transition-metal ions from a magma. Science, N.Y., 144 (3621): 1001-1003.

BURNS, R.G.; FYFE, W.S. 1967: Crystal-Field theory and the geochemistry of transition elements. Researches in Geochemistry Vol. 2: 259-285. Abelson, P.H. (ed.), Wiley - New York, London, Sydney.

CHALLIS, G.A.; LAUDER, W.R. 1966: The genetic position of "Alpine" type ultramafic rocks. Bull. Volcan., 29: 283-306.

CHAYES, F. 1965: On the level of silica saturation in andesite. Ann. Rep. Dir. Geophys. Lab. Wash., 1964-1965: 155-159.

CLARK, R.H. 1960 a: Andesite lavas of the North Island, New Zealand. Int. Geol. Congr., Norden, 1960 pt 13: 123-131.

CLARK, R.H. 1960 b: Petrology of the volcanic rocks of Tongariro Subdivision. Appendix 2 in Gregg, D.R., The geology of Tongariro Subdivision. Bull. N.Z. geol. Surv., n.s., 40: 107-123.

DEER, W.A.; HOWIE, R.A.; ZUSSMAN, J. 1963: Rock forming minerals, Vol. 2. Chain Silicates, Longmans, Green; London.

DEGENS, E.T.; WILLIAMS, E.G.; KEITH, M.L. 1957: Environmental studies of Carboniferous sediments. Part I. Geochemical criteria for differentiating marine and fresh-water shales. Bull. Am. Ass. Petrol. Geol., 41: 2427-2455.

DEGENS, E.T.; WILLIAMS, E.G.; KEITH, M.L. 1958: Environmental studies of Carboniferous sediments. Part II. Application of geochemical criteria. Bull. Am. Ass. Petrol. Geol., 42: 981-997.

DICKINSON, W.R. 1968: Circum-pacific andesite types. J. geophys. Res., 73: 2261-2269.

DICKINSON, W.R.; HATHERTON, T. 1967: Andesitic volcanism and seismicity around the pacific. Science, N.Y., 157: 801-803

DUNCAN, A.R.; TAYLOR, S.R. 1968: Trace element analyses of magnetites from andesitic and dacitic lavas from Bay of Plenty, New Zealand. Contr. Mineral. Petrol., 20: 30-33.

ELLIS, A.J.; SEWELL, J.R. 1963: Boron in waters and rocks of New Zealand hydrothermal areas. N.Z. Jl Sci., 6: 589-606.

EWART, A. 1963: Petrology and petrogenesis of the Quaternary pumice ash in the Taupo Area, New Zealand. J. Petrology, 4, (3): 392-431.

EWART, A.; STIPP, J.J. 1968: Petrogenesis of the volcanic rocks of the Central North Island, New Zealand, as indicated by a study of Sr^{87}/Sr^{86} ratios, and Sr, Rb, K, U, and Th abundances. Geochim. cosmochim. Acta, 32: 699-736.

EWART, A.; TAYLOR, S.R. 1969: Trace element geochemistry of the rhyolitic volcanic rocks, Central North Island, New Zealand, phenocryst data. Contr. Mineral. Petrol., 22: 127-146.

EWART, A.; TAYLOR, S.R.; CAPP, A.C. 1968: Trace and minor element geochemistry of the rhyolitic volcanic rocks, Central North Island, New Zealand. Total rock and residual liquid data. Contr. Mineral. Petrol., 18: 76-104.

FLEMING, C.A. 1952: The White Island trench: a sub-marine graben in the Bay of Plenty, New Zealand. Proc. Pacif. 7th Sci. Congr., 3: 210-213.

GILL, J.B. (in press): Geochemistry of Viti Levu, Fiji, and its evolution as an island arc.

GRANGE, L.J. 1937: The geology of the Rotorua-Taupo subdivision. Bull. N.Z. geol. Surv. n.s. 37.

GREEN, T.H.; RINGWOOD, A.E. 1968: Genesis of the calc-alkaline igneous rock suite. Contr. Mineral. Petrol., 18: 105-162.

HAMILTON, R.R.; GALE, A.W. 1968: Seismicity and structure of North Island, New Zealand. J. geophys. Res., 73: 3859-3876.

HARLOFF, C. 1927: Zonal structure in plagioclases. Leid. geol. Meded., 2: 99-114.

HASKIN, L.A.; FREY, F.A. 1966: Dispersed and not-so-rare Earths. Science, N.Y., 152: (3720): 299-314.

HASKIN, L.A.; FREY, F.A.; SCHMITT, R.A.; SMITH, R.H. 1966: Meteoritic, solar and terrestrial rare-earth distributions. Phys. Chem. Earth, 7: 167-322.

HATHERTON, T. 1968: "Miogeosynclinal" andesites. Earth & Planet. Sci. Lett. (Neth.), 4: 441-447.

HATHERTON, T. 1969: The geophysical significance of calc-alkaline andesites in New Zealand. N.Z. Jl Geol. Geophys., 12: 436-459.

HATHERTON, T.; DICKINSON, W.R. 1968: Andesitic volcanism and seismicity in New Zealand. J. geophys. Res., 73: 4615-4619.

HEALY, J. 1962: Structure and volcanism in the Taupo Volcanic Zone, New Zealand. 'Crust of the Pacific Basin', Geophys. Monogr. 6: 151-157.

HEALY, J. 1964: Volcanic mechanisms in the Taupo Volcanic Zone, New Zealand. N.Z. Jl Geol. Geophys., 7 (1): 6-23.

HEALY, J. 1967: Geological History of the Whakatane District. Whakatane & District Historical Soc., Historical Rev., 15 (1): 9-27.

HEALY, J.; EWART, A. 1965: Coastal section - Matata to Otamarakau. In N.Z. Volcanology, Central Volcanic Region, Dep. Scient. ind. Res. Information Series 50: 132-139.

HEALY, J.; SCHOFIELD, J.C.; THOMPSON, B.N. 1964: Sheet 5 - Rotorua. Geological map of New Zealand. 1:250,000. N.Z. Dep. Scient. ind. Res. Wellington

HEIER, K.S.; COMPSTON, W.; MCDOUGALL, I. 1965: Thorium and uranium concentrations, and the isotopic composition of strontium in the differentiated Tasmanian dolerites. Geochim. cosmochim. Acta, 29: 643-659.

KOLBE, P.; TAYLOR, S.R. 1966: Geochemical investigations of the granitic rocks of the Snowy Mts area, New South Wales. J. geol. Soc. Aust., 13: 1-25.

KUNO, H. 1960: High-alumina basalt. J. Petrology, 1: 121-145.

KUNO, H. 1968: Origin of andesite and its bearing on the Island Arc structure. Bull. Volcan., 32: 141-176.

LE MAITRE, R.W. 1968: Chemical variation within and between volcanic rock series - A statistical approach. J. Petrology, 9: 220-252.

LEWIS, J.F. 1968 a: Tauhara volcano, Taupo Zone. Part II - Mineralogy and petrology. N.Z. Jl Geol. Geophys., 11 (3): 651-684.

LEWIS, J.F. 1968 b: Trace elements, variation in alkalis, and the ratio Sr^{87}/Sr^{86} in selected rocks from the Taupo Volcanic Zone. N.Z. Jl Geol. Geophys., 11 (3), 608-629.

MANSON, V. 1967: Geochemistry of basaltic rocks: major elements. p. 215-269 in Basalts, Vol. 1., Hess, H.H. & Poldervaart, A. (ed.); Wiley, New York.

MODRINIAK, N.; STUDT, F.E. 1959: Geological structure of the Taupo-Tarawera district. N.Z. Jl Geol. Geophys., 2 (4): 654-684.

MACPHERSON, E.O. 1944: Notes on the Geology of Whakatane District and Whale Island. N.Z. Jl Sci. Technol., 26 (2B), 66-76.

NORRISH, K.; CHAPPELL, B.W. 1967: X-ray fluorescence spectrography. in Physical Methods in Determinative Mineralogy. J. Zussman (ed.) Academic Press, London & New York.

OSBORN, E.F. 1959: Role of oxygen pressure in the crystallisation and differentiation of basaltic magma. Am. J. Sci., 257: 609-647.

OSBORN, E.F. 1962: Reaction series for subalkaline igneous rocks based on different oxygen pressure conditions. Am. Miner., 47: 211-226.

OSBORN, E.F. 1969: The complementariness of orogenic andesite and alpine peridotite. Geochim. cosmochim. Acta, 33: 307-324.

PEARCE, T.H. 1968: A contribution to the theory of variation diagrams. Contr. Mineral. Petrol., 19: 142-157.

POLDERVAART, A.; PARKER, A.B. 1964: The crystallisation index as a parameter of igneous differentiation in binary variation diagrams. Am. J. Sci., 262: 281-289.

PRINZ, M. 1967: Geochemistry of basaltic rocks: trace elements. in Basalts, Vol. 1., p. 270-323 Hess, H.H. & Poldervaart, A (ed.); Wiley, New York.

RINGWOOD, A.E. 1955: The principles governing trace element behaviour during magmatic crystallisation. Part II: The role of complex formation. Geochim. cosmochim. Acta, 7: 242-254.

ROEDER, P.L.; OSBORN, E.F. 1966 a: Fractional crystallisation trends in the system $Mg_2 SiO_4$ - $Ca Al_2 Si_2O_8$ - FeO - Fe_2O_3 - SiO_2 over the range of oxygen partial pressures of 10^{-11} to $10^{-0.7}$ atm. Bull. Volcan., 29: 659-668.

ROEDER, P.L.; OSBORN, E.F. 1966 b: Experimental data for the system MgO - FeO - Fe_2O_3 - $Ca Al_2 Si_2O_8$ - SiO_2 and their petrological implications. Am. J. Sci., 264: 428-480.

SCHOFIELD, J.C. 1968: Regional aspects of Cainozoic volcanology in the North Island of New Zealand - crustal fusion produces intermediate magma. N.Z. Jl Geol. Geophys., 11 (2): 277-290.

SHAW, D.M. 1954: Trace elements in pelitic rocks, I, II. Bull. geol. Soc. Am., 65: 1151-1166, 1167-1182.

SMITH, J.V.; GAY, P. 1958: The powder patterns and lattice parameters of plagioclase felspars. II. Mineralog. Mag., 31: 744-762.

STEINER, A. 1958: Petrogenetic implications of the 1954 Ngauruhoe lava and its xenoliths. N.Z. Jl Geol. Geophys., 1 (2): 325-363.

STUDT, F.E. 1958: Geophysical reconnaissance at Kawerau, New Zealand. N.Z. Jl Geol. Geophys., 1 (2): 219-246.

TAYLOR, G.A. 1958: The 1951 eruption of Mount Lamington, Papua. Bull. Bur. Miner. Resour. Aust. 38.

TAYLOR, S.R. 1965 a: Geochemical analysis by spark source mass spectrography. Geochim. cosmochim. Acta, 29: 1243-1262.

TAYLOR, S.R. 1965 b: The application of trace element data to problems in petrology. Phys. Chem. Earth, 6: 133-213.

TAYLOR, S.R. 1968: Geochemistry of andesites. in Origin and distribution of the elements. L.H. Ahrens (ed.); Pergamon, Oxford & New York.

TAYLOR, S.R. 1969: Trace element chemistry of andesites and associated calc-alkaline rocks. I.U.M.P. Sci. Rep. 16. (Proc. Andesite Conference, Oregon), 43-63.

TAYLOR, S.R.; CAPP, A.C.; GRAHAM, A.L.; BLAKE, D.H. 1969: Trace element abundances in andesites II. Saipan, Bougainville and Fiji. Contr. Mineral. Petrol., 23: 1-26.

TAYLOR, S.R.; EWART, A.; CAPP, A.C.1968: Leucogranites and rhyolites: Trace element evidence for fractional crystallisation and partial melting. Lithos 1, 2: 179-186.

TAYLOR, S.R.; KAYE, M.; WHITE, A.J.R.; DUNCAN, A.R.; EWART, A. 1969: Genetic significance of Co, Cr, Ni, Sc and V content of andesites. Geochim. cosmochim. Acta, 33: 275-286.

TAYLOR, S.R.; WHITE, A.J.R. 1965: Geochemistry of andesites and the growth of continents. Nature, Lond., 208 (5007): 271-273.

TAYLOR, S.R.; WHITE, A.J.R. 1966: Trace element abundances in andesites. Bull. Volcan., 29: 177-194.

THOMPSON, B.N. 1964: Quaternary volcanism of the Central Volcanic Region. N.Z. Jl Geol. Geophys., 7 (1): 45-66.

THOMPSON, B.N.; KERMODE, L.O.; EWART, A. 1965: New Zealand volcanology. Central Volcanic Region. N.Z. Dep scient. ind. Res. Inf. Ser. 50.

THORNTON, C.P.; TUTTLE, O.F. 1960: Chemistry of igneous rocks I. Differentiation index. Am. J. Sci., 258: 664-684.

TUREKIAN, K.K.; WEDEPOHL, K.H. 1961: Distribution of the elements in some major units of the earth's crust. Bull. geol. Soc. Am. 72: 175-192.

VANCE, J.A. 1962: Zoning in igneous plagioclase: normal and oscillatory zoning. Am. J. Sci., 260: 746-760.

VANCE, J.A. 1965: Zoning in igneous plagioclase: patchy zoning. J. Geol., 73 (4): 636-651.

WAGER, L.R.; BROWN, G.M.; WADSWORTH, W.J. 1960: Types of igneous cumulates. J. Petrology, 1: 73-85.

WEBER, J.N.; MIDDLETON, G.V. 1961: Geochemistry of the turbidites of the Normanskill and Charny formations. II - distribution of trace elements. Geochim. cosmochim. Acta, 22: 244-288.

WILLIAMS, H. 1932: The history and character of volcanic Domes. Univ. Calif. Publs. geol. Sci. 21: 51-146.

Kawerau

Lake Pupuwharau

Tarawera River

Ignimbrite Roof Dome

North Dome

Northern Base Flows

Western Base Flows

Main Dome

Southern Base Flows

Lahar Fan

N

W

S

1a

1b

2a

2b

3a

3b

3c

6a

6b

6c

Aa

Ab

Ac

Ba

Bb

Ca

Cb

Da

Db

Dc

Dd

Ea

8a

8b

11a

1

2

3

4

5

6

7

8

9

10

11

SCALE

0 0·25 0·5 0·75 1·0 Miles

0 250 500 750 1000 1250 1500 Metres

LEGEND

- 1b — LAVA FLOW, COULÉE, OR DOME
- LAHAR DEBRIS AND/OR SCREE
- POSITION OF FLOW BOUNDARY KNOWN
- POSITION OF FLOW BOUNDARY INFERRED
- 1 / 2 — FLOW 1 YOUNGER THAN FLOW 2
- 1 / 2 — RELATIVE AGES OF FLOW 1 AND FLOW 2 NOT KNOWN
- ●3 — VOLCANIC VENT

15 16 17 18 19 420000 E 21

510000 N 09 08 07 06 05

Fig. 3. - Interpretive Map of Edgecumbe. Where flows can be ascribed to a particular vent they are given the vent number, and a number of flows apparently from the same vent are termed a flow series. The relative age of the flows in each flow series is indicated by the letters 'a', 'b' and 'c' after the vent number, indicating increasing age with 'a' being the youngest recognised flow from that vent. In cases where a flow series can be recognised but the vent from which it was erupted is not recognisable, then all the flows in any one series are identified by capital letters. Thus flow series A contains three flows: Aa, Ab and Ac, in order of increasing age.

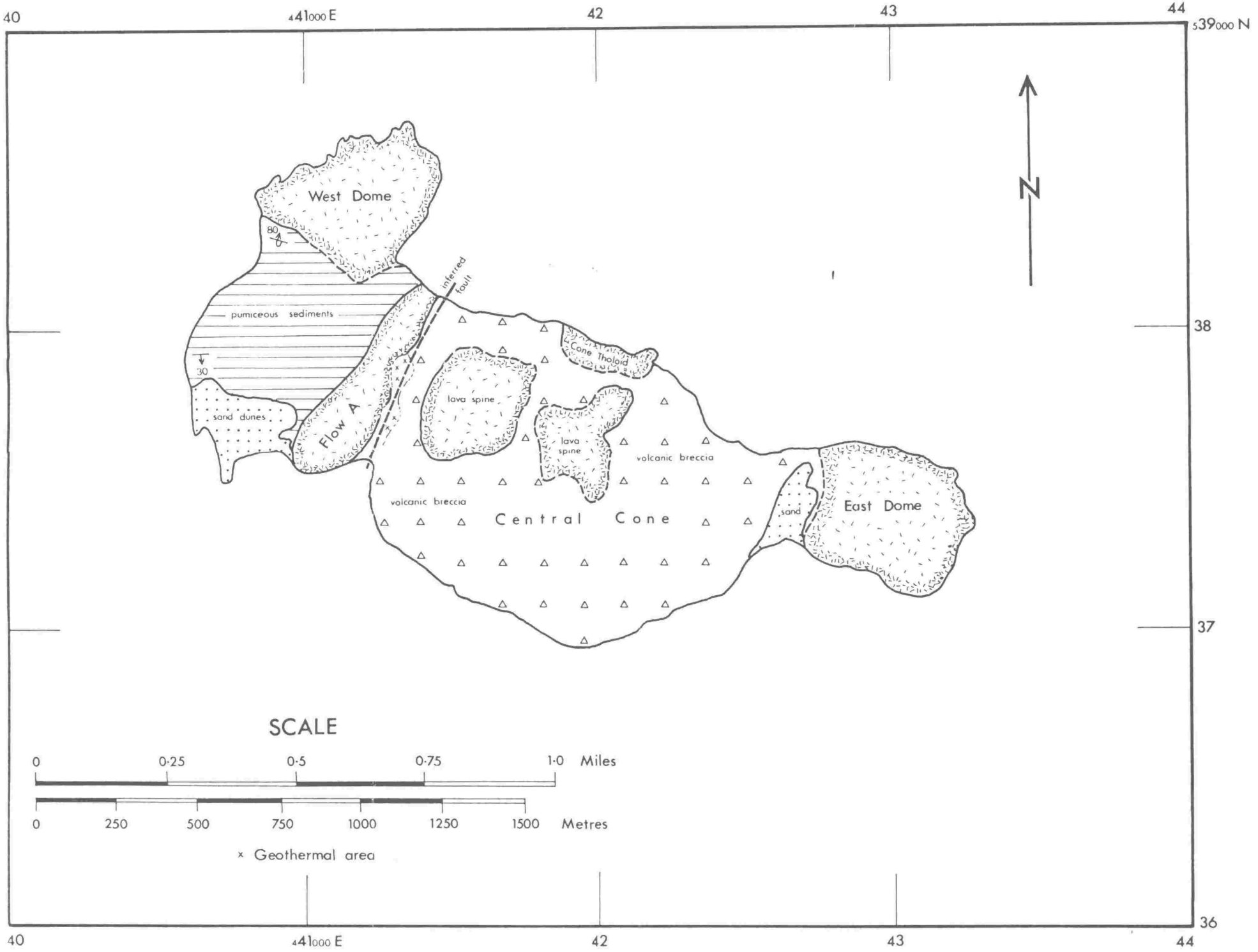
40
441000 E
42
43
44
539000 N
West Dome
80
pumiceous sediments
30
sand dunes
Flow A
inferred fault
lava spine
Cone Tholoid
lava spine
volcanic breccia
volcanic breccia
Central Cone
sand
East Dome
N
38
37
36
SCALE
0
0·25
0·5
0·75
1·0 Miles
0
250
500
750
1000
1250
1500 Metres
× Geothermal area

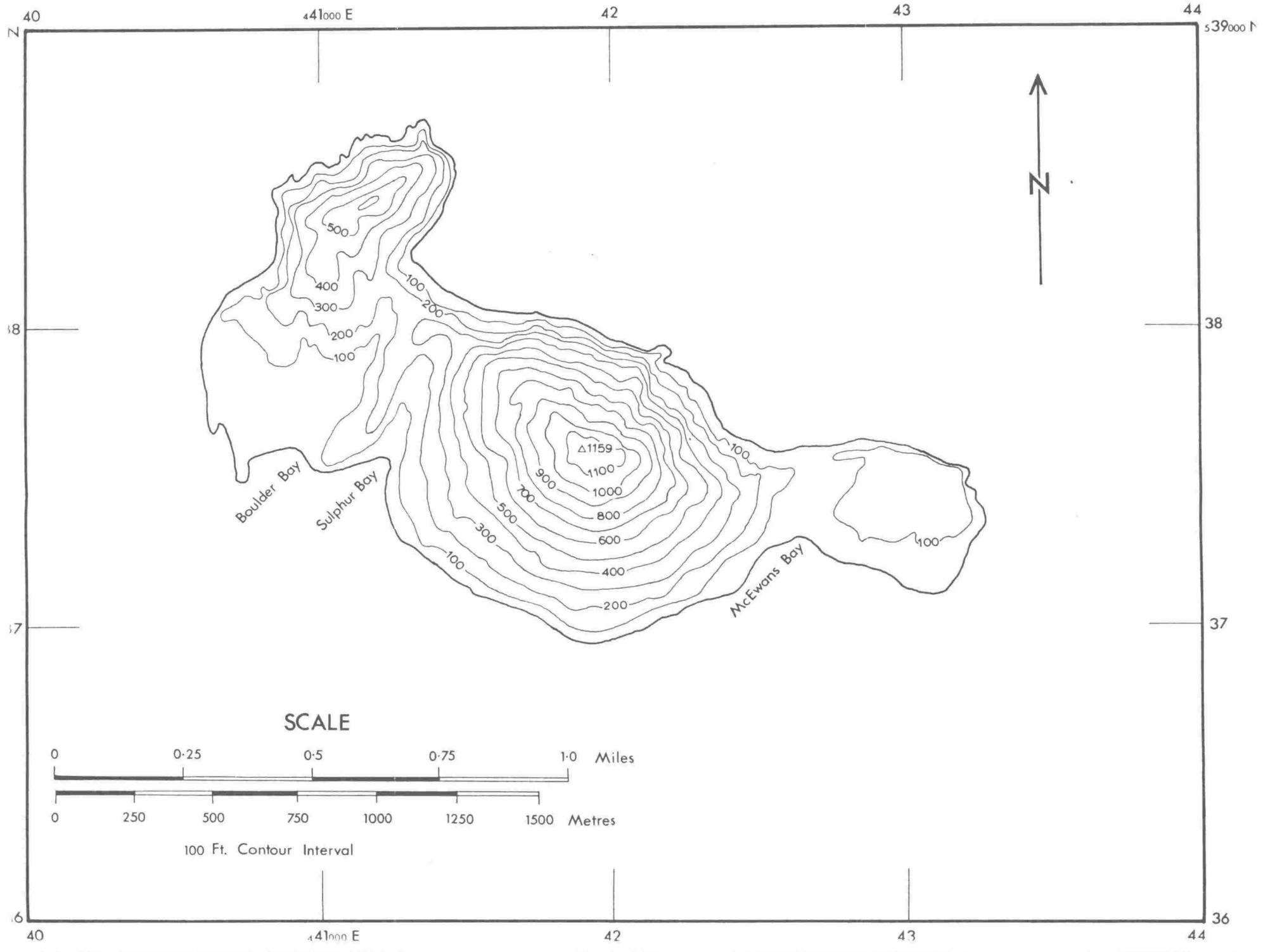
40
441000 E
42
43
44
N
539000 N
38
37
36
N
500
400
300
200
100
100
200
△1159
1100
1000
900
800
700
600
500
400
300
200
100
100
100
Boulder Bay
Sulphur Bay
McEwans Bay
SCALE
0
0·25
0·5
0·75
1·0 Miles
0
250
500
750
1000
1250
1500 Metres
100 Ft. Contour Interval

15 16 17 18 19 ▲20000 E 21

s10000 N

09 08 07 06 05

N

SCALE

0 0·25 0·5 0·75 1·0 Miles

0 250 500 750 1000 1250 1500 Metres

50 Ft. Contour Interval

Drawn from N.Z.M.S. 2 N77/5,6

TABLE 30

CORRELATION MATRIX - WHALE ISLAND

14 samples (no xenolith data is included)

53 variables

see Table 29 for list of abbreviations used.

Significance levels:	95%	$\|r\| >$	0.497
	99%	$\|r\| >$	0.623
	99.9%	$\|r\| >$	0.742

TABLE 31

CORRELATION MATRIX - EDGECUMBE & WHALE ISLAND

24 samples (no xenolith data is included)

53 variables

see Table 29 for list of abbreviations used.

Significance levels:	95%	$\|r\|$	$>$	0.381
	99%	$\|r\|$	$>$	0.487
	99.9%	$\|r\|$	$>$	0.597